

HYBRIDIZATION IN THE NORTHERN FLICKER (*COLAPTES AURATUS*) REVEALS  
THE GENOMIC ARCHITECTURE OF FEATHER COLORATION

A Dissertation

Presented to the Faculty of the Graduate School  
of Cornell University

In Partial Fulfillment of the Requirements for the Degree of  
Doctor of Philosophy

by

Stephanie Maria Aguillon

August 2021

© 2021 Stefanie Maria Aguillon

HYBRIDIZATION IN THE NORTHERN FLICKER (*COLAPTES AURATUS*) REVEALS  
THE GENOMIC ARCHITECTURE OF FEATHER COLORATION

Stephanie Maria Aguillon, Ph. D.

Cornell University 2021

Birds possess a remarkable diversity of feather coloration—from dark blacks and grays to bright reds and yellows. The genetic bases of these color differences have been sought for a long time, but we are just beginning to be able to understand the relationship between genotype and phenotype in non-model systems. Here, I perform an in-depth analysis of phenotypic and genotypic variation in the northern flicker complex (*Colaptes auratus*), a common North American woodpecker, to further our understanding of feather coloration in birds. For this work, I leverage the extensive hybridization between the yellow-shafted and red-shafted subspecies of the northern flicker in the Great Plains. This hybrid zone has been studied intensely for many years due to their distinct coloration differences, most notably the difference in the wing and tail color (the eponymous “shaft”) which varies from brilliant yellow to salmon red. I first assess phenotypic variation across an identical transect of the hybrid zone in historic and contemporary sampling periods, and document a westward movement of the hybrid zone towards the range of the red-shafted flicker. I then explore population genetic patterns using a reduced-representation genomic sequencing approach and am able to separately cluster the taxa for the first time, but identify an extremely low-level of baseline divergence nonetheless. Finally, I use whole-genome sequencing and subsequent targeted sequencing to identify regions of the genome associated with the

coloration differences in the flickers and assess how interactions between these genomic regions influence coloration. Collectively, these studies have furthered our understanding of the long-studied flicker hybrid zone and the genetic basis of coloration in birds.

## BIOGRAPHICAL SKETCH

Stephanie Maria Aguilon grew up in Sierra Vista, Arizona. Her grandfather, Frank J. Wood, instilled in her a love of the natural world through frequent fishing and camping trips (often to Patagonia Lake State Park), and many afternoons spent watching nature documentaries or discussing plants and animals on the front porch. After completing her early education at Buena High School, Stephanie was the first member of her family to go to college and attended the University of Arizona in Tucson, AZ. There, she participated in research opportunities through the UA/NASA Space Grant Program and the NSF Research Experience for Undergraduates. The fall semester of her junior year, Stephanie took an ornithology course with Renée A. Duckworth, who changed the course of her future by introducing her to birds and evolutionary biology. She switched majors to complete a combined five-year B.S./M.S. program working on western bluebirds with Renée. Stephanie graduated from the University of Arizona *summa cum laude* and with Honors with a B.S. in Ecology and Evolutionary Biology in 2013, and was selected as the Outstanding Senior for the department. She graduated with a M.S. in Ecology and Evolutionary Biology from the University of Arizona in 2014. Stephanie then joined the labs of Richard G. Harrison and Irby J. Lovette in Ecology and Evolutionary Biology at Cornell University to pursue her PhD.

This dissertation is dedicated to Frank J. Wood (March 6, 1946 – July 3, 2017) and Richard G. Harrison (November 19, 1945 – April 12, 2016), the two people I most wanted to be here when I finished.

## ACKNOWLEDGEMENTS

There are many, many people that helped make this dissertation possible. I would first like to thank my advisors Irby Lovette and Richard (Rick) Harrison, and my committee members Jeremy Searle, Maren Vitousek, and Leo Campagna. Individually and collectively, you really helped get me to the finish line. I am so deeply appreciative of my parents, Carrie and Jose Aguilon, who sacrificed so much to ensure that I had the opportunity to get to where I am today. You have both been so endlessly supportive as I have pursued this winding academic path. Thank you to Jen Walsh, for your unofficial advising and enduring friendship throughout this process. You have been such an important mentor both personally and professionally, and I cannot thank you enough. I am so grateful you ended up at Cornell for your post-doc, allowing our paths to cross.

Thank you to Bronwyn Butcher, Vanya Rohwer, Charles Dardia, Dave Toews, Rusty Ligon, and Steve Bogdanowicz for guidance and assistance in the lab, field, and museum. Brianna Mims, Augie Kramer, and Tayler Brooks additionally provided important help in the field. Thank you to Renée Duckworth for your thoughtful guidance and support along the way, and to Alex Badyaev for your insistence that Rick's lab was a great choice for me. Thank you to all of my lab mates (past and present), including *undergrads* Chloe Mikles, Jose Gamarra, Kelsie Lopez, and Vicens Vila-Coury; *grads* Petra Deane, Ezra Lencer, Henry Kunerth, Trevor Sless, Nick Mason, Jacob Berv, Natalie Hofmeister, Tram Nguyen, Amelia-Juliette Demery, Sarah Khalil, and Bryce Robinson; and *postdocs* Nancy Chen, Scott Taylor, Leo Campagna, Dave Toews, Jose Andres, Jen Walsh, Gavin Leighton, Rusty Ligon, Eliot Miller, Conor Taff, Shawn Billerman, Daniel Hooper, Natalia García, Sabrina McNew, Gemma Clucas, and Carrie Branch. Special thanks to Megan Bishop for providing the beautiful flicker

illustrations—they really elevated my dissertation! Thank you to the staff of the Department of Ecology and Evolutionary Biology and the Cornell Lab of Ornithology, including Patty Jordan, Carol Damm, Micky Zifchock, Zhila Sadri, LuAnne Kenjerska, John Howell, Brian Mlodzinski, Gary Oltz, Jolene Gardner, Jennifer Holleran, Chad Westmiller, Sally Blinn, and Manley Gavich. Particular thanks to Karen Harvey and Karl Karlson for always keeping the second floor of Corson-Mudd and the Fuller EvoBio Lab, respectively, clean and tidy. I always appreciated your friendly faces as you checked in.

I have made so many terrific friends during my time in Ithaca and I will do my best to acknowledge as many of you as I can here (sorry for any lapses in memory!). First and foremost, thank you to Gregor Siegmund for your wonderful friendship. Getting to know you during our time at Cornell has been an absolute joy. Who knew where being assigned to the same office at the beginning of grad school would take us! Particular thanks for putting up with my incessant rhyming and bad puns during the pandemic. Thanks to Natalie Hofmeister and Amelia Demery for your amazing friendships. I am so lucky to have gotten to spend my time here with you two insightful ladies. Also, so many thanks to Amelia for introducing me to D&D. You have been such a great DM and I have had so much fun being a part of Team Richard with Natalie, Clarice Guan, Charlotte Levy, Cinnamon Mittan, Katie Holmes, Sarah Khalil, Rachael Mady, and Monique Pipkin. D&D really kept me sane during the pandemic. (I do hope Zarna gets to cast fireball against Irig the Dark before I leave here though!) Thanks to the Pizza Pals, Gregor, Kate Eisen, and Ian Hunter, for welcoming me into your pizza posse and keeping up Pizza Wednesdays virtually. And so many thanks to Kate for keeping me physically active in the pool and mentally active outside the pool! Thanks to Team Charismatic Megafauna, particularly the long-time members Gregor and

Trevor Sless, for your continued domination of Darwin Day Trivia during our time here. Thanks also to Liz Duskey for bringing so much laughter and nerdiness to my life. Thanks to Marsha Durbin, Nora Springer, Diana Travis, and the Tompkins County SPCA doggie playgroups for bringing me into the fold and allowing me to watch your dogs at play every Sunday. Finally, thanks to Erin Morrison. Although we met long before I moved to Ithaca, your influence personally and professionally has been so important. You really helped to set me on this journey and I cannot thank you enough. I have continued to enjoy our catch ups at conferences—from Brazil to Alaska—and I hope we will continue that tradition into the future.

A variety of organizations provided fellowship and research funding for me to conduct this work. I am incredibly grateful to the NSF Graduate Research Fellowship Program (GRFP; award DGE-1144153), SUNY Diversity Fellowship, American Association of University Women (AAUW) American Dissertation Fellowship, Cornell Provost Diversity Fellowship, Cornell Lab of Ornithology Ivy Fellowship, and Cornell Lab of Ornithology Anna Marie Brown Fund for providing fellowship funding allowing me to focus on my research. This work would not have been possible without research funding, which was generously provided by the Cornell Lab of Ornithology Athena Fund, Garden Club of America Frances M. Peacock Scholarship, Richard G. Harrison Fund, Betty Miller Francis '47 Fund for Field Research, Cornell Lab of Ornithology Sally Merrill Sutcliffe Endowment, Andrew W. Mellon Student Research Grant, American Ornithological Society Hesse Award, Wilson Ornithological Society Research Award, Paul P. Feeny Graduate Student Research Fund, and Cornell Sigma Xi Grant-in-Aid-of-Research.

Finally, I would be remiss if I did not fully acknowledge the amount of loss I have suffered during my PhD and the people that have helped support me. Before

starting at Cornell, I was quite naïve to loss. But during my PhD, my co-advisor Rick Harrison died suddenly while on sabbatical in Australia (April 2016), my grandfather Frank Wood died after a long battle with COPD caused by a lifetime of smoking (July 2017), my heart dog Chiquita nearly died twice but received life-saving care first with a blood transfusion when she was on death's door from internal bleeding (December 2017) and later with an emergency cholecystectomy (February 2019), I left a ten-year relationship (January 2019), and then Chiquita was diagnosed with pancreatic carcinoma and I had to let her go less than a month later (November 2019). I truly suspect at many other institutions I would not have continued on with my degree. I am so grateful for the flexibility and extra time I have been given at Cornell that has allowed me to finish; I definitely would not have had the strength to do so without the support of the following people. Thanks first and foremost to my advisor Irby Lovette. You really stepped in to help keep me going when Rick died, and have been so incredibly supportive during all of my other personal losses. I cannot thank you enough. Thanks also to Jeremy Searle and Monica Geber for providing support after Rick died and always checking in on my well-being. Thanks to Gregor and Natalie for helping to take care of Chiquita while I was in Arizona when my Ganpa was in hospice. Thank you to Jen Walsh and Bronwyn Butcher for giving me a place to stay and a shoulder to cry on when I struck out on my own and had nowhere else to go. I really appreciate that you did not let me sleep on my office floor. Special thanks and my eternal gratitude to the Cornell University Hospital for Animals (specifically the Emergency and Critical Care Service, Dr. Adam Miller, and the many rotating vet students), VCA Colonial Animal Hospital, and Embrace Pet Insurance for giving me extra time with Chiquita. The last months of Chiquita's life were some of the hardest I have ever experienced, and I am so fortunate I did not have to go through them alone.

Gregor was there 24/7 for many weeks, helping to provide her intense daily care and helping me take her to get all the smells one last time. I really could not have done it without you. Thank you from the bottom of my heart. Natalie, Amelia, Sarah Khalil, Kate Eisen, Jen Walsh, and Tram Nguyen provided food, encouragement, puzzles, flowers, craft breaks, and checked in on us frequently. I cannot tell you how much I appreciated your many kindnesses. And finally, thanks to my Mom for coming all the way from Arizona to be with us at the end.

## TABLE OF CONTENTS

BIOGRAPHICAL SKETCH .....	iii
DEDICATION .....	iv
ACKNOWLEDGEMENTS.....	v
PREFACE .....	xii
Resumen en español .....	xii
Dissertation Introduction.....	xiii
References .....	xvi
<b>1. RAPID MOVEMENT OF AN AVIAN HYBRID ZONE .....</b>	<b>1</b>
1.1 Abstract.....	1
1.2 Introduction .....	2
1.3 Methods.....	6
1.4 Results.....	12
1.5 Discussion .....	19
1.6 References .....	23
<b>2. A FLICKER OF HOPE: GENOMIC DATA DISTINGUISH NORTHERN FLICKER TAXA DESPITE LOW LEVELS OF DIVERGENCE.....</b>	<b>28</b>
2.1 Abstract.....	28
2.2 Introduction .....	29
2.3 Methods.....	34
2.4 Results.....	41
2.5 Discussion .....	50
2.6 References .....	54
<b>3. EXTENSIVE HYBRIDIZATION REVEALS MULTIPLE COLORATION GENES UNDERLYING A COMPLEX PLUMAGE PHENOTYPE.....</b>	<b>62</b>
3.1 Abstract.....	62
3.2 Introduction .....	63
3.3 Results and Discussion.....	66
3.4 Conclusions.....	75
3.5 Methods.....	76
3.6 References .....	81
<b>4. INTERACTING GENOMIC REGIONS SHAPE THE COLORATION OF MULTIPLE PHENOTYPES IN THE NORTHERN FLICKER.....</b>	<b>90</b>
4.1 Abstract.....	90
4.2 Introduction .....	91

4.3 Methods.....	94
4.4 Results.....	98
4.5 Discussion .....	101
4.6 References .....	109
A. CHAPTER 1 APPENDIX .....	115
B. CHAPTER 2 APPENDIX .....	129
C. CHAPTER 3 APPENDIX .....	140
D. CHAPTER 4 APPENDIX .....	159

## PREFACE

### Resumen en español

Las aves poseen una enorme diversidad en la coloración del plumaje: presentando desde negros y grises hasta rojos y amarillos brillantes. A pesar de llevar mucho tiempo buscando las bases genéticas de estas diferencias de color, los biólogos evolutivos apenas estamos empezando a comprender la relación entre el genotipo y fenotipo en organismos que no son modelos genéticos. En este trabajo realizo un análisis en profundidad de la variación fenotípica y genotípica en *Colaptes auratus auratus* y *Colaptes auratus cafer*, dos carpinteros de América del Norte, para elucidar el funcionamiento de las bases genéticas de la coloración del plumaje. Para llevar a cabo este objetivo, aprovecho la extensa zona híbrida entre *C. a. auratus* y *C. a. cafer* en la región de las Grandes Llanuras de América del Norte. Esta zona híbrida se ha estudiado intensamente durante muchos años debido a las marcadas diferencias de coloración entre *C. a. auratus* y *C. a. cafer*, particularmente la diferencia en el color de las alas y la cola (que varían del amarillo a rojo). Primero, evalué la variación fenotípica en dos transectas idénticas de la zona híbrida en períodos de muestreo históricos y contemporáneos, y documenté un movimiento hacia el oeste de la zona híbrida, hacia el área de distribución del *C. a. cafer*. En segundo lugar, exploro los patrones genéticos de la población utilizando secuenciación de nueva generación y utilizando estos datos logro diferenciar los taxones por primera vez, pero sin embargo identifiqué un bajo nivel de divergencia. Por último, utilizo la secuenciación completa del genoma y la secuenciación dirigida para identificar las regiones del genoma asociadas a las diferencias de coloración en *Colaptes auratus* y evaluar cómo las interacciones entre estas regiones genómicas producen color. En conjunto, estos estudios han ampliado nuestra

comprensión de la zona híbrida entre *C. a. auratus* y *C. a. cafer* y la base genética de la coloración del plumaje en las aves.

## **Dissertation Introduction**

I have had a keen interest in hybridization and hybrid zones since I began my PhD. I found the idea that interbreeding between species occurred frequently in nature and could be used to understand important aspects of the evolutionary process utterly fascinating. Rick Harrison, my late advisor, described hybrid zones as “windows on evolutionary process” in 1990, and this has clearly proven to be true in the genomics era. Hybrid zones, the geographical regions where interbreeding occurs, have provided numerous important insights. Scientists are now routinely using hybrid zones to understand topics as disparate as adaptive introgression (Chhatre et al. 2018; Walsh et al. 2018), the genetic basis of morphology (Brelsford et al. 2017; Powell et al. 2021) and behavior (Delmore et al. 2016), barriers to gene flow (Larson et al. 2013; Hooper et al. 2019), and even climate change (Taylor et al. 2014; Billerman et al. 2016; Larson et al. 2019)

Of particular interest to me has been the burgeoning literature using hybrid zones to study the genetic basis of coloration in birds. Hybrid zones have helped to uncover the genetic basis of color in bird species as varied as European crows (Poelstra et al. 2015; Knief et al. 2019) and wagtails (Semenov et al. 2021), African tinkerbirds (Kirschel et al. 2020), Australian grassfinches (Hooper et al. 2019), and various species of North American warblers (Toews et al. 2016; Brelsford et al. 2017; Wang et al. 2020). Although melanin pigmentation (blacks, grays, and browns) is still much better

understood than carotenoid pigmentation (bright reds, oranges, and yellows) in birds (Hubbard et al. 2010; Toews et al. 2017), hybrid zones have helped provide insights into both pigment types.

My interest in hybrid zones and bird coloration collided the day Rick went searching through his office file cabinets to find a stack of classic papers on the Great Plains hybrid zones. This region of North America is considered to be a suture zone where many hybrid zones—of various taxa—co-occur geographically (Rising 1983; Swenson and Howard 2004). There are five bird hybrid zones in this suture zone that have a long history of study: indigo and lazuli buntings (Sibley and Short 1959; Kroodsma 1975; Baker and Baker 1990; Baker and Johnson 1998; Carling and Brumfield 2008; Carling et al. 2010; Carling and Zuckerberg 2011; Carling and Thomassen 2012), spotted and eastern towhees (Sibley and West 1959), black-headed and rose-breasted grosbeaks (West 1962; Anderson and Daugherty 1974; Mettler and Spellman 2009), Bullock's and Baltimore orioles (Sibley and Short 1964; Rising 1969, 1970; Rohwer and Manning 1990; Rising 1996; Carling et al. 2011; Jacobsen and Omland 2012; Walsh et al. 2020), and the red-shafted and yellow-shafted flicker (Short 1965; Moore and Buchanan 1985; Grudzien and Moore 1986; Grudzien et al. 1987; Moore 1987; Fletcher and Moore 1992; Moore and Price 1993).

I read through this stack of classic papers with Rick's penciled notes in the margins with interest and was particularly intrigued by the hybrid zone in the flickers. Despite having very distinct phenotypic differences between the two hybridizing taxa across a number of plumage patches (Short 1965; Wiebe and Moore 2020), no genetic differences (mitochondrial or nuclear) had been identified (Grudzien and Moore 1986; Grudzien et al. 1987; Moore et al. 1991; Fletcher and Moore 1992) and no modern genomic sequencing techniques had yet been applied. After discussions with my co-

advisors, Rick and Irby Lovette, and multiple visits to the Cornell University Museum of Vertebrates (CUMV) to look at specimens, I decided to focus my PhD research on flickers.

Yellow-shafted (*Colaptes auratus auratus*) and red-shafted (*Colaptes auratus cafer*<sup>1</sup>) flickers are common woodpeckers distributed widely across much of North America. The flickers differ across a number of plumage characteristics—wing and tail (“shaft”) color, ear covert color, crown color, male malar stripe color, throat color, and the presence/absence of the nuchal patch—but are largely ecologically similar otherwise (similar diets, habitats, behavior, etc.). These two taxa are currently classified as subspecies within the “northern flicker,” as they come into secondary contact in a large hybrid zone in the Great Plains, extending from northern Texas up to Alaska following the rain shadow of the Rocky Mountains. Hybridization is widespread within the hybrid zone and hybrid individuals can be easily identified by their plumage. Despite this extensive hybridization, there is no evidence for assortative mating in the southern (US) part of the hybrid zone (Bock 1971; Moore 1987) and only weak evidence in the northern (Canadian) part (Wiebe 2000; Flockhart and Wiebe 2007; Wiebe and Vitousek 2015). Moreover, there are no clear fitness consequences of hybridization (Moore and Koenig 1986; Wiebe and Bortolotti 2002; Flockhart and Wiebe 2009), and in fact, the hybrid zone has been hypothesized to represent a case of “bounded hybrid superiority” (Moore and Price 1993)—where hybrids actually have higher fitness than parental types within the region of the hybrid zone.

In this dissertation, I first focus exclusively on the six plumage differences and

---

<sup>1</sup> The sub-specific epithet of the red-shafted flicker is based on a term that is an extreme racial slur against Black Africans, particularly in South Africa. Thus, I refrain from using the scientific names for these species whenever possible in my dissertation, and instead refer to the flickers by their common names.

use CUMV specimens to assess movement of the flicker hybrid zone over time (Chapter 1). I then use various genomic sequencing approaches to understand: population genetic patterns across the species complex (Chapter 2), the regions of the genome that create their coloration differences (Chapter 3), and how these genomic regions interact to produce the plumage color (Chapter 4). Collectively, this research has furthered our understanding of the long-studied flicker hybrid zone, as well as our understanding of the genetic basis of coloration in birds. By conducting both extensive phenotypic and extensive genomic analyses, I have made my work comparable to previous studies in the flickers, while also pushing our understanding of the group forward—identifying differences in the genome for the first time. Moreover, by leveraging their extensive hybridization, I have made important discoveries about the genetic basis of both melanin and carotenoid plumage coloration in birds.

## References

- Anderson, B. W. and R. J. Daugherty. 1974. Characteristics and reproductive biology of grosbeaks (*Pheucticus*) in the hybrid zone in South Dakota. *The Wilson Bulletin* 86:1-11.
- Baker, M. C. and E. M. Baker. 1990. Reproductive behavior of female buntings: isolating mechanisms in a hybridizing pair of species. *Evolution* 44:332-338.
- Baker, M. C. and M. S. Johnson. 1998. Allozymic and morphometric comparisons among indigo and lazuli buntings and their hybrids. *Auk* 115:537-542.
- Billerman, S. M., M. A. Murphy, and M. D. Carling. 2016. Changing climate mediates sapsucker (*Aves: Sphyrapicus*) hybrid zone movement. *Ecol. Evol.* 6:7976-7990.
- Bock, C. E. 1971. Pairing in hybrid flicker populations in eastern Colorado. *Auk* 88:921-924.

- Brelsford, A., D. P. L. Toews, and D. E. Irwin. 2017. Admixture mapping in a hybrid zone reveals loci associated with avian feather coloration. *Proc. R. Soc. B* 284:20171106.
- Carling, M. D. and R. T. Brumfield. 2008. Haldane's rule in an avian system: using cline theory and divergence population genetics to test for differential introgression of mitochondrial, autosomal, and sex-linked loci across the *Passerina* bunting hybrid zone. *Evolution* 62:2600-2615.
- Carling, M. D., I. J. Lovette, and R. T. Brumfield. 2010. Historical divergence and gene flow: coalescent analyses of mitochondrial, autosomal and sex-linked loci in *Passerina* buntings. *Evolution* 64:1762-1772.
- Carling, M. D., L. G. Serene, and I. J. Lovette. 2011. Using historical DNA to characterize hybridization between Baltimore Orioles (*Icterus galbula*) and Bullock's Orioles (*I. bullockii*). *Auk* 128:61-68.
- Carling, M. D. and H. A. Thomassen. 2012. The role of environmental heterogeneity in maintaining reproductive isolation between hybridizing *Passerina* (Aves: Cardinalidae) buntings. *Int. J. Ecol.* 2012:1-11.
- Carling, M. D. and B. Zuckerberg. 2011. Spatio-temporal changes in the genetic structure of the *Passerina* bunting hybrid zone. *Mol. Ecol.* 20:1166-1175.
- Chhatre, V. E., L. M. Evans, S. P. DiFazio, and S. R. Keller. 2018. Adaptive introgression and maintenance of a trispecies hybrid complex in range-edge populations of *Populus*. *Mol. Ecol.* 27:4820-4838.
- Delmore, K. E., D. P. Toews, R. R. Germain, G. L. Owens, and D. E. Irwin. 2016. The genetics of seasonal migration and plumage color. *Curr. Biol.* 26:2167-2173.
- Fletcher, S. D. and W. S. Moore. 1992. Further analysis of allozyme variation in the northern flicker, in comparison with mitochondrial DNA variation. *Condor* 94:988-991.
- Flockhart, D. T. T. and K. L. Wiebe. 2007. The role of weather and migration in assortative pairing within the northern flicker (*Colaptes auratus*) hybrid zone. *Evol. Ecol. Res.* 9:887-903.
- Flockhart, D. T. T. and K. L. Wiebe. 2009. Absence of reproductive consequences of

- hybridization in the northern flicker (*Colaptes auratus*) hybrid zone. *Auk* 126:351-358.
- Grudzien, T. A. and W. S. Moore. 1986. Genetic differentiation between the yellow-shafted and red-shafted subspecies of the northern flicker. *Biochem. Syst. Ecol.* 14:451-453.
- Grudzien, T. A., W. S. Moore, J. R. Cook, and D. Tagle. 1987. Genic population structure and gene flow in the northern flicker (*Colaptes auratus*) hybrid zone. *Auk* 104:654-664.
- Harrison, R. G. 1990. Hybrid zones: windows on evolutionary process. *Oxford Surveys in Evolutionary Biology* 7:69-128.
- Hooper, D. M., S. C. Griffith, and T. D. Price. 2019. Sex chromosome inversions enforce reproductive isolation across an avian hybrid zone. *Mol. Ecol.* 28:1246-1262.
- Hubbard, J. K., J. A. Uy, M. E. Hauber, H. E. Hoekstra, and R. J. Safran. 2010. Vertebrate pigmentation: from underlying genes to adaptive function. *Trends Genet.* 26:231-239.
- Jacobsen, F. and K. E. Omland. 2012. Extensive introgressive hybridization within the northern oriole group (Genus *Icterus*) revealed by three-species isolation with migration analysis. *Ecol Evol* 2:2413-2429.
- Kirschel, A. N. G., E. C. Nwankwo, D. Pierce, S. M. Lukhele, M. Moysi, B. O. Ogolowa, S. C. Hayes, A. Monadjem, and A. Brelsford. 2020. *CYP2J19* mediates carotenoid colour introgression across a natural avian hybrid zone. *Mol. Ecol.* 29:4970-4984.
- Knief, U., C. M. Bossu, N. Saino, B. Hansson, J. Poelstra, N. Vijay, M. Weissensteiner, and J. B. W. Wolf. 2019. Epistatic mutations under divergent selection govern phenotypic variation in the crow hybrid zone. *Nat. Ecol. Evol.* 3:570-576.
- Kroodsma, R. L. 1975. Hybridization in buntings (*Passerina*) in North Dakota and eastern Montana. *Auk* 92:66-80.
- Larson, E. L., J. A. Andres, S. M. Bogdanowicz, and R. G. Harrison. 2013. Differential introgression in a mosaic hybrid zone reveals candidate barrier genes. *Evolution* 67:3653-3661.

- Larson, E. L., R. M. Tinghitella, and S. A. Taylor. 2019. Insect hybridization and climate change. *Front. Ecol. Evol.* 7:348.
- Mettler, R. D. and G. M. Spellman. 2009. A hybrid zone revisited: molecular and morphological analysis of the maintenance, movement, and evolution of a Great Plains avian (Cardinalidae: *Pheucticus*) hybrid zone. *Mol. Ecol.* 18:3256-3267.
- Moore, W. S. 1987. Random mating in the northern flicker hybrid zone: implications for the evolution of bright and contrasting plumage patterns in birds. *Evolution* 41:539-546.
- Moore, W. S. and D. B. Buchanan. 1985. Stability of the northern flicker hybrid zone in historical times: implications for adaptive speciation theory. *Evolution* 39:135-151.
- Moore, W. S., J. H. Graham, and J. T. Price. 1991. Mitochondrial DNA variation in the northern flicker (*Colaptes auratus*, Aves). *Mol. Biol. Evol.* 8:327-344.
- Moore, W. S. and W. D. Koenig. 1986. Comparative reproductive success of yellow-shafted, red-shafted, and hybrid flickers across a hybrid zone. *Auk* 103:42-51.
- Moore, W. S. and J. T. Price. 1993. The nature of selection in the northern flicker hybrid zone and its implications for speciation theory. Pp. 196-225 in R. G. Harrison, ed. *Hybrid Zones and the Evolutionary Process*. Oxford University Press, Oxford, UK.
- Poelstra, J. W., N. Vijay, M. P. Hoepfner, and J. B. Wolf. 2015. Transcriptomics of colour patterning and coloration shifts in crows. *Mol. Ecol.* 24:4617-4628.
- Powell, D. L., C. Payne, S. M. Banerjee, M. Keegan, E. Bashkirova, R. Cui, P. Andolfatto, G. G. Rosenthal, and M. Schumer. 2021. The genetic architecture of variation in the sexually selected sword ornament and its evolution in hybrid populations. *Curr. Biol.*
- Rising, J. D. 1969. A comparison of metabolism and evaporative water loss of Baltimore and Bullock Orioles. *Comp. Biochem. Physiol.* 31:915-925.
- Rising, J. D. 1970. Morphological variation and evolution in some North American orioles. *Syst. Zool.* 19:315-351.

- Rising, J. D. 1983. The Great Plains Hybrid Zones. Pp. 131-157 in R. F. Johnston, ed. Current Ornithology. Plenum Press, New York.
- Rising, J. D. 1996. The stability of the oriole hybrid zone in western Kansas. Condor 98:658-663.
- Rohwer, S. and J. Manning. 1990. Differences in timing and number of molts for Baltimore and Bullock's orioles: implications to hybrid fitness and theories of delayed plumage maturation. Condor 92:125-140.
- Semenov, G., E. Linck, E. D. Enbody, R. B. Harris, D. R. Khaydarov, P. Alström, L. Andersson, and S. A. Taylor. 2021. Asymmetric introgression reveals the genetic architecture of a plumage trait. Nat. Commun. 12:1019.
- Short, L. L. 1965. Hybridization in the flickers (*Colaptes*) of North America. Bull. Am. Mus. Nat. Hist. N. Y. 129:307-428.
- Sibley, C. G. and L. L. Short. 1959. Hybridization in the buntings (*Passerina*) of the Great Plains. Auk 76:443-463.
- Sibley, C. G. and L. L. Short. 1964. Hybridization in the orioles of the Great Plains. Condor 66:130-150.
- Sibley, C. G. and D. A. West. 1959. Hybridization in the rufous-sided towhees of the Great Plains. Auk 76:326-338.
- Swenson, N. G. and D. J. Howard. 2004. Do suture zones exist? Evolution 58:2391-2397.
- Taylor, S. A., T. A. White, W. M. Hochachka, V. Ferretti, R. L. Curry, and I. Lovette. 2014. Climate-mediated movement of an avian hybrid zone. Curr. Biol. 24:671-676.
- Toews, D. P. L., N. R. Hofmeister, and S. A. Taylor. 2017. The evolution and genetics of carotenoid processing in animals. Trends Genet. 33:171-182.
- Toews, D. P. L., S. A. Taylor, R. Vallender, A. Brelsford, B. G. Butcher, P. W. Messer, and I. J. Lovette. 2016. Plumage genes and little else distinguish the genomes of hybridizing warblers. Curr. Biol. 26:2313-2318.

- Walsh, J., S. M. Billerman, V. G. Rohwer, B. G. Butcher, and I. J. Lovette. 2020. Genomic and plumage variation across the controversial Baltimore and Bullock's oriole hybrid zone. *Auk* 137.
- Walsh, J., A. I. Kovach, B. J. Olsen, W. G. Shriver, and I. J. Lovette. 2018. Bidirectional adaptive introgression between two ecologically divergent sparrow species. *Evolution* 72:2076-2089.
- Wang, S., S. Rohwer, D. R. de Zwaan, D. P. L. Toews, I. J. Lovette, J. Mackenzie, and D. E. Irwin. 2020. Selection on a small genomic region underpins differentiation in multiple color traits between two warbler species. *Evol. Lett.* 4:502-515.
- West, D. A. 1962. Hybridization in grosbeaks (*Pheucticus*) of the Great Plains. *Auk* 79:399-424.
- Wiebe, K. L. 2000. Assortative mating by color in a population of hybrid northern flickers. *Auk* 117:525-529.
- Wiebe, K. L. and G. R. Bortolotti. 2002. Variation in carotenoid-based color in northern flickers in a hybrid zone. *The Wilson Bulletin* 114:393-400.
- Wiebe, K. L. and W. S. Moore. 2020. Northern Flicker (*Colaptes auratus*), version 1.0 in P. G. Rodewald, ed. *Birds of the World*. Cornell Lab of Ornithology, Ithaca, New York, USA.
- Wiebe, K. L. and M. N. Vitousek. 2015. Melanin plumage ornaments in both sexes of northern flicker are associated with body condition and predict reproductive output independent of age. *Auk* 132:507-517.

## CHAPTER 1

### RAPID MOVEMENT OF AN AVIAN HYBRID ZONE

#### **Abstract**

Natural hybrid zones have provided important insights into many aspects of the evolutionary process. Hybrid zone movement has been of particular interest, as the geographic stability or instability can help to disentangle the underlying biological processes that maintain hybridization in nature. Here, we leverage replicated sampling of an identical transect across the hybrid zone of the yellow-shafted and red-shafted flicker over a 60-year period (1955-1957 to 2016-2018) to understand hybrid zone dynamics and assess movement. Flickers differ in six distinct phenotypic traits that we characterize using two separate phenotyping approaches: categorical scoring and multi-spectral photography. Estimates of the center of the hybrid zone using geographic cline analyses suggest the hybrid zone has shifted ~90 km westward and towards the range of the red-shafted flicker since the mid-1950s. Comparisons between phenotyping approaches were broadly similar, suggesting categorical scoring of phenotypes adequately summarizes the variation present in flickers. By comparing to previous work in the same region of the hybrid zone, it appears likely that movement of the hybrid zone occurred rapidly in the years since 1982, prior to which the hybrid zone had been stable over the previous century. Thus, it is possible that the movement observed across our two sampling periods is the result of rapid changes in climate in recent decades.

## Introduction

Hybridization and individuals of hybrid origin have provided unique insights into the process of speciation (Barton and Hewitt 1985; Harrison 1993; Harrison and Larson 2014). Hybrid zones, geographical regions where differentiated taxa interbreed and produce hybrids, have long-been described as “windows on evolutionary process” as they provide opportunities to assess the outcome of natural hybridization and recombination over many generations (Harrison 1990). This has led to discoveries about adaptive introgression (e.g., Scriber 2011; Walsh et al. 2018), the genetic architecture of important traits (e.g., Delmore et al. 2016; Powell et al. 2020), and barriers to gene flow (e.g., Larson et al. 2013; Hooper et al. 2019).

Additionally, the geographic locations of hybrid zones can also provide important insights, and hybrid zone movement on the landscape has been of particular interest. Although the potential for hybrid zones to move has been known for a long time (Barton and Hewitt 1985), it was not until much more recently that the empirical evidence for hybrid zone movement became unequivocal (Buggs 2007). The increase in molecular sampling techniques has been especially helpful in elucidating this pattern further, as it is now possible to identify signatures of historical hybrid zone movement in the genome itself (e.g., Wielstra et al. 2017; van Riemsdijk et al. 2019; Wielstra 2019). Hybrid zones may move for a number of reasons, including differences in population density of the hybridizing taxa (Barton 1979), asymmetric hybridization (Konishi and Takata 2004), or changes in the environment (Taylor et al. 2015). The potential for hybrid zone movement caused by rapid changes in climate has recently been receiving increased attention (Taylor et al. 2014; Billerman et al. 2016; Ryan et al. 2018; Wang et al. 2019; Wielstra 2019), and in fact, hybrid zones may prove to be important “windows on climate change” (Taylor et al. 2015).

Here, we assess movement in the long-studied hybrid zone between the yellow-shafted (*Colaptes auratus auratus*) and red-shafted (*C. a. cafer*<sup>2</sup>) flickers (e.g., Short 1965; Moore and Buchanan 1985; Moore and Koenig 1986; Wiebe 2000; Flockhart and Wiebe 2009). Flickers are common woodpeckers widely distributed across wooded areas of North America—red-shafted flickers in the west and yellow-shafted flickers in the east (Wiebe and Moore 2020). These two forms come into secondary contact in an extensive hybrid zone in the Great Plains that roughly follows the Rocky Mountains from northern Texas to southern Alaska (Figure 1.1). This hybrid zone has intrigued naturalists since at least the mid-1800s (Audubon et al. 1897), as hybridization is clearly visible due to differences across six distinct phenotypic traits (Figure 1.1, Table 1.1; Short 1965). There is mixed evidence of assortative mating based on these phenotypes, with no evidence in the southern portion of the hybrid zone (Bock 1971; Moore 1987) and weak but significant evidence in the northern portion of the hybrid zone (Wiebe 2000; Flockhart and Wiebe 2007; Wiebe and Vitousek 2015). Despite this mixed evidence, no fitness consequences of hybridization have been identified in any part of the hybrid zone (Moore and Koenig 1986; Wiebe and Bortolotti 2002; Flockhart and Wiebe 2009). Our previous work has demonstrated the extremely low levels of genomic divergence between red-shafted and yellow-shafted flickers (Aguillon et al. 2018), with the few differentiated regions of the genome being associated with phenotypic differences (Aguillon et al. 2021). Thus, patterns in the phenotypic traits of the flicker hybrid zone additionally are a good indicator of genomic patterns at the few

---

<sup>2</sup> The subspecific epithet of the red-shafted flicker is based on a term that is an extreme racial slur against Black Africans, particularly in South Africa. We include the official scientific name here, but purposefully refer to the flickers only by their common names in the remainder of the manuscript. We have elsewhere proposed the name be officially changed to *Colaptes auratus lathamii* (Aguillon and Lovette 2019), but this name is not yet officially accepted.

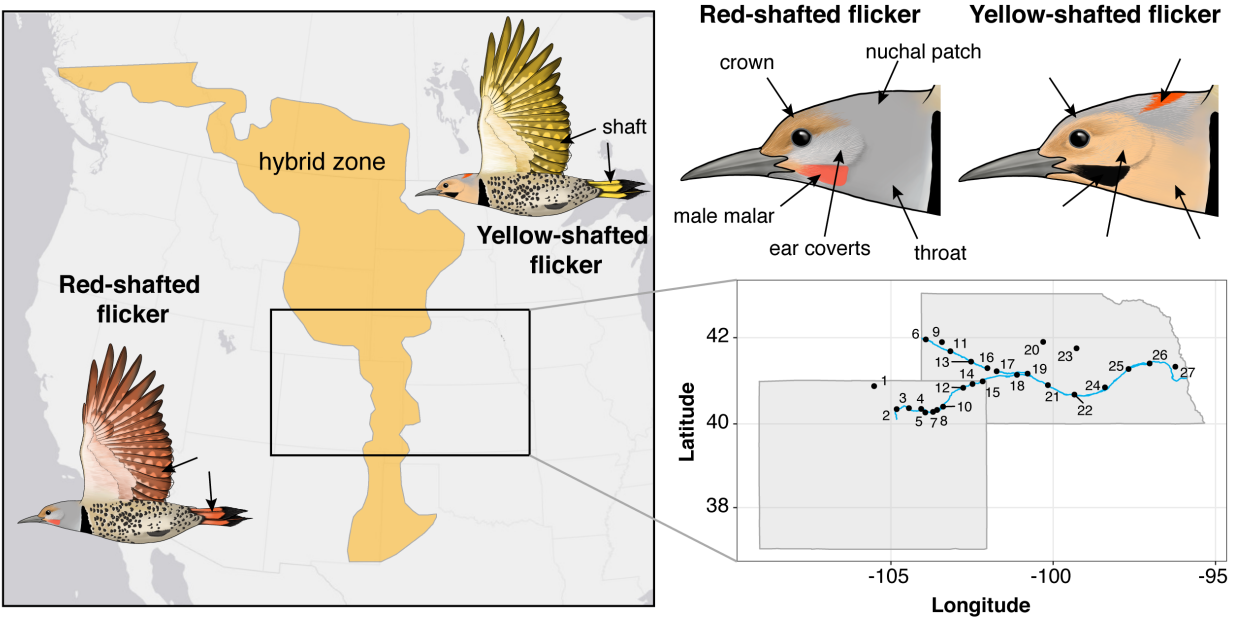


**Figure 1.1.** Geographic extent of the hybrid zone between red-shafted and yellow-shafted flickers as estimated in Moore and Price (1993), focused on the extent in the southern portion of the hybrid zone. The inset map of Colorado and Nebraska depicts the sampling transect along the Platte River with sampling localities used in the geographic cline analyses indicated with numbers (as in Table A3). The six primary phenotypic differences are shown with arrows on the flicker illustrations (provided by M. Bishop) and specific coloration differences are described in Table 1.1.

**Table 1.1.** Primary phenotypic trait differences between the flickers. See Figure 1.1 for illustrations of these differences.

<b>Trait</b>	<b>Yellow-shafted flicker</b>	<b>Red-shafted flicker</b>
Crown color	Gray	Brown
Ear covert color	Tan	Gray
Male malar stripe color	Black	Red
Nuchal patch	Present, broad	Absent
Shaft color	Bright yellow	Salmon red
Throat color	Tan	Gray

differentiated regions of the genome that do exist.

We assess movement of the flicker hybrid zone by comparing two sampling periods of an identical transect separated by approximately 60 years (Figure 1.1 inset). We compare two separate approaches to quantify flicker plumage differences: categorical scoring and multi-spectral photography. Using geographic cline analyses, we estimate the center and width of the phenotypic clines in the historic and contemporary sampling periods of the hybrid zone (separately for the six phenotypic traits and using an overall score). Finally, we compare the cline centers and widths between the two sampling periods to assess changes in location and shape of the hybrid zone.

## **Methods**

### *Study system and sampling*

Yellow-shafted and red-shafted flickers are common woodpeckers that are widely distributed across North America, and come into secondary contact in a broad hybrid zone in the Great Plains (Figure 1.1). The flickers differ across six primary plumage characteristics (Figure 1.1): wing and tail (the eponymous “shaft”) color, crown color, ear covert color, throat color, male malar stripe color, and the presence/absence of the nuchal patch on the nape of the neck (Short 1965). Table 1.1 includes details on the differences between the two parental forms. In brief, these birds differ vividly in the shaft color (bright yellow in the yellow-shafted flicker versus salmon red in the red-shafted flicker) and in the overall coloring of the face and head. Although there is some geographic variation in the intensity of the coloration within each taxon (Wiebe and Moore 2020), the differences between the two taxa are far greater than any within taxa

variation that exists. Hybrids can exhibit various combinations of the six parental traits, as well as traits intermediate to the parental traits.

The most extensive study of phenotypic variation and hybridization was undertaken by Lester L. Short, in which he collected specimens intensively along the Platte River in Nebraska and Colorado from 1955-1957 (inset in Figure 1.1; Short 1965). The flicker hybrid zone transect collected by Short remains one of the most special components of the ornithological collection in the Cornell University Museum of Vertebrates (CUMV). During the spring and summer of 2016-2018, the CUMV re-sampled flickers along the Platte River to amass a modern-day transect of the flicker hybrid zone (revisiting many of Short's original collection localities). This was additionally supplemented by mist-netting and banding individuals during 2016.

Henceforth, we will use "historic" and "contemporary" to refer to flickers sampled from 1955-1957 and 2016-2018, respectively. We focus here on adults to avoid confounding patterns due to immature plumage in juveniles. We include 252 flickers from the historic transect (all vouchered in the CUMV) and 107 flickers from the contemporary transect (91 specimens vouchered in the CUMV and 16 individuals that were banded, photographed, and released). We group the sexes together across all analyses except for those on the malar stripe (the only sexually dimorphic character in flickers), where we include only males (138 from the historic transect and 72 from the contemporary transect). Table A1 includes details on the individuals included in this study.

### *Phenotypic scoring*

*Qualitative scoring.* We scored plumage characters of historic and contemporary flickers sampled in the hybrid zone on a categorical scale from 0 (pure yellow-shafted) to 4

(pure red-shafted) for each of the six phenotypic traits following a protocol slightly modified from (Short 1965). See Table A2 for details on the trait descriptions used for scoring. This method has been used extensively within the flicker system (e.g., Moore and Buchanan 1985; Moore 1987; Wiebe 2000; Flockhart and Wiebe 2007; Aguilon et al. 2021), so is comparable to previous work. The main modification from Short (1965) was differences in scoring of the shaft color based on an increased understanding of carotenoid pigmentation, particularly around orange feather coloration (e.g., Hudon et al. 2017). We additionally calculated an overall phenotypic hybrid index by summing across the trait scores and standardizing to range from 0 to 1. This standardization additionally makes comparisons between males and females possible because females lack the red/black malar stripe present in males. All scoring was conducted by SMA to ensure consistency.

*Multispectral photography and quantitative scoring.* We additionally collected images of all of the contemporary CUMV flicker specimens, plus a handful of examples of allopatric individuals from both taxa (4 yellow-shafted and 8 red-shafted; Table A1), to obtain a more quantitative assessment of phenotypic traits following Ligon et al. (2018). We took RAW format images under standardized conditions using a Canon 7D camera (Tokyo, Japan) with full-spectrum quartz conversion and fitted with a Novoflex Noflexar 35 mm lens. Specimens were illuminated by two eyeColor arc lamps (Iwasaki, Tokyo, Japan) that simulate CIE-recommended daylight (D65) and were diffused through 0.5 mm polytetrafluoroethylene sheets. The lamps include a UV-blocking coating, which was removed prior to image collection. To capture the important aspects of flicker plumage, each specimen was photographed from three viewing angles: ventral (flat on its back), dorsal (flat on its belly), and lateral (on its left side). Additionally, for each viewing

angle, we used filters (Baader, Mammendorf, Germany) to take two photographs: one capturing visible light between 400-700 nm and one capturing only UV light between 300-400 nm. All specimens were photographed against a blank white background and included size and color standards. For visible light photographs, we used a shutter speed of 1/6" and ISO of 400, and for UV photographs those parameters were increased to 4" and 3200, respectively.

Visible and UV photographs were used to create standardized multispectral image files for each specimen and viewing angle using the Multispectral Image Calibration and Analysis Toolbox (micaToolbox; Troscianko and Stevens 2015) in ImageJ (Schneider et al. 2012). Standardized multispectral images combine, equalize, and linearize the different color channels from the two photographs (Stevens et al. 2007). We identified regions of interest (ROI) within each flicker as follows: throat and shaft with the ventral viewing angle; crown and nuchal patch with the dorsal viewing angle; and ear coverts and malar stripe with the lateral viewing angle. We then used the micaToolbox to estimate the color sensitivity of our camera/lens combination and generate a custom mapping function to convert colors in the image to stimulation values corresponding to an avian visual space (the Eurasian blue tit, *Cyanistes caeruleus*). We used the Batch Multispectral Image Analysis option in the micaToolbox to output values for each color channel (red, green, blue, UV) and luminance within each ROI, as well as the overall area of the ROI (important only for the nuchal patch).

### *Cline analyses*

To evaluate the distribution of phenotypic traits across the hybrid zone, we fit a series of geographic cline models using the Metropolis-Hastings Markov chain Monte Carlo algorithm employed in the HZAR package (Derryberry et al. 2014) in R v.3.6.2 (R Core

Team 2018). HZAR can only estimate one-dimensional clines and requires samples to be grouped into separate localities with an estimated distance for each locality from the start of the cline (Figure 1.1, Table A3). We grouped samples based on sampling location, set the start of the cline to the western-most locality sampled in the Rocky Mountains, and determined the mean latitude across all localities. We then used the 'distm' function within the geosphere package (Hijmans 2019) in R to calculate the distance (in km) each locality was from the start of the cline along the mean latitude value, using the longitude of the locality and assuming an ellipsoid shape. Despite the spread in localities along the North and South forks of the Platte River, using the mean latitude to calculate distance seems to be a conservative approach. Even using the minimum or maximum latitude value in this method results in the farthest eastern locality being only 10 km different from the values used here.

For qualitative phenotype scores of historic and contemporary flicker specimens, we fit three separate models in HZAR for each phenotypic trait that varied in the number of cline shape parameters estimated: (1) fixed starting/ending trait values and no exponential tails; (2) free starting/ending trait values and no exponential tails; and (3) free starting/ending trait values and exponential tails estimated on both ends of the cline. Within each trait, the three models were then compared using AICc scores to select the top model. Due to the non-normal distribution for the majority of the quantitative phenotype scores we used HZAR's cline models for frequency data typically used for allele frequencies (implemented with 'hzar.doMolecularData1DPops') by dividing each score by 4 to transform to range from 0-1. Comparisons of the standardized hybrid index between the different modelling methods in HZAR resulted in nearly identical results, so this seems like a reasonable approach.

For quantitative phenotype scores from the photographs of contemporary

flickers, we first compared the color channel and luminance values (for the shaft, throat, crown, ear coverts, and malar stripe) and area (for the nuchal patch) to the distance along the hybrid zone transect using simple linear regressions ('lm' in the stats package) in R (Figure A1). We then isolated image parameters with slopes significantly different from 0 (either positive or negative) for geographic cline analyses in HZAR. We fit five separate models for each value using the 'hzar.doNormalData1DRaw' function, the three described above for qualitative scores, in addition to: (4) free starting/ending trait values and an exponential tail estimated on the left side of the cline only; and (5) free starting/ending trait values and an exponential tail estimated on the right side of the cline only. Within each trait, the five models were then compared using AICc scores to select the top model. Allopatric individuals were included in this analysis by placing them 100 km past the cline on either side. Despite focusing only on image parameters with significantly non-zero slopes, in some cases the modelling did not resolve clear geographic clines (typically when slopes were only very slightly non-zero). Thus, to provide useful comparisons to the clines produced from the qualitative phenotypic scoring, we retain here just those clines that were clearly resolved (asterisks in Figure A1). Additionally, some image parameters resulted in two models with similar AIC scores. We focus here just on the best model if both clines were well resolved or on the well-resolved cline (if one was not).

For all traits and scoring methods, we focus on the means and estimated log likelihood intervals of the cline center and width (which are estimated from all models regardless of model type). We use the cline centers to assess whether clines are coincident geographically (i.e., occur in the same place), and the cline widths to assess whether clines are concordant (i.e., have the same shape).

## Results

### *Geographic clines from qualitative scoring*

For the historic transect, the best-fitting cline models for all individual traits (other than ear coverts) and the overall hybrid index was model #2 and included free starting/ending values and no exponential tails (Figure 1.2A, Table A4). The ear coverts, however, were best explained by model #1 that included fixed starting/ending values. The clines for the six phenotypic traits are broadly overlapping with similar estimated cline centers, though the cline for the ear coverts is slightly displaced from the others towards the west (Figure 1.2A, 1.3B; Table A4). Across the six phenotypic traits, the average cline center was 223 (166-274) km east of the transect start, which is situated near locality 12 (Crook, Colorado; Figure 1.1, Table A3). The cline widths for four of the phenotypic traits were similar, but the clines for the ear coverts and throat were wider (though the confidence intervals overlap; Figure A2, Table A4). The average cline width across the six phenotypic traits was 148 (35-311) km (Figure A2). The cline for the overall hybrid index has parameters similar to averaging over the six phenotypic traits (center = 229 (162-276) km; width = 129 (3-334) km), and nicely coincides with the clines for individual traits (Figure 1.2A).

For the contemporary transect, the best-fitting cline model for all individual traits and the overall hybrid index was model #1, which included fixed starting/ending values and no exponential tails (Figure 1.2B, Table A4). The clines for the six phenotypic traits were broadly overlapping with similar estimated cline centers, though the clines for the male malar and throat were slightly displaced towards the east (Figure 1.2B, 1.3B; Table A4). Across the six phenotypic traits, the average cline center was 143 (91-180) km east of the transect start, situated in the region between localities 6 (Morrill, Nebraska) and 7 (E Fort Morgan, Colorado; Figure 1.1, Table A3). The cline widths were

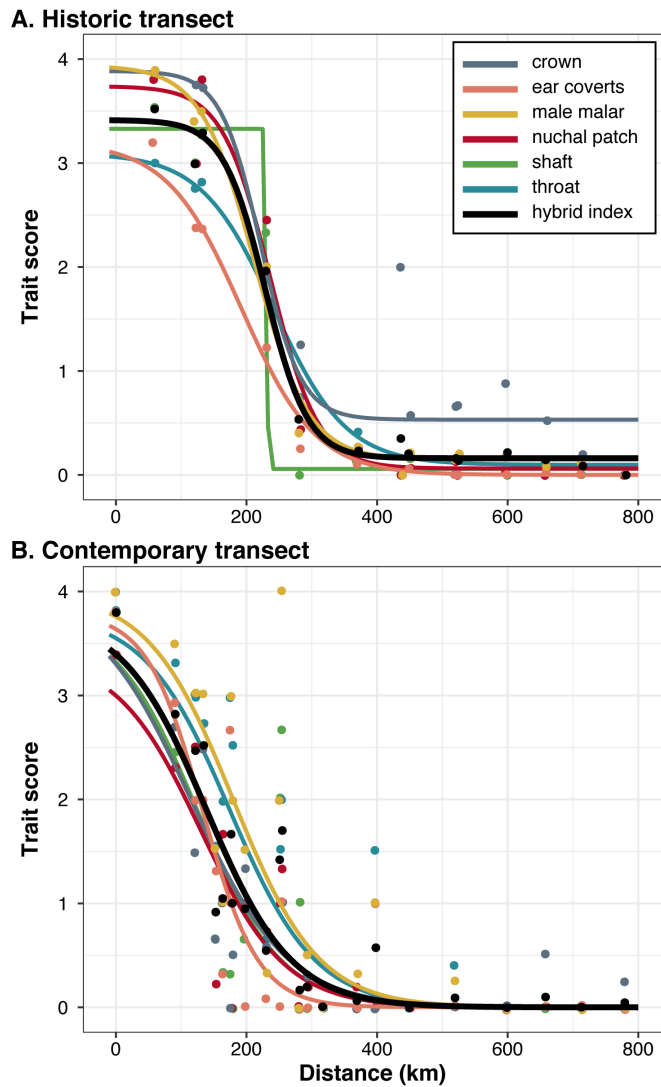


**Figure 1.2.** Geographic clines for the qualitative scoring of six phenotypic traits and overall hybrid index as estimated for the (A) historic and (B) contemporary transects. Separate traits are indicated by different colors and the overall hybrid index is shown as a thick black line. Points indicate the average trait score at each sampling locality and are jittered for visualization purposes. Corresponding model outputs are available in Table A4.

additionally broadly similar across the six phenotypic traits, although the width of the ear covert cline was slightly smaller (Figure A2, Table A4). The average cline width across the six phenotypic traits was 251 (160-441) km (Figure A2). The cline for the overall hybrid index has parameters similar to averaging over the six phenotypic traits (center = 139 (87-175) km; width = 261 (168-451) km), and coincides with the clines for individual traits (Figure 1.2B).

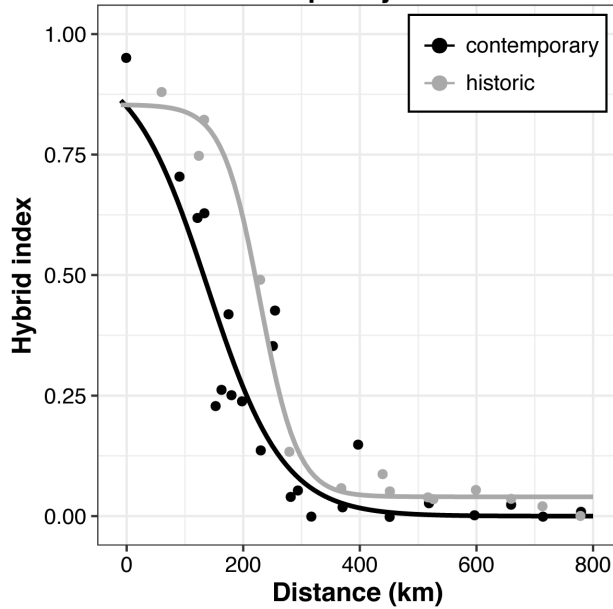
#### *Comparison of historic and contemporary geographic clines*

The historic and contemporary geographic clines for the hybrid index are offset from each other, with the contemporary cline center located 90 km west of the historic cline center (Figure 1.3A, Table A4). Despite this offset, the confidence intervals of the cline centers do overlap slightly (Figure 1.3B, Table A4; historic = 162-276 km, contemporary = 87-175 km). The pattern of the contemporary cline being displaced from the historic cline in the western direction is repeated across each of the six phenotypic traits (Figure 1.3B, Table A4; minimum displacement is 33 km in the male malar and maximum displacement is 107 km in the crown and shaft), with the confidence intervals not overlapping between historic and contemporary cline centers for the crown, nuchal patch, and shaft. The widths of the geographic clines tended to be larger in the contemporary transect than in the historic transect across the analyses, but the confidence intervals were broadly overlapping and the reverse pattern was true in the ear coverts (Figure A2).

#### *Geographic clines from quantitative scoring*

Geographic cline analysis using quantitative scoring from multispectral photography resulted in well-resolved clines from 11 image parameters across the six phenotypic

### A. Historic vs. contemporary transects



### B. Comparison of cline centers

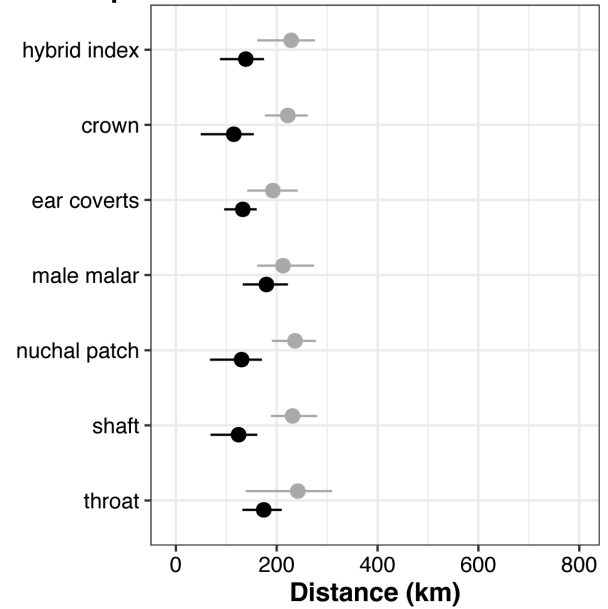


**Figure 1.3.** (A) Geographic clines from the qualitative scoring of overall hybrid index as estimated for the historic (gray) and contemporary (black) transects demonstrate the ~90 km westward displacement of the contemporary cline. (B) Estimated cline centers with confidence intervals for the geographic clines estimated from qualitative scoring of the overall hybrid index and six phenotypic traits.

traits (Figure 1.3, Table A5): area in nuchal patch; luminance in throat; long wave (red channel) in ear coverts, male malar, shaft, and throat; medium wave (green channel) in male malar and shaft; short wave (blue channel) in crown and male malar; and UV wave in crown. The best-fitting cline models were a combination of model #1 (fixed starting/ending values and no exponential tails; 3 models), model #2 (free starting/ending values and no exponential tails; 5 models), and model #5 (free starting/ending values and an exponential tail estimated on the right side of the cline; 3 models). The estimated cline centers varied across the different phenotypic traits and image parameters from a low of 44 (1-90) km east of the transect start for the short wave parameter in the crown to a high of 205 (189-212) km east of the transect start for the short wave parameter in the malar stripe (Figure 1.5; Table A5). Overall, the average cline center across the quantitative trait analyses was 134 (80-178) km east of the transect start, which is situated near locality 6 (Morrill, Nebraska; Figure 1.1, Table A3). The clines additionally varied in width across the different phenotypic traits and image parameters from a low of 2 (0-14) km for the long wave parameter in the shaft to a high of 358 (293-447) km for the long wave parameter in the male malar stripe (Figure A3, Table A5). The average cline width across the quantitative trait analyses was 101 (57-187) km.

#### *Comparison of geographic clines from qualitative and quantitative scoring*

The cline centers were broadly similar between the qualitative and quantitative scoring methods across the six phenotypic traits with confidence intervals that were largely overlapping (Figure 1.4; Table A4, A5). Averaging across the individual traits within each scoring method resulted in remarkably similar cline centers (qualitative scoring: 143 (91-180) km east of the transect start; quantitative scoring: 134 (80-178) km east of

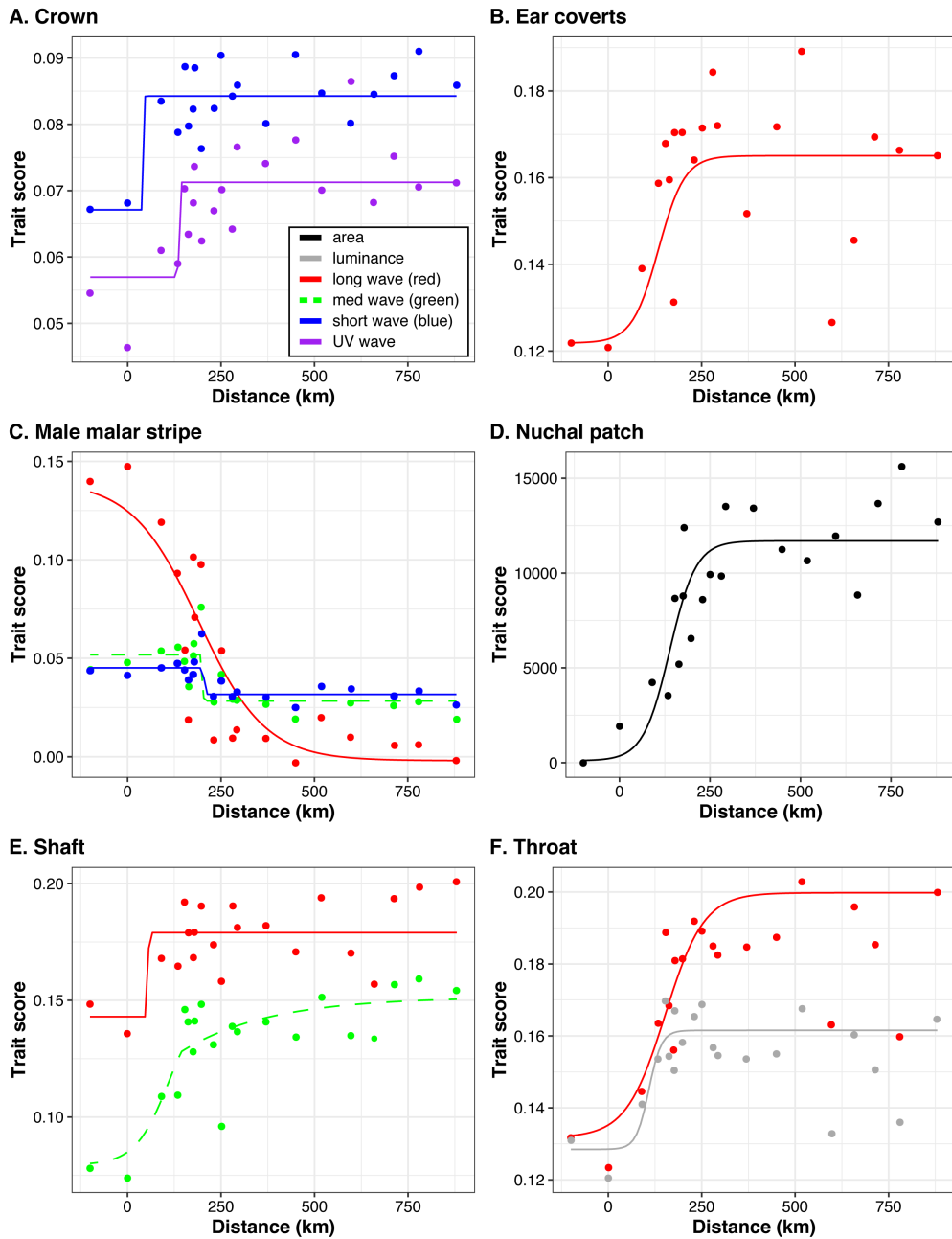


**Figure 1.4.** Geographic clines from the quantitative scoring of six image parameters across the six phenotypic traits. Image parameters are indicated by different colors (legend in A), with the medium wave channel (green) shown with a dashed line for ease of differentiation. Points indicate the average trait score at each sampling locality. Corresponding model outputs are available in Table A5.

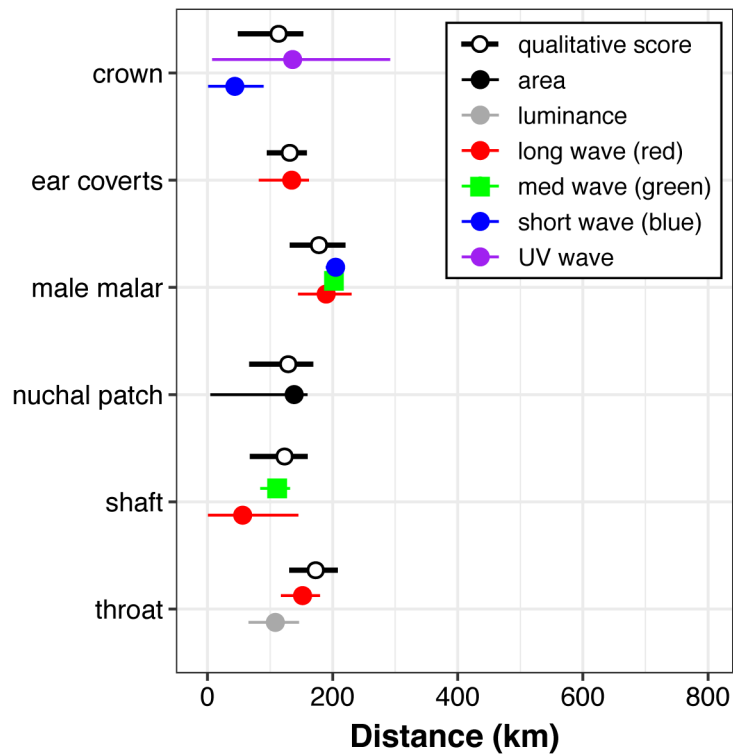


**Figure 1.5.** Estimated cline centers with confidence intervals from the qualitative (open circles) and quantitative (closed, colored circles) scoring of six phenotypic traits in the contemporary transect. The medium wave channel (green) is shown with a square symbol for ease of differentiation.

the transect start). As described above, this places the cline center between or near locality 6 (Morrill, Nebraska) and 7 (E Fort Morgan, Colorado). The estimated cline widths did vary between the qualitative and quantitative scoring methods (Figure A2, A3; Table A4, A5), particularly because a number of the clines from the quantitative scoring had sharp transitions with narrow widths along the transect (e.g., crown, the long wave parameter in the shaft).

## **Discussion**

Hybrid zones have long been viewed as windows into the evolutionary process (e.g., Harrison 1993; Harrison and Larson 2014, 2016): providing insight into the early stages of speciation, barriers to gene exchange, and the genetic basis of important traits. The northern flicker hybrid zone in the Great Plains of North America was an important study system in the early development of ideas about hybrid zone dynamics in nature (Moore and Buchanan 1985; Moore and Price 1993). In this study, we assessed phenotypic patterns across the flicker hybrid zone by comparing historic (1955-1957) and contemporary (2015-2018) sampling periods of an identical transect to understand hybrid zone dynamics across time and space.

In both the historic and contemporary transects, we find that geographic clines for all six phenotypic traits of interest and the overall hybrid index largely co-localize in space (Figure 1.2). Geographic cline analyses estimated the cline center for the historic transect to be situated near Crook, Colorado (sampling location 12; Figure 1.1), which recapitulates the conclusions in Short (1965) using the same specimens. For the contemporary transect, the cline center has shifted approximately 90 km westward (Figure 1.2) and is situated between Morrill, Nebraska (locality 6) and E. Fort Morgan,

Colorado (locality 7). This westward shift in the hybrid zone in the contemporary flickers is repeated across all six phenotypic traits and the overall hybrid index (Figure 1.2B), although the confidence intervals are completely non-overlapping in only three analyses (crown, nuchal patch, and shaft). This apparent movement in the flicker hybrid zone differs greatly from previous work done in this region of the hybrid zone that instead found stability when comparing samples from 1889-1968 and 1981-1982 (Moore and Buchanan 1985), though movement has been suspected previously in the northern portion of the hybrid zone (McGillivray and Biermann 1987). Although the range of years in the early sampling point in Moore and Buchanan (1985) is quite large (79 years), 69% of their samples are from the 1950s and later (see their Table 1.1), which broadly overlaps with our historical transect sampling. Yet they did not find evidence for hybrid zone movement between their two sampling points. Thus, the finding in our study that the flicker hybrid zone has shifted westward is surprising, and suggests that the movement has occurred in the last ~35 years (i.e., after the study by Moore and Buchanan 1985). This further suggests that the rate of movement of the hybrid zone has been quite rapid: ~2.5 km/year.

The region of hybridization between the flickers is located in the Great Plains suture zone (Swenson and Howard 2004), where environmental factors are known to hold avian hybrid zones geographically in place (Swenson 2006). As there are well-documented cases of avian hybrid zone movement due to climate change over shorter time periods than we find here (e.g., Taylor et al. 2014), and climate change is known to influence hybrid zones more generally (reviewed in Taylor et al. 2015; Larson et al. 2019), it is possible that the movement in the flicker hybrid zone is related to rapid changes in climate in recent decades. Indeed, similar climate-mediated movement has been found in the *Sphyrapicus* woodpecker hybrid zone as a result of climate-related

range shifts in the hybridizing species (Billerman et al. 2016). Moreover, a similar ~100 km westward shift was documented in the Great Plains hybrid zone between the lazuli and indigo buntings (*Passerina amoena* and *P. cyanea*) over the period from 1955-1969 to 2004-2007 (Carling and Zuckerberg 2011). The westward movement of both the flicker and bunting hybrid zones over a similar time period underscores the likely role of exogenous factors in controlling the movement of these hybrid zones.

Unfortunately, the potential for hybrid zone movement due to ecological factors makes it difficult to compare alternative hypotheses regarding the underlying maintenance of the flicker hybrid zone. Movement of a hybrid zone may occur under both a tension zone model (Key 1968) and an environmental selection gradient model (May et al. 1975) given ecological change (Buggs 2007; Wielstra 2019). In the tension zone model, selection is endogenous and a balance between selection against hybrids and parental dispersal into the hybrid zone influences the location of the hybrid zone (Barton and Hewitt 1985; Barton and Hewitt 1989). Under this model, hybrid zones typically stabilize in density troughs (Barton and Hewitt 1985) and an ecological change that influences population density on the landscape can cause movement of the hybrid zone. However, a similar change of hybrid zone location would occur under an environmental selection gradient model where the selection maintaining the hybrid zone is exogeneous. For instance, if there is ecological change that expands or moves the geographic area where hybrids have higher fitness than parentals (e.g., under a hybrid superiority model; Moore 1977; Moore and Price 1993), there can be hybrid zone movement to track this change. The movement of the flicker hybrid zone rapidly over recent decades suggests it is likely tied to changes in climate and thus, makes it difficult to disentangle these two hypotheses of hybrid zone maintenance.

Geographic cline analyses using the qualitative (Figure 1.2B) and quantitative

(Figure 1.4) scoring approaches of the flicker phenotypes in the contemporary transect led to broadly similar results. In fact, the estimated cline centers and confidence intervals were overlapping for all six phenotypic traits between the two scoring methods (Figure 1.5). In some cases, the cline center from qualitative scoring was closer to one particular image parameter from the quantitative scoring (e.g., in crown, shaft, and throat; Figure 1.5), but it never differed completely from all image parameters. The one difference we did find between the qualitative and quantitative scoring methods was in the estimated cline widths (Figure A2, A3). In a number of cases, clines from the quantitative scoring method were much narrower than clines from the qualitative scoring (primarily image parameters with width estimates close to zero). However, when comparing widths of all of the image parameters for a given trait with the qualitative scoring for that trait, only the crown had completely non-overlapping confidence intervals between all image parameters and the qualitative scoring, suggesting the differences are not actually that substantial. Overall, the broad overlap between the geographic clines from the qualitative and quantitative scoring approaches suggests that the qualitative scoring (shown in Table A2) is a good representation of the variation present across the six phenotypic differences in flickers.

In this study, we assess the location of the hybrid zone between the red-shafted and yellow-shafted flicker across space and time using geographic cline analyses in identical transects. We find evidence that the hybrid zone has shifted ~90 km westwards (towards the range of the red-shafted flicker) over the past ~60 years, perhaps as a result of changing climate in the Great Plains. Moreover, by comparing to previous work in this portion of the hybrid zone (Moore and Buchanan 1985), it appears likely that this hybrid zone movement has occurred in the years since the early 1980s. Our comparisons across phenotypic traits and scoring methods suggest that qualitative

scoring of phenotypes in flickers provides a good approximation of the existing phenotypic variation. Moreover, our previous work showed that the genomic differences between red-shafted and yellow-shafted flickers are almost exclusively related to differences in phenotypic characteristics (Aguillon et al. 2021), so assessments of flicker phenotype additionally represent a good proxy for differences at the genomic level.

## References

- Aguillon, S. M., L. Campagna, R. G. Harrison, and I. J. Lovette. 2018. A flicker of hope: genomic data distinguish northern flicker taxa despite low levels of divergence. *Auk* 135:748-766.
- Aguillon, S. M. and I. J. Lovette. 2019. Change the specific/subspecific/morphological group name of the red-shafted flicker from *cafer* to *lathamii*. AOS North American Classification Committee 2019-A-10:66-71.
- Aguillon, S. M., J. Walsh, and I. J. Lovette. 2021. Extensive hybridization reveals multiple coloration genes underlying a complex plumage phenotype. *Proc. R. Soc. B* 288:20201805.
- Audubon, J. J., M. R. Audubon, and E. Coues. 1897. *Audubon and His Journals*. Scribner, New York.
- Barton, N. H. 1979. The dynamics of hybrid zones. *Heredity* 43:341-359.
- Barton, N. H. and G. M. Hewitt. 1985. Analysis of hybrid zones. *Annu. Rev. Ecol. Syst.* 16:113-148.
- Barton, N. H. and G. M. Hewitt. 1989. Adaptation, speciation and hybrid zones. *Nature* 341:497-503.
- Billerman, S. M., M. A. Murphy, and M. D. Carling. 2016. Changing climate mediates sapsucker (Aves: *Sphyrapicus*) hybrid zone movement. *Ecol. Evol.* 6:7976-7990.

- Bock, C. E. 1971. Pairing in hybrid flicker populations in eastern Colorado. *Auk* 88:921-924.
- Buggs, R. J. 2007. Empirical study of hybrid zone movement. *Heredity* 99:301-312.
- Carling, M. D. and B. Zuckerberg. 2011. Spatio-temporal changes in the genetic structure of the *Passerina* bunting hybrid zone. *Mol. Ecol.* 20:1166-1175.
- Delmore, K. E., D. P. Toews, R. R. Germain, G. L. Owens, and D. E. Irwin. 2016. The genetics of seasonal migration and plumage color. *Curr. Biol.* 26:2167-2173.
- Derryberry, E. P., G. E. Derryberry, J. M. Maley, and R. T. Brumfield. 2014. HZAR: hybrid zone analysis using an R software package. *Mol. Ecol. Resour.* 14:652-663.
- Flockhart, D. T. T. and K. L. Wiebe. 2007. The role of weather and migration in assortative pairing within the northern flicker (*Colaptes auratus*) hybrid zone. *Evol. Ecol. Res.* 9:887-903.
- Flockhart, D. T. T. and K. L. Wiebe. 2009. Absence of reproductive consequences of hybridization in the northern flicker (*Colaptes auratus*) hybrid zone. *Auk* 126:351-358.
- Harrison, R. G. 1990. Hybrid zones: windows on evolutionary process. *Oxford Surveys in Evolutionary Biology* 7:69-128.
- Harrison, R. G. 1993. *Hybrid Zones and the Evolutionary Process*. Oxford University Press, New York.
- Harrison, R. G. and E. L. Larson. 2014. Hybridization, introgression, and the nature of species boundaries. *J. Hered.* 105:795-809.
- Harrison, R. G. and E. L. Larson. 2016. Heterogenous genome divergence, differential introgression, and the origin and structure of hybrid zones. *Mol. Ecol.* 25:2454-2466.
- Hijmans, R. C. 2019. geosphere: spherical trigonometry. R package version 1.5-10.
- Hooper, D. M., S. C. Griffith, and T. D. Price. 2019. Sex chromosome inversions enforce reproductive isolation across an avian hybrid zone. *Mol. Ecol.* 28:1246-1262.

- Hudon, J., R. J. Driver, N. H. Rice, T. L. Lloyd-Evans, J. A. Craves, and D. P. Shustack. 2017. Diet explains red flight feathers in yellow-shafted flickers in eastern North America. *Auk* 134:22-33.
- Key, K. H. L. 1968. The concept of stasipatric speciation. *Syst. Zool.* 17:14-22.
- Konishi, M. and K. Takata. 2004. Impact of asymmetrical hybridization followed by sterile F1 hybrids on species replacement in *Pseudorasbora*. *Conserv. Genet.* 5:463-474.
- Larson, E. L., J. A. Andres, S. M. Bogdanowicz, and R. G. Harrison. 2013. Differential introgression in a mosaic hybrid zone reveals candidate barrier genes. *Evolution* 67:3653-3661.
- Larson, E. L., R. M. Tinghitella, and S. A. Taylor. 2019. Insect hybridization and climate change. *Front. Ecol. Evol.* 7:348.
- Ligon, R. A., C. D. Diaz, J. L. Morano, J. Troscianko, M. Stevens, A. Moskeland, T. G. Laman, and E. Scholes. 2018. Evolution of correlated complexity in the radically different courtship signals of birds-of-paradise. *PLoS Biol.* 16:e2006962.
- May, R. M., J. A. Endler, and R. E. McMurtrie. 1975. Gene frequency clines in the presence of selection opposed by gene flow. *Am. Nat.* 109:659-676.
- McGillivray, W. B. and G. C. Biermann. 1987. Expansion of the zone of hybridization of northern flickers in Alberta. *Wilson Bull.* 99:690-692.
- Moore, W. S. 1977. An evaluation of narrow hybrid zones in vertebrates. *Q. Rev. Biol.* 52:263-277.
- Moore, W. S. 1987. Random mating in the northern flicker hybrid zone: implications for the evolution of bright and contrasting plumage patterns in birds. *Evolution* 41:539-546.
- Moore, W. S. and D. B. Buchanan. 1985. Stability of the northern flicker hybrid zone in historical times: implications for adaptive speciation theory. *Evolution* 39:135-151.
- Moore, W. S. and W. D. Koenig. 1986. Comparative reproductive success of yellow-shafted, red-shafted, and hybrid flickers across a hybrid zone. *Auk* 103:42-51.

- Moore, W. S. and J. T. Price. 1993. The nature of selection in the northern flicker hybrid zone and its implications for speciation theory. Pp. 196-225 *in* R. G. Harrison, ed. Hybrid Zones and the Evolutionary Process. Oxford University Press, Oxford, UK.
- Powell, D. L., M. García-Olazábal, M. Keegan, P. Reilly, K. Du, A. P. Díaz-Loyo, S. Banerjee, D. Blakkan, D. Reich, P. Andolfatto, G. G. Rosenthal, M. Scharti, and M. Schumer. 2020. Natural hybridization reveals incompatible alleles that cause melanoma in swordtail fish. *Science* 368:731-736.
- R Core Team. 2018. R: A language and environment for statistical computing. R Foundation for Statistical Computing, Vienna, Austria.
- Ryan, S. F., J. M. Deines, J. M. Scriber, M. E. Pfrender, S. E. Jones, S. J. Emrich, and J. J. Hellmann. 2018. Climate-mediated hybrid zone movement revealed with genomics, museum collection, and simulation modeling. *Proc. Natl. Acad. Sci. USA* 115:E2284-E2291.
- Schneider, C. A., W. S. Rasband, and K. W. Eliceiri. 2012. NIH Image to ImageJ: 25 years of image analysis. *Nat. Methods* 9:671-675.
- Scriber, J. M. 2011. Impacts of climate warming on hybrid zone movement: geographically diffuse and biologically porous “species borders”. *Insect Sci.* 18:121-159.
- Short, L. L. 1965. Hybridization in the flickers (*Colaptes*) of North America. *Bull. Am. Mus. Nat. Hist. N. Y.* 129:307-428.
- Stevens, M., C. A. Párraga, I. C. Cuthill, J. C. Partridge, and T. S. Troscianko. 2007. Using digital photography to study animal coloration. *Biol. J. Linn. Soc.* 90:211-237.
- Swenson, N. G. 2006. Gis-based niche models reveal unifying climatic mechanisms that maintain the location of avian hybrid zones in a North American suture zone. *J. Evol. Biol.* 19:717-725.
- Swenson, N. G. and D. J. Howard. 2004. Do suture zones exist? *Evolution* 58:2391-2397.
- Taylor, S. A., E. L. Larson, and R. G. Harrison. 2015. Hybrid zones: windows on climate change. *Trends Ecol. Evol.* 30:398-406.

- Taylor, S. A., T. A. White, W. M. Hochachka, V. Ferretti, R. L. Curry, and I. Lovette. 2014. Climate-mediated movement of an avian hybrid zone. *Curr. Biol.* 24:671-676.
- Troscianko, J. and M. Stevens. 2015. Image calibration and analysis toolbox—a free software suite for objectively measuring reflectance, colour and pattern. *Methods Ecol Evol* 6:1320-1331.
- van Riemsdijk, I., R. K. Butlin, B. Wielstra, and J. W. Arntzen. 2019. Testing an hypothesis of hybrid zone movement for toads in France. *Mol. Ecol.* 28:1070-1083.
- Walsh, J., A. I. Kovach, B. J. Olsen, W. G. Shriver, and I. J. Lovette. 2018. Bidirectional adaptive introgression between two ecologically divergent sparrow species. *Evolution* 72:2076-2089.
- Wang, S., S. Rohwer, K. Delmore, and D. E. Irwin. 2019. Cross-decades stability of an avian hybrid zone. *J. Evol. Biol.* 32:1242-1251.
- Wiebe, K. L. 2000. Assortative mating by color in a population of hybrid northern flickers. *Auk* 117:525-529.
- Wiebe, K. L. and G. R. Bortolotti. 2002. Variation in carotenoid-based color in northern flickers in a hybrid zone. *The Wilson Bulletin* 114:393-400.
- Wiebe, K. L. and W. S. Moore. 2020. Northern Flicker (*Colaptes auratus*), version 1.0 in P. G. Rodewald, ed. *Birds of the World*. Cornell Lab of Ornithology, Ithaca, New York, USA.
- Wiebe, K. L. and M. N. Vitousek. 2015. Melanin plumage ornaments in both sexes of northern flicker are associated with body condition and predict reproductive output independent of age. *Auk* 132:507-517.
- Wielstra, B. 2019. Historical hybrid zone movement: more pervasive than appreciated. *J. Biogeogr.* 46:1300-1305.
- Wielstra, B., T. Burke, R. K. Butlin, A. Avcı, N. Üzüm, E. Bozkurt, K. Olgun, and J. W. Arntzen. 2017. A genomic footprint of hybrid zone movement in crested newts. *Evol. Lett.* 1:93-101.

## CHAPTER 2

### A FLICKER OF HOPE: GENOMIC DATA DISTINGUISH NORTHERN FLICKER TAXA DESPITE LOW LEVELS OF DIVERGENCE<sup>3</sup>

#### **Abstract**

Next-generation sequencing technologies are increasingly being employed to explore patterns of genomic variation in avian taxa previously characterized using morphology and/or traditional genetic markers. The hybridization dynamics of the Northern Flicker complex have received considerable attention, primarily due to the conspicuous plumage differences among these birds and the geographically extensive hybrid zone between the Red-shafted (*Colaptes auratus cafer*) and Yellow-shafted (*Colaptes auratus auratus*) flickers in the Great Plains region of North America. However, no traditional molecular techniques have been able to differentiate these two morphologically well-defined taxa from one another, or conclusively from the closely related Gilded Flicker (*Colaptes chrysoides*). Here, we use a next-generation sequencing approach to assess the genetic diversity and evolutionary history of these three taxa. We confirm the overall low levels of differentiation found using traditional molecular markers, but are able to distinguish between the three taxa for the first time, using a dataset of thousands of SNP loci distributed across the genome. Through demographic modeling and phylogenetic reconstructions, we find that Red-shafted and Yellow-shafted flickers are likely sister taxa, and that their divergence from the Gilded Flicker was comparatively older. The low level of divergence and lack of fixed differences in our dataset between

---

<sup>3</sup> Aguillon, SM, L Campagna, RG Harrison, IJ Lovette. 2018. A flicker of hope: Genomic data distinguish Northern Flicker taxa despite low levels of divergence. *The Auk: Ornithological Advances* 135(3): 748-766.

Red-shafted and Yellow-shafted flickers, in particular, suggests whole genome re-sequencing may be necessary to assess the dynamics of their hybridization and identify the genetic basis of their striking differences in plumage.

## **Introduction**

Most bird species and subspecies were initially recognized and described based on similarities or differences in morphological characters, often those related to plumage. With the advent of molecular techniques, many of these taxa have been revisited using genetic markers, and there have been many situations both in which new cryptic species have been discovered based on high levels of genetic differentiation (e.g., Weir et al. 2016; Garg et al. 2016) or in which morphologically distinct taxa show surprisingly low levels of genetic distinctiveness (e.g., Toews et al. 2016a; Campagna et al. 2017; Poelstra et al. 2014; Mason and Taylor 2015). Until fairly recently, these molecular data have largely been derived from a limited sample of the genome (i.e. ‘traditional’ molecular markers, such as mitochondrial genes, a small number of nuclear genes, or AFLP markers). Next-generation sequencing technologies provide the opportunity for substantially increased genomic-scale resolution through greater data abundance and increased coverage of the genome. It can therefore be profitable to use these genomic methods to revisit taxa previously studied with morphology and traditional molecular markers. In extreme situations where very little genomic divergence exists and traditional molecular markers were insufficient to distinguish morphologically diagnosable taxa, whole-genome sequencing may be the only way to identify the rare differentiated regions of the genome (e.g., Toews et al. 2016a; Campagna et al. 2017; Poelstra et al. 2014).

Hybrid zones and contact zones of many taxa (including birds, mammals, and trees) cluster in the Great Plains of North America (Rising 1983; Swenson and Howard 2005) and five of the avian hybrid zones have been intensely studied since the late 1950s (Sibley and Short 1964; Short 1965; Anderson and Daugherty 1974; Sibley and Short 1959; Sibley and West 1959). These five hybrid zones are the product of secondary contact between easterly and westerly distributed taxa, yet differ in location and geographic extent and include (with western taxa listed first in each pair): Lazuli (*Passerina amoena*) and Indigo buntings (*P. cyanea*); Red-shafted (*Colaptes auratus cafer*<sup>4</sup>) and Yellow-shafted flickers (*C. auratus auratus*); Black-headed (*Pheucticus melanocephalus*) and Rose-breasted grosbeaks (*P. ludovicianus*); Bullock's (*Icterus bullockii*) and Baltimore orioles (*I. galbula*); and Spotted (*Pipilo maculatus*) and Eastern towhees (*P. erythrophthalmus*). Research in these systems has shaped our general understanding of hybrid zones and the speciation process (Moore 1977; Rising 1996; Mettler and Spellman 2009; Moore and Price 1993), as well as criteria for defining species (Sibley and Short 1964, 1959).

The hybrid zone between the western Red-shafted Flicker and the eastern Yellow-shafted Flicker has received considerable attention (e.g. Short 1965; Moore and Buchanan 1985; Moore and Koenig 1986; Moore and Price 1993; Anderson 1971; Wiebe 2000; Wiebe and Bortolotti 2002). Red-shafted and Yellow-shafted flickers are common woodpeckers distributed across much of North America. They have an extensive hybrid zone spanning from northern Texas to southern Alaska, roughly following the rain

---

<sup>4</sup> The subspecific epithet of the red-shafted flicker is based on a term that is an extreme racial slur against Black Africans, particularly in South Africa. We include the official scientific name here, but purposefully refer to the flickers only by their common names in the remainder of the manuscript. We have elsewhere proposed the name be officially changed to *Colaptes auratus lathamii* (Aguillon and Lovette 2019), but this name is not yet officially accepted.

shadow of the Rocky Mountains in the western Great Plains (Figure 2.1; Wiebe and Moore 2017). Red-shafted and Yellow-shafted flickers are currently classified as subspecies within the Northern Flicker complex that also includes the Gilded Flicker (*Colaptes chrysoides*) species, along with geographically disjunct Northern Flicker subspecies from Central America (Guatemalan Flicker; *Colaptes auratus mexicanoides*) and the Caribbean (Cuban Flicker; *Colaptes auratus chrysocaulosus*). Gilded Flickers were once also considered a subspecies of the Northern Flicker (American Ornithologists' Union 1995); they have been elevated to full species status because hybridization between regionally sympatric Red-shafted and Gilded flickers occurs rarely, likely owing to differences in habitat use (Short 1965; Johnson 1969). Taxa in this complex vary primarily in six distinct plumage characters—nuchal patch presence, crown color, ear covert color, throat color, malar stripe color, and “shaft” color (i.e. wing and tail color)—and hybrids exhibit various combinations of parental traits and traits intermediate to the parental traits (Figure 2.1; Wiebe and Moore 2017). This conspicuous and apparently polygenic phenotypic variation makes the Northern Flicker particularly intriguing from a genomic perspective because, to date, genetic markers have not been found that differentiate these taxa (Grudzien and Moore 1986; Grudzien et al. 1987; Fletcher and Moore 1992; Moore et al. 1991).

Early investigations using allozymes (Grudzien and Moore 1986; Grudzien et al. 1987; Fletcher and Moore 1992) and mitochondrial DNA (Moore et al. 1991) found no diagnostic differentiation between Red-shafted, Yellow-shafted, and Gilded flickers. Modest geographic variation exists in mitochondrial haplotype frequencies across the continental US, but it is not related in any clear way to the three named taxa or the hybrid zone between Red-shafted and Yellow-shafted flickers (Moore et al. 1991). Instead, Moore et al. (1991) distinguished two major haplotype clusters—a north and

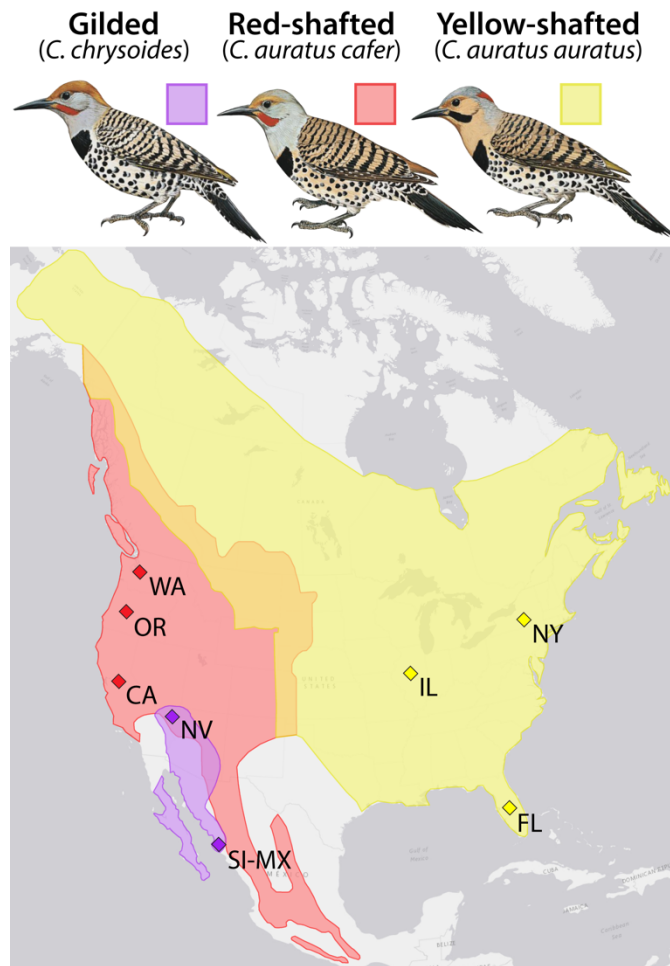


**Figure 2.1.** Phenotypic variation and distribution of the three focal taxa from the Northern Flicker complex: Gilded Flicker (purple), Red-shafted Flicker (red), and Yellow-shafted Flicker (yellow). The orange region of the map shows the approximate location of the hybrid zone between Red-shafted and Yellow-shafted flickers in the North American Great Plains. Diamonds represent sampling locations. See Table B1 for details on individuals sampled from each location. Distributions were redrawn from the Birds of North America in ArcGIS (ESRI, Redlands, CA) and bird illustrations are from the Handbook of the Birds of the World.

east cluster that crosses the hybrid zone and a southwest cluster—which they suggest could be due to historical isolation of the southwest populations or their adaptation to the arid conditions found in deserts of the US Southwest. Additionally, the mitochondrial haplotypes of Gilded Flickers were closely related to those found in Red-shafted Flickers in the southwest clade (Moore et al. 1991). No parallel geographic variation was identified using nuclear markers (allozymes) in a subsequent study and no significant divergence of Gilded Flickers from Red-shafted and Yellow-shafted flickers was found (Fletcher and Moore 1992). A recent study has attempted to differentiate the subgroups within the overall Northern Flicker complex using a genomic technique, but its power of inference for the most closely related forms was limited by the inclusion of only a small number of individuals of each taxon (Manthey et al. 2017). Manthey et al. (2017) were able to identify differences in the geographically isolated Guatemalan and Cuban flickers, but were unable to unambiguously resolve differences in the remaining three taxa.

Here, we take a reduced-representation genomic sequencing approach using more extensive sampling of Red-shafted, Yellow-shafted, and Gilded flickers across their range to better characterize genetic differentiation within the Northern Flicker complex. In this study, we purposefully sample populations located at a substantial distance from the Great Plains hybrid zone to define the underlying genetic diversity and genetic structure among individuals that are unlikely to have undergone genetic introgression via recent hybridization. Although we find quite low levels of overall genomic differentiation, we are able to clearly and conclusively distinguish the three taxa genetically for the first time. We first describe patterns of genetic structure and differentiation between the three flicker taxa and then model their demographic and evolutionary histories.

## Methods

### *Sampling*

We obtained tissue samples from 40 Northern Flickers from three of the five subgroups: Red-shafted Flickers (*Colaptes auratus cafer*),  $n = 14$ ; Yellow-shafted Flickers (*Colaptes auratus auratus*),  $n = 21$ ; and Gilded Flickers (*Colaptes chrysoides*),  $n = 5$ . Due to issues with data quality in downstream analyses, two individuals were ultimately removed from the dataset (one Red-shafted and one Yellow-Shafted flicker), leaving a total of 38 individuals (details in Table B1). We included samples from widely spaced localities within the geographic range of each taxon to better assess their general levels of genetic variation (Figure 2.1). Our intention was to characterize genetic differentiation between the taxa independent of current hybridization (as much as is possible given the substantial extent of hybridization), hence all Red-shafted and Yellow-shafted flicker samples were from localities at least 500 km away from the present-day hybrid zone. However, three of the samples included in our study (those from Nevada) were from an area of range overlap with Red-shafted Flickers.

### *Molecular laboratory methods*

Genomic DNA was isolated from each sample using DNEasy tissue extraction kits following the manufacturer's protocol (Qiagen, Valencia, CA, USA). We used double-digest restriction site-associated DNA sequencing (ddRAD) following the protocol of Peterson et al. (2012) with modifications as described in (Thrasher et al. 2018) to generate genomic data. ddRAD is a technique in which genomic DNA is digested with two restriction enzymes that cut the DNA into small fragments distributed throughout the genome. It is a cost-effective method for single nucleotide polymorphism (SNP) discovery and genotyping in non-model organisms (Peterson et al. 2012). For each

individual, we used approximately 500 ng of DNA at a standardized concentration of 50 ng/ $\mu$ l. All DNA concentrations were determined using a Qubit fluorometer (Life Technologies, NY, USA). DNA was digested with the restriction enzymes SbfI (8 bp recognition site) and MspI (4 bp recognition site; New England BioLabs, MA, USA). The ends of the digested DNA were ligated to P1 and P2 adaptors using T4 DNA Ligase (New England BioLabs). P1 adaptors were ligated to the 5' end of the digested DNA and contained an SbfI compatible overhang and an inline barcode (between 5 and 7 bp long) to identify individual samples bioinformatically later in the analysis. P2 adaptors were ligated to the 3' end of the digested DNA and contained an MspI compatible overhang. Digestion/ligation reactions included 250 times more P2 than P1 adaptor to reflect the differences in abundance of SbfI/P1 and MspI/P2 restriction sites in the genome.

We pooled samples with unique P1 barcodes into two different indexing groups after digestion/ligation. The DNA in each index group was purified with 1.5 $\times$  Agencourt AMPure XP beads (Beckman Coulter, CA, USA) to remove enzymes and small DNA fragments. We size-selected fragments between 400 and 700 bp using Blue Pippin (Sage Science, MA, USA). To incorporate the full Illumina TruSeq primer sequences and unique indexing primers into each library, we performed low cycle number PCR with Phusion High-Fidelity DNA Polymerase (New England BioLabs), with the following thermocycling profile: 98 $^{\circ}$  C for 30 s followed by 11 cycles at 98 $^{\circ}$  C for 5 s, 60 $^{\circ}$  C for 25 s, and 72 $^{\circ}$  C for 10 s with a final extension at 72 $^{\circ}$  C for 5 min. We visualized the product of this amplification on a 1% agarose gel and performed a final 0.7 $\times$  AMPure cleanup to eliminate DNA fragments smaller than 200 bp. Libraries were visualized on a fragment Bioanalyzer (Agilent Technologies, CA, USA) to precisely determine fragment size distribution. The index groups were combined at equimolar

ratios and sequenced on one Illumina HiSeq 2500 lane (single-end, 150 bp) at the Cornell University Biotechnology Resource Center in conjunction with samples from another project.

### *Quality filtering and SNP calling*

We used the FASTX-Toolkit ([http://hannonlab.cshl.edu/fastx\\_toolkit/](http://hannonlab.cshl.edu/fastx_toolkit/)) to perform quality filtering (FASTX Quality Filter) by removing sequence reads if a single base had a Phred quality score below 10, and/or if more than 5% of bases had a Phred quality score below 20. The remaining reads were demultiplexed using the `process_radtags` command in STACKS 1.44 (Catchen et al. 2011). We applied additional filtering and only retained reads that met the following conditions: they passed the Illumina chastity filter, they contained an intact SbfI RAD site, they contained one of the unique barcodes assigned to each sample (employing the `rescue barcodes` option, allowing one mismatch), and they did not contain Illumina indexing adaptors (reads with one mismatch with the adaptor sequence were also discarded). This resulted in 38.5 million sequence reads retained after filtering. To accommodate differences in the length of inline barcodes, all sequence reads were trimmed at their 3' end to 140bp (FASTX Trimmer).

Sequences were assembled de novo into a catalog using the `ustacks/cstacks/sstacks` pipeline controlled by the `denovo_map` program in STACKS. Sequence reads from the same individual were aligned to each other and considered a locus ("stack") based on a minimum depth of coverage of at least 10 reads ( $m$ ). We allowed five mismatches between aligned reads within individuals ( $M$ ) and five mismatches between aligned loci from different individuals ( $n$ ), resulting in a catalog of 63,259 unique loci. Average read depth across loci and individuals in the catalog was

44.9× (see Table B2 for details on individual coverage and missing data). We used the populations program within STACKS to export SNP data for downstream analyses. We required that a SNP be present in a minimum of 80% of all individuals with a minimum stack depth of 20 to be retained. We exported all SNPs from each RAD locus (16,670 SNPs) and additionally retained a subset of SNPs that included the first SNP per locus and a minor allele frequency (MAF) threshold of 10% (1,911 SNPs) for analyses that require unlinked data (e.g. STRUCTURE).

We compared our de novo assembly to a reference-based assembly using the pstacks/cstacks/sstacks pipeline controlled by the ref\_map program in STACKS. Sequence reads were aligned to the Downy Woodpecker (*Picoides pubescens*) genome assembly (Gilbert et al. 2014; Zhang et al. 2014) with BOWTIE2 2.3.0 (Langmead et al. 2009). The average overall alignment across individuals was 65.8% [range = 53.9-69.6%] (Gilded: 67.7% [65.9-69.0%], Red-shafted: 64.6% [53.9-69.6%], Yellow-shafted: 66.2% [55.7-69.1%]). The reference-based catalog assembly is able to accommodate indels and does not require alignment of reads within individuals ( $M$ ). We allowed five mismatches between aligned loci from different individuals ( $n$ ). The reference-based assembly resulted in a catalog of 27,108 loci. Average read depth across loci and individuals in the catalog was 46.6× (see Table B2 for details on individual coverage and missing data). We used the populations program within STACKS to export SNP data using the same requirements as for the de novo assembly. We exported all SNPs from each stack (8,943 SNPs) and additionally created a subset of SNPs that included only the first SNP per stack (1,584 SNPs) for analyses that require unlinked data (e.g. SNAPP).

We checked the consistency between the de novo and reference-based assemblies and found high concordance. Overall, 97.2% of the loci from the reference-based catalog aligned to loci in the de novo catalog and 62.7% in the reciprocal alignment using a

custom Perl script with BLASTN 2.3.0 and an Expect ( $E$ ) value of  $<1.0 \times 10^{-10}$  (Altschul et al. 1990). Because we obtained similar results in the downstream analyses using SNPs from the de novo and reference-based assemblies (see results), we primarily present results from the de novo marker set here. However, some of the analyses required the use of the reference-based assembly and we indicate this where relevant.

### *Genetic differentiation and spatial population genetic structure*

We calculated a measure of population differentiation with overall (genome-wide) pairwise estimates of  $F_{ST}$  and per SNP  $F_{ST}$  between the three Northern Flicker taxa and between the populations within each taxon using the 'basic.stats' function in the hierfstat package (Goudet 2005) in R 3.4.0 (R Core Team 2017). We report Nei's  $F_{ST}$  (Nei 1987) to correct for sampling differences between the taxa, but values were comparable with other  $F_{ST}$  estimates (see results). We used the 'summary' function in the adegenet package (Jombart 2008) in R to generate observed and expected heterozygosity estimates for each taxon. Observed heterozygosity can be used as a proxy for levels of inbreeding in a population with lower values suggesting more inbreeding or small population sizes. To visualize genetic clustering in the data, we performed a principal component analysis (PCA) using the 'snpgdsPCA' function in the SNPRelate package (Zheng et al. 2012) in R. PCA can be used to transform large datasets of correlated variables into uncorrelated principle components. As PCAs do not handle missing data well, we have removed three individuals from the PCA with large amounts of missing data (but have retained them elsewhere in the study; see Table B2). We also analyzed hierarchical genetic structure using an analysis of molecular variance (AMOVA) with the function 'poppr.amova' in the poppr package (Kamvar et al. 2014) in R. Significance was determined using 999 permutations. Comparing the three variance components in

an AMOVA ( $F_{IT}$ ,  $F_{IS}$ ,  $F_{ST}$ ) can provide further evidence for the presence of population structure.

To identify genetic structure within the Northern Flicker complex, we assigned individuals to genetic clusters using STRUCTURE 2.3.4 (Pritchard et al. 2000) using the de novo dataset with the first SNP per stack and a 10% minor allele frequency threshold. We implemented the admixture ancestry model with correlated allele frequencies, but did not use the default allele frequency prior, instead setting it to the one estimated from the data ( $\lambda = 1.47$ ). We conducted 10 runs for each value of  $K = 1-5$ ; each run consisted of 300,000 generations following a burn-in of 200,000. The most likely value of  $K$  was determined following the  $\Delta K$  method described by Evanno et al. (2005) and implemented in STRUCTURE HARVESTER 0.6.94 (Earl and vonHoldt 2011). We averaged results across the 10 runs using the greedy algorithm in the program CLUMPP 1.1.2 (Jakobsson and Rosenberg 2007) and visualized results using DISTRUCT 1.1 (Rosenberg 2003).

#### *Outlier analysis*

We used BayeScan 2.1 (Foll and Gaggiotti 2008) to identify outlier SNPs putatively under selection. BayeScan uses a combination of  $F_{ST}$  and allele frequency differences to determine if a locus is under natural selection. It does this by assessing if alpha (the locus-specific component of  $F_{ST}$ ) is necessary to explain the observed pattern of diversity in a given locus using reversible-jump MCMC. In locus models that include alpha, positive values suggest diversifying selection, while negative values suggest purifying or balancing selection. We scanned all SNPs across the three Northern Flicker taxa and allowed for a false discovery rate of 1%. Additionally, we evaluated all SNPs within the top 0.1% of the  $F_{ST}$  distribution ( $F_{ST} \geq 0.8198$ ). For all outlier SNPs identified using both

methods, we assessed homology to the Zebra Finch (*Taeniopygia guttata*) genome using BLASTN (Altschul et al. 1990). We required an  $E$  value of  $<1.0 \times 10^{-5}$ ,  $>70\%$  identity score, and  $>50\%$  query coverage to assign a match.

### *Tree building*

To infer a species tree we used SNAPP 1.3.0 (Bryant et al. 2012) implemented in BEAST 2.4.5 (Bouckaert et al. 2014). In order to root the tree with sequences from the Downy Woodpecker, we used the 1,584 SNPs from the reference-based assembly (which included one SNP per locus and were not filtered by minor allele frequency). Because SNAPP is computationally intensive, we selected five individuals from each taxon (with little missing data) to build the tree (see Table B2 for samples chosen). We ran SNAPP for 1.5 million generations (with the first 10% set as burn-in) using default priors and saving the output every 1,000 generations. The monophyly of the three flickers was enforced following Shakya et al. (2017). We designated an initial tree with the Downy Woodpecker as an outgroup and the three flickers as a polytomy for the ingroup. We visually assessed convergence using Tracer 1.6.0 (Rambaut et al. 2014), and determined estimated sample sizes (ESS) were sufficiently large when they reached  $>200$  for estimated parameters. We visualized the full set of resulting species trees using DensiTree 2.2.6 (Bouckaert 2010; Bouckaert and Heled 2014) which shows fuzziness in parts of the tree that have higher uncertainty.

### *Modeling of demographic history*

To estimate demographic history, including divergence times, effective population sizes, and gene flow, we used the Generalized Phylogenetic Coalescent Sampler (G-PhoCS) program 1.2.3 (Gronau et al. 2011). G-PhoCS is based on a full coalescent

isolation-with-migration model and allows asymmetric gene flow between taxa. G-PhoCS uses haplotype data with no filtering for minor allele frequency to model demography. Thus, we obtained sequence data from the reference-based STACKS assembly from all 38 individuals for this analysis, including 140 bp haplotypes from 1,671 RAD loci (8,943 SNPs) using both variable and invariant haplotypes. The G-PhoCS model had 13 free parameters: 6 migration rates, 3 current and 2 ancestral effective population sizes, and 2 divergence times.

We ran G-PhoCS using the standard MCMC settings described in Gronau et al. (2011) and Freedman et al. (2014) and default parameters with 50,000 burn-in generations and 500,000 additional sampling generations. We visually assessed all runs using Tracer 1.6.0 (Rambaut et al. 2014) to ensure they showed adequate mixing and convergence. We converted the resulting mutation-scaled parameter estimates from the posterior distributions to generations and individuals by assuming an average mutation rate of  $10^{-9}$  mutations per bp per generation (Kumar and Subramanian 2002). As this mutation rate is an approximation, we focus the interpretation and discussion of results on relative comparisons between different parameter estimates, rather than their absolute values. We measured gene flow as the number of migrants per generation. The models implemented in G-PhoCS are conditioned upon a given phylogenetic topology. Thus, we ran G-PhoCS with each of the three possible starting three-taxon trees.

## **Results**

### *Genetic variation in the Northern Flicker complex*

PCA revealed clear genetic differentiation among Red-shafted, Yellow-shafted, and Gilded flickers (Figure 2.2A), with PC1 and PC2 explaining 5.62% and 3.57% of the

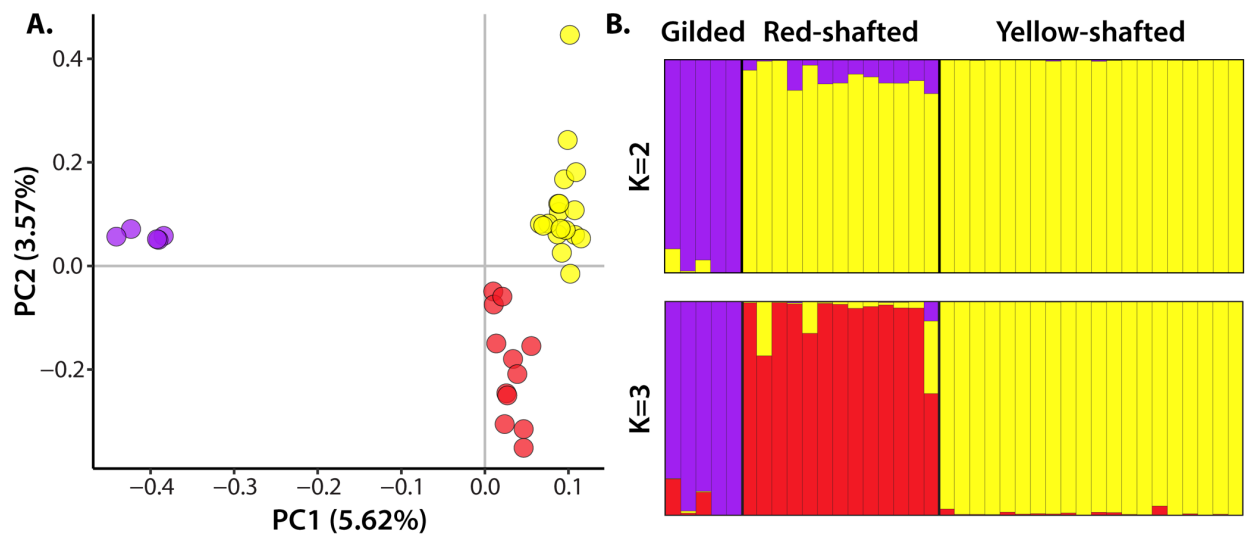


**Figure 2.2.** Genetic structure within the Northern Flicker complex showing the ability to differentiate the three taxa using multiple analytical methods. **(A)** Principal component analysis based on 16,670 SNPs with Gilded Flickers shown in purple, Red-shafted Flickers in red, and Yellow-shafted Flickers in yellow. **(B)** STRUCTURE plots for  $K = 2$  and  $K = 3$  based on 1,911 SNPs (one per locus with 10% MAF filtering). The  $\Delta K$  method preferred  $K = 2$ , but  $K = 3$  had the highest log likelihood (see Figure B3) and provides an increased ability to differentiate Red-shafted and Yellow-shafted flickers.

variation, respectively. Subsequent PC axes explained little additional variation and did not further distinguish these a priori groups (Figure B1). PC1 clearly split Gilded Flickers from both Red-shafted and Yellow-shafted flickers and also provided a slight split between most Red-shafted and Yellow-shafted individuals, while PC2 further separated Red-shafted Flickers from Yellow-shafted Flickers. PCA results were similar from the de novo (Figure 2.2A) and reference-based SNP datasets (Figure B2A).

Using the  $\Delta K$  method, STRUCTURE assigned individuals to two genetic clusters, corresponding to the split between Gilded Flickers and all Red-shafted and Yellow-shafted individuals (Figure 2.2B). Although  $K = 2$  had the highest  $\Delta K$  value,  $K = 3$  had a slightly higher mean log likelihood (Figure B3) and further differentiates Red-shafted Flickers from Yellow-shafted Flickers (Figure 2.2B). The same results were obtained using the reference-based SNP dataset (Figure B2B). To further explore the distinction between  $K = 2$  and  $K = 3$ , we subsequently ran STRUCTURE only on Red-shafted and Yellow-shafted individuals using a subset of 1,737 SNPs found only in those two groups (i.e. we used STACKS to output a new set of SNPs while excluding Gilded Flickers). We conducted 10 runs for each value of  $K = 1-5$  following the same protocol as described in the Methods section. We found  $K = 2$  was strongly preferred in this STRUCTURE analysis with both the highest  $\Delta K$  value and the highest mean log likelihood (Figure B4). Although individual assignments to genetic clusters matching a priori groups were high in the original STRUCTURE run, there were also some signatures indicating possible admixture or incomplete lineage sorting. In particular, the three Gilded Flickers from Nevada (where their range overlaps with Red-shafted Flickers; first three bars in Figure 2.2B,  $K = 3$ ) had partial assignment to the Red-shafted cluster, while the two Gilded Flickers from Sinaloa, Mexico did not (last two bars in Figure 2.2B,  $K = 3$ ). Additionally, Red-shafted and Yellow-shafted flickers also had some partial

assignments to the alternative cluster, though this was more apparent in Red-shafted Flickers.

We assessed patterns of per-SNP observed heterozygosity and pairwise  $F_{ST}$ , as well as patterns of hierarchical structure using AMOVA (Figure 2.3). Mean observed heterozygosity was lower in Gilded Flickers (0.0941) than in Red-shafted (0.1213) or Yellow-shafted (0.1165) flickers (Figure 2.3A). Average pairwise  $F_{ST}$  between the three groups reflects the differences observed in the PC and STRUCTURE analyses (Figure 2.3B, Table 2.1), with low overall mean  $F_{ST}$  between Red-shafted and Yellow-shafted flickers (0.0181) and substantially higher mean  $F_{ST}$  between Red-shafted and Gilded flickers (0.1160) and Yellow-shafted and Gilded flickers (0.1386). Although we present here  $F_{ST}$  estimates using a correction for differing sample sizes,  $F_{ST}$  estimates that do not include this correction showed qualitatively similar patterns (Table B3). Average pairwise  $F_{ST}$  values between populations within the three taxa were low overall, with the highest mean  $F_{ST}$  between the Nevada and Sinaloa populations in the Gilded Flicker (0.0547; Table B4). However, our sample sizes may be too small to reliably estimate  $F_{ST}$  between populations within the three taxa. Results from an AMOVA (Figure 2.3C) indicated that 6.4% of the molecular variance explained differences among groups ( $F_{ST}$ ;  $P < 0.001$ ), 6.3% explained differences among individuals within groups ( $F_{IS}$ ;  $P < 0.001$ ), and 87.3% explained differences within individuals ( $F_{IT}$ ;  $P < 0.001$ ).

#### *Signatures of selection through outlier detection*

We identified 46 outlier SNPs (0.28% of all SNPs) using BayeScan across all three flicker taxa (Figure B5). All outlier SNPs were determined to be under directional selection (i.e. had a positive alpha value). Half of the identified SNPs had an  $F_{ST}$  greater than 0.90 between Yellow-shafted and Gilded flickers with an  $F_{ST}$  less than 0.50 between Red-

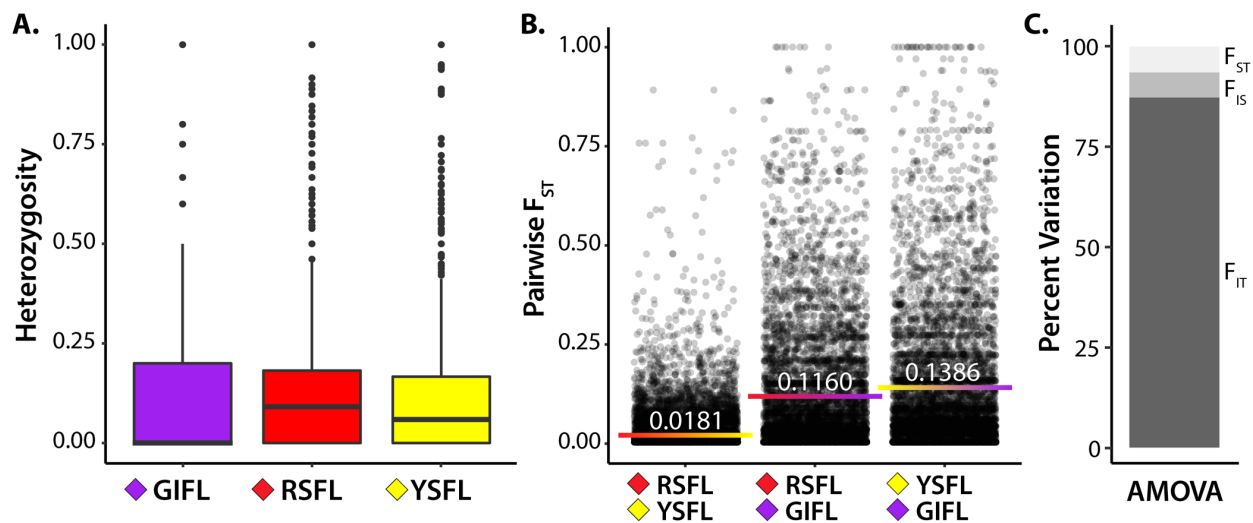


**Figure 2.3.** Estimates of (A) observed heterozygosity and (B) pairwise  $F_{ST}$  within the Northern Flicker complex for 16,670 SNPs. Estimates of heterozygosity are shown as boxplots with the range between the first and third quartile indicated with color and a thick black line for the median.  $F_{ST}$  values are shown for each SNP and the overall mean values are noted on each bar. Observed heterozygosity is higher in Red-shafted and Yellow-shafted flickers than in Gilded Flickers and estimates of pairwise  $F_{ST}$  are substantially lower in comparisons between Red-shafted and Yellow-shafted flickers than in either comparison with Gilded Flickers. (C) Results from an analysis of molecular variance (AMOVA) showing that most of the molecular variance is found within individuals ( $F_{ST}$ : among groups,  $F_{IS}$ : among individuals within groups,  $F_{IT}$ : within individuals). Taxa abbreviations: GIFL = Gilded Flicker, RSFL = Red-shafted Flicker, YSFL = Yellow-shafted Flicker.

**Table 2.1.** Pairwise  $F_{ST}$  estimates for 16,670 SNPs with mean  $F_{ST}$  shown below the diagonal, and median and range (in brackets) shown above.

	<b>Gilded Flickers</b>	<b>Red-shafted Flickers</b>	<b>Yellow-shafted Flickers</b>
<b>Gilded Flickers</b>	—	0.0745 [0-1.0]	0.0843 [0-1.0]
<b>Red-shafted Flickers</b>	0.1160	—	0.0200 [0-0.8912]
<b>Yellow-shafted Flickers</b>	0.1386	0.0181	—

shafted and Gilded flickers, suggesting fixed or nearly fixed differences with Gilded Flickers were driving many of the SNPs identified using BayeScan. Repeating the BayeScan analysis after excluding Gilded Flickers resulted in no outlier SNPs being identified. We identified an additional 8 SNPs within the top 0.1% of the  $F_{ST}$  distribution that were not originally identified using BayeScan. A number of the outliers we identified in both methods aligned to homologous genes in the Zebra Finch using our stringent matching criteria (Table B5).

#### *Evolutionary relationships and demographic history in the Northern Flicker complex*

The SNAPP species tree grouped Red-shafted and Yellow-shafted flickers as sister taxa connected by relatively short branch lengths (Figure 2.4). The cloudogram revealed higher levels of uncertainty in the branch length separating Gilded Flickers from the clade of Red-shafted and Yellow-shafted flickers. Despite this uncertainty, SNAPP consistently identified this tree topology with a posterior probability of 1 for all nodes.

We used G-PhoCS to estimate demographic parameters under each of the three possible three-taxon starting trees. Models with Yellow-shafted or Red-shafted flickers as the outgroup produced similar parameter estimates to each other, but strongly differed from models with Gilded Flickers as the outgroup (Figure B6). Because of the strong support in the SNAPP analysis for the tree topology with Gilded Flicker as the outgroup, we present results for this model (Figure 2.5). We found evidence for a split between Red-shafted and Yellow-shafted flickers that was approximately 16 times more recent than their common ancestor's split with Gilded Flickers. The current effective population sizes were comparable between Red-shafted and Yellow-shafted flickers, with Yellow-shafted Flickers having a slightly larger population size. However, their effective population sizes were approximately 40-50 times larger than the Gilded

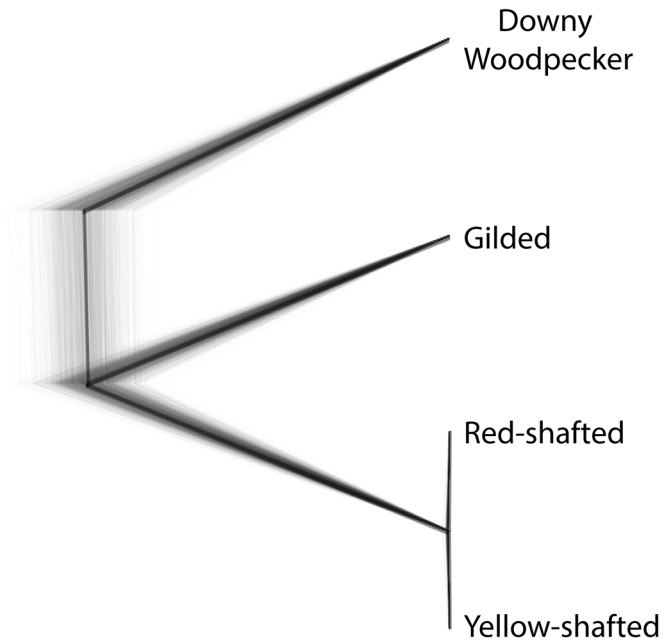


**Figure 2.4.** Species tree for the three focal taxa of the Northern Flicker complex inferred from 1,584 SNPs from the reference-based assembly using SNAPP. The consensus tree (thick line) is shown on top of a cloudogram of post-burn-in trees, each shown with a thin gray line. The darker shades of gray in the cloudogram imply greater degree of overlap between individual trees. Posterior probabilities equal 1 for all nodes.

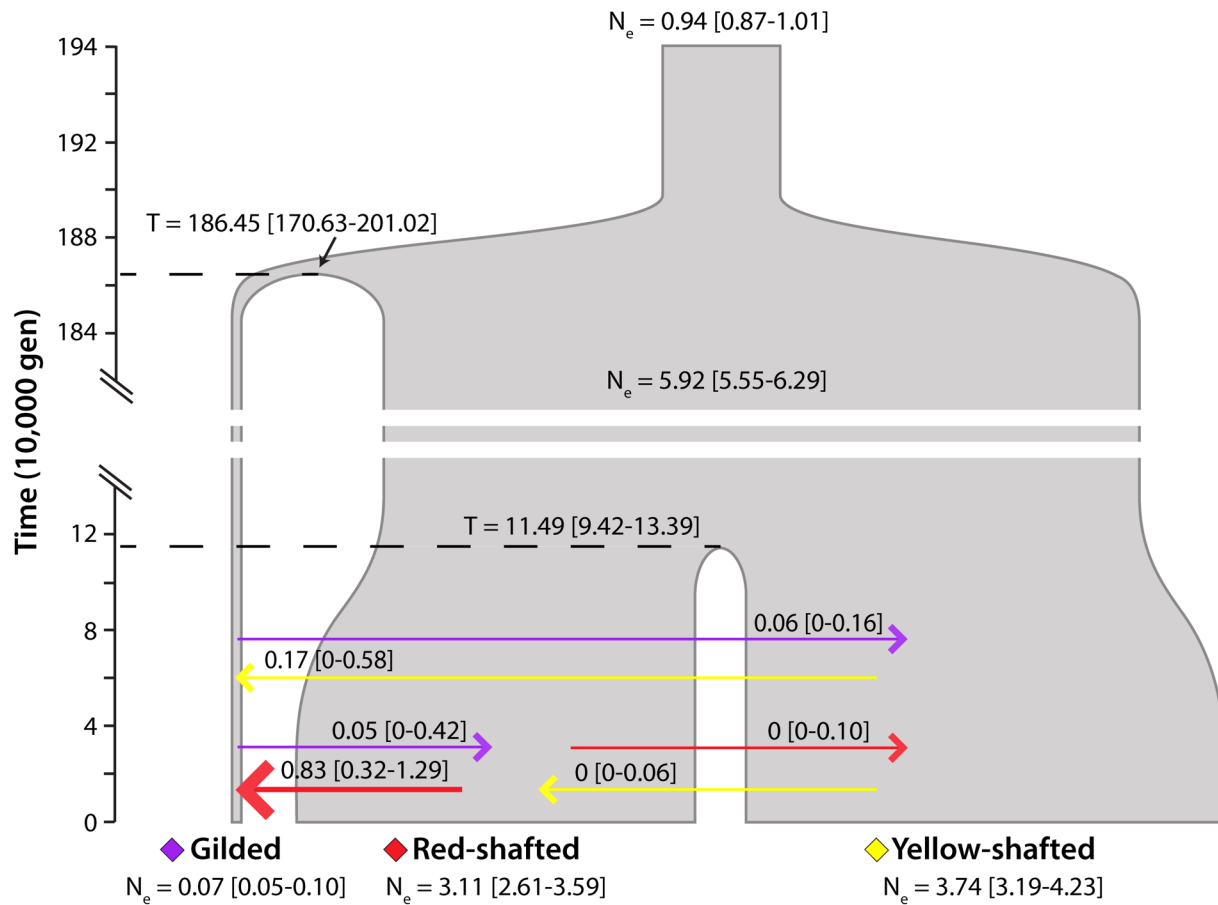


**Figure 2.5.** The phylogeny of the three Northern Flicker taxa drawn to scale to represent estimates of effective population sizes ( $N_e$ , in millions of individuals) and divergence times (dotted lines;  $T$ , in 10,000 generations) from G-PhoCS. Gene flow is shown as arrows between lineages (in migrants per generation). All parameter estimates are expressed as medians with the 95% Bayesian CI in brackets. Interpretation should be focused on relative comparisons between parameter estimates, rather than the actual value of the estimates, as we based calculations on an approximate mutation rate of  $10^{-9}$  mutations per bp per generation. See Figure B6 for parameter estimates from all G-PhoCS models.

Flicker's current effective population size. We estimated gene flow between the three taxa in all possible directions and in most cases our estimates could not be distinguished from zero. The only exception was evidence for gene flow from Red-shafted Flickers into Gilded Flickers.

## **Discussion**

Next-generation sequencing technologies are playing an increasingly large part in ornithology (reviewed in Toews et al. 2016c) and can be used to revisit previously studied systems with increased power and resolution, often providing new insights into the evolution or other aspects of such systems. In this study we revisited three of the five taxa in the well-studied Northern Flicker complex using ddRAD sequencing: Red-shafted, Yellow-shafted, and Gilded flickers. Previous studies using traditional molecular markers were unable to identify genetic differences separating these morphologically distinct taxa (Grudzien and Moore 1986; Grudzien et al. 1987; Fletcher and Moore 1992; Moore et al. 1991) and even several hundred SNPs with a small panel of individuals did not provide much increased resolution (Manthey et al. 2017). Here, the combination of increased sampling and a different genomic sequencing method has allowed us to clearly differentiate Red-shafted, Yellow-shafted, and Gilded flickers genetically for the first time (Figure 2.2). Nevertheless, we find levels of differentiation to be low overall, consistent with previous studies using both traditional molecular markers (Grudzien and Moore 1986; Grudzien et al. 1987; Fletcher and Moore 1992; Moore et al. 1991) and genomic sequencing (Manthey et al. 2017). Moreover, our estimates of  $F_{ST}$  are similar to those in Manthey et al. (2017) despite the differences in molecular methods and sampling. Differentiation between Red-shafted and Yellow-

shafted flickers is particularly low (Table 2.1, Figure 2.3B-C): mean  $F_{ST}$  between them was only 0.0181 and we found no SNPs. This level of differentiation is in the low range of comparable estimates from other recent radiations and hybridizing avian taxa (Walsh et al. 2017; Toews et al. 2016b; Burri et al. 2015; Delmore et al. 2015; Poelstra et al. 2014), though not as low as that found in some systems (Capuchino seedeaters: Campagna et al. 2017; Golden-winged and Blue-winged warblers: Toews et al. 2016a; Darwin's Finches: Chaves et al. 2016, Lamichhaney et al. 2015). Estimates of observed heterozygosity and  $F_{ST}$  in the Gilded Flicker are suggestive of small population sizes within its limited geographic range: Gilded Flickers have the lowest observed heterozygosity (Figure 2.3A) and elevated genetic differentiation from both Red-shafted (0.1160) and Yellow-shafted flickers (0.1386; Figure 2.3B).

We identified only a small number of SNPs that exhibited elevated levels of divergence between the three flicker taxa (Table B5). In total, 17 SNPs were in the top 0.1% of the  $F_{ST}$  distribution ( $F_{ST} \geq 0.8198$ ) and we identified 42 SNPs under directional selection through BayeScan (9 of which were in the top 0.1% of the distribution). Estimates of  $F_{ST}$  between the different taxa in these outlier SNPs suggest that fixed or nearly fixed differences with Gilded Flickers are driving the results from BayeScan. Moreover, excluding Gilded Flickers from the BayeScan analysis resulted in the absence of outlier SNPs between Red-shafted and Yellow-shafted flickers. The low number of SNPs under directional selection in the Gilded Flicker could be the consequence of their small effective population size leading to a predominant effect of genetic drift.

We were able to annotate only 14% of the outlier SNPs. Of these few candidate genes, we did not find any that were clearly related to the phenotypic differentiation in the three flicker taxa. Regions under selection in the flickers deserve further attention, but it is likely that a whole-genome sequencing approach will be necessary to identify

the genetic differences responsible for generating their distinct plumage phenotypes. This is particularly true for comparisons between Red-shafted and Yellow-shafted flickers, as we did not identify fixed SNPs between these two taxa and found only 7 SNPs that exceeded an  $F_{ST}$  of 0.75.

Despite the low overall levels of differentiation, we were able to describe some aspects of the evolutionary history in this species complex for the first time. We found high support for Red-shafted and Yellow-shafted flickers being each other's closest relatives (Figure 2.4), which contrasts with the uncertain and differing tree topologies found in previous studies (Dufort 2015; Manthey et al. 2017). In fact, to our knowledge, this is the first highly supported phylogeny for these three taxa. Given the high degree of genetic similarity between these three flickers, it is unsurprising that previous studies using a few nuclear or mitochondrial genes were unable to discern their evolutionary relationships. The evolutionary history of this group has long been a mystery, particularly as Gilded Flickers resemble Red-shafted Flickers in most characters (but with a more rusty-colored crown and yellow wing and tail feathers).

In this study, we additionally provide improved insights into the demographic history of the Northern Flicker complex over evolutionary time (Figure 2.5). We find evidence for a split between Red-shafted and Yellow-shafted flickers that is approximately 16 times more recent than their ancestor's split with Gilded Flickers, suggesting the low differentiation between Red-shafted and Yellow-shafted flickers is largely due to their recent common ancestry. As we found in other analyses, we again see evidence for a small effective population size in Gilded Flickers (~40-50 times smaller than in Red-shafted or Yellow-shafted flickers). However, we cannot assess if the Gilded Flicker experienced any bottlenecks since its split from its common ancestor with Red-shafted and Yellow-shafted flickers, as the demographic modeling approach

is restricted to one shared ancestral and one contemporary effective population size estimate per taxon.

Our estimates of gene flow between taxa were largely indistinguishable from zero—gene flow from Red-shafted Flickers into Gilded Flickers is the only exception (CI = 0.32-1.29 migrants/generation). This finding seems counterintuitive given the large amount of known hybridization that currently occurs between Red-shafted and Yellow-shafted flickers in the Great Plains (Moore 1987; Moore and Buchanan 1985; Wiebe 2000; Wiebe and Moore 2017). However, we note that our estimates of gene flow reflect our choice of sampling locations: we specifically used samples away from the hybrid zone. Moreover, the estimate of gene flow between Red-shafted and Gilded flickers may be overestimated relative to other comparisons because we included three (of five) Gilded Flicker samples from the area of overlap between the two taxa in Nevada (Figure 2.1). These three individuals additionally showed signatures consistent with admixture with Red-shafted Flickers in the STRUCTURE analyses (first three bars in Figure 2.2B,  $K = 3$ ). It is likely that repeating the analysis with samples closer to the hybrid zone between Red-shafted and Yellow-shafted flickers would result in higher estimates of gene flow between them. However, the results from this study suggest that the effects of gene flow between Red-shafted and Yellow-shafted flickers may be geographically limited since strong signatures of gene flow do not seem to extend throughout the entire geographic range despite frequent hybridization that has been ongoing for many generations. This is consistent with the geographically limited area where phenotypically hybrid individuals are found. Additionally, it is also possible that the majority of the genome has been homogenized between Red-shafted and Yellow-shafted flickers with only small regions that remain differentiated (likely related to differences in plumage). Although the majority of the genome may have introgressed

across the hybrid zone, it is possible that these small regions experience strong selection against introgression. We are currently further exploring this possibility using whole genome sequencing.

In this study, we present an updated view of the evolutionary history of the Northern Flicker complex. Although we are able to differentiate Red-shafted, Yellow-shafted, and Gilded flickers for the first time using genetic markers, we also confirm the overall very low levels of divergence found in previous studies using traditional molecular markers (Grudzien and Moore 1986; Grudzien et al. 1987; Fletcher and Moore 1992; Moore et al. 1991). The low level of overall genomic differentiation that we find presents a promising opportunity for future studies to use whole genome sequencing to identify highly differentiated regions of the genome and distinguish them from background levels of differentiation. Employing these techniques in the hybrid zone between Red-shafted and Yellow-shafted flickers would additionally provide a more thorough understanding of hybridization than has previously been possible in this system, allowing us to pair studies of both phenotypes and genotypes. Moreover, the distinct phenotypic differences and frequent hybridization presents a clear opportunity to associate differentiated genomic regions with observed phenotypes. The recent divergence and distinct phenotypic differences suggests a few genes of large effect may be responsible for the morphological differentiation.

## References

- Altschul, S. F., W. Gish, W. Miller, E. W. Myers, and D. J. Lipman (1990). Basic Local Alignment Search Tool. *Journal of Molecular Biology* 215:403-410.
- American Ornithologists' Union (1995). Fortieth supplement to the American Ornithologists' Union *Check-list of North American Birds*. *The Auk* 112:819-830.

- Anderson, B. W. (1971). Man's influence on hybridization in two avian species in South Dakota. *The Condor* 73:342-347.
- Anderson, B. W., and R. J. Daugherty (1974). Characteristics and reproductive biology of grosbeaks (*Pheucticus*) in the hybrid zone in South Dakota. *The Wilson Bulletin* 86:1-11.
- Bouckaert, R., and J. Heled (2014). DensiTree 2: Seeing trees through the forest. *bioRxiv*.
- Bouckaert, R., J. Heled, D. Kuhnert, T. Vaughan, C. H. Wu, D. Xie, M. A. Suchard, A. Rambaut, and A. J. Drummond (2014). BEAST 2: a software platform for Bayesian evolutionary analysis. *PLoS Computational Biology* 10:e1003537.
- Bouckaert, R. R. (2010). DensiTree: making sense of sets of phylogenetic trees. *Bioinformatics* 26:1372-1373.
- Bryant, D., R. Bouckaert, J. Felsenstein, N. A. Rosenberg, and A. RoyChoudhury (2012). Inferring species trees directly from biallelic genetic markers: bypassing gene trees in a full coalescent analysis. *Molecular Biology and Evolution* 29:1917-1932.
- Burri, R., A. Nater, T. Kawakami, C. F. Mugal, P. I. Olason, L. Smeds, A. Suh, L. Dutoit, S. Bureš, L. Z. Garamszegi, S. Hogner, et al. (2015). Linked selection and recombination rate variation drive the evolution of the genomic landscape of differentiation across the speciation continuum of *Ficedula* flycatchers. *Genome* 25:1656-1665.
- Campagna, L., M. Repenning, L. F. Silveira, C. S. Fontana, P. L. Tubaro, and I. J. Lovette (2017). Repeated divergent selection on pigmentation genes in a rapid finch radiation. *Science Advances* 3:1-11.
- Catchen, J. M., A. Amores, P. Hohenlohe, W. Cresko, and J. H. Postlethwait (2011). Stacks: building and genotyping loci de novo from short-read sequences. *G3* 1:171-182.
- Chaves, J. A., E. A. Cooper, A. P. Hendry, J. Podos, L. F. De Leon, J. A. Raeymaekers, W. O. MacMillan, and J. A. Uy (2016). Genomic variation at the tips of the adaptive radiation of Darwin's finches. *Molecular Ecology* 25:5282-5295.
- Delmore, K. E., S. Hubner, N. C. Kane, R. Schuster, R. L. Andrew, F. Camara, R. Guigo, and D. E. Irwin (2015). Genomic analysis of a migratory divide reveals candidate

- genes for migration and implicates selective sweeps in generating islands of differentiation. *Molecular Ecology* 24:1873-1888.
- Dufort, M. J. (2015). An augmented supermatrix phylogeny of the avian family Picidae reveals uncertainty deep in the family tree. *Molecular Phylogenetics and Evolution* 94:313-326.
- Earl, D. A., and B. M. vonHoldt (2011). STRUCTURE HARVESTER: a website and program for visualizing STRUCTURE output and implementing the Evanno method. *Conservation Genetics Resources* 4:359-361.
- Evanno, G., S. Regnaut, and J. Goudet (2005). Detecting the number of clusters of individuals using the software STRUCTURE: a simulation study. *Molecular Ecology* 14:2611-2620.
- Fletcher, S. D., and W. S. Moore (1992). Further analysis of allozyme variation in the Northern Flicker, in comparison with mitochondrial DNA variation. *The Condor* 94:988-991.
- Foll, M., and O. Gaggiotti (2008). A genome-scan method to identify selected loci appropriate for both dominant and codominant markers: a Bayesian perspective. *Genetics* 180:977-993.
- Freedman, A. H., I. Gronau, R. M. Schweizer, D. Ortega-Del Vecchyo, E. Han, P. M. Silva, M. Galaverni, Z. Fan, P. Marx, B. Lorente-Galdos, H. Beale, et al. (2014). Genome sequencing highlights the dynamic early history of dogs. *PLoS Genetics* 10:e1004016.
- Garg, K. M., R. Tizard, N. S. Ng, E. Cros, A. Dejtardol, B. Chattopadhyay, N. Pwint, M. Packert, and F. E. Rheindt (2016). Genome-wide data help identify an avian species-level lineage that is morphologically and vocally cryptic. *Molecular Phylogenetics and Evolution* 102:97-103.
- Gilbert, M. P., E. D. Jarvis, B. Li, C. Li, The Avian Genome Consortium, J. Wang, and G. Zhang (2014). Genomic data of the Downy Woodpecker (*Picoides pubescens*). GigaScience Database.
- Goudet, J. (2005). HIERFSTAT, a package for R to compute and test hierarchical *F*-statistics. *Molecular Ecology Notes* 5:184-186.

- Gronau, I., M. J. Hubisz, B. Gulko, C. G. Danko, and A. Siepel (2011). Bayesian inference of ancient human demography from individual genome sequences. *Nature Genetics* 43:1031-1034.
- Grudzien, T. A., and W. S. Moore (1986). Genetic differentiation between the yellow-shafted and red-shafted subspecies of the northern flicker. *Biochemical Systematics and Ecology* 14:451-453.
- Grudzien, T. A., W. S. Moore, J. R. Cook, and D. Tagle (1987). Genic population structure and gene flow in the northern flicker (*Colaptes auratus*) hybrid zone. *The Auk* 104:654-664.
- Jakobsson, M., and N. A. Rosenberg (2007). CLUMPP: a cluster matching and permutation program for dealing with label switching and multimodality in analysis of population structure. *Bioinformatics* 23:1801-1806.
- Johnson, N. K. (1969). Three papers on variation in flickers (*Colaptes*). *The Wilson Bulletin* 81:225-230.
- Jombart, T. (2008). adegenet: a R package for the multivariate analysis of genetic markers. *Bioinformatics* 24:1403-1405.
- Kamvar, Z. N., J. F. Tabima, and N. J. Grunwald (2014). Poppr: an R package for genetic analysis of populations with clonal, partially clonal, and/or sexual reproduction. *PeerJ* 2:e281.
- Kumar, S., and S. Subramanian (2002). Mutation rates in mammalian genomes. *Proceedings of the National Academy of Sciences* 99:803-808.
- Lamichhaney, S., J. Berglund, M. S. Almen, K. Maqbool, M. Grabherr, A. Martinez-Barrio, M. Promerova, C. J. Rubin, C. Wang, N. Zamani, B. R. Grant, et al. (2015). Evolution of Darwin's finches and their beaks revealed by genome sequencing. *Nature* 518:371-375.
- Langmead, B., C. Trapnell, M. Pop, and S. L. Salzberg (2009). Ultrafast and memory-efficient alignment of short DNA sequences to the human genome. *Genome Biology* 10:R25.

- Manthey, J. D., M. Geiger, and R. G. Moyle (2017). Relationships of morphological groups in the northern flicker superspecies complex (*Colaptes auratus* & *C. chrysoides*). *Systematics and biodiversity* 15:183-191.
- Mason, N. A., and S. A. Taylor (2015). Differentially expressed genes match bill morphology and plumage despite largely undifferentiated genomes in a Holarctic songbird. *Molecular Ecology* 24:3009-3025.
- Mettler, R. D., and G. M. Spellman (2009). A hybrid zone revisited: molecular and morphological analysis of the maintenance, movement, and evolution of a Great Plains avian (*Cardinalidae: Pheucticus*) hybrid zone. *Molecular Ecology* 18:3256-3267.
- Moore, W. S. (1977). An evaluation of narrow hybrid zones in vertebrates. *The Quarterly Review of Biology* 52:263-277.
- Moore, W. S. (1987). Random mating in the northern flicker hybrid zone: implications for the evolution of bright and contrasting plumage patterns in birds. *Evolution* 41:539-546.
- Moore, W. S., and D. B. Buchanan (1985). Stability of the northern flicker hybrid zone in historical times: implications for adaptive speciation theory. *Evolution* 39:135-151.
- Moore, W. S., J. H. Graham, and J. T. Price (1991). Mitochondrial DNA variation in the northern flicker (*Colaptes auratus*, Aves). *Molecular Biology and Evolution* 8:327-344.
- Moore, W. S., and W. D. Koenig (1986). Comparative reproductive success of yellow-shafted, red-shafted, and hybrid flickers across a hybrid zone. *The Auk* 103:42-51.
- Moore, W. S., and J. T. Price (1993). The nature of selection in the northern flicker hybrid zone and its implications for speciation theory. Pages 196-225 in *Hybrid zones and the evolutionary process* (Harrison, R. G., Ed.). Oxford University Press, Oxford, UK.
- Nei, M. (1987). *Molecular Evolutionary Genetics*. Columbia University Press, New York.

- Peterson, B. K., J. N. Weber, E. H. Kay, H. S. Fisher, and H. E. Hoekstra (2012). Double digest RADseq: an inexpensive method for de novo SNP discovery and genotyping in model and non-model species. *PLoS One* 7:e37135.
- Poelstra, J. W., N. Vijay, C. M. Bossu, H. Lantz, B. Ryll, I. Muller, V. Baglione, P. Unneberg, M. Wikelski, M. G. Grabherr, and J. B. Wolf (2014). The genomic landscape underlying phenotypic integrity in the face of gene flow in crows. *Science* 344:1410-1414.
- Pritchard, J. K., M. Stephens, and P. Donnelly (2000). Inference of population structure using multilocus genotype data. *Genetics* 155:945-959.
- R Core Team (2017). R: A language and environment for statistical computing. R Foundation for Statistical Computing, Vienna, Austria.
- Rambaut, A., M. A. Suchard, D. Xie, and A. J. Drummond (2014). Tracer v1.6.
- Rising, J. D. (1983). The Great Plains Hybrid Zones. Pages 131-157 in *Current Ornithology* (Johnston, R. F., Ed.). Plenum Press, New York.
- Rising, J. D. (1996). The stability of the oriole hybrid zone in western Kansas. *The Condor* 98:658-663.
- Rosenberg, N. A. (2003). DISTRUCT: a program for the graphical display of population structure. *Molecular Ecology Notes* 4:137-138.
- Shakya, S. B., J. Fuchs, J. M. Pons, and F. H. Sheldon (2017). Tapping the woodpecker tree for evolutionary insight. *Molecular Phylogenetics and Evolution* 116:182-191.
- Short, L. L. (1965). Hybridization in the flickers (*Colaptes*) of North America. *Bulletin of the American Museum of Natural History*, New York 129:307-428.
- Sibley, C. G., and L. L. Short (1959). Hybridization in the buntings (*Passerina*) of the Great Plains. *The Auk* 76:443-463.
- Sibley, C. G., and L. L. Short (1964). Hybridization in the orioles of the Great Plains. *The Condor* 66:130-150.

- Sibley, C. G., and D. A. West (1959). Hybridization in the rufous-sided towhees of the Great Plains. *The Auk* 76:326-338.
- Swenson, N. G., and D. J. Howard (2005). Clustering of contact zones, hybrid zones, and phylogeographic breaks in North America. *The American Naturalist* 166:581-591.
- Thrasher, D. J., B. G. Butcher, L. Campagna, M. S. Webster, and I. J. Lovette (2018). Double-digest RAD sequencing outperforms microsatellite loci at assigning paternity and estimating relatedness: A proof of concept in a highly promiscuous bird. *Molecular Ecology Resources*. <http://dx.doi.org/10.1111/1755-0998.12771>
- Toews, D. P., S. A. Taylor, R. Vallender, A. Brelsford, B. G. Butcher, P. W. Messer, and I. J. Lovette (2016a). Plumage genes and little else distinguish the genomes of hybridizing warblers. *Current Biology* 26:2313-2318.
- Toews, D. P. L., A. Brelsford, C. Grossen, B. Milá, and D. E. Irwin (2016b). Genomic variation across the yellow-rumped warbler species complex. *The Auk* 133:698-717.
- Toews, D. P. L., L. Campagna, S. A. Taylor, C. N. Balakrishnan, D. T. Baldassarre, P. E. Deane-Coe, M. G. Harvey, D. M. Hooper, D. E. Irwin, C. D. Judy, N. A. Mason, et al. (2016c). Genomic approaches to understanding population divergence and speciation in birds. *The Auk* 133:13-30.
- Walsh, J., I. J. Lovette, V. Winder, C. S. Elphick, B. J. Olsen, G. Shriver, and A. I. Kovach (2017). Subspecies delineation amid phenotypic, geographic and genetic discordance in a songbird. *Molecular Ecology* 26:1242-1255.
- Weir, J. T., O. Haddrath, H. A. Robertson, R. M. Colbourne, and A. J. Baker (2016). Explosive ice age diversification of kiwi. *Proceedings of the National Academy of Sciences, USA* 113:E5580-E5587.
- Wiebe, K. L. (2000). Assortative mating by color in a population of hybrid northern flickers. *The Auk* 117:525-529.
- Wiebe, K. L., and G. R. Bortolotti (2002). Variation in carotenoid-based color in northern flickers in a hybrid zone. *The Wilson Bulletin* 114:393-400.

- Wiebe, K. L., and W. S. Moore (2017). Northern Flicker (*Colaptes auratus*), version 3.0. in The Birds of North America (Rodewald, P. G., Ed.). Cornell Lab of Ornithology, Ithaca, New York, USA.
- Zhang, G., C. Li, Q. Li, B. Li, D. M. Larkin, C. Lee, J. F. Storz, A. Antunes, M. J. Greenwold, R. W. Meredith, A. Ödeen, et al. (2014). Comparative genomics reveals insights into avian genome evolution and adaptation. *Science* 346:1311-1320.
- Zheng, X., D. Levine, J. Shen, S. M. Gogarten, C. Laurie, and B. S. Weir (2012). A high-performance computing toolset for relatedness and principal component analysis of SNP data. *Bioinformatics* 28:3326-3328.

## CHAPTER 3

### EXTENSIVE HYBRIDIZATION REVEALS MULTIPLE COLORATION GENES UNDERLYING A COMPLEX PLUMAGE PHENOTYPE<sup>5</sup>

#### **Abstract**

Coloration is an important target of both natural and sexual selection. Discovering the genetic basis of colour differences can help us to understand how this visually striking phenotype evolves. Hybridizing taxa with both clear colour differences and shallow genomic divergences are unusually tractable for associating coloration phenotypes with their causal genotypes. Here, we leverage the extensive admixture between two common North American woodpeckers—yellow-shafted and red-shafted flickers—to identify the genomic bases of six distinct plumage patches involving both melanin and carotenoid pigments. Comparisons between flickers across ~7.25 million genome-wide SNPs show that these two forms differ at only a small proportion of the genome (mean  $F_{ST} = 0.008$ ). Within the few highly differentiated genomic regions, we identify 368 SNPs significantly associated with four of the six plumage patches. These SNPs are linked to multiple genes known to be involved in melanin and carotenoid pigmentation. For example, a gene (*CYP2J19*) known to cause yellow to red colour transitions in other birds is strongly associated with the yellow versus red differences in the wing and tail feathers of these flickers. Additionally, our analyses suggest novel links between known melanin genes and carotenoid coloration. Our finding of patch-specific control of plumage coloration adds to the growing body of literature suggesting colour diversity

---

<sup>5</sup> Aguillon, SM, J Walsh, IJ Lovette. 2021. Extensive hybridization reveals multiple coloration genes underlying a complex plumage phenotype. *Proceedings of the Royal Society B* 288(1943): 20201805.

in animals could be created through selection acting on novel combinations of coloration genes.

## **Introduction**

Coloration is a visually striking and extraordinarily variable phenotype in animals that drives both natural and sexual selection, and can ultimately drive the process of speciation [1-3]. In recent decades, biologists have been increasingly interested in connecting variation in coloration to an underlying genotype, with much of the focus placed on genes of large effect that influence whole-body coloration differences [3-10]. However, in recent years the use of anonymous genomic scans and admixture mapping has facilitated the discovery of genomic regions involved in coloration of smaller, discrete patches on the body [11-16]. Increasing empirical evidence of patch-specific control of coloration suggests extensive phenotypic diversity could be created through selection acting on novel combinations of coloration genes [17-22].

Low levels of background genomic divergence—either due to experimental crosses, recent speciation, or ongoing introgression—in taxa that differ primarily in colour have allowed for identification of candidate coloration genes in numerous systems [6, 14, 21, 23]. However, what we know about the genes involved in coloration varies extensively depending on the type of pigment involved. The pathways involved in melanin coloration (greys, blacks, browns, and dark reds) are better characterized [5], compared to carotenoid coloration (bright reds, yellows, and oranges) for which only a handful of underlying genes have been identified [24, 25]. This difference is due to differences in pigment acquisition—melanins are produced endogenously, while carotenoids must be acquired through the diet and are subsequently biochemically

processed [24]—and the ability to study melanins in humans and other model systems [5].

Birds with low levels of background divergence have served as particularly powerful non-model systems for discovering the genetic bases of melanin and carotenoid coloration [6, 8, 11, 12, 14, 18, 20, 26-28], as they often exhibit discrete feather patches that differ in colour and pigment type across the body [19]. Yet, despite the substantial variation in pigmentation across birds, the genetic bases of melanin and carotenoid coloration have only rarely been studied together in the same system (but see [11, 14, 16]), though the genes involved are not currently known to overlap in function or co-localize in the genome [3, 5]. Here, we leverage the extensive natural phenotypic variation between yellow-shafted (*Colaptes auratus auratus*) and red-shafted (*C. a. cafer*<sup>6</sup>) flickers, common woodpeckers that hybridize in North America [29], to identify the genomic underpinnings of plumage coloration and explore the connections between melanin and carotenoid pigmentation. The two flickers differ in the coloration of six distinct feather patches: wing and tail (the eponymous “shaft”), nuchal patch, ear coverts, throat, crown, and male malar stripe (Figure 3.1A; Table C1) [30]. The pigments vary depending on the feather patch, with melanins (throat, ear coverts, crown), carotenoids (wing and tail, nuchal patch), and both melanins and carotenoids (male malar stripe) being involved [31, 32]. Previous molecular work has highlighted the very low baseline genetic divergence between these two taxa [33-38]. Importantly, there is extensive ongoing hybridization and backcrossing where the flickers meet in a

---

<sup>6</sup> The subspecific epithet of the red-shafted flicker is etymologically based on a term referring to an African people that is an extreme racial slur. This nomenclatural history places users of this official Linnaean name in the unfortunate situation of perpetuating this slur. We include the official Linnaean name in this one line, but otherwise purposefully refer to these taxa by their common names. Aguillon and Lovette have elsewhere proposed the scientific name for the red-shafted flicker be changed to *Colaptes auratus lathami*, but this name is not yet widely accepted [42].

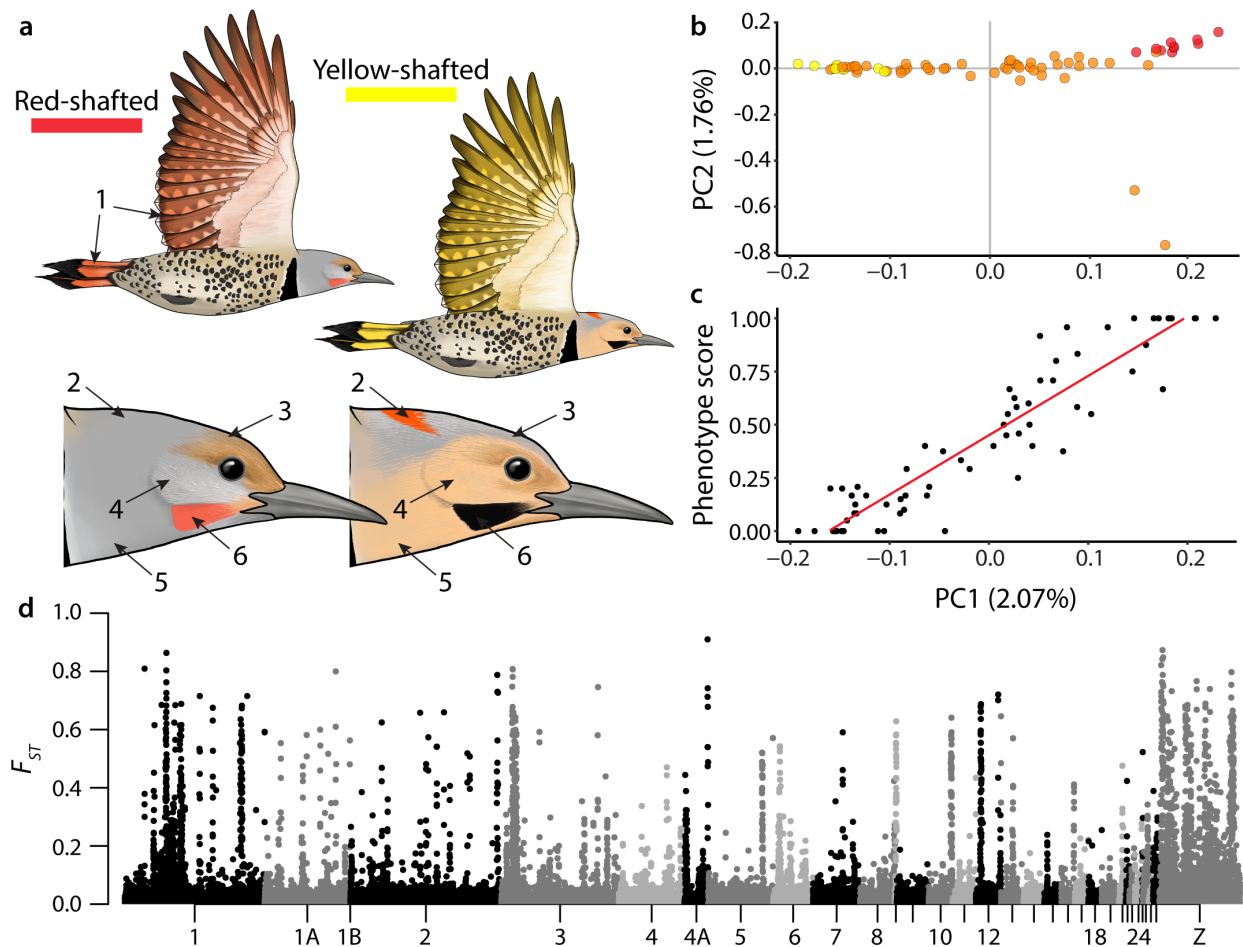


**Figure 3.1.** (A) Coloration differences between red-shafted and yellow-shafted flickers: (1) wing and tail (the eponymous “shaft”), (2) nuchal patch, (3) crown, (4) ear coverts, (5) throat, and (6) male malar stripe. Pigmentation is based on carotenoids (wing and tail, nuchal patch), melanins (crown, ear coverts, throat), and both carotenoids and melanins (male malar stripe). Illustrations by Megan Bishop. (B) Principal component analysis (PCA) separately clusters yellow-shafted (yellow points), red-shafted (red points), and hybrid (orange points) flickers using the dataset of approximately 7.25 million genome-wide SNPs. (C) PC1 is significantly associated with overall phenotype score ( $\rho = 0.94$ ,  $p < 2.2 \times 10^{-16}$ ), where variation ranges from 0 for pure yellow-shafted flickers to 1 for pure red-shafted flickers. (D) The distribution of genetic differentiation ( $F_{ST}$ ) between allopatric yellow-shafted flickers and allopatric red-shafted flickers across the whole genome. Individual points show the weighted mean  $F_{ST}$  for 25kb windows. Chromosome positions are based on alignment to the zebra finch genome.

secondary contact zone in the Great Plains of North America (Figure C1). Admixed and backcrossed hybrids exhibit the full range of possible trait combinations across the six feather patches [30, 39, 40] and occasional transgressive phenotypes [41].

Their combination of low genome-wide divergence, clear phenotypic differences, and extensive hybridization makes flickers an exceptional non-model system in which to explore the genomic basis of feather coloration. Further, the variation in both melanin and carotenoid pigmentation provides an opportunity to explore the potential interactions between genes involved in both pigment types. We compare whole genomes of phenotypically admixed individuals from the hybrid zone along with allopatric red-shafted and yellow-shafted individuals. Here, we (1) assess the genomic landscape of divergence between allopatric flickers and (2) capitalize on a dataset of phenotypically variable hybrid flickers to perform association tests between the genomic markers and the six plumage traits. We leverage these complementary and independent approaches to identify SNPs that are significantly associated with plumage differences. We then (3) search for candidate pigmentation genes present near these SNPs and (4) discuss potential mechanisms connecting melanin and carotenoid genes with individual plumage patches.

## **Results and Discussion**

### *The genomic landscape of divergence in flickers*

We conducted whole genome re-sequencing of 10 allopatric red-shafted, 10 allopatric yellow-shafted, and 48 hybrid flickers (Table C2), resulting in approximately 7.25 million SNPs distributed across the genome. Red-shafted and yellow-shafted flickers clustered separately in a principal component analysis (PCA) with hybrids extending

between the two parental taxa on PC1 (Figure 3.1B; 2.07% of the variation) and clustering separately from them on PC3 and PC4 (Figure C2; 1.68% and 1.65% of the variation, respectively). We estimated  $F_{ST}$  values between the allopatric red-shafted and allopatric yellow-shafted individuals in nonoverlapping 25kb windows to search for divergent regions of the genome. Differentiation across all windows was low between the allopatric individuals (mean genome-wide  $F_{ST} = 0.008$ , mean autosomal  $F_{ST} = 0.007$ , mean Z-linked  $F_{ST} = 0.041$ ), but we identified a number of regions with elevated  $F_{ST}$  estimates relative to the background (Figure 3.1D). Across the entire dataset, we found only a small number of SNPs that were fixed (780 SNPs with  $F_{ST} = 1$ , 0.011% of the total) or nearly fixed (2,156 SNPs with  $F_{ST} > 0.90$ , 0.030% of the total).

We scored the six differing plumage patches (Figure 3.1A) in the flickers to obtain a score ranging from 0 (yellow-shafted) to 1 (red-shafted). See Methods for details on the phenotypic scoring. We found that PC1 was strongly correlated with the overall phenotype score (Figure 3.1C,  $\rho = 0.94$ ,  $p < 2.2 \times 10^{-16}$ ) and with each individual trait separately (Figure C3). Further, a PCA based on 780 fixed SNPs between allopatric red-shafted and allopatric yellow-shafted flickers resulted in the first PC axis explaining a majority of the variation (55.56%) and individuals spread along PC1 based on overall phenotype score (Figure C4). Taken together, these findings suggest that the few divergent genomic regions between allopatric flickers ( $F_{ST}$  peaks in Figure 3.1D) are associated with the loci responsible for their coloration differences.

#### *Multiple, discrete genomic regions shape the complex plumage phenotype*

We took advantage of the plumage trait variation among hybrid flickers to conduct genome-wide associations (GWAs) for each of the six plumage patches to test whether

particular  $F_{ST}$  divergence peaks were associated with plumage coloration (see Figure C5 and C6 for illustrations and trait variation of hybrids). By focusing only on hybrid individuals, the results of our GWA analyses are independent from our assessment of genomic divergence between allopatric individuals (shown in Figure 3.1D). Because red-shafted and yellow-shafted flickers do not differ ecologically [29] and hybrid flickers with variable trait combinations were sampled from the same geographic transect, we expect any associations identified in the GWAs to be related to differences in plumage coloration. 368 SNPs (0.005% of the total) were significantly associated with plumage patches using a significance threshold of  $\alpha = 0.0000001$  ( $-\log_{10}(\alpha) = 7$ ), with 19 SNPs identified in more than one analysis (Figure 3.2; Table C3 and Figure C7). We found significant associations between multiple SNPs and plumage for four of the six focal traits, excluding throat colour (only 1 SNP identified) and crown colour (no SNPs identified). We validated our associations to ensure the identified regions represent real associations between plumage patches and genotype using randomized GWA analyses (Figure C8; see Methods for details).

The GWA analyses revealed several genomic regions that were significantly associated with the coloration of the wing and tail, nuchal patch, ear coverts, and male malar stripe (Figure 3.2; Table C3). In several cases, we identified regions of the genome that were significantly associated with multiple plumage traits (e.g., at the end of chromosome 1 and the beginning of chromosome 3). However, we also identified regions of the genome that were unique to a single GWA analysis (e.g., associations between wing and tail colour and regions on chromosomes 5, 8, and 12). These findings suggest multiple mechanisms influencing coloration in flickers: some genomic regions exert pleiotropic control over the coloration of multiple plumage patches, while other

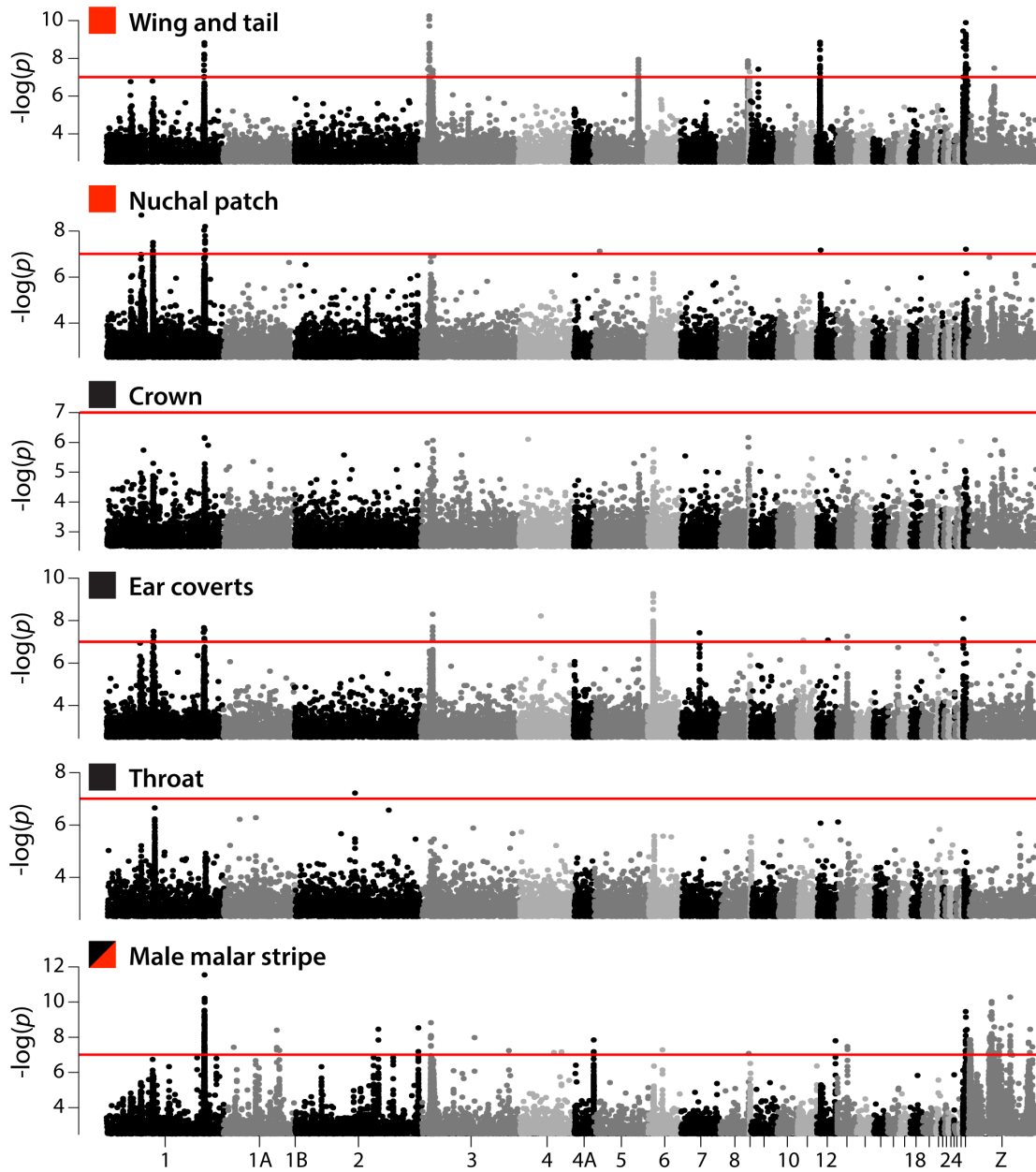


**Figure 3.2.** Results from the genome-wide associations (GWAs) of hybrid flickers comparing individual SNPs with coloration differences in the six plumage patches. Pigment type is indicated by the square next to the trait name (red = carotenoid, black = melanin, red and black = carotenoid and melanin). Some peaks of significant SNPs are present in GWAs of multiple phenotypic traits, while other peaks are unique to a single GWA, suggesting multiple mechanisms influence coloration in flickers. The red line represents the significance threshold of  $-\log_{10}(p) = 7$ . Chromosome positions are based on alignment to the zebra finch genome. For visualization purposes we show only points with  $-\log_{10}(p) > 2.5$ .

genomic regions control the coloration of a single plumage patch (perhaps as loci of large effect). The presence of potential genetic incompatibilities influencing wing and tail colour in hybrid flickers makes understanding the interactions between these genomic regions of particular importance [41]. By taking complementary, yet independent, approaches in the GWAs and  $F_{ST}$  analyses, we find that genomic regions identified in the GWAs of hybrid flickers largely lie within regions of the genome with elevated  $F_{ST}$  between allopatric flickers (peaks in Figure 3.1D; Figure C9). However, not all genomic regions with elevated  $F_{ST}$  were associated with variation in coloration (e.g., the first peak on chromosome 4A, the peak on chromosome 10, and multiple peaks on the Z chromosome).

*Melanin and carotenoid genes both associate with carotenoid plumage in flickers*

To identify candidate genes associated with plumage variation, we searched for all genes within 20kb of SNPs that were significantly associated with plumage patches. Using this approach, we identified a total of 112 genes (Table C4). Here, we highlight 12 genes (Table 3.1, Figure 3.3) that are known or suspected to be involved in melanin or carotenoid pigmentation in other systems: 7 of these candidates are known to be directly involved with pigmentation [6, 8, 43], 3 are suspected to be involved in pigmentation based on the function of related genes [8], and 2 were identified in previous associations with feather coloration in birds [11, 26].

We find a strong association between wing and tail colour and the genomic region on chromosome 8 containing the gene *CYP2J19* (Figure 3.3C, Table 3.1), which codes for a cytochrome P450 enzyme. *CYP2J19* upregulation via an introgressed variant is causal in changing the typical yellow-feathered canary (*Serinus canaria*) into the “red factor” canary [6] and the lack of a functional copy in zebra finch (*Taeniopygia guttata*) is

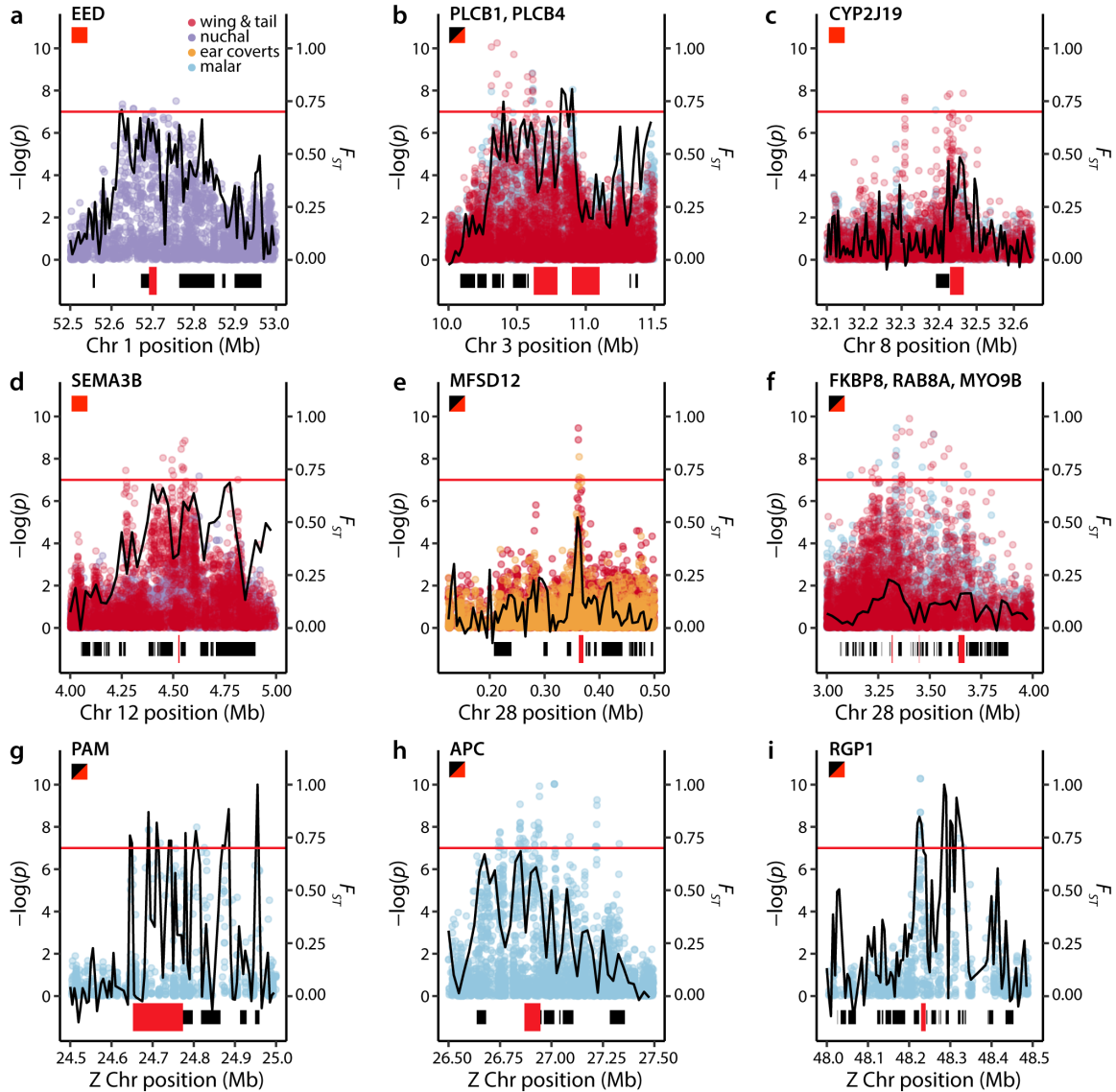


**Figure 3.3.** Patterns of genetic differentiation and GWA significance around nine genomic regions of interest containing 12 candidate coloration genes (Table 3.1). Significance values from the GWA analyses are shown as points coloured by the analyses they were identified in (legend in panel A). The horizontal red lines indicate the GWA significance threshold of  $-\log_{10}(p) = 7$ . Weighted mean  $F_{ST}$  between allopatric red-shafted and allopatric yellow-shafted flickers estimated in 25kb (B, D, F, H) or 5kb (A, C, E, G, I) windows are shown as black lines in each panel. Genes contained within the plotted area are shown as bars at the bottom of each panel, with the red bars indicating the locations of focal genes. When multiple focal genes are located within a single panel, they are listed at the top of the panel in the order of their physical location (from left to right). Pigment types of the trait(s) significantly associated with the focal genes are indicated by the squares under the gene names (red = carotenoid, black = melanin, red and black = carotenoid and melanin). Chromosome positions are based on alignment to the zebra finch genome.

**Table 3.1.** Candidate coloration genes located within 20kb of SNPs that were significantly associated with plumage patches in the GWAs. Pigment types of the trait(s) significantly associated with the SNPs are indicated by the coloured squares (red = carotenoid, black = melanin, red and black = carotenoid and melanin). The full list of identified genes is presented in the Table C4.

Gene	Fig	Chr	Associated Trait(s)	Rationale
EED	3a	1	 nuchal	known melanin gene [8]
PLCB1	3b	3	 malar	known melanin gene [8]
PLCB4	3b	3	 malar, wing and tail	known melanin gene [8]
CYP2J19	3c	8	 wing and tail	known carotenoid gene [6, 43]
SEMA3B	3d	12	 wing and tail	related to known melanin gene family (SEMA) [8]
MFSD12	3e	28	 ear coverts, wing and tail	candidate melanin gene [23, 26]
FKBP8	3f	28	 malar, wing and tail	known melanin gene [8]
RAB8A	3f	28	 malar, wing and tail	related to known melanin gene family (RABs) [8]
MYO9B	3f	28	 malar, wing and tail	related to known melanin genes (MYO5A, MYO7A) [8]
PAM	3g	Z	 malar	known melanin gene [8]
APC	3h	Z	 malar	known melanin gene, candidate carotenoid gene [8, 12]
RGP1	3i	Z	 malar	candidate melanin gene [11]

implicated in the “yellowbeak” phenotype in which the normally red beak and legs are instead yellow [43]. It is currently one of only two genes known to be involved in red coloration in birds, and evidence of its functioning in natural systems is increasing [44-47]. Our identification of *CYP2J19* in the GWA for wing and tail coloration suggests that it mediates this yellow versus red trait difference in flickers and provides further support for its importance in red coloration across diverse avian lineages.

The majority of our identified candidate genes for carotenoid plumage patches in the flickers (Table 3.1) are known or suspected to affect melanin pigmentation in other organisms (henceforth “melanin genes”). In some cases, we find melanin genes are associated with both melanin and carotenoid traits in a single region of the genome (*PLCB1* and *PLCB4* (Figure 3.3B) on chromosome 3, and *MFSD12* (Figure 3.3E) and *FKBP8*, *RAM8A*, and *MYO9B* (Figure 3.3F) on chromosome 28), while in other cases, we find melanin genes associated with a single trait (malar stripe) that uses both pigment types (*PAM* (Figure 3.3G), *APC* (Figure 3.3H), and *RGP1* (Figure 3.3I) on the Z chromosome). Most unusually, we identify two regions containing known or suspected melanin genes (*EED* (Figure 3.3A) on chromosome 1 and *SEMA3B* (Figure 3.3D) on chromosome 12) that are associated only with carotenoid-based traits. To our knowledge, of these 12 melanin genes only *APC* has previously been linked to carotenoid pigmentation (in an associational study [12]), in addition to its known link to melanin pigmentation [8].

#### *Potential mechanisms linking melanin genes with carotenoid traits*

Melanin and carotenoid pigmentation derive from different biochemical pathways [48] and the genes involved in the different processes are not currently known to co-localize in the genome or exert influence over each other [3, 5]. Thus, our finding in flickers of

repeated associations between different carotenoid traits and melanin genes was unexpected. Although we lack a complete annotation of the flicker reference genome and therefore may have missed some causal genes, we repeatedly found associations between known carotenoid traits and melanin genes from different regions of the genome. Here, we outline three non-mutually exclusive explanations for these associations that link melanin genes with carotenoid plumage coloration.

First, some of the association patterns we identify in the GWAs suggest pleiotropic effects of melanin genes: we find multiple plumage patches (carotenoid and melanin) associated with the same region of the genome (Figure 3.3B, E, F). This could occur through regulatory genes typically involved in melanin pigmentation evolving to control the expression of both melanins and carotenoids. Similar pleiotropy has been found in two different warbler species (*Setophaga*), where associations between a single genomic region and multiple aspects of carotenoid and melanin plumage differences have been identified [11, 16]. The finding of possible pleiotropic effects on melanin and carotenoid plumage in woodpeckers and warblers, distantly related bird taxa, suggests pleiotropic effects of melanin genes may be widespread.

Second, melanin genes could be associated with carotenoid traits because the trait differences we observe are actually due to a combination of both pigments. Melanin genes associated with the male malar stripe (Figure 3.3B, F-I) exemplify this mechanism: red pigments are present in the malar stripes of both red-shafted and yellow-shafted flickers, and yellow-shafted flickers subsequently overlay melanin to produce a black malar stripe that masks the red pigment [31, 49]. Beyond this one situation where melanic pigments completely overlay a carotenoid trait, it is also possible that the two pigments are used in concert within the feathers to produce the observed colour (as in [50, 51]). Additionally, melanins serve a number of other

functions in feathers apart from coloration (e.g., feather structure and stability [52, 53], UV protection [54], resistance to bacterial degradation [55]), so differences in patterns of plumage pigmentation relating to these other factors could also exist.

Finally, rather than controlling the upregulation and co-deposition of melanins with carotenoids, our results suggest the intriguing possibility that these genes may instead control the absence of melanin within the feathers. A reduction of melanin is necessary for the bright red and yellow coloration to be visible, and it is possible that the two taxa have differential levels of melanin reduction in their feathers or that they use different molecular pathways to reduce melanin deposition. In particular, the associations between the nuchal patch with *EED* (Figure 3.3A) and the nuchal patch and wing and tail colour with *SEMA3B* (Figure 3.3D), suggests the potential for melanin genes to play a direct role in carotenoid traits. This finding opens up a novel area of inquiry aimed at understanding the interactions between melanin genes and the production and display of carotenoid traits. Exploring differences in gene expression in these coloured feather patches could help to better understand the mechanisms underlying these associations.

## **Conclusions**

The extensive hybridization between red-shafted and yellow-shafted flickers, in combination with their clear phenotypic differences, has allowed us to separately connect phenotypic differences with individual genomic regions. Here, we identify a complex relationship linking pigmentation genes with modular plumage patches: we find that some genomic regions associate with multiple plumage patches, while others associate with a single plumage patch. We provide evidence for a novel link between

known melanin genes and carotenoid traits, and additionally identify *CYP2J19* as a strong candidate related to red versus yellow coloration differences. The patch-specific control of plumage coloration that we identify here, and increasingly found in other systems [reviewed in 19], suggests the possibility that colour diversity across birds could be created through selection to produce novel combinations of coloration genes each exerting control on a separate body patch.

## Methods

### *Sample collection and plumage scoring*

We obtained tissue samples from allopatric yellow-shafted flickers from New York ( $n = 5$ ) and Florida ( $n = 5$ ), and allopatric red-shafted flickers from Oregon ( $n = 5$ ) and California ( $n = 5$ ). These allopatric samples allowed us to characterize genomic differentiation between the flickers far from the region of current hybridization. Additionally, we sampled flickers with variable phenotypes ( $n = 48$ ) from a sampling transect across the hybrid zone in Nebraska and Colorado following the Platte River. See Table C2 for details on included samples.

Red-shafted and yellow-shafted flickers differ in colour across six distinct plumage characters: wing and tail, nuchal patch, crown, ear coverts, throat, and male malar stripe (Figure 3.1A) [29]. Hybrids exhibit various combinations of parental traits and traits intermediate to the parental traits (Figure C5). We scored plumage characters on a scale from 0 (pure yellow-shafted) to 4 (pure red-shafted) following a protocol slightly modified from [30] (Table C1), an approach that has been taken in many previous studies of the northern flicker hybrid zone [e.g., 39, 40, 56, 57]. We additionally calculated an overall phenotype score by adding the scores for the six individual traits

and standardizing to range from 0 to 1 to include both sexes (as all females lack a malar stripe). To ensure consistency, all scoring was conducted by a single individual (SMA). Hybrid flickers were chosen for genotyping in this study to maximize power in the GWA analyses: we selected a panel of hybrids that exhibited high variation in their combination of plumage traits (Figure C6).

#### *Reference genome assembly and annotation*

We sequenced and assembled the genome of a male yellow-shafted flicker (CUMV 57446). DNA was extracted using the Genra Puregene Tissue Kit following the manufacturer's protocol (Qiagen, California, USA) to isolate high molecular weight DNA. Three libraries were prepared and sequenced by the Cornell Weill Medical College genomics core facility—one 180bp fragment library and two mate-pair libraries (3kb and 8kb insert size)—across three lanes of an Illumina HiSeq2500 using the rapid run mode. The two mate-pair libraries were multiplexed on a single lane, while the fragment library was run across two lanes. The three lanes of sequencing generated ~481 million raw paired-end reads.

We assembled the reference genome using ALLPATHS-LG v.52488 [58] and assessed the quality of the assembly using QUAST v.4.0 [59] and BUSCO v.3.1.0 [60]. The reference assembly had a total length of 1.10 Gb distributed across 22,654 scaffolds with an N50 of 1.57 Mb. Using BUSCO, we searched for a set of 2,586 conserved, single-copy orthologs found across vertebrates. Our flicker reference genome contained a single, complete copy of 87.2% of these genes and a fragment of an additional 6.7%. Of the remaining genes, 0.4% were identified multiple times and 5.7% were completely missing. To obtain more precise information on chromosome position, we additionally assigned individual scaffolds to chromosomes based on assignments in the Ensembl

zebra finch (*Taeniopygia guttata*) reference genome v.3.2.4 release 91 [61] using the ‘Chromosemble’ function in Satsuma [62].

We annotated the reference genome using the MAKER v.2.31 pipeline [63]. We first used RepeatModeler v.1.0 [64] to generate a library of repetitive sequences present in the assembly and RepeatMasker v.4.0 [65] to soft mask these repeats. We then produced gene models by running two iterations of MAKER: the first iteration produces ab initio gene predictions, while the second iteration uses the gene models predicted from the first to improve performance. We used the Ensembl expressed sequence tags (ESTs) and protein database from the zebra finch (v.3.2.4 downloaded July 2017) [61] to train MAKER. This pipeline annotated a total of 12,141 genes (62.4% of the total). 97.3% of the proteins predicted by MAKER matched zebra finch proteins using BLAST [66].

#### *Low coverage re-sequencing and variant discovery*

We performed low coverage re-sequencing of the genomes of 68 flickers. Genomic DNA was extracted from each sample using DNeasy blood and tissue extraction kits (Qiagen, California, USA) and DNA concentrations were determined using a Qubit fluorometer (Life Technologies, California, USA). We used 200 ng of DNA from each sample to prepare individually barcoded libraries with a 550bp insert size following the protocol for the TruSeq Nano DNA Library Prep kit (Illumina, California, USA). The libraries were pooled into three groups and sequenced separately on an Illumina NextSeq500 lane (2×150bp) at the Cornell University Biotechnology Resource Center.

We assessed the quality of individual libraries using FastQC v.0.11.5 (<http://www.bioinformatics.babraham.ac.uk/projects/fastqc/>) and subsequently performed trimming, adapter removal, and initial quality filtering using

AdapterRemoval v.2.1.1 [67]. We required a minimum Phred quality score of 10 and merged overlapping paired-end reads. Filtered sequences were aligned to the northern flicker reference genome using Bowtie2 v.2.2.8 [68] with the very sensitive, local option. Alignment statistics were obtained from Qualimap v.2.2.1 [69]; the average alignment rate across all samples was 92.3%. Alignment rates were comparable across the different taxa: red-shafted flickers (91.9%), yellow-shafted flickers (91.8%), and hybrid flickers (92.6%). After filtering and aligning to the reference, the mean depth of coverage was 4.1X (range: 1.6X – 11.4X).

All resulting SAM files were converted to BAM files, sorted, and indexed using SAMtools v.1.3 [70]. We used Picard Tools v.2.8.2 (<https://broadinstitute.github.io/picard/>) to mark PCR duplicates and subsequently realigned around indels and fixed mate-pairs using GATK v.3.8.1 [71]. Variant discovery and genotyping for the 68 flickers was performed using the unified genotyper module in GATK. We used the following hard filtering parameters to remove variants from the output file:  $QD < 2.0$ ,  $FS > 40.0$ ,  $MQ < 20.0$ , and  $HaplotypeScore > 12.0$ . Subsequently, we filtered out variants that were not biallelic, had a minor allele frequency less than 5%, had a mean depth of coverage less than 3X or greater than 50X, or had more than 20% missing data across all individuals in the dataset. This pipeline produced 7,233,334 SNPs genotyped across all 68 flickers. We repeated the analyses with a variety of other SNP calling tools, including ANGSD [72] and the haplotype caller module in GATK [71]. We obtained qualitatively similar results across all analyses, and so here choose to present results from SNP calling with unified genotyper in GATK.

### *Population genomic analyses*

We visualized genetic clustering in the SNP dataset by performing a principal

component analysis (PCA) using the 'snpgdsPCA' function in the SNPRelate package [73] in R v.3.5.2 [74]. We characterized genome-wide patterns of divergence between allopatric red-shafted and allopatric yellow-shafted flickers by calculating  $F_{ST}$  using VCFtools v.0.1.16 [75] across 5 and 25 kb windows and individual SNPs. We visualized the results using the 'manhattan' function in the qqman package [76] in R.

### *Genotype-phenotype associations*

We used GEMMA v.0.98 (Genome-wide Efficient Mixed Model Association) [77] to associate genotypic variation at SNPs with variation in the six plumage traits for the 48 hybrid flickers while controlling for levels of relatedness. The GEMMA analysis requires a complete SNP dataset, so we first used BEAGLE v.4.1 [78] to impute missing data in the dataset. We transformed the imputed dataset into binary PLINK BED format using VCFtools v.0.1.16 [75] and PLINK v.1.09 [79]. We calculated a relatedness matrix in GEMMA using the centred relatedness matrix option (-gk 1). We conducted separate univariate linear mixed models for each phenotypic trait and used the Wald test (p\_wald) with a significance threshold of  $\alpha = 0.0000001$  ( $-\log_{10}(\alpha) = 7$ ) to identify significant associations between SNPs and phenotypes. To visualize the results, we used the 'manhattan' function in the qqman package [76] in R.

To validate the resulting associations, we repeated the GEMMA analysis using a dataset with randomized phenotypes. Instead of generating artificial phenotypic scores, we retained the true phenotypic scoring across all plumage traits, but randomized the individual assignment. If the GEMMA analysis was identifying real associations between genotype and phenotype, we expected few SNPs to exceed our significance threshold in this randomized analysis. In strong contrast to the true results, we found

only 5 significant SNPs across the six randomized analyses and no clustering of significant SNPs in any genomic region (Figure C8).

### *Functional characterization of candidate genes*

We compiled a list of genes within a 20kb buffer of SNPs significantly associated with phenotype using Geneious v.11.1.5 [80]. To characterize putative candidate genes, we used ontology information from the zebra finch Ensembl database [61] and functional information from the Uniprot database [81]. We additionally compared the identified list of genes to known genes involved in pigmentation. We were able to compare our gene list to 428 genes known to be involved in melanin pigmentation [8], and searched for the three gene families known to be involved in carotenoid pigmentation ( $\beta$ -carotene oxygenases, scavenger receptors, and cytochrome P450s) [24] and genes identified in recent analyses of pigmentation in other bird species [11, 12, 14, 16, 26].

### **References**

1. Cuthill I.C., Allen W.L., Arbuckle K., Caspers B., Chaplin G., Hauber M.E., Hill G.E., Jablonski N.G., Jiggins C.D., Kelber A., et al. 2017 The biology of color. *Science* **357**, eaan0221. (doi:10.1126/science.aan0221).
2. Hill G.E., McGraw K.J. 2006 *Bird Coloration: Function and Evolution*. Cambridge, Massachusetts: Harvard University Press.
3. Orteu A., Jiggins C.D. 2020 The genomics of coloration provides insights into adaptive evolution. *Nat. Rev. Genet.* **21**, 461-475. (doi:10.1038/s41576-020-0234-z).
4. Hoekstra H.E., Hirschmann R.J., Bunday R.A., Insel P.A., Crossland J.P. 2006 A single amino acid mutation contributes to adaptive beach mouse color pattern. *Science* **313**, 101-104. (doi:10.1126/science.1126121).

5. Hubbard J.K., Uy J.A., Hauber M.E., Hoekstra H.E., Safran R.J. 2010 Vertebrate pigmentation: from underlying genes to adaptive function. *Trends Genet.* **26**, 231-239. (doi:10.1016/j.tig.2010.02.002).
6. Lopes R.J., Johnson J.D., Toomey M.B., Ferreira M.S., Araujo P.M., Melo-Ferreira J., Andersson L., Hill G.E., Corbo J.C., Carneiro M. 2016 Genetic basis for red coloration in birds. *Curr. Biol.* **26**, 1427-1434. (doi:10.1016/j.cub.2016.03.076).
7. Mundy N.I. 2005 A window on the genetics of evolution: *MC1R* and plumage colouration in birds. *Proc. R. Soc. B* **272**, 1633-1640. (doi:10.1098/rspb.2005.3107).
8. Poelstra J.W., Vijay N., Hoepfner M.P., Wolf J.B. 2015 Transcriptomics of colour patterning and coloration shifts in crows. *Mol. Ecol.* **24**, 4617-4628. (doi:10.1111/mec.13353).
9. San-Jose L.M., Roulin A. 2017 Genomics of coloration in natural animal populations. *Phil. Trans. R. Soc. B* **372**, 20160337. (doi:10.1098/rstb.2016.0337).
10. Uy J.A., Cooper E.A., Cutie S., Concannon M.R., Poelstra J.W., Moyle R.G., Filardi C.E. 2016 Mutations in different pigmentation genes are associated with parallel melanism in island flycatchers. *Proc. R. Soc. B* **283**, 20160731. (doi:10.1098/rspb.2016.0731).
11. Brelsford A., Toews D.P.L., Irwin D.E. 2017 Admixture mapping in a hybrid zone reveals loci associated with avian feather coloration. *Proc. R. Soc. B* **284**, 20171106. (doi:10.1098/rspb.2017.1106).
12. Gao G., Xu M., Bai C., Yang Y., Li G., Xu J., Wei Z., Min J., Su G., Zhou X., et al. 2018 Comparative genomics and transcriptomics of *Chrysolophus* provide insights into the evolution of complex plumage coloration. *Gigascience* **7**, giy113. (doi:10.1093/gigascience/giy113).
13. Kim K.W., Jackson B.C., Zhang H., Toews D.P.L., Taylor S.A., Greig E.I., Lovette I.J., Liu M.M., Davison A., Griffith S.C., et al. 2019 Genetics and evidence for balancing selection of a sex-linked colour polymorphism in a songbird. *Nat. Commun.* **10**, 1852. (doi:10.1038/s41467-019-09806-6).
14. Toews D.P.L., Taylor S.A., Vallender R., Brelsford A., Butcher B.G., Messer P.W., Lovette I.J. 2016 Plumage genes and little else distinguish the genomes of hybridizing warblers. *Curr. Biol.* **26**, 2313-2318. (doi:10.1016/j.cub.2016.06.034).

15. Toomey M.B., Marques C.I., Andrade P., Araujo P.M., Sabatino S., Gazda M.A., Afonso S., Lopes R.J., Corbo J.C., Carneiro M. 2018 A non-coding region near *Follistatin* controls head colour polymorphism in the Gouldian finch. *Proc. R. Soc. B* **285**, 20181788. (doi:10.1098/rspb.2018.1788).
16. Wang S., Rohwer S., de Zwaan D.R., Toews D.P.L., Lovette I.J., Mackenzie J., Irwin D.E. 2020 Selection on a small genomic region underpins differentiation in multiple color traits between two warbler species. *Evol. Lett.* (doi:10.1002/evl3.198).
17. Mazo-Vargas A., Concha C., Livraghi L., Massardo D., Wallbank R.W.R., Zhang L., Papador J.D., Martinez-Najera D., Jiggins C.D., Kronforst M.R., et al. 2017 Macroevolutionary shifts of *WntA* function potentiate butterfly wing-pattern diversity. *Proc. Natl. Acad. Sci. USA* **114**, 10701-10706. (doi:10.1073/pnas.1708149114).
18. Campagna L., Repenning M., Silveira L.F., Fontana C.S., Tubaro P.L., Lovette I.J. 2017 Repeated divergent selection on pigmentation genes in a rapid finch radiation. *Sci. Adv.* **3**, e1602404. (doi:10.1126/sciadv.1602404).
19. Funk E.R., Taylor S.A. 2019 High-throughput sequencing is revealing genetic associations with avian plumage color. *Auk* **136**, 1-7. (doi:10.1093/auk/ukz048/5585843).
20. Stryjewski K.F., Sorenson M.D. 2017 Mosaic genome evolution in a recent and rapid avian radiation. *Nat. Ecol. Evol.* **1**, 1912-1922. (doi:10.1038/s41559-017-0364-7).
21. Van Belleghem S.M., Rastas P., Papanicolaou A., Martin S.H., Arias C.F., Supple M.A., Hanly J.J., Mallet J., Lewis J.J., Hines H.M., et al. 2017 Complex modular architecture around a simple toolkit of wing pattern genes. *Nat. Ecol. Evol.* **1**, 0052. (doi:10.1038/s41559-016-0052).
22. Zhang L., Mazo-Vargas A., Reed R.D. 2017 Single master regulatory gene coordinates the evolution and development of butterfly color and iridescence. *Proc. Natl. Acad. Sci. USA* **114**, 10707-10712. (doi:10.1073/pnas.1709058114).
23. Rodriguez A., Mundy N.I., Ibanez R., Prohl H. 2020 Being red, blue and green: the genetic basis of coloration differences in the strawberry poison frog (*Oophaga pumilio*). *BMC Genomics* **21**, 301. (doi:10.1186/s12864-020-6719-5).
24. Toews D.P.L., Hofmeister N.R., Taylor S.A. 2017 The evolution and genetics of carotenoid processing in animals. *Trends Genet.* **33**, 171-182. (doi:10.1016/j.tig.2017.01.002).

25. Walsh N., Dale J., McGraw K.J., Pointer M.A., Mundy N.I. 2012 Candidate genes for carotenoid coloration in vertebrates and their expression profiles in the carotenoid-containing plumage and bill of a wild bird. *Proc. R. Soc. B* **279**, 58-66. (doi:10.1098/rspb.2011.0765).
26. Abolins-Abols M., Kornobis E., Ribeca P., Wakamatsu K., Peterson M.P., Ketterson E.D., Mila B. 2018 Differential gene regulation underlies variation in melanic plumage coloration in the dark-eyed junco (*Junco hyemalis*). *Mol. Ecol.* **27**, 4501-4515. (doi:10.1111/mec.14878).
27. Cooke T.F., Fischer C.R., Wu P., Jiang T.X., Xie K.T., Kuo J., Doctorov E., Zehnder A., Khosla C., Chuong C.M., et al. 2017 Genetic mapping and biochemical basis of yellow feather pigmentation in budgerigars. *Cell* **171**, 427-439.e421. (doi:10.1016/j.cell.2017.08.016).
28. Gazda M.A., Araújo P.M., Lopes R.J., Toomey M.B., Andrade P., Afonso S., Marques C., Nunes L., Pereira P., Trigo S., et al. 2020 A genetic mechanism for sexual dichromatism in birds. *Science* **368**, 1270-1274. (doi:10.1126/science.aba0803).
29. Wiebe K.L., Moore W.S. 2017 Northern Flicker (*Colaptes auratus*), version 3.0. In *The Birds of North America* (ed. Rodewald P.G.). Ithaca, New York, USA, Cornell Lab of Ornithology.
30. Short L.L. 1965 Hybridization in the flickers (*Colaptes*) of North America. *Bull. Am. Mus. Nat. Hist. N. Y.* **129**, 307-428.
31. Hudon J., Wiebe K.L., Pini E., Stradi R. 2015 Plumage pigment differences underlying the yellow-red differentiation in the northern flicker (*Colaptes auratus*). *Comp. Biochem. Phys. B* **183**, 1-10. (doi:10.1016/j.cbpb.2014.12.006).
32. Wiebe K.L., Vitousek M.N. 2015 Melanin plumage ornaments in both sexes of northern flicker are associated with body condition and predict reproductive output independent of age. *Auk* **132**, 507-517. (doi:10.1642/auk-14-281.1).
33. Aguilon S.M., Campagna L., Harrison R.G., Lovette I.J. 2018 A flicker of hope: genomic data distinguish northern flicker taxa despite low levels of divergence. *Auk* **135**, 748-766. (doi:10.1642/auk-18-7.1).
34. Fletcher S.D., Moore W.S. 1992 Further analysis of allozyme variation in the northern flicker, in comparison with mitochondrial DNA variation. *Condor* **94**, 988-991. (doi:10.2307/1369295).

35. Grudzien T.A., Moore W.S. 1986 Genetic differentiation between the yellow-shafted and red-shafted subspecies of the northern flicker. *Biochem. Syst. Ecol.* **14**, 451-453. (doi:10.1016/0305-1978(86)90033-5).
36. Grudzien T.A., Moore W.S., Cook J.R., Tagle D. 1987 Genic population structure and gene flow in the northern flicker (*Colaptes auratus*) hybrid zone. *Auk* **104**, 654-664. (doi:10.1093/auk/104.4.654).
37. Manthey J.D., Geiger M., Moyle R.G. 2017 Relationships of morphological groups in the northern flicker superspecies complex (*Colaptes auratus* & *C. chrysoides*). *Syst. Biodivers.* **15**, 183-191. (doi:10.1080/14772000.2016.1238020).
38. Moore W.S., Graham J.H., Price J.T. 1991 Mitochondrial DNA variation in the northern flicker (*Colaptes auratus*, Aves). *Mol. Biol. Evol.* **8**, 327-344. (doi:10.1093/oxfordjournals.molbev.a040656).
39. Moore W.S., Buchanan D.B. 1985 Stability of the northern flicker hybrid zone in historical times: implications for adaptive speciation theory. *Evolution* **39**, 135-151. (doi:10.2307/2408523).
40. Moore W.S. 1987 Random mating in the northern flicker hybrid zone: implications for the evolution of bright and contrasting plumage patterns in birds. *Evolution* **41**, 539-546. (doi:10.1111/j.1558-5646.1987.tb05824.x).
41. Hudon J., Wiebe K.L., Stradi R. 2021 Disruptions of feather carotenoid pigmentation in a subset of hybrid northern flickers (*Colaptes auratus*) may be linked to genetic incompatibilities. *Comp. Biochem. Phys. B* **251**, 110510. (doi:10.1016/j.cbpb.2020.110510).
42. Aguillon S.M., Lovette I.J. 2019 Change the specific/subspecific/morphological group name of the red-shafted flicker from *cafer* to *lathamii*. *AOS North American Classification Committee 2019-A-10*, 66-71.
43. Mundy N.I., Stapley J., Bennison C., Tucker R., Twyman H., Kim K.-W., Burke T., Birkhead T.R., Andersson S., Slate J. 2016 Red carotenoid coloration in the zebra finch is controlled by a cytochrome P450 gene cluster. *Curr. Biol.* **26**, 1435-1440. (doi:10.1016/j.cub.2016.04.047).
44. Hooper D.M., Griffith S.C., Price T.D. 2019 Sex chromosome inversions enforce reproductive isolation across an avian hybrid zone. *Mol. Ecol.* **28**, 1246-1262. (doi:10.1111/mec.14874).

45. Kirschel A.N.G., Nwankwo E.C., Pierce D., Lukhele S.M., Moysi M., Ogolowa B.O., Hayes S.C., Monadjem A., Brelsford A. 2020 *CYP2J19* mediates carotenoid colour introgression across a natural avian hybrid zone. *Mol. Ecol.* (doi:10.1111/mec.15691).
46. Twyman H., Prager M., Mundy N.I., Andersson S. 2018 Expression of a carotenoid-modifying gene and evolution of red coloration in weaverbirds (Ploceidae). *Mol. Ecol.* **27**, 449-458. (doi:10.1111/mec.14451).
47. Khalil S., Welklin J.F., McGraw K.J., Boersma J., Schwabl H., Webster M.S., Karubian J. 2020 Testosterone regulates *CYP2J19*-linked carotenoid signal expression in male red-backed fairywrens (*Malurus melanocephalus*). *Proc. R. Soc. B* **287**, 20201687. (doi:10.1098/rspb.2020.1687).
48. Hill G.E., McGraw K.J. 2006 *Bird Coloration: Mechanisms and Measurements*. Cambridge, Massachusetts: Harvard University Press.
49. Test F.H. 1942 The nature of red, yellow, and orange pigments in woodpeckers of the genus *Colaptes*. *Univ. Calif. Publ. Zool.* **46**, 371-390.
50. Hofmann C.M., McGraw K.J., Cronin T.W., Omland K.E. 2007 Melanin coloration in New World orioles I: carotenoid masking and pigment dichromatism in the orchard oriole complex. *J. Avian Biol.* **38**, 163-171. (doi:10.1111/j.2007.0908-8857.03803.x).
51. McGraw K.J., Wakamatsu K., Clark A.B., Yasukawa K. 2004 Red-winged blackbirds *Agelaius phoeniceus* use carotenoids and melanin pigments to color their epaulets. *J. Avian Biol.* **35**, 543-550. (doi:10.1111/j.0908-8857.2004.03345.x).
52. Bonser R.H.C. 1995 Melanin and the abrasion resistance of feathers. *Condor* **97**, 590-591.
53. Kose M., Møller A.P. 1999 Sexual selection, feather breakage and parasites: the importance of white spots in the tail of the barn swallow (*Hirundo rustica*). *Behav. Ecol. Sociobiol.* **45**, 430-436. (doi:10.1007/s002650050581).
54. Ward J.M., Blount J.D., Ruxton G.D., Houston D.C. 2002 The adaptive significance of dark plumage for birds in desert environments. *Ardea* **90**, 311-323.
55. Peele A.M., Burt E.H., Jr., Schroeder M.R., Greenberg R.S. 2009 Dark color of the coastal plain swamp sparrow (*Melospiza georgiana nigrescens*) may be an evolutionary

response to occurrence and abundance of salt-tolerant feather-degrading bacillin in its plumage. *Auk* **126**, 531-535. (doi:10.1525/auk.2009.08142).

56. Flockhart D.T.T., Wiebe K.L. 2007 The role of weather and migration in assortative pairing within the northern flicker (*Colaptes auratus*) hybrid zone. *Evol. Ecol. Res.* **9**, 887-903.

57. Wiebe K.L. 2000 Assortative mating by color in a population of hybrid northern flickers. *Auk* **117**, 525-529.

58. Gnerre S., MacCallum I., Przybylski D., Ribeiro F.J., Burton J.N., Walker B.J., Sharpe T., Hall G., Shea T.P., Sykes S., et al. 2011 High-quality draft assemblies of mammalian genomes from massively parallel sequence data. *Proc. Natl. Acad. Sci. USA* **108**, 1513-1518. (doi:10.1073/pnas.1017351108).

59. Gurevich A., Saveliev V., Vyahhi N., Tesler G. 2013 QUASt: quality assessment tool for genome assemblies. *Bioinformatics* **29**, 1072-1075. (doi:10.1093/bioinformatics/btt086).

60. Simão F.A., Waterhouse R.M., Ioannidis P., Kriventseva E.V., Zdobnov E.M. 2015 BUSCO: assessing genome assembly and annotation completeness with single-copy orthologs. *Bioinformatics* **31**, 3210-3212. (doi:10.1093/bioinformatics/btv351).

61. Aken B.L., Achuthan P., Akanni W., Amode M.R., Bernsdorff F., Bhai J., Billis K., Carvalho-Silva D., Cummins C., Clapham P., et al. 2017 Ensembl 2017. *Nucleic Acids Res.* **45**, D635-D642. (doi:10.1093/nar/gkw1104).

62. Grabherr M.G., Russell P., Meyer M., Mauceli E., Alföldi J., Di Palma F., Lindblad-Toh K. 2010 Genome-wide synteny through highly sensitive sequence alignment: Satsuma. *Bioinformatics* **26**, 1145-1151. (doi:10.1093/bioinformatics/btq102).

63. Cantarel B.L., Korf I., Robb S.M., Parra G., Ross E., Moore B., Holt C., Sánchez Alvarado A., Yandell M. 2008 MAKER: an easy-to-use annotation pipeline designed for emerging model organism genomes. *Genome Res.* **18**, 188-196. (doi:10.1101/gr.6743907).

64. Smit A.F.A., Hubley R. 2008 RepeatModeler Open-1.0. (<http://www.repeatmasker.org>).

65. Smit A.F.A., Hubley R., Green P. 2013 RepeatMasker Open-4.0. (<http://www.repeatmasker.org>).

66. Altschul S.F., Gish W., Miller W., Myers E.W., Lipman D.J. 1990 Basic Local Alignment Search Tool. *J. Mol. Biol.* **215**, 403-410. (doi:10.1016/S0022-2836(05)80360-2).
67. Lindgreen S. 2012 AdapterRemoval: easy cleaning of next-generation sequencing reads. *BMC Res. Notes* **5**, 337. (doi:10.1186/1756-0500-5-337).
68. Langmead B., Salzberg S.L. 2012 Fast gapped-read alignment with Bowtie 2. *Nat. Methods* **9**, 357-359. (doi:10.1038/nmeth.1923).
69. Okonechnikov K., Conesa A., García-Alcalde F. 2016 Qualimap 2: advanced multi-sample quality control for high-throughput sequencing data. *Bioinformatics* **32**, 292-294. (doi:10.1093/bioinformatics/btv566).
70. Li H., Handsaker B., Wysoker A., Fennell T., Ruan J., Homer N., Marth G., Abecasis G., Durbin R., 1000 Genome Project Data Processing Subgroup. 2009 The Sequence Alignment/Map format and SAMtools. *Bioinformatics* **25**, 2078-2079. (doi:10.1093/bioinformatics/btp352).
71. McKenna A., Hanna M., Banks E., Sivachenko A., Cibulskis K., Kernytsky A., Garimella K., Altshuler D., Gabriel S., Daly M., et al. 2010 The Genome Analysis Toolkit: a MapReduce framework for analyzing next-generation DNA sequencing data. *Genome Res.* **20**, 1297-1303. (doi:10.1101/gr.107524.110).
72. Korneliussen T.S., Albrechtsen A., Nielsen R. 2014 ANGSD: Analysis of Next Generation Sequencing Data. *BMC Bioinformatics* **15**, 356. (doi:10.1186/s12859-014-0356-4).
73. Zheng X., Levine D., Shen J., Gogarten S.M., Laurie C., Weir B.S. 2012 A high-performance computing toolset for relatedness and principal component analysis of SNP data. *Bioinformatics* **28**, 3326-3328. (doi:10.1093/bioinformatics/bts606).
74. R Core Team. 2018 R: A language and environment for statistical computing. (Vienna, Austria, R Foundation for Statistical Computing).
75. Danecek P., Auton A., Abecasis G., Albers C.A., Banks E., DePristo M.A., Handsaker R.E., Lunter G., Marth G.T., Sherry S.T., et al. 2011 The variant call format and VCFtools. *Bioinformatics* **27**, 2156-2158. (doi:10.1093/bioinformatics/btr330).
76. Turner S.D. 2014 qqman: an R package for visualizing GWAS results using Q-Q and manhattan plots. bioRxiv. (doi:10.1101/005165).

77. Zhou X., Stephens M. 2012 Genome-wide efficient mixed-model analysis for association studies. *Nat. Genet.* **44**, 821-824. (doi:10.1038/ng.2310).
78. Browning S.R., Browning B.L. 2007 Rapid and accurate haplotype phasing and missing-data inference for whole-genome association studies by use of localized haplotype clustering. *Am. J. Hum. Genet.* **81**, 1084-1097. (doi:10.1086/521987).
79. Purcell S., Neale B., Todd-Brown K., Thomas L., Ferreira M., Bender D., Maller J., Sklar P., de Bakker P., Daly M., et al. 2007 PLINK: a toolset for whole-genome association and population-based linkage analysis. *Am. J. Hum. Genet.* **81**, 559-575. (doi:10.1086/519795).
80. Kearse M., Moir R., Wilson A., Stones-Havas S., Cheung M., Sturrock S., Buxton S., Cooper A., Markowitz S., Duran C., et al. 2012 Geneious Basic: an integrated and extendable desktop software platform for the organization and analysis of sequence data. *Bioinformatics* **28**, 1647-1649. (doi:10.1093/bioinformatics/bts199).
81. UniProt Consortium. 2019 UniProt: a worldwide hub of protein knowledge. *Nucleic Acids Res.* **47**, D506-D515. (doi:10.1093/nar/gky1049)

## CHAPTER 4

### INTERACTING GENOMIC REGIONS SHAPE THE COLORATION OF MULTIPLE PHENOTYPES IN THE NORTHERN FLICKER

#### **Abstract**

The number of genes related to coloration in birds has been rapidly increasing, aided by systems with low levels of baseline divergence. It has become clear that multiple genomic regions are often related to color differences in particular plumage patches, yet to date, few studies have assessed the role of epistatic interactions between these genomic regions. Here, we take advantage of the hybridizing yellow-shafted and red-shafted flickers to assess epistatic interactions between genomic regions that produce the ear covert (melanin) and shaft (carotenoid) color. Using targeted sequencing to obtain high-quality genotype calls, we first validate the genotype-phenotype relationships of SNPs found previously using low-coverage whole genome sequencing. We then use these genotype calls to identify significant epistatic interactions in producing color in both the ear coverts and the shaft. This represents the first time that epistatic interactions have been identified in traits produced with carotenoid or pheomelanin pigments in wild birds. Although in the majority of cases we are unable to identify specific genes within the interacting genomic regions, in the two interactions where we can, we find a known carotenoid gene (CYP2J19) interacting with known melanin genes (MFSD12, FKBP8) to produce the shaft color, adding an additional layer to the novel relationship we identified previously linking melanin genes to carotenoid traits in flickers.

## Introduction

Coloration is an important phenotype driving both natural and sexual selection in animals (Hill and McGraw 2006; Cuthill et al. 2017) and our understanding of the genetic basis of coloration differences has been increasing rapidly in recent years (reviewed in Orteu and Jiggins 2020). Birds with low levels of background genomic divergence have provided particularly useful non-model systems for associating phenotypes with particular genotypes (reviewed in Funk and Taylor 2019), as they provide the opportunity to conduct admixture mapping (e.g., Brelsford et al. 2017; Hooper et al. 2019; Aguillon et al. 2021) and anonymous genomic scans (e.g., Toews et al. 2016; Campagna et al. 2017; Stryjewski and Sorenson 2017). Although our understanding of the genetic basis of both melanin (blacks, grays, browns) and carotenoid (reds, oranges, yellows) pigmentation has increased, we still know comparatively more about the endogenously produced melanin plumage patches than we do about the exogenously obtained and biochemically processed carotenoid plumage patches (Hubbard et al. 2010; Toews et al. 2017).

Patch-specific control of plumage coloration, where a particular gene or genomic region controls the coloration of a discrete patch of the body (rather than whole-body coloration), seems to be a general pattern in birds (Funk and Taylor 2019). In fact, shuffling these genomic regions into different combinations may be one of the ways plumage diversification has occurred in birds. Across studies, there are occasionally single genomic regions identified as being important in producing the color of a particular plumage patch (Lopes et al. 2016; Mundy et al. 2016; Uy et al. 2016; Cooke et al. 2017; Toomey et al. 2018; Vickrey et al. 2018; Kim et al. 2019; Gazda et al. 2020a; Gazda et al. 2020b; Wang et al. 2020), often in birds that have been subjected to extensive artificial selection or small population sizes. More commonly in wild birds,

multiple genomic regions are found to be important in producing coloration differences (Toews et al. 2016; Brelsford et al. 2017; Campagna et al. 2017; Stryjewski and Sorenson 2017; Abolins-Abols et al. 2018; Hooper et al. 2019; Knief et al. 2019; Aguillon et al. 2021; Semenov et al. 2021).

Despite the clear evidence for multiple regions being important in the production of coloration phenotypes, only two studies to date have assessed the role of epistatic interactions in the production of coloration in wild birds (Knief et al. 2019; Semenov et al. 2021), though more is known in other non-avian taxa about such epistatic interactions (e.g., butterflies: Mazo-Vargas et al. 2017; Lewis et al. 2019). In both carrion/hooded crows (*Corvus corone*, *C. corvix*; (Knief et al. 2019)) and white wagtails (*Motacilla alba alba*, *M. a. personata*; (Semenov et al. 2021)), there are two genomic regions that are strongly associated with differences in color, and epistatic interactions between these regions play a role in producing the observed color phenotypes. These two studies represent important steps forward in our understanding of avian coloration genetics, and demonstrate the likely common role for epistasis in bird coloration. However, these two studies both focus on melanin pigmentation and more specifically on eumelanin (responsible for black and gray pigments). So despite these advances, there is still little information currently available on how regions of the genome interact to produce coloration in birds in general.

Here, we leverage the distinct coloration differences and extensive hybridization between yellow-shafted (*Colaptes auratus auratus*) and red-shafted (*C. a. cafer*<sup>7</sup>) flickers to

---

<sup>7</sup> The subspecific epithet of the red-shafted flicker is based on a term that is an extreme racial slur against Black Africans, particularly in South Africa. We include the official scientific name here, but purposefully refer to the flickers only by their common names in the remainder of the manuscript. We have elsewhere proposed the name be officially changed to *Colaptes auratus lathamii* (Aguillon and Lovette 2019), but this name is not yet officially accepted.

assess the involvement of epistatic interactions in producing coloration across multiple body patches created with both carotenoid and melanin pigments. Flickers are common woodpeckers distributed across wooded areas of North America (Wiebe and Moore 2020), and come into secondary contact in the Great Plains where hybridization occurs readily (Short 1965; Moore 1987). The two taxa differ in coloration across a number of plumage patches that are derived from melanin and carotenoid pigments (Hudon et al. 2015). Our previous work in this system has identified the extremely low levels of genomic divergence between these two taxa (Aguillon et al. 2018) and we used this low background differentiation to associate phenotypic differences with specific genomic regions (Aguillon et al. 2021). In this study, we focus on two traits where we have previously identified multiple genomic regions associated with coloration: the eponymous “shaft” (wing and tail) color, and ear covert color. The shaft varies from bright yellow in yellow-shafted flickers to salmon red in red-shafted flickers, and it is a carotenoid-based trait, whereas the melanin-based ear coverts vary from tan in yellow-shafted flickers to gray in red-shafted flickers (likely resulting from a difference in pheomelanin content).

We conduct targeted sequencing to generate high-quality genotype calls of markers previously found to be associated with the shaft and ear covert colors. We thereby assayed a large panel of individuals from allopatric populations of both taxa and from the region of the hybrid zone in Nebraska and Colorado. We first verify the previously identified genotype-phenotype associations using this larger panel of individuals. We then test for additive and epistatic interactions between all two-locus comparisons within each phenotypic trait. This represents the first test of epistasis in multiple traits in the same avian system and the first test in coloration based on carotenoid and pheomelanin pigmentation.

## Methods

### *Sampling and phenotypic scoring*

Yellow-shafted and red-shafted flickers differ primarily across six plumage characteristics: shaft color, crown color, ear covert color, throat color, male malar stripe color, and the presence/absence of the nuchal patch (Short 1965). Hybrids exhibit combinations of the six parental traits, as well as colors intermediate to the parentals. We have previously taken advantage of this mixing to identify regions of the genome involved in differences in the shaft, ear coverts, malar stripe, and nuchal patch (Aguillon et al. 2021). We obtained blood or tissue samples from 190 flickers, and focus here on a subset of 136 individuals with high data quality that are from either a transect across the hybrid zone (N=103) or allopatric populations (N=33; Table D1). We scored the color of the ear coverts and shaft of flickers sampled in the hybrid zone on a categorical scale from 0 (pure yellow-shafted) to 4 (pure red-shafted) following a protocol slightly modified from Short (1965) and used elsewhere (Moore and Buchanan 1985; Moore 1987; Aguillon et al. 2021). For individuals from allopatric populations, we assume a score of 0 for yellow-shafted flickers and 4 for red-shafted flickers, which seems appropriate given the much lower variability within the allopatric populations compared to between the populations.

### *Molecular methods*

Genomic DNA was extracted from each sample using DNeasy blood and tissue extraction kits following the manufacturer's protocol (Qiagen, California, USA). DNA concentrations were determined using a Qubit fluorometer (Life Technologies, California, USA) and we diluted all samples to 20-30 ng/ $\mu$ l. We performed targeted sequencing of regions of the genome identified as significantly associated with

coloration differences in the ear coverts and shaft in Aguillon et al. (2021) by performing a multiplex PCR (Table D2; Figure D1, D2). First, we developed forward and reverse primers from the yellow-shafted flicker reference genome (Aguillon et al. 2021) that flanked SNPs of interest using the primer design tool in Geneious Prime v.2020.1.2. (www.geneious.com) and ordered through Integrated DNA Technologies (New Jersey, USA). Primers optimally were 20bp in length with a melting point between 58-66°C and produced a product of ~300bp in size. To allow for multiplexing, the primers included an adaptor overhang for subsequent barcoding. Next, we conducted the first round of PCR which amplifies these targeted regions for each individual sample. We suspended primers at a 250  $\mu$ M concentration in TE buffer and then used 1.4  $\mu$ l of each primer to produce a primer mix (plus 1xTE to reach a final volume of 500  $\mu$ l). For each reaction, we combined 2  $\mu$ l DNA, 5  $\mu$ l 2X Qiagen Multiplex PCR Master Mix, 0.3  $\mu$ l primer mix, and 3.7  $\mu$ l water (for a total reaction volume of 11  $\mu$ l) and performed the PCR under the following thermocycling profile: 95°C for 5 minutes followed by 30 cycles at 95°C for 30 sec, 62°C for 90 sec, and 72°C for 30 sec, with a final extension at 68°C for 10 min. Concentrations were quantified for a handful of PCR products across each plate using the Qubit fluorometer and the plates were then diluted to a concentration of 2-5 ng/ $\mu$ l. Next, we conducted the second round of PCR which uses the adaptor overhangs on the primers to attach uniquely identifiable Illumina barcode pairs to each sample. For each reaction, we combined 2  $\mu$ l of the product from the first PCR, 1.1  $\mu$ l 10X Buffer (ThermoFisher Scientific, Massachusetts, USA), 0.33  $\mu$ l 50 mM MgCl<sub>2</sub>, 0.22  $\mu$ l 10 mM dNTPs, 0.05  $\mu$ l Platinum Taq DNA Polymerase (ThermoFisher Scientific), and 4.3  $\mu$ l water (for a total reaction volume of 8  $\mu$ l) and performed the PCR under the following thermocycling profile: 95°C for 2 min followed by 7 cycles at 95°C for 30 sec, 55°C for 30 sec, and 72°C for 30 sec, 1 cycle of 95°C for 10 sec, 55°C for 3 min with a 0.1°C/per

second ramp, 72°C for 30 sec, and a final extension at 72°C for 5 min. After this final PCR, we pooled all samples and performed a 1:1 cleanup using Serapure beads to remove enzymes and small DNA fragments. Samples were visualized on a fragment Bioanalyzer (Agilent Technologies, California, USA) to assess the success of the PCR and were then sequenced on one Illumina MiSeq lane (single-end, 300bp) at the Cornell University Biotechnology Resource Center.

#### *Quality filtering and variant calling*

We performed trimming and adaptor removal using cutadapt v.2.1 (Martin 2011). We subsequently assessed the quality of individual samples using FastQC v.0.11.8 ([www.bioinformatics.babraham.ac.uk/projects/fastqc](http://www.bioinformatics.babraham.ac.uk/projects/fastqc)) and MultiQC v.1.7 (Ewels et al. 2016). We made a reference FASTA file from the reference genome of the yellow-shafted flicker (Aguillon et al. 2021) for each targeted region and aligned reads to this reference using Bowtie2 v.2.3.5 (Langmead and Salzberg 2012) with the sensitive alignment option. All resulting SAM files were converted to BAM files and sorted using SAMtools v.1.11 (Li et al. 2009). We used the multibamqc option within QualiMap v.2.2.1 (Okonechnikov et al. 2016) to run a final quality check on all samples. Individuals with an average sequencing length less than 200bp were removed. These samples also had fewer sequencing reads, lower percent duplications, and higher percent failed sequencing reads, so we believe this is a useful proxy for overall sample sequencing quality. Variant discovery and genotyping on the remaining samples was performed using bcftools (Li 2011) within the SamTools package. We then used VCFtools v.0.1.16 (Danecek et al. 2011) to output only the SNP of interest from each targeted region.

### *Genetic structure in the dataset*

All data processing and visualizations, except where indicated otherwise, use the tidyverse package (Wickham et al. 2019) in R v.3.6.2 (R Core Team 2018). To explore genetic clustering in the dataset, we first performed a principal components analysis (PCA) using the 'snpgdsPCA' function in the SNPRelate package (Zheng et al. 2012) in R. We performed analyses separately for the loci associated with ear covert and shaft color. We ran linear models comparing the PC1 values to the trait score using the 'lm' function in the base stats package in R. To identify genetic structure across the samples, we additionally used STRUCTURE v.2.3.2 (Pritchard et al. 2000) to assign individuals to genetic clusters. We performed this analysis separately for the loci for ear covert and shaft color. Rather than grouping individuals based on their location of origin, we instead grouped individuals based on their trait color score. Within STRUCTURE we used the admixture ancestry model with correlated allele frequencies and estimated the allele frequency prior for the data ( $\lambda=1.3754$  for shaft color and  $\lambda=1.0408$  for ear covert color) with an initial run of  $K=1$ . We conducted 10 runs for each value of  $K=1-5$  with 60,000 generations following a burn-in of 20,000 generations. We determined the most likely value of  $K$  using the  $\Delta K$  method (Evanno et al. 2005) implemented in STRUCTURE HARVESTER v.0.6.94 (Earl and vonHoldt 2011). We averaged results across the runs using the 'full search' option within CLUMPP v.1.1.2 (Jakobsson and Rosenberg 2007) and visualized the results using DISTRUCT v.1.1 (Rosenberg 2003) and a custom R script.

### *Interactions between genomic regions*

To understand how different loci interact with each other to produce the phenotype, we fitted a series of additive linear models using the 'lm' function in the stats package in

base R following the approach used in Knief et al. (2019). Separately for loci involved in the ear covert color and the shaft color, we first fit additive models for all potential two-locus combinations. We then fit base additive models with an additional interaction term to identify any epistatic interactions. To test for significant differences between the additive and epistatic models for each two-locus combination, we used the ‘anova’ function in the stats package in base R (comparing the additive model to each one-locus model, and the interaction model to the additive model). Because the number of loci in our dataset results in a prohibitively large number of two-locus comparisons and the simultaneous problem of multiple statistical tests (particularly so for the shaft color loci), we limited our comparisons to a single locus for each genomic region (Table D3). These different genomic regions largely corresponded to different chromosomes, except for chromosome 28 where we define two separate regions (see Table D2). For each region, we selected the locus with the highest significance score in the GWA analysis and the least amount of missing data (as it is necessary to have a complete dataset to statistically compare the two models). It was necessary to remove a single individual from the interaction analysis due to missing data at one of the chosen loci. We used the multiple  $R^2$  from the linear models to estimate the variance explained by additive or interaction effects.

## **Results**

### *Quality of sequencing results*

We obtained genotypes for 54 SNPs of interest for the ear covert (N=9) and shaft (N=45) color in 136 individuals. Mean sequencing coverage for individuals across the dataset was 399X (Figure D3A), which did not differ between allopatric and hybrid zone

samples (371X for allopatric, 408X for hybrid zone;  $p = 0.537$ ). Sequencing coverage was variable across the SNPs of interest (Figure D4; overall mean = 388X), but because we removed individuals with low quality data, levels of missing data were quite low (mean = 3.34%; Figure D3B). The relationships between individual SNP genotypes and phenotypes with our expanded sampling (ear coverts: Figure D1, shaft: Figure D2) validate the genotype-phenotype associations reported in Aguillon et al. (2021).

### *Genetic structure*

PCAs based on the SNPs associated with ear covert color (Figure 4.1A) and shaft color (Figure 4.1C) separated individuals along PC1 based on phenotype. Individuals with higher PC1 scores had more yellow-shafted-like phenotypes and individuals with lower PC1 scores had more red-shafted-like phenotypes (ear coverts: Figure D5A,  $\rho = -0.7322$ ,  $p < 2.2 \times 10^{-16}$ ; shaft: Figure D5B,  $\rho = -0.8298$ ,  $p < 2.2 \times 10^{-16}$ ). PC1 explained a large proportion of the variation for both the ear coverts (43.93%) and the shaft (40.69%) color.

Using the  $\Delta K$  method, STRUCTURE optimally assigned individuals to 2 genetic clusters for both the ear covert color (Figure 4.1B, D6) and the shaft color (Figure 4.1D, D6). These genetic clusters distinguished individuals based on phenotype such that individuals with yellow-shafted traits (score = 0) had higher ancestry proportions for one cluster, and individuals with red-shafted traits (score = 4) had higher ancestry proportions for the alternative cluster (STRUCTURE plots separated out by individuals are shown in Figure D6, and summaries within phenotype scores are shown in Figure 4.1B and 4.1D). Individuals with intermediate traits (score = 1, 2, or 3) had correspondingly intermediate ancestry proportions for the two clusters.

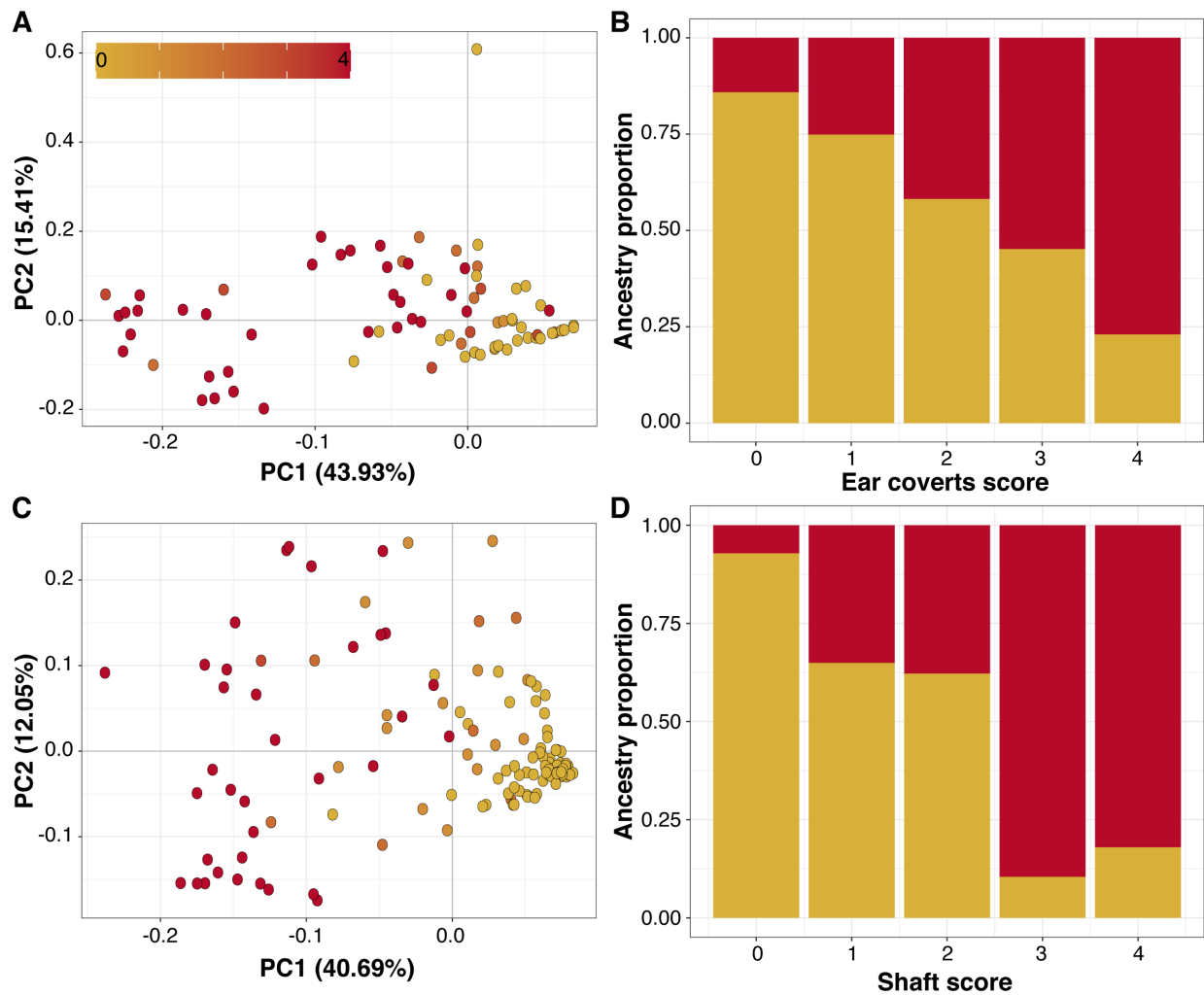


**Figure 4.1.** Genetic structuring within the dataset is explained by ear covert color (top panels) and shaft color (bottom panels). (A, C) Principal component analyses separate individuals along PC1 based on phenotype score (indicated by the color of the points; legend in panel A). Figure D5 shows the significant correlations between PC1 and phenotype. (B, D) STRUCTURE analyses identified  $K=2$  as the optimal number of genetic clusters and separated individuals based on their phenotype score. The bar plots summarize the ancestry proportions of all individuals at each phenotype score. Figure D6 shows the STRUCTURE plots partitioned by individuals.

### *Interactions between genomic regions*

We selected a representative SNP from each genomic region as described in the Methods to conduct pairwise comparisons between regions (Table D3). Additive models for all two-locus comparisons were statistically better at explaining trait differences than either single-locus model for both ear covert (Table 4.1) and shaft (Table 4.2) color (i.e.,  $\text{phenotype}=\text{SNP1}+\text{SNP2}$  was better than either  $\text{phenotype}=\text{SNP1}$  or  $\text{phenotype}=\text{SNP2}$  models). For ear covert color, we found that 3 of the 6 comparisons—chrom 1 vs. chrom 6, chrom 1 vs. chrom 13, and chrom 13 vs. chrom 28 (region A)—were additionally better explained by an interaction model than an additive model (Figure 4.2, Table 4.1; i.e.,  $\text{phenotype}=\text{SNP1}+\text{SNP2}+\text{SNP1}\times\text{SNP2}$  was better than  $\text{phenotype}=\text{SNP1}+\text{SNP2}$ ). For shaft color, we found that 8 of the 21 comparisons were better explained by an interaction model (Figure 4.3, Table 4.2): chrom 1 vs. 5, chrom 1 vs. 12, chrom 1 vs. chrom 28 (region A), chrom 1 vs. chrom 28 (region B), chrom 3 vs. chrom 28 (region B), chrom 8 vs. chrom 28 (region A), chrom 8 vs. chrom 28 (region B), and chrom 12 vs. chrom 28 (region A).

### **Discussion**

The extensive hybridization between red-shafted and yellow-shafted flickers represents a powerful opportunity to study the interactions between genomic regions in producing both melanin and carotenoid pigmentation simultaneously in the same system. Here, we use a targeted sequencing approach to obtain genotypes of 54 SNPs identified as important in the ear covert (pheomelanin) and shaft (carotenoid) coloration differences in flickers across 136 individuals to better understand the role of epistatic interactions in producing coloration in these birds, a topic about which little is currently known.

**Table 4.1.** Results for the two-locus models explaining ear covert color

<b>Chromosome comparison</b>	<b>Best model</b>	<b>Variance (%)</b>	<b>p-value*</b>	<b>Model comparison p-value<sup>†</sup></b>
1 vs 6	Interaction	38.51	$6.68 \times 10^{-14}$	0.02856
1 vs 13	Interaction	47.69	$< 2.2 \times 10^{-16}$	0.02188
1 vs 28A	Additive	39.48	$3.14 \times 10^{-15}$	-
6 vs 13	Additive	38.22	$1.24 \times 10^{-14}$	-
6 vs 28A	Additive	44.23	$< 2.2 \times 10^{-16}$	-
13 vs 28A	Interaction	45.48	$< 2.2 \times 10^{-16}$	0.006512

\* significance level of the best model

<sup>†</sup> significance when comparing the additive and interaction models; shown only when the interaction model is the best model

**Table 4.2.** Results for the two-locus models explaining shaft color

<b>Chromosome comparison</b>	<b>Best model</b>	<b>Variance (%)</b>	<b>p-value*</b>	<b>Model comparison p-value<sup>†</sup></b>
1 vs 3	Additive	62.73	$< 2.2 \times 10^{-16}$	-
1 vs 5	Interaction	46.23	$< 2.2 \times 10^{-16}$	0.02109
1 vs 8	Additive	58.86	$< 2.2 \times 10^{-16}$	-
1 vs 12	Interaction	54.43	$< 2.2 \times 10^{-16}$	0.03244
1 vs 28A	Interaction	49.32	$< 2.2 \times 10^{-16}$	0.002167
1 vs 28B	Interaction	49.62	$< 2.2 \times 10^{-16}$	0.0004524
3 vs 5	Additive	62.14	$< 2.2 \times 10^{-16}$	-
3 vs 8	Additive	67.5	$< 2.2 \times 10^{-16}$	-
3 vs 12	Additive	64.07	$< 2.2 \times 10^{-16}$	-
3 vs 28A	Additive	63.4	$< 2.2 \times 10^{-16}$	-
3 vs 28B	Interaction	68.06	$< 2.2 \times 10^{-16}$	0.01724
5 vs 8	Additive	58.04	$< 2.2 \times 10^{-16}$	-
5 vs 12	Additive	50.28	$< 2.2 \times 10^{-16}$	-
5 vs 28A	Additive	48.26	$< 2.2 \times 10^{-16}$	-
5 vs 28B	Additive	46.28	$< 2.2 \times 10^{-16}$	-
8 vs 12	Additive	59.51	$< 2.2 \times 10^{-16}$	-
8 vs 28A	Interaction	67.02	$< 2.2 \times 10^{-16}$	0.007017
8 vs 28B	Interaction	65.52	$< 2.2 \times 10^{-16}$	0.00661
12 vs 28A	Interaction	56.17	$< 2.2 \times 10^{-16}$	0.01425
12 vs 28B	Additive	54.19	$< 2.2 \times 10^{-16}$	-
28A vs 28B	Additive	35.58	$2.48 \times 10^{-13}$	-

\* significance level of the best model

<sup>†</sup> significance when comparing the additive and interaction models; shown only when the interaction model is the best model

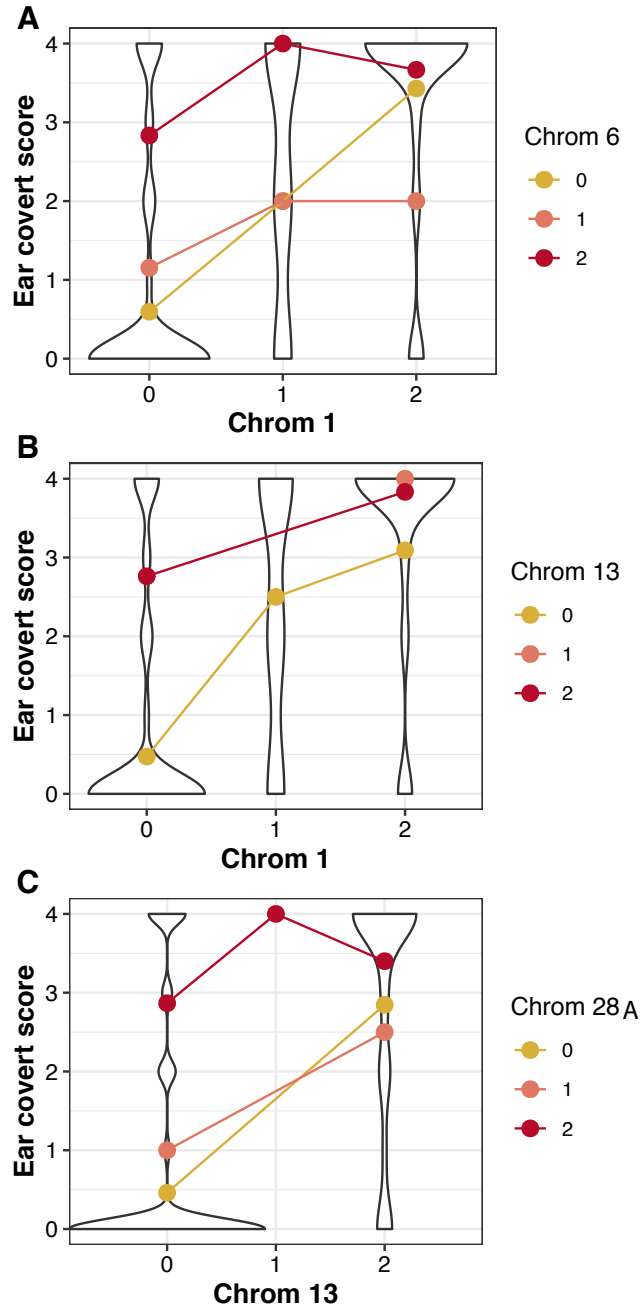


**Figure 4.2.** The two-locus models for ear cover color that were best explained by including interactions. Given a particular genotype at the first locus (x-axis), the colored lines show the relationship between ear cover color for each genotype at the second locus (legend). Violin plots show the distribution of ear cover scores for each genotype of the first locus. 0 = homozygote for the reference allele, 1 = heterozygote, 2 = homozygote for the alternate allele. Full model results are shown in Table 4.1.

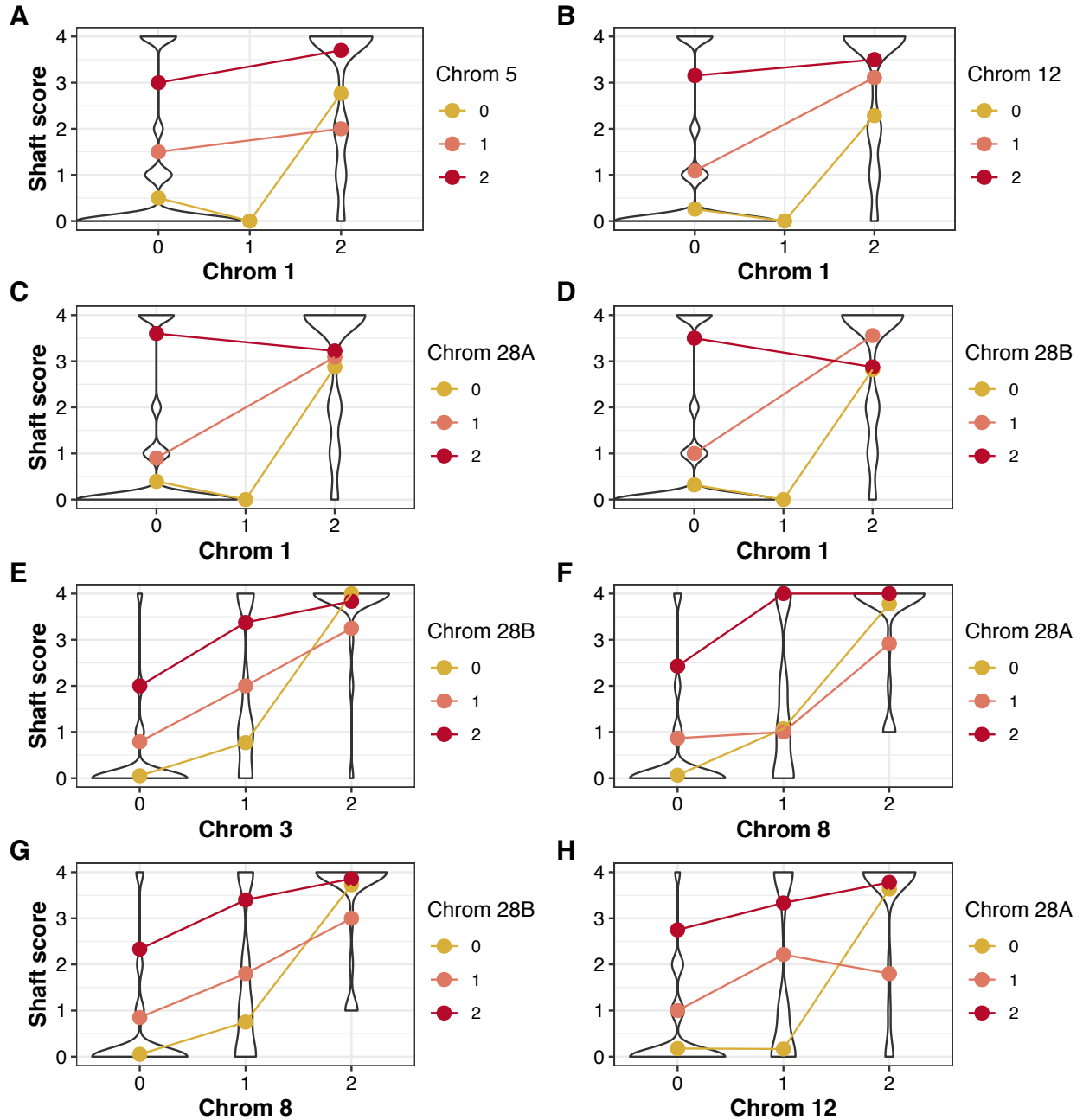


**Figure 4.3.** The two-locus models for shaft color that were best explained by including interactions. Given a particular genotype at the first locus (x-axis), the colored lines show the relationship between shaft color for each genotype at the second locus (legend). Violin plots show the distribution of shaft scores for each genotype of the first locus. 0 = homozygote for the reference allele, 1 = heterozygote, 2 = homozygote for the alternate allele. Full model results are shown in Table 4.2.

Validating the relationship between genotype and phenotype is an important first step in evaluating this genetic dataset. Although the targeted SNPs were chosen based on previous genome-wide associations (Aguillon et al. 2021), we had fewer individuals and lower coverage data in that study. By increasing the number of individuals included here and performing a PCR-based sequencing approach, we have increased power in our ability to associate genotypes and phenotypes. Importantly, we find that the targeted SNPs are indeed associated with coloration differences in the ear coverts (Figure D1) and shaft (Figure D2) as expected, validating the results from our original genome-wide associations. Moreover, genetic clustering analyses nicely separate individuals based on their phenotype score (Figure 4.1), as would also be expected, further suggesting that these genomic regions are important in creating these phenotypic differences. The targeted SNPs have a clear relationship with the ear covert and shaft coloration, and thereby present a clear opportunity to test for epistatic interactions in producing coloration in the flickers.

We found that every two-locus additive comparison was better at explaining phenotypic differences than either individual locus independently (for both the ear coverts and the shaft). Additionally, we found significant interactive effects in 3 of 6 comparisons of genomic regions for ear covert coloration (Table 4.1, Figure 4.2) and in 8 of 21 comparisons for shaft coloration (Table 4.2, Figure 4.3). Significant interactive effects with chromosome 1 were common for both the ear coverts and shaft. The general pattern across all of the significant epistatic interaction models has two aspects. First, having more alternate alleles at the first locus (i.e., a genotype of 1 or 2) results in a higher phenotype score (more red-shafted). In general, individuals with two alternate alleles had a more red-shafted phenotype than individuals with only one alternate allele. Second, variation in the genotype of the second locus had little phenotypic effect

in individuals with two alternate alleles at the first locus, but did account for remaining variation in the other genotypes at the first locus (having more alternate alleles at the second locus resulted in a higher phenotype score).

There were relatively few identified genes near the majority of the SNPs used in the interaction analyses in our study, so we do not find any clear relationship between particular genes and the identified epistatic interactions when comparing across all of the significant interaction models. The two exceptions are the significant interactions for shaft color between chromosome 8 and the two regions on chromosome 28 (Figure 4.3F, 4.3G; Table 4.2). The SNP on chromosome 8 is located within the gene *CYP2J19*, which is one of the only genes already known to be involved in yellow to red coloration differences in birds (Lopes et al. 2016; Mundy et al. 2016). The regions on chromosome 28 are nearby the genes *MFSD12* (region A) and *FKBP8* (region B), both known to be involved in melanin pigmentation (Poelstra et al. 2015; Rodriguez et al. 2020). *MFSD12*, in particular, has been implicated in pheomelanin synthesis and eumelanin inhibition in humans, mice, and birds (Crawford et al. 2017; Abolins-Abols et al. 2018). This repeated association between melanin genes and carotenoid traits is an intriguing, novel pattern in flickers that we have discussed at length previously (see Aguilon et al. 2021). Here, we find an additional layer to this relationship: significant interactions between genes involved in carotenoid and melanin pigmentation to produce the overall carotenoid phenotype. These two interactions indicate that the production of red ketolated carotenoids (from *CYP2J19*) is by itself not enough to produce the full red-shafted flicker phenotype, but it must instead be paired with changes in melanin pigmentation. The underlying mechanisms might include either decreasing deposition of melanin overall to allow the carotenoids to be more visible (with *FKBP8*), or by preferentially depositing red-brown pheomelanins that mask the underlying black eumelanin

pigments (with MFSD12).

The two previous studies on epistatic relationships in coloration of carrion and hooded crows and subspecies of the white wagtail have focused entirely on melanin pigmentation, particularly the extent of black eumelanin (Knief et al. 2019; Semenov et al. 2021). In both examples, there are only two regions of the genome that are significantly associated with plumage coloration, one containing a gene with a clear link to melanin pigmentation and the other containing genes with a less clear link. In both the crows (Knief et al. 2019) and the wagtails (Semenov et al. 2021), they find an epistatic relationship between the two identified genomic regions that together create the observed phenotype. The interactions in flickers are much more complex, as flickers differ across many more plumage patches and at many more coloration-related loci, and therefore there are more than two genotype-phenotype associations for each plumage patch (Aguillon et al. 2021). Nonetheless, we also find significant epistatic interactions between multiple genomic regions to produce the coloration of these two traits: ear coverts and shaft. Moreover, for the first time, we have identified epistatic interactions in producing carotenoid and pheomelanin coloration. Intriguingly, in the two interactions in the shaft where we can identify genes in both regions, we find a known carotenoid gene interacting with known melanin genes. Although the field has come far in identifying regions of the genome associated with coloration differences, understanding the interactions between these genomic regions is a promising next step towards thoroughly understanding the genomic basis of coloration in birds. The complexity of the overall phenotype and the number of genotype-phenotype associations in flickers allowed for an assessment of interactions across many genomic regions in both melanin and carotenoid traits. Our results suggest interactions between different genomic regions may be common in avian coloration, and future work should

attempt to disentangle these interactions across multiple systems.

## References

- Abolins-Abols, M., E. Kornobis, P. Ribeca, K. Wakamatsu, M. P. Peterson, E. D. Ketterson, and B. Mila. 2018. Differential gene regulation underlies variation in melanic plumage coloration in the dark-eyed junco (*Junco hyemalis*). *Mol. Ecol.* 27:4501-4515.
- Aguillon, S. M., L. Campagna, R. G. Harrison, and I. J. Lovette. 2018. A flicker of hope: genomic data distinguish northern flicker taxa despite low levels of divergence. *Auk* 135:748-766.
- Aguillon, S. M. and I. J. Lovette. 2019. Change the specific/subspecific/morphological group name of the red-shafted flicker from *cafer* to *lathami*. AOS North American Classification Committee 2019-A-10:66-71.
- Aguillon, S. M., J. Walsh, and I. J. Lovette. 2021. Extensive hybridization reveals multiple coloration genes underlying a complex plumage phenotype. *Proc. R. Soc. B* 288:20201805.
- Brelsford, A., D. P. L. Toews, and D. E. Irwin. 2017. Admixture mapping in a hybrid zone reveals loci associated with avian feather coloration. *Proc. R. Soc. B* 284:20171106.
- Campagna, L., M. Repenning, L. F. Silveira, C. S. Fontana, P. L. Tubaro, and I. J. Lovette. 2017. Repeated divergent selection on pigmentation genes in a rapid finch radiation. *Sci. Adv.* 3:e1602404.
- Cooke, T. F., C. R. Fischer, P. Wu, T. X. Jiang, K. T. Xie, J. Kuo, E. Doctorov, A. Zehnder, C. Khosla, C. M. Chuong, and C. D. Bustamante. 2017. Genetic mapping and biochemical basis of yellow feather pigmentation in budgerigars. *Cell* 171:427-439.e421.
- Crawford, N. G., D. E. Kelly, M. E. B. Hansen, M. H. Beltrame, S. Fan, S. L. Bowman, E. Jewett, A. Ranciaro, S. Thompson, Y. Lo, S. P. Pfeifer, J. D. Jensen, M. C. Campbell, W. Beggs, F. Hormozdiari, S. W. Mpoloka, G. G. M, T. Nyambo, D. W. Meskel, G. Belay, J. Haut, NISC Comparative Sequencing Program, H. Rothschild, L. Zon, Y. Zhou, M. A. Kovacs, M. Xu, T. Zhang, K. Bishop, J. Sinclair, C. Rivas, E. Elliot, J. Choi, S. A. Li, B. Hicks, S. Burgess, C. Abnet, D. E. Watkins-Chow, E. Oceana, Y. S. Song, E. Eskin, K. M. Brown, M. S. Marks, S. K.

- Loftus, W. J. Pavan, M. Yeager, S. Chanock, and S. A. Tishkoff. 2017. Loci associated with skin pigmentation identified in African populations. *Science* 358:eaan8433.
- Cuthill, I. C., W. L. Allen, K. Arbuckle, B. Caspers, G. Chaplin, M. E. Hauber, G. E. Hill, N. G. Jablonski, C. D. Jiggins, A. Kelber, J. Mappes, J. Marshall, R. Merrill, D. Osorio, R. Prum, N. W. Roberts, A. Roulin, H. M. Rowland, T. N. Sherratt, J. Skelhorn, M. P. Speed, M. Stevens, M. C. Stoddard, D. Stuart-Fox, L. Talas, E. Tibbetts, and T. Caro. 2017. The biology of color. *Science* 357:eaan0221.
- Danecek, P., A. Auton, G. Abecasis, C. A. Albers, E. Banks, M. A. DePristo, R. E. Handsaker, G. Lunter, G. T. Marth, S. T. Sherry, G. McVean, R. Durbin, and G. Genomes Project Analysis. 2011. The variant call format and VCFtools. *Bioinformatics* 27:2156-2158.
- Earl, D. A. and B. M. vonHoldt. 2011. STRUCTURE HARVESTER: a website and program for visualizing STRUCTURE output and implementing the Evanno method. *Conserv. Genet. Res.* 4:359-361.
- Evanno, G., S. Regnaut, and J. Goudet. 2005. Detecting the number of clusters of individuals using the software STRUCTURE: a simulation study. *Mol. Ecol.* 14:2611-2620.
- Ewels, P., M. Magnusson, S. Lundin, and M. Kaller. 2016. MultiQC: summarize analysis results for multiple tools and samples in a single report. *Bioinformatics* 32:3047-3048.
- Funk, E. R. and S. A. Taylor. 2019. High-throughput sequencing is revealing genetic associations with avian plumage color. *Auk* 136:1-7.
- Gazda, M. A., P. M. Araújo, R. J. Lopes, M. B. Toomey, P. Andrade, S. Afonso, C. Marques, L. Nunes, P. Pereira, S. Trigo, G. E. Hill, J. C. Corbo, and M. Carneiro. 2020a. A genetic mechanism for sexual dichromatism in birds. *Science* 368:1270-1274.
- Gazda, M. A., M. B. Toomey, P. M. Araujo, R. J. Lopes, S. Afonso, C. A. Myers, K. Serres, P. D. Kiser, G. E. Hill, J. C. Corbo, and M. Carneiro. 2020b. Genetic basis of de novo appearance of carotenoid ornamentation in bare parts of canaries. *Mol. Biol. Evol.* 37:1317-1328.

- Hill, G. E. and K. J. McGraw. 2006. Bird Coloration: Function and Evolution. Harvard University Press, Cambridge, Massachusetts.
- Hooper, D. M., S. C. Griffith, and T. D. Price. 2019. Sex chromosome inversions enforce reproductive isolation across an avian hybrid zone. *Mol. Ecol.* 28:1246-1262.
- Hubbard, J. K., J. A. Uy, M. E. Hauber, H. E. Hoekstra, and R. J. Safran. 2010. Vertebrate pigmentation: from underlying genes to adaptive function. *Trends Genet.* 26:231-239.
- Hudon, J., K. L. Wiebe, E. Pini, and R. Stradi. 2015. Plumage pigment differences underlying the yellow-red differentiation in the northern flicker (*Colaptes auratus*). *Comp. Biochem. Phys. B* 183:1-10.
- Jakobsson, M. and N. A. Rosenberg. 2007. CLUMPP: a cluster matching and permutation program for dealing with label switching and multimodality in analysis of population structure. *Bioinformatics* 23:1801-1806.
- Kim, K. W., B. C. Jackson, H. Zhang, D. P. L. Toews, S. A. Taylor, E. I. Greig, I. J. Lovette, M. M. Liu, A. Davison, S. C. Griffith, K. Zeng, and T. Burke. 2019. Genetics and evidence for balancing selection of a sex-linked colour polymorphism in a songbird. *Nat. Commun.* 10:1852.
- Knief, U., C. M. Bossu, N. Saino, B. Hansson, J. Poelstra, N. Vijay, M. Weissensteiner, and J. B. W. Wolf. 2019. Epistatic mutations under divergent selection govern phenotypic variation in the crow hybrid zone. *Nat. Ecol. Evol.* 3:570-576.
- Langmead, B. and S. L. Salzberg. 2012. Fast gapped-read alignment with Bowtie 2. *Nat. Methods* 9:357-359.
- Lewis, J. J., R. C. Geltman, P. C. Pollak, K. E. Rondem, S. M. Van Belleghem, M. J. Hubisz, P. R. Munn, L. Zhang, C. Benson, A. Mazo-Vargas, C. G. Danko, B. A. Counterman, R. Papa, and R. D. Reed. 2019. Parallel evolution of ancient, pleiotropic enhancers underlies butterfly wing pattern mimicry. *Proc. Natl. Acad. Sci. USA* 116:24174-24183.
- Li, H. 2011. A statistical framework for SNP calling, mutation discovery, association mapping and population genetical parameter estimation from sequencing data. *Bioinformatics* 27:2987-2993.

- Li, H., B. Handsaker, A. Wysoker, T. Fennell, J. Ruan, N. Homer, G. Marth, G. Abecasis, R. Durbin, and 1000 Genome Project Data Processing Subgroup. 2009. The Sequence Alignment/Map format and SAMtools. *Bioinformatics* 25:2078-2079.
- Lopes, R. J., J. D. Johnson, M. B. Toomey, M. S. Ferreira, P. M. Araujo, J. Melo-Ferreira, L. Andersson, G. E. Hill, J. C. Corbo, and M. Carneiro. 2016. Genetic basis for red coloration in birds. *Curr. Biol.* 26:1427-1434.
- Martin, M. 2011. Cutadapt removes adaptor sequences from high-throughput sequencing reads. *EMBnet.journal* 17:10-12.
- Mazo-Vargas, A., C. Concha, L. Livraghi, D. Massardo, R. W. R. Wallbank, L. Zhang, J. D. Papador, D. Martinez-Najera, C. D. Jiggins, M. R. Kronforst, C. J. Breuker, R. D. Reed, N. H. Patel, W. O. McMillan, and A. Martin. 2017. Macroevolutionary shifts of *WntA* function potentiate butterfly wing-pattern diversity. *Proc. Natl. Acad. Sci. USA* 114:10701-10706.
- Moore, W. S. 1987. Random mating in the northern flicker hybrid zone: implications for the evolution of bright and contrasting plumage patterns in birds. *Evolution* 41:539-546.
- Moore, W. S. and D. B. Buchanan. 1985. Stability of the northern flicker hybrid zone in historical times: implications for adaptive speciation theory. *Evolution* 39:135-151.
- Mundy, N. I., J. Stapley, C. Bennison, R. Tucker, H. Twyman, K.-W. Kim, T. Burke, T. R. Birkhead, S. Andersson, and J. Slate. 2016. Red carotenoid coloration in the zebra finch is controlled by a cytochrome P450 gene cluster. *Curr. Biol.* 26:1435-1440.
- Okonechnikov, K., A. Conesa, and F. García-Alcalde. 2016. Qualimap 2: advanced multi-sample quality control for high-throughput sequencing data. *Bioinformatics* 32:292-294.
- Orteu, A. and C. D. Jiggins. 2020. The genomics of coloration provides insights into adaptive evolution. *Nat. Rev. Genet.* 21:461-475.
- Poelstra, J. W., N. Vijay, M. P. Hoepfner, and J. B. Wolf. 2015. Transcriptomics of colour patterning and coloration shifts in crows. *Mol. Ecol.* 24:4617-4628.

- Pritchard, J. K., M. Stephens, and P. Donnelly. 2000. Inference of population structure using multilocus genotype data. *Genetics* 155:945-959.
- R Core Team. 2018. R: A language and environment for statistical computing. R Foundation for Statistical Computing, Vienna, Austria.
- Rodriguez, A., N. I. Mundy, R. Ibanez, and H. Prohl. 2020. Being red, blue and green: the genetic basis of coloration differences in the strawberry poison frog (*Oophaga pumilio*). *BMC Genomics* 21:301.
- Rosenberg, N. A. 2003. DISTRUCT: a program for the graphical display of population structure. *Mol. Ecol. Notes* 4:137-138.
- Semenov, G., E. Linck, E. D. Enbody, R. B. Harris, D. R. Khaydarov, P. Alström, L. Andersson, and S. A. Taylor. 2021. Asymmetric introgression reveals the genetic architecture of a plumage trait. *Nat. Commun.* 12:1019.
- Short, L. L. 1965. Hybridization in the flickers (*Colaptes*) of North America. *Bull. Am. Mus. Nat. Hist. N. Y.* 129:307-428.
- Stryjewski, K. F. and M. D. Sorenson. 2017. Mosaic genome evolution in a recent and rapid avian radiation. *Nat. Ecol. Evol.* 1:1912-1922.
- Toews, D. P. L., N. R. Hofmeister, and S. A. Taylor. 2017. The evolution and genetics of carotenoid processing in animals. *Trends Genet.* 33:171-182.
- Toews, D. P. L., S. A. Taylor, R. Vallender, A. Brelsford, B. G. Butcher, P. W. Messer, and I. J. Lovette. 2016. Plumage genes and little else distinguish the genomes of hybridizing warblers. *Curr. Biol.* 26:2313-2318.
- Toomey, M. B., C. I. Marques, P. Andrade, P. M. Araujo, S. Sabatino, M. A. Gazda, S. Afonso, R. J. Lopes, J. C. Corbo, and M. Carneiro. 2018. A non-coding region near *Follistatin* controls head colour polymorphism in the Gouldian finch. *Proc. R. Soc. B* 285:20181788.
- Uy, J. A., E. A. Cooper, S. Cutie, M. R. Concannon, J. W. Poelstra, R. G. Moyle, and C. E. Filardi. 2016. Mutations in different pigmentation genes are associated with parallel melanism in island flycatchers. *Proc. R. Soc. B* 283:20160731.

- Vickrey, A. I., R. Bruders, Z. Kronenberg, E. Mackey, R. J. Bohlender, E. T. Maclary, R. Maynez, E. J. Osborne, K. P. Johnson, C. D. Huff, M. Yandell, and M. D. Shapiro. 2018. Introgression of regulatory alleles and a missense coding mutation drive plumage pattern diversity in the rock pigeon. *eLife* 7.
- Wang, S., S. Rohwer, D. R. de Zwaan, D. P. L. Toews, I. J. Lovette, J. Mackenzie, and D. E. Irwin. 2020. Selection on a small genomic region underpins differentiation in multiple color traits between two warbler species. *Evol. Lett.* 4:502-515.
- Wickham, H., M. Averick, J. Bryan, W. Chang, L. D. A. McGowan, R. François, G. Grolemund, A. Hayes, L. Henry, J. Hester, M. Kuhn, T. L. Pedersen, E. Miller, S. M. Bache, K. Müller, J. Ooms, D. Robinson, D. P. Seidel, V. Spinu, K. Takahashi, D. Vaughan, C. Wilke, K. Woo, and H. Yutani. 2019. Welcome to the Tidyverse. *J. Open Source Softw.* 4:1686.
- Wiebe, K. L. and W. S. Moore. 2020. Northern Flicker (*Colaptes auratus*), version 1.0 in P. G. Rodewald, ed. *Birds of the World*. Cornell Lab of Ornithology, Ithaca, New York, USA.
- Zheng, X., D. Levine, J. Shen, S. M. Gogarten, C. Laurie, and B. S. Weir. 2012. A high-performance computing toolset for relatedness and principal component analysis of SNP data. *Bioinformatics* 28:3326-3328.

CHAPTER 1 APPENDIX

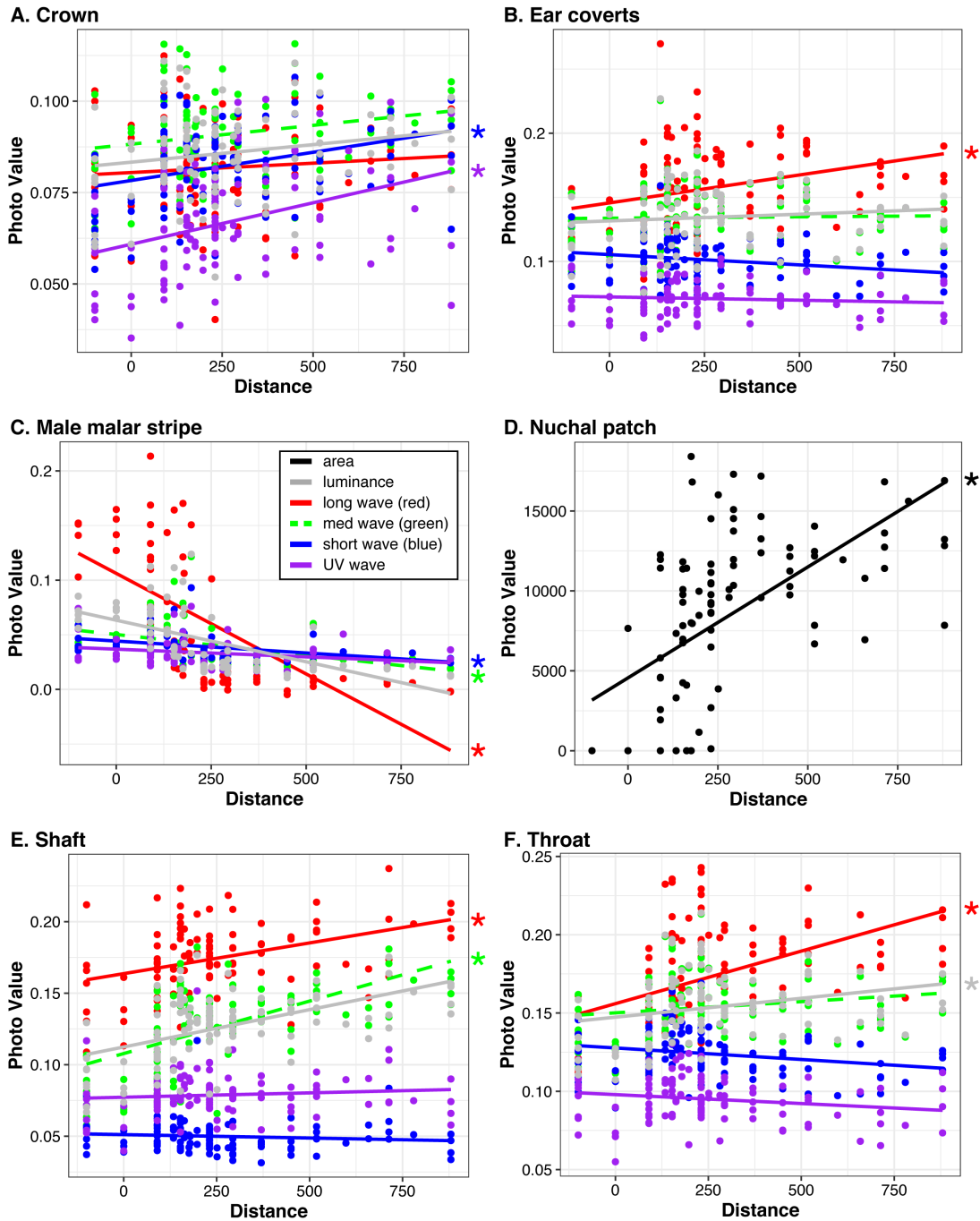


**Figure A1.** Relationships between the six phenotypic traits and the six image parameters from the multispectral photography. Image parameters are indicated by different colors (legend in C), with the medium wave channel (green) shown with a dashed line for ease of differentiation. Image parameters that resulted in well-resolved clines (Figure 1.4) are indicated with an asterisk on the right side of the plot.

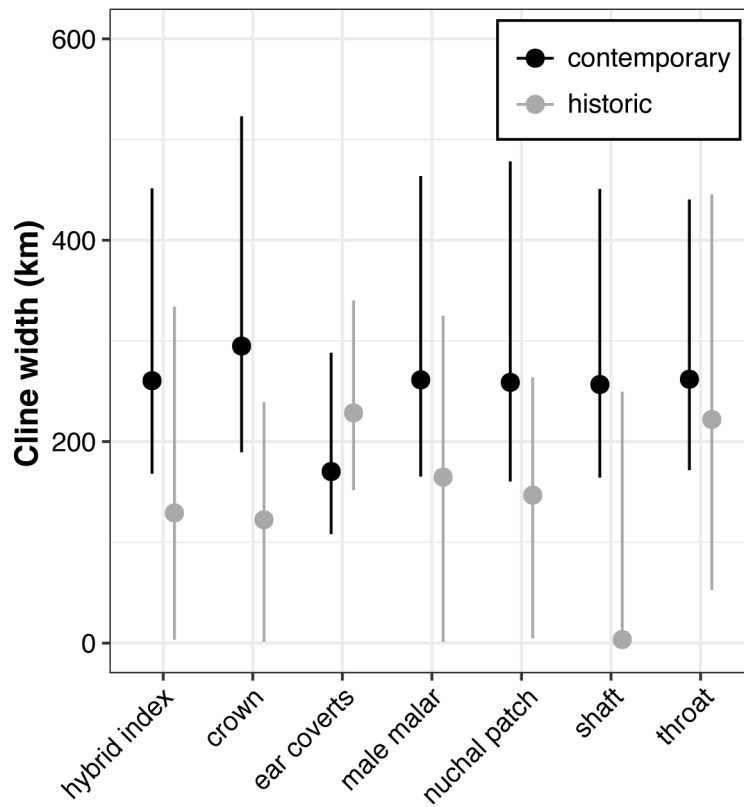


**Figure A2.** Estimated cline widths with confidence intervals for the geographic clines estimated from qualitative scoring in the historic (gray) and contemporary (black) transects.

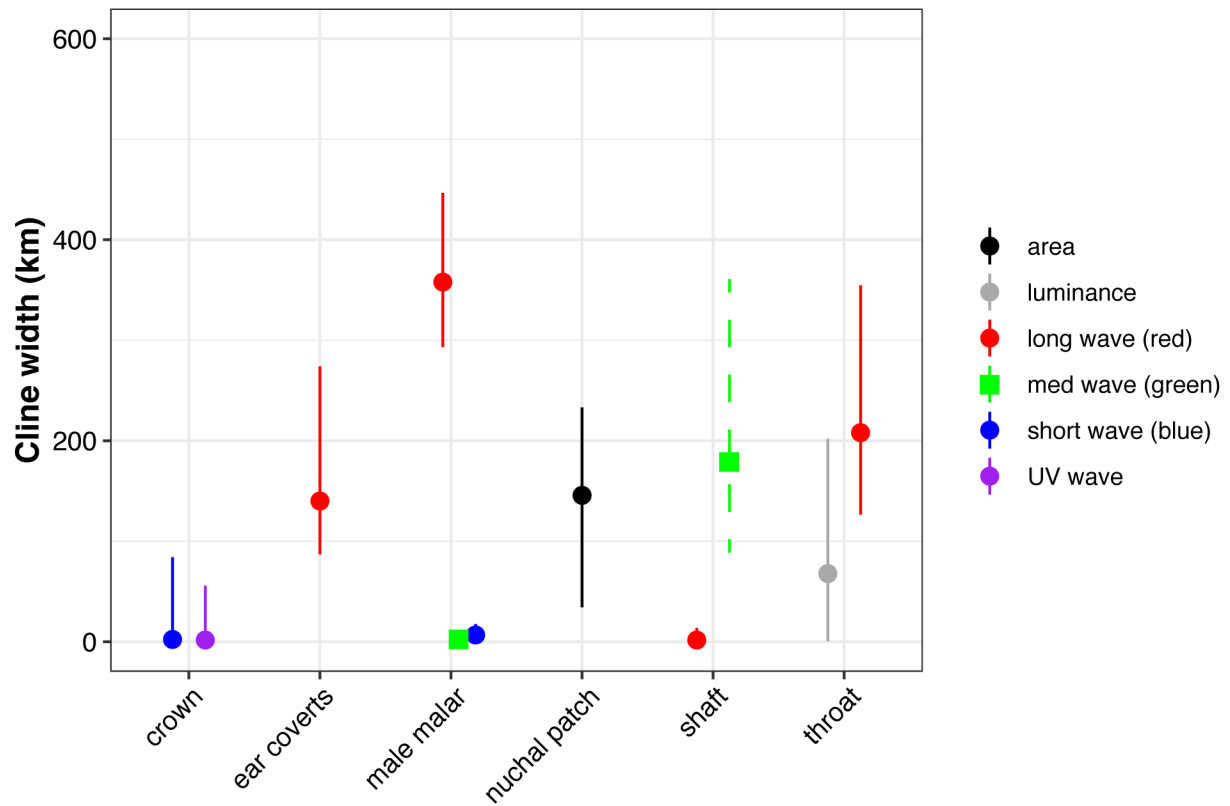


**Figure A3.** Estimated cline widths with confidence intervals for the geographic clines estimated from quantitative scoring of six image parameters across the six phenotypic traits. Image parameters are indicated by different colors, with the medium wave channel (green) shown with a dashed line and square symbol for ease of differentiation.

**Table A1.** Detailed information on samples included in this study. Locality ID/Name correspond to values in Figure 1.1 and Table A3. Phenotype scores range from 0 (yellow-shafted) to 4 (red-shafted). The overall hybrid index has been transformed to range from 0 to 1 to allow comparisons between the sexes.

Sample ID	Year	County	State	Latitude	Longitude	Transect	Locality ID	Locality Name	Sex	Crown	Ear Coverts	Malar	Nuchal	Shaft	Throat	Hybrid Index
28110	1956	Weld	Colorado	40.346603	-104.82279	historic	2	Greeley	Male	4	4	4	4	4	4	1
28111	1956	Weld	Colorado	40.346603	-104.82279	historic	2	Greeley	Female	4	4	NA	3	4	3	0.9
28112	1956	Weld	Colorado	40.346603	-104.82279	historic	2	Greeley	Male	4	4	4	4	4	4	1
28113	1956	Weld	Colorado	40.346603	-104.82279	historic	2	Greeley	Female	4	4	NA	4	4	3	0.95
28116	1956	Weld	Colorado	40.346603	-104.82279	historic	2	Greeley	Male	4	4	4	4	4	4	1
28123	1956	Weld	Colorado	40.346603	-104.82279	historic	2	Greeley	Female	4	2	NA	4	4	3	0.85
28125	1956	Weld	Colorado	40.346603	-104.82279	historic	2	Greeley	Male	4	4	4	4	4	3	0.95833333
28127	1956	Weld	Colorado	40.346603	-104.82279	historic	2	Greeley	Male	4	3	4	3	2	2	0.75
28128	1956	Weld	Colorado	40.346603	-104.82279	historic	2	Greeley	Male	4	1	3	3	4	2	0.70833333
28129	1956	Weld	Colorado	40.346603	-104.82279	historic	2	Greeley	Female	4	0	NA	4	4	1	0.65
28132	1956	Weld	Colorado	40.346603	-104.82279	historic	2	Greeley	Male	3	2	4	4	3	2	0.75
28133	1956	Weld	Colorado	40.346603	-104.82279	historic	2	Greeley	Female	3	4	NA	4	4	3	0.9
28136	1956	Weld	Colorado	40.346603	-104.82279	historic	2	Greeley	Male	4	4	4	4	4	4	1
28139	1956	Weld	Colorado	40.346603	-104.82279	historic	2	Greeley	Female	4	4	NA	4	3	3	0.9
28140	1956	Weld	Colorado	40.346603	-104.82279	historic	2	Greeley	Male	4	4	4	4	1	4	0.875
28085	1956	Morgan	Colorado	40.350895	-104.06117	historic	4	Orchard	Male	4	2	NA	3	4	4	NA
28086	1956	Morgan	Colorado	40.350895	-104.06117	historic	4	Orchard	Female	4	3	NA	4	4	3	0.9
28095	1956	Morgan	Colorado	40.350895	-104.06117	historic	4	Orchard	Male	4	4	4	3	4	3	0.91666667
28103	1956	Morgan	Colorado	40.350895	-104.06117	historic	4	Orchard	Male	3	2	4	2	4	3	0.75
28104	1956	Morgan	Colorado	40.350895	-104.06117	historic	4	Orchard	Female	4	2	NA	4	2	3	0.75
28105	1956	Morgan	Colorado	40.350895	-104.06117	historic	4	Orchard	Male	4	3	4	4	2	3	0.83333333
28106	1956	Morgan	Colorado	40.350895	-104.06117	historic	4	Orchard	Male	3	0	2	0	1	0	0.25
28109	1956	Morgan	Colorado	40.350895	-104.06117	historic	4	Orchard	Male	4	3	3	4	3	3	0.83333333
28087	1956	Morgan	Colorado	40.267982	-103.94052	historic	5	W Fort Morgan	Male	3	3	4	4	4	3	0.875
28090	1956	Morgan	Colorado	40.267982	-103.94052	historic	5	W Fort Morgan	Female	4	2	NA	4	4	3	0.85
28091	1956	Morgan	Colorado	40.267982	-103.94052	historic	5	W Fort Morgan	Female	4	3	NA	4	4	3	0.9
28097	1956	Morgan	Colorado	40.267982	-103.94052	historic	5	W Fort Morgan	Male	4	2	2	NA	2	3	NA
28098	1956	Morgan	Colorado	40.267982	-103.94052	historic	5	W Fort Morgan	Male	3	2	4	4	4	3	0.83333333
28099	1956	Morgan	Colorado	40.267982	-103.94052	historic	5	W Fort Morgan	Female	4	3	NA	4	4	3	0.9
28100	1956	Morgan	Colorado	40.267982	-103.94052	historic	5	W Fort Morgan	Male	4	3	4	3	4	3	0.875
28101	1956	Morgan	Colorado	40.267982	-103.94052	historic	5	W Fort Morgan	Male	4	3	3	4	2	3	0.79166667
28102	1956	Morgan	Colorado	40.267982	-103.94052	historic	5	W Fort Morgan	Female	4	3	NA	4	4	4	0.95
28107	1956	Morgan	Colorado	40.267982	-103.94052	historic	5	W Fort Morgan	Male	3	0	4	3	2	0	0.5
28108	1956	Morgan	Colorado	40.267982	-103.94052	historic	5	W Fort Morgan	Female	4	2	NA	4	2	3	0.75
28072	1956	Logan	Colorado	40.853691	-102.70736	historic	12	Crook	Male	0	0	0	0	0	0	0
28073	1956	Logan	Colorado	40.853691	-102.70736	historic	12	Crook	Female	1	0	NA	0	0	0	0.05
28075	1956	Logan	Colorado	40.853691	-102.70736	historic	12	Crook	Male	3	0	1	3	3	0	0.41666667
28076	1956	Logan	Colorado	40.853691	-102.70736	historic	12	Crook	Female	2	2	NA	3	4	2	0.65
28077	1956	Logan	Colorado	40.853691	-102.70736	historic	12	Crook	Female	3	1	NA	4	1	3	0.6
28078	1956	Logan	Colorado	40.853691	-102.70736	historic	12	Crook	Female	1	0	NA	4	1	2	0.4
28079	1956	Logan	Colorado	40.853691	-102.70736	historic	12	Crook	Male	1	1	3	0	4	3	0.5
28080	1956	Logan	Colorado	40.853691	-102.70736	historic	12	Crook	Male	4	4	4	4	4	4	1
28084	1956	Logan	Colorado	40.853691	-102.70736	historic	12	Crook	Female	2	3	NA	4	4	3	0.8
28026	1956	Deuel	Nebraska	40.981292	-102.18304	historic	15	Big Springs	Female	3	0	NA	0	0	0	0.15
28027	1956	Deuel	Nebraska	40.981292	-102.18304	historic	15	Big Springs	Female	3	0	NA	0	0	0	0.15
28028	1956	Deuel	Nebraska	40.981292	-102.18304	historic	15	Big Springs	Male	0	0	0	0	0	0	0
28029	1956	Deuel	Nebraska	40.981292	-102.18304	historic	15	Big Springs	Male	0	0	0	0	0	3	0.125
28030	1956	Deuel	Nebraska	40.981292	-102.18304	historic	15	Big Springs	Male	1	2	1	1	0	3	0.33333333
28031	1956	Deuel	Nebraska	40.981292	-102.18304	historic	15	Big Springs	Male	1	0	1	NA	0	0	NA
28032	1956	Deuel	Nebraska	40.981292	-102.18304	historic	15	Big Springs	Male	1	0	0	2	0	0	0.125

(Table A1 continued)

28033	1956	Deuel	Nebraska	40.981292	-102.18304	historic	15	Big Springs	Female	1	0	NA	0	0	0	0.05
28036	1956	Lincoln	Nebraska	41.144314	-101.11275	historic	18	Sutherland	Male	2	3	4	3	4	4	0.83333333
28037	1956	Lincoln	Nebraska	41.144314	-101.11275	historic	18	Sutherland	Female	0	0	NA	0	0	0	0
28038	1956	Lincoln	Nebraska	41.144314	-101.11275	historic	18	Sutherland	Male	0	0	0	2	0	0	0.08333333
28040	1956	Lincoln	Nebraska	41.144314	-101.11275	historic	18	Sutherland	Male	1	0	0	0	0	0	0.04166667
28041	1956	Lincoln	Nebraska	41.144314	-101.11275	historic	18	Sutherland	Male	NA	0	0	0	0	0	NA
28048	1956	Lincoln	Nebraska	41.144457	-101.12705	historic	18	Sutherland	Male	NA	0	0	0	0	0	NA
28049	1957	Lincoln	Nebraska	41.144457	-101.12705	historic	18	Sutherland	Male	0	0	0	0	0	2	0.08333333
28050	1957	Lincoln	Nebraska	41.144457	-101.12705	historic	18	Sutherland	Male	0	0	0	0	0	0	0
28051	1957	Lincoln	Nebraska	41.144457	-101.12705	historic	18	Sutherland	Female	0	0	NA	0	0	0	0
28052	1957	Lincoln	Nebraska	41.144457	-101.12705	historic	18	Sutherland	Female	0	0	NA	0	0	3	0.15
28053	1957	Lincoln	Nebraska	41.144457	-101.12705	historic	18	Sutherland	Male	0	0	0	0	0	0	0
28054	1957	Lincoln	Nebraska	41.144457	-101.12705	historic	18	Sutherland	Female	0	0	NA	0	0	0	0
28055	1957	Lincoln	Nebraska	41.144457	-101.12705	historic	18	Sutherland	Female	0	0	NA	0	0	0	0
28056	1957	Lincoln	Nebraska	41.144457	-101.12705	historic	18	Sutherland	Female	0	0	NA	0	0	0	0
28057	1957	Lincoln	Nebraska	41.144457	-101.12705	historic	18	Sutherland	Male	0	0	0	0	0	0	0
28058	1957	Lincoln	Nebraska	41.144457	-101.12705	historic	18	Sutherland	Male	1	0	0	0	0	0	0.04166667
28059	1957	Lincoln	Nebraska	41.144457	-101.12705	historic	18	Sutherland	Male	0	0	0	0	0	0	0
28060	1957	Lincoln	Nebraska	41.144457	-101.12705	historic	18	Sutherland	Female	0	0	NA	1	0	0	0.05
28061	1957	Lincoln	Nebraska	41.144457	-101.12705	historic	18	Sutherland	Female	0	0	NA	0	0	0	0
28062	1957	Lincoln	Nebraska	41.144457	-101.12705	historic	18	Sutherland	Male	0	0	0	0	0	1	0.04166667
28063	1957	Lincoln	Nebraska	41.144457	-101.12705	historic	18	Sutherland	Male	0	0	0	0	0	0	0
28064	1957	Lincoln	Nebraska	41.144457	-101.12705	historic	18	Sutherland	Female	0	0	NA	0	0	0	0
28065	1957	Lincoln	Nebraska	41.144457	-101.12705	historic	18	Sutherland	Female	1	0	NA	0	0	0	0.05
28066	1957	Lincoln	Nebraska	41.144457	-101.12705	historic	18	Sutherland	Male	0	0	0	0	0	2	0.08333333
28067	1957	Lincoln	Nebraska	41.144457	-101.12705	historic	18	Sutherland	Female	1	0	NA	0	0	0	0.05
28068	1957	Lincoln	Nebraska	41.144457	-101.12705	historic	18	Sutherland	Male	0	0	0	0	0	0	0
28069	1957	Lincoln	Nebraska	41.144457	-101.12705	historic	18	Sutherland	Female	0	0	NA	0	0	0	0
28070	1957	Lincoln	Nebraska	41.144457	-101.12705	historic	18	Sutherland	Female	0	0	NA	0	0	0	0
28071	1957	Lincoln	Nebraska	41.144457	-101.12705	historic	18	Sutherland	Female	1	0	NA	0	0	0	0.05
26115	1955	Thomas	Nebraska	41.903358	-100.31039	historic	20	Halsey	Male	3	0	0	0	0	0	0.125
26116	1955	Thomas	Nebraska	41.903358	-100.31039	historic	20	Halsey	Female	1	0	NA	0	0	0	0.05
27986	1956	Dawson	Nebraska	40.899611	-100.14843	historic	21	Gothenberg	Male	1	0	1	0	0	0	0.08333333
27987	1956	Dawson	Nebraska	40.899611	-100.14843	historic	21	Gothenberg	Female	0	0	NA	0	0	0	0
27988	1956	Dawson	Nebraska	40.899611	-100.14843	historic	21	Gothenberg	Female	1	0	NA	0	0	0	0.05
27989	1956	Dawson	Nebraska	40.899611	-100.14843	historic	21	Gothenberg	Male	1	0	0	0	0	0	0.04166667
27990	1956	Dawson	Nebraska	40.899611	-100.14843	historic	21	Gothenberg	Male	0	0	0	0	0	0	0
27991	1956	Dawson	Nebraska	40.899611	-100.14843	historic	21	Gothenberg	Female	0	0	NA	0	0	0	0
27992	1956	Dawson	Nebraska	40.899611	-100.14843	historic	21	Gothenberg	Female	0	0	NA	0	0	0	0
27993	1956	Dawson	Nebraska	40.899611	-100.14843	historic	21	Gothenberg	Female	3	0	NA	0	0	0	0.15
27994	1956	Dawson	Nebraska	40.899611	-100.14843	historic	21	Gothenberg	Female	2	0	NA	0	0	0	0.1
27995	1956	Dawson	Nebraska	40.899611	-100.14843	historic	21	Gothenberg	Male	0	0	1	0	0	0	0.04166667
27996	1956	Dawson	Nebraska	40.899611	-100.14843	historic	21	Gothenberg	Male	2	0	0	0	0	0	0.08333333
27997	1956	Dawson	Nebraska	40.899611	-100.14843	historic	21	Gothenberg	Female	0	0	NA	0	0	0	0
27998	1956	Dawson	Nebraska	40.899611	-100.14843	historic	21	Gothenberg	Female	1	0	NA	0	0	0	0.05
27999	1956	Dawson	Nebraska	40.899611	-100.14843	historic	21	Gothenberg	Male	2	0	1	0	0	0	0.125
28000	1957	Dawson	Nebraska	40.899611	-100.14843	historic	21	Gothenberg	Male	0	0	0	0	3	0	0.125
28001	1957	Dawson	Nebraska	40.899611	-100.14843	historic	21	Gothenberg	Male	0	0	0	1	0	0	0.04166667
28002	1957	Dawson	Nebraska	40.899611	-100.14843	historic	21	Gothenberg	Male	0	0	0	0	0	0	0
28003	1957	Dawson	Nebraska	40.899611	-100.14843	historic	21	Gothenberg	Male	3	0	0	0	0	0	0.125
28005	1957	Dawson	Nebraska	40.899611	-100.14843	historic	21	Gothenberg	Male	0	0	0	0	0	0	0
28008	1957	Dawson	Nebraska	40.899611	-100.14843	historic	21	Gothenberg	Male	0	0	0	1	0	0	0.04166667
28009	1957	Dawson	Nebraska	40.899611	-100.14843	historic	21	Gothenberg	Male	0	0	1	0	0	0	0.04166667
28010	1957	Dawson	Nebraska	40.899611	-100.14843	historic	21	Gothenberg	Male	0	0	0	0	0	0	0
28011	1957	Dawson	Nebraska	40.899611	-100.14843	historic	21	Gothenberg	Male	1	0	0	0	0	0	0.04166667
28012	1957	Dawson	Nebraska	40.899611	-100.14843	historic	21	Gothenberg	Male	0	2	0	0	0	3	0.20833333

(Table A1 continued)

28013	1957	Dawson	Nebraska	40.899611	-100.14843	historic	21	Gothenberg	Female	0	0	NA	0	0	0	0
28014	1957	Dawson	Nebraska	40.899611	-100.14843	historic	21	Gothenberg	Female	0	0	NA	0	0	0	0
28015	1957	Dawson	Nebraska	40.899611	-100.14843	historic	21	Gothenberg	Female	0	0	NA	0	0	0	0
28017	1957	Dawson	Nebraska	40.899611	-100.14843	historic	21	Gothenberg	Male	0	0	0	0	0	2	0.08333333
28018	1957	Dawson	Nebraska	40.899611	-100.14843	historic	21	Gothenberg	Female	0	0	NA	0	2	0	0.1
28020	1957	Dawson	Nebraska	40.899611	-100.14843	historic	21	Gothenberg	Female	2	0	NA	0	0	0	0.1
28021	1957	Dawson	Nebraska	40.899611	-100.14843	historic	21	Gothenberg	Male	0	0	0	0	0	0	0
28022	1957	Dawson	Nebraska	40.899611	-100.14843	historic	21	Gothenberg	Female	0	0	NA	0	0	1	0.05
28023	1957	Dawson	Nebraska	40.899611	-100.14843	historic	21	Gothenberg	Male	0	0	0	0	0	0	0
27958	1956	Phelps	Nebraska	40.686493	-99.337838	historic	22	Elm Creek	Male	0	0	0	0	0	0	0
27961	1956	Phelps	Nebraska	40.686493	-99.337838	historic	22	Elm Creek	Female	2	0	NA	0	0	0	0.1
27963	1956	Phelps	Nebraska	40.686493	-99.337838	historic	22	Elm Creek	Male	0	0	0	0	0	0	0
27964	1956	Phelps	Nebraska	40.686493	-99.337838	historic	22	Elm Creek	Male	0	0	1	0	0	0	0.04166667
27965	1956	Phelps	Nebraska	40.686493	-99.337838	historic	22	Elm Creek	Female	0	0	NA	0	0	0	0
27966	1956	Phelps	Nebraska	40.686493	-99.337838	historic	22	Elm Creek	Female	0	0	NA	2	0	0	0.1
27967	1956	Phelps	Nebraska	40.686493	-99.337838	historic	22	Elm Creek	Male	0	0	0	0	0	0	0
27968	1956	Phelps	Nebraska	40.686493	-99.337838	historic	22	Elm Creek	Male	0	0	0	0	0	0	0
27969	1956	Phelps	Nebraska	40.686493	-99.337838	historic	22	Elm Creek	Female	0	0	NA	0	0	0	0
27970	1956	Phelps	Nebraska	40.686493	-99.337838	historic	22	Elm Creek	Male	1	0	0	0	0	0	0.04166667
27971	1956	Phelps	Nebraska	40.686493	-99.337838	historic	22	Elm Creek	Female	0	0	NA	0	0	0	0
27972	1956	Phelps	Nebraska	40.686493	-99.337838	historic	22	Elm Creek	Male	0	0	0	0	0	0	0
27973	1956	Phelps	Nebraska	40.686493	-99.337838	historic	22	Elm Creek	Male	1	0	0	0	0	0	0.04166667
27975	1957	Phelps	Nebraska	40.686493	-99.337838	historic	22	Elm Creek	Male	3	0	0	0	0	0	0.125
27976	1957	Phelps	Nebraska	40.686493	-99.337838	historic	22	Elm Creek	Male	1	0	0	0	0	0	0.04166667
27977	1957	Phelps	Nebraska	40.686493	-99.337838	historic	22	Elm Creek	Female	1	0	NA	1	0	0	0.1
27978	1957	Phelps	Nebraska	40.686493	-99.337838	historic	22	Elm Creek	Female	1	0	NA	0	0	0	0.05
27979	1957	Phelps	Nebraska	40.686493	-99.337838	historic	22	Elm Creek	Male	0	0	0	0	0	0	0
27980	1957	Phelps	Nebraska	40.686493	-99.337838	historic	22	Elm Creek	Female	0	0	NA	0	0	0	0
27981	1957	Phelps	Nebraska	40.686493	-99.337838	historic	22	Elm Creek	Male	3	0	0	0	0	0	0.125
27983	1957	Phelps	Nebraska	40.686493	-99.337838	historic	22	Elm Creek	Female	2	0	NA	0	0	0	0.1
27984	1957	Phelps	Nebraska	40.686493	-99.337838	historic	22	Elm Creek	Male	0	0	1	0	0	0	0.04166667
27985	1957	Phelps	Nebraska	40.686493	-99.337838	historic	22	Elm Creek	Male	0	0	0	0	0	0	0
26119	1955	Loup	Nebraska	41.756348	-99.282391	historic	23	Burwell	Male	0	0	1	0	0	0	0.04166667
26121	1955	Loup	Nebraska	41.756348	-99.282391	historic	23	Burwell	Female	0	0	NA	0	0	0	0
26122	1955	Loup	Nebraska	41.756348	-99.282391	historic	23	Burwell	Male	2	0	0	0	0	0	0.08333333
26123	1955	Loup	Nebraska	41.756348	-99.282391	historic	23	Burwell	Male	0	0	0	0	0	0	0
26126	1955	Loup	Nebraska	41.756348	-99.282391	historic	23	Burwell	Male	0	0	0	0	0	0	0
26129	1955	Loup	Nebraska	41.756348	-99.282391	historic	23	Burwell	Male	2	0	0	0	0	0	0.08333333
26079	1955	Howard	Nebraska	41.170793	-98.459716	historic	24	Grand Island	Female	3	0	NA	0	0	0	0.15
26080	1955	Howard	Nebraska	41.170793	-98.459716	historic	24	Grand Island	Male	0	0	1	0	0	0	0.04166667
26081	1955	Howard	Nebraska	41.170793	-98.459716	historic	24	Grand Island	Female	0	0	NA	0	0	0	0
26082	1955	Howard	Nebraska	41.170793	-98.459716	historic	24	Grand Island	Female	2	0	NA	0	0	0	0.1
26085	1955	Howard	Nebraska	41.170793	-98.459716	historic	24	Grand Island	Female	2	0	NA	0	0	0	0.1
26087	1955	Howard	Nebraska	41.170793	-98.459716	historic	24	Grand Island	Female	2	0	NA	0	0	0	0.1
26088	1955	Greeley	Nebraska	41.446867	-98.710826	historic	24	Grand Island	Male	3	0	0	0	0	0	0.125
26092	1955	Adams	Nebraska	40.456467	-98.39133	historic	24	Grand Island	Male	0	0	0	0	0	0	0
26093	1955	Adams	Nebraska	40.456467	-98.39133	historic	24	Grand Island	Male	2	0	1	0	0	3	0.25
26095	1955	Adams	Nebraska	40.456467	-98.39133	historic	24	Grand Island	Male	1	0	0	0	0	0	0.04166667
26096	1955	Adams	Nebraska	40.456467	-98.39133	historic	24	Grand Island	Male	0	0	0	0	0	0	0
26098	1955	Adams	Nebraska	40.456467	-98.39133	historic	24	Grand Island	Female	3	0	NA	0	0	0	0.15
26139	1955	Hall	Nebraska	40.826569	-98.385575	historic	24	Grand Island	Male	0	0	0	0	0	0	0
26140	1955	Hall	Nebraska	40.826569	-98.385575	historic	24	Grand Island	Female	1	0	NA	0	0	0	0.05
26144	1955	Hall	Nebraska	40.826569	-98.385575	historic	24	Grand Island	Male	0	0	0	0	0	0	0
26145	1955	Hall	Nebraska	40.826569	-98.385575	historic	24	Grand Island	Male	0	0	0	0	0	0	0
26147	1955	Hall	Nebraska	40.826569	-98.385575	historic	24	Grand Island	Female	0	0	NA	0	0	0	0
26149	1955	Hall	Nebraska	40.826569	-98.385575	historic	24	Grand Island	Female	2	0	NA	0	0	0	0.1

(Table A1 continued)

26160	1955	Howard	Nebraska	41.170793	-98.459716	historic	24	Grand Island	Male	1	0	0	0	0	3	0.16666667
27932	1956	Hall	Nebraska	40.826569	-98.385575	historic	24	Grand Island	Female	2	0	NA	1	0	0	0.15
27933	1956	Hall	Nebraska	40.826569	-98.385575	historic	24	Grand Island	Male	0	0	0	0	0	0	0
27934	1956	Hall	Nebraska	40.826569	-98.385575	historic	24	Grand Island	Male	1	0	0	0	0	0	0.04166667
27935	1956	Hall	Nebraska	40.826569	-98.385575	historic	24	Grand Island	Male	0	0	0	0	0	1	0.04166667
27936	1956	Hall	Nebraska	40.826569	-98.385575	historic	24	Grand Island	Male	0	0	0	0	0	0	0
27937	1956	Hall	Nebraska	40.826569	-98.385575	historic	24	Grand Island	Male	0	0	1	0	0	0	0.04166667
27938	1956	Hall	Nebraska	40.826569	-98.385575	historic	24	Grand Island	Male	0	0	0	0	0	0	0
27939	1956	Hall	Nebraska	40.826569	-98.385575	historic	24	Grand Island	Female	1	0	NA	0	0	0	0.05
27940	1956	Hall	Nebraska	40.826569	-98.385575	historic	24	Grand Island	Male	0	0	0	0	0	0	0
27942	1956	Hall	Nebraska	40.826569	-98.385575	historic	24	Grand Island	Male	0	0	1	0	0	0	0.04166667
27943	1957	Hall	Nebraska	40.826569	-98.385575	historic	24	Grand Island	Female	0	0	NA	0	0	0	0
27944	1957	Hall	Nebraska	40.826569	-98.385575	historic	24	Grand Island	Male	0	0	0	0	0	0	0
27945	1957	Hall	Nebraska	40.826569	-98.385575	historic	24	Grand Island	Male	1	0	0	0	0	0	0.04166667
27946	1957	Hall	Nebraska	40.826569	-98.385575	historic	24	Grand Island	Female	1	0	NA	0	0	0	0.05
27947	1957	Hall	Nebraska	40.826569	-98.385575	historic	24	Grand Island	Female	2	0	NA	0	0	0	0.1
27948	1957	Hall	Nebraska	40.826569	-98.385575	historic	24	Grand Island	Male	0	0	0	0	0	0	0
27949	1957	Hall	Nebraska	40.826569	-98.385575	historic	24	Grand Island	Male	0	0	0	0	0	0	0
27950	1957	Hall	Nebraska	40.826569	-98.385575	historic	24	Grand Island	Male	1	0	0	0	0	0	0.04166667
27951	1957	Hall	Nebraska	40.826569	-98.385575	historic	24	Grand Island	Female	1	0	NA	0	0	0	0.05
27952	1957	Hall	Nebraska	40.826569	-98.385575	historic	24	Grand Island	Female	2	0	NA	0	0	0	0.1
27953	1957	Hall	Nebraska	40.826569	-98.385575	historic	24	Grand Island	Female	0	0	NA	0	0	0	0
27954	1957	Hall	Nebraska	40.826569	-98.385575	historic	24	Grand Island	Female	1	0	NA	0	0	0	0.05
27956	1957	Hall	Nebraska	40.826569	-98.385575	historic	24	Grand Island	Female	2	0	NA	0	0	0	0.1
27891	1956	Polk	Nebraska	41.275898	-97.686277	historic	25	Silver Creek	Male	0	0	0	0	0	0	0
27892	1956	Polk	Nebraska	41.275898	-97.686277	historic	25	Silver Creek	Female	0	0	NA	0	0	0	0
27893	1956	Polk	Nebraska	41.275898	-97.686277	historic	25	Silver Creek	Female	2	0	NA	0	0	0	0.1
27894	1956	Polk	Nebraska	41.275898	-97.686277	historic	25	Silver Creek	Female	1	0	NA	0	0	0	0.05
27895	1956	Polk	Nebraska	41.275898	-97.686277	historic	25	Silver Creek	Female	0	1	NA	0	0	2	0.15
27896	1956	Polk	Nebraska	41.275898	-97.686277	historic	25	Silver Creek	Female	0	0	NA	0	0	0	0
27897	1956	Polk	Nebraska	41.275898	-97.686277	historic	25	Silver Creek	Female	0	0	NA	0	0	0	0
27898	1956	Polk	Nebraska	41.275898	-97.686277	historic	25	Silver Creek	Female	0	0	NA	0	0	0	0
27900	1956	Polk	Nebraska	41.275898	-97.686277	historic	25	Silver Creek	Male	0	0	0	0	0	0	0
27904	1956	Polk	Nebraska	41.275898	-97.686277	historic	25	Silver Creek	Male	1	0	1	0	0	0	0.08333333
27905	1956	Polk	Nebraska	41.275898	-97.686277	historic	25	Silver Creek	Female	2	0	NA	0	0	0	0.1
27906	1956	Polk	Nebraska	41.275898	-97.686277	historic	25	Silver Creek	Male	3	0	0	0	0	0	0.125
27909	1956	Polk	Nebraska	41.275898	-97.686277	historic	25	Silver Creek	Female	1	0	NA	0	0	0	0.05
27912	1956	Polk	Nebraska	41.275898	-97.686277	historic	25	Silver Creek	Male	1	0	0	0	0	0	0.04166667
27913	1957	Polk	Nebraska	41.275898	-97.686277	historic	25	Silver Creek	Male	0	0	0	0	0	0	0
27914	1957	Polk	Nebraska	41.275898	-97.686277	historic	25	Silver Creek	Male	0	0	0	0	0	0	0
27915	1957	Polk	Nebraska	41.275898	-97.686277	historic	25	Silver Creek	Female	1	0	NA	0	0	0	0.05
27916	1957	Polk	Nebraska	41.275898	-97.686277	historic	25	Silver Creek	Female	0	0	NA	0	0	0	0
27918	1957	Polk	Nebraska	41.275898	-97.686277	historic	25	Silver Creek	Male	2	0	0	0	0	0	0.08333333
27919	1957	Polk	Nebraska	41.275898	-97.686277	historic	25	Silver Creek	Female	0	0	NA	0	0	0	0
27920	1957	Polk	Nebraska	41.275898	-97.686277	historic	25	Silver Creek	Female	0	0	NA	0	0	0	0
27921	1957	Polk	Nebraska	41.275898	-97.686277	historic	25	Silver Creek	Female	0	0	NA	0	0	0	0
27923	1957	Polk	Nebraska	41.275898	-97.686277	historic	25	Silver Creek	Female	0	0	NA	0	0	0	0
27925	1957	Polk	Nebraska	41.275898	-97.686277	historic	25	Silver Creek	Male	0	0	0	0	0	0	0
27926	1957	Polk	Nebraska	41.275898	-97.686277	historic	25	Silver Creek	Female	1	0	NA	0	0	0	0.05
27927	1957	Polk	Nebraska	41.275898	-97.686277	historic	25	Silver Creek	Male	0	0	0	0	0	1	0.04166667
27928	1957	Polk	Nebraska	41.275898	-97.686277	historic	25	Silver Creek	Male	0	0	0	0	0	0	0
27929	1957	Polk	Nebraska	41.275898	-97.686277	historic	25	Silver Creek	Male	0	0	0	0	3	0	0.125
27930	1957	Polk	Nebraska	41.275898	-97.686277	historic	25	Silver Creek	Male	0	0	0	0	0	0	0
27854	1956	Colfax	Nebraska	41.418285	-97.035706	historic	26	Schuyler	Male	0	0	0	0	0	0	0
27855	1956	Colfax	Nebraska	41.418285	-97.035706	historic	26	Schuyler	Male	0	0	0	0	0	0	0
27856	1956	Colfax	Nebraska	41.418285	-97.035706	historic	26	Schuyler	Male	0	0	0	0	0	0	0

(Table A1 continued)

27858	1956	Colfax	Nebraska	41.418285	-97.035706	historic	26	Schuyler	Female	0	0	NA	0	0	0	0
27859	1956	Colfax	Nebraska	41.418285	-97.035706	historic	26	Schuyler	Female	0	0	NA	0	0	0	0
27860	1956	Colfax	Nebraska	41.418285	-97.035706	historic	26	Schuyler	Male	0	0	1	0	0	0	0.04166667
27861	1956	Colfax	Nebraska	41.418285	-97.035706	historic	26	Schuyler	Male	0	0	0	0	0	0	0
27862	1956	Colfax	Nebraska	41.418285	-97.035706	historic	26	Schuyler	Male	0	0	0	0	0	0	0
27863	1956	Colfax	Nebraska	41.418285	-97.035706	historic	26	Schuyler	Male	0	0	1	0	0	0	0.04166667
27864	1956	Colfax	Nebraska	41.418285	-97.035706	historic	26	Schuyler	Male	0	0	0	0	0	0	0
27865	1956	Colfax	Nebraska	41.418285	-97.035706	historic	26	Schuyler	Male	0	0	0	0	0	0	0
27866	1956	Colfax	Nebraska	41.418285	-97.035706	historic	26	Schuyler	Female	0	0	NA	0	0	0	0
27867	1956	Colfax	Nebraska	41.418285	-97.035706	historic	26	Schuyler	Male	0	0	0	0	0	1	0.04166667
27868	1956	Colfax	Nebraska	41.418285	-97.035706	historic	26	Schuyler	Male	0	0	0	0	0	0	0
27869	1956	Colfax	Nebraska	41.418285	-97.035706	historic	26	Schuyler	Male	0	0	0	0	0	0	0
27870	1956	Colfax	Nebraska	41.418285	-97.035706	historic	26	Schuyler	Male	0	0	0	0	0	0	0
27871	1956	Colfax	Nebraska	41.418285	-97.035706	historic	26	Schuyler	Female	1	0	NA	0	0	0	0.05
27872	1956	Colfax	Nebraska	41.418285	-97.035706	historic	26	Schuyler	Female	1	0	NA	0	0	0	0.05
27873	1956	Colfax	Nebraska	41.418285	-97.035706	historic	26	Schuyler	Female	0	0	NA	0	0	0	0
27874	1956	Colfax	Nebraska	41.418285	-97.035706	historic	26	Schuyler	Female	0	0	NA	0	0	0	0
27875	1957	Colfax	Nebraska	41.418285	-97.035706	historic	26	Schuyler	Female	0	0	NA	0	0	0	0
27876	1957	Colfax	Nebraska	41.418285	-97.035706	historic	26	Schuyler	Female	1	0	NA	0	0	0	0.05
27877	1957	Colfax	Nebraska	41.418285	-97.035706	historic	26	Schuyler	Female	0	0	NA	0	0	0	0
27878	1957	Colfax	Nebraska	41.418285	-97.035706	historic	26	Schuyler	Male	0	0	0	0	0	0	0
27879	1957	Colfax	Nebraska	41.418285	-97.035706	historic	26	Schuyler	Male	0	0	0	0	0	0	0
27880	1957	Colfax	Nebraska	41.418285	-97.035706	historic	26	Schuyler	Female	0	0	NA	0	0	0	0
27881	1957	Colfax	Nebraska	41.418285	-97.035706	historic	26	Schuyler	Female	0	0	NA	0	0	0	0
27882	1957	Colfax	Nebraska	41.418285	-97.035706	historic	26	Schuyler	Male	0	0	0	0	0	1	0.04166667
27883	1957	Colfax	Nebraska	41.418285	-97.035706	historic	26	Schuyler	Male	1	0	0	0	0	0	0.04166667
27884	1957	Colfax	Nebraska	41.418285	-97.035706	historic	26	Schuyler	Female	0	0	NA	0	0	0	0
27885	1957	Colfax	Nebraska	41.418285	-97.035706	historic	26	Schuyler	Female	0	0	NA	1	0	0	0.05
27886	1957	Colfax	Nebraska	41.418285	-97.035706	historic	26	Schuyler	Female	0	0	NA	0	0	1	0.05
27887	1957	Colfax	Nebraska	41.418285	-97.035706	historic	26	Schuyler	Female	2	0	NA	0	0	0	0.1
27888	1956	Colfax	Nebraska	41.418285	-97.035706	historic	26	Schuyler	Female	1	0	NA	0	0	0	0.05
27889	1956	Colfax	Nebraska	41.418285	-97.035706	historic	26	Schuyler	Female	0	0	NA	3	0	0	0.15
27890	1956	Colfax	Nebraska	41.418285	-97.035706	historic	26	Schuyler	Female	0	0	NA	0	0	0	0
27853	1957	Washington	Nebraska	41.520252	-96.072984	historic	27	Eastern	Male	0	0	0	0	0	0	0
58063	2018	Larimer	Colorado	40.877545	-105.45918	contemporary	1	Western	Male	4	4	4	4	3	4	0.95833333
58066	2018	Larimer	Colorado	40.9534225	-105.51859	contemporary	1	Western	Male	4	4	4	4	4	3	0.95833333
58077	2018	Larimer	Colorado	40.9281916	-105.53019	contemporary	1	Western	Male	4	4	4	4	4	4	1
58078	2018	Larimer	Colorado	40.9278115	-105.52583	contemporary	1	Western	Male	4	4	4	1	4	4	0.875
1833-36503	2016	Larimer	Colorado	40.683309	-105.55056	contemporary	1	Western	Male	4	3	4	4	4	4	0.95833333
57967	2017	Weld	Colorado	40.3946389	-104.49341	contemporary	3	Kersey	Male	1	4	3	0	1	4	0.54166667
58062	2018	Weld	Colorado	40.3672611	-104.44124	contemporary	3	Kersey	Male	4	4	4	4	4	4	1
58070	2018	Weld	Colorado	40.3672611	-104.44124	contemporary	3	Kersey	Male	4	4	4	0	1	4	0.70833333
58071	2018	Weld	Colorado	40.3672611	-104.44124	contemporary	3	Kersey	Male	3	4	4	3	2	4	0.83333333
58075	2018	Weld	Colorado	40.3672611	-104.44124	contemporary	3	Kersey	Female	4	4	NA	4	4	4	1
58076	2018	Weld	Colorado	40.3672611	-104.44124	contemporary	3	Kersey	Female	0	3	NA	1	0	4	0.4
58089	2018	Weld	Colorado	40.3672611	-104.44124	contemporary	3	Kersey	Male	1	3	4	2	4	3	0.70833333
58149	2018	Weld	Colorado	40.3672611	-104.44124	contemporary	3	Kersey	Male	3	0	4	0	4	0	0.45833333
58150	2018	Weld	Colorado	40.3672611	-104.44124	contemporary	3	Kersey	Male	2	2	2	3	4	3	0.66666667
58151	2018	Weld	Colorado	40.3672611	-104.44124	contemporary	3	Kersey	Female	1	0	NA	1	1	1	0.2
58152	2018	Weld	Colorado	40.3672611	-104.44124	contemporary	3	Kersey	Male	4	4	4	4	4	4	1
58153	2018	Weld	Colorado	40.3672611	-104.44124	contemporary	3	Kersey	Male	4	4	4	4	1	4	0.875
58154	2018	Weld	Colorado	40.3672611	-104.44124	contemporary	3	Kersey	Male	4	2	2	4	2	4	0.75
1803-25408	2016	Morgan	Colorado	40.35563	-104.09725	contemporary	4	Orchard	Female	2	2	NA	4	2	3	0.65
1833-36502	2016	Morgan	Colorado	40.35563	-104.09725	contemporary	4	Orchard	Male	1	2	3	1	4	3	0.58333333
56726	2016	Scotts Bluff	Nebraska	41.9671694	-103.93139	contemporary	6	Morrill	Male	0	0	1	0	4	0	0.20833333
56727	2016	Scotts Bluff	Nebraska	41.9671694	-103.93139	contemporary	6	Morrill	Male	4	2	4	3	4	3	0.83333333

(Table A1 continued)

56736	2016	Scotts Bluff	Nebraska	41.9671694	-103.93139	contemporary	6	Morrill	Male	4	4	4	3	2	4	0.875
58064	2018	Scotts Bluff	Nebraska	41.9364698	-103.90436	contemporary	6	Morrill	Female	2	2	NA	4	0	4	0.6
57987	2017	Morgan	Colorado	40.2825194	-103.70253	contemporary	7	E Fort Morgan	Male	0	0	0	0	0	0	0
57988	2017	Morgan	Colorado	40.2825194	-103.70253	contemporary	7	E Fort Morgan	Male	1	3	2	0	1	4	0.45833333
58079	2018	Morgan	Colorado	40.2825194	-103.70253	contemporary	7	E Fort Morgan	Male	2	3	3	0	0	2	0.41666667
58080	2018	Morgan	Colorado	40.2825194	-103.70253	contemporary	7	E Fort Morgan	Male	3	4	2	1	3	4	0.70833333
58081	2018	Morgan	Colorado	40.2825194	-103.70253	contemporary	7	E Fort Morgan	Female	0	0	NA	0	0	0	0
58082	2018	Morgan	Colorado	40.2825194	-103.70253	contemporary	7	E Fort Morgan	Female	0	0	NA	0	0	0	0
58088	2018	Morgan	Colorado	40.2825194	-103.70253	contemporary	7	E Fort Morgan	Male	0	2	1	0	0	2	0.20833333
58094	2018	Morgan	Colorado	40.2825194	-103.70253	contemporary	7	E Fort Morgan	Female	0	0	NA	0	1	2	0.15
58097	2018	Morgan	Colorado	40.2825194	-103.70253	contemporary	7	E Fort Morgan	Male	0	0	1	1	1	0	0.125
57642	2017	Morgan	Colorado	40.3298	-103.56721	contemporary	8	Brush	Female	0	0	NA	1	1	3	0.25
58060	2018	Morgan	Colorado	40.3221972	-103.60051	contemporary	8	Brush	Female	1	0	NA	4	0	0	0.25
58083	2018	Morgan	Colorado	40.3298	-103.56721	contemporary	8	Brush	Male	2	1	1	0	0	3	0.29166667
58067	2018	Scotts Bluff	Nebraska	41.8984992	-103.42772	contemporary	9	Minatare	Male	0	0	2	0	0	2	0.16666667
58068	2018	Scotts Bluff	Nebraska	41.8984992	-103.42772	contemporary	9	Minatare	Male	0	4	3	3	0	4	0.58333333
58069	2018	Scotts Bluff	Nebraska	41.8984992	-103.42772	contemporary	9	Minatare	Male	0	4	4	0	1	3	0.5
58074	2018	Morgan	Colorado	40.4047694	-103.39182	contemporary	10	Merino	Male	0	0	3	0	0	2	0.20833333
58090	2018	Morgan	Colorado	40.4047694	-103.39182	contemporary	10	Merino	Male	1	2	1	0	0	3	0.29166667
56724	2016	Morrill	Nebraska	41.6895056	-103.16821	contemporary	11	Bridgeport	Male	0	0	2	0	1	0	0.125
56725	2016	Morrill	Nebraska	41.6895056	-103.16821	contemporary	11	Bridgeport	Male	0	0	1	0	1	0	0.08333333
56734	2016	Morrill	Nebraska	41.6895056	-103.16821	contemporary	11	Bridgeport	Female	4	0	NA	3	0	3	0.5
57607	2017	Logan	Colorado	40.8388917	-102.81204	contemporary	12	Crook	Female	0	0	NA	0	0	1	0.05
57608	2017	Logan	Colorado	40.8388917	-102.81204	contemporary	12	Crook	Female	2	0	NA	4	1	0	0.35
57609	2017	Logan	Colorado	40.8388917	-102.81204	contemporary	12	Crook	Male	0	0	1	0	1	0	0.08333333
57610	2017	Logan	Colorado	40.8388917	-102.81204	contemporary	12	Crook	Female	3	0	NA	4	4	0	0.55
57986	2017	Logan	Colorado	40.8388917	-102.81204	contemporary	12	Crook	Female	0	0	NA	0	1	2	0.15
58059	2018	Logan	Colorado	40.8388917	-102.81204	contemporary	12	Crook	Female	0	0	NA	0	0	0	0
58061	2018	Logan	Colorado	40.8388917	-102.81204	contemporary	12	Crook	Male	0	0	0	0	0	0	0
58072	2018	Logan	Colorado	40.8388917	-102.81204	contemporary	12	Crook	Male	0	0	0	0	0	2	0.08333333
58073	2018	Logan	Colorado	40.8388917	-102.81204	contemporary	12	Crook	Female	0	0	NA	0	0	0	0
58084	2018	Logan	Colorado	40.8388917	-102.81204	contemporary	12	Crook	Male	2	0	0	0	1	1	0.16666667
58085	2018	Logan	Colorado	40.8388917	-102.81204	contemporary	12	Crook	Female	1	1	NA	3	2	2	0.45
58086	2018	Logan	Colorado	40.8388917	-102.81204	contemporary	12	Crook	Female	0	0	NA	0	0	0	0
58087	2018	Logan	Colorado	40.8388917	-102.81204	contemporary	12	Crook	Male	0	0	0	0	0	1	0.04166667
58092	2018	Logan	Colorado	40.8388917	-102.81204	contemporary	12	Crook	Male	1	0	1	0	0	0	0.08333333
58093	2018	Logan	Colorado	40.8388917	-102.81204	contemporary	12	Crook	Female	0	0	NA	0	0	1	0.05
58065	2018	Garden	Nebraska	41.4499137	-102.53066	contemporary	13	Lisco	Male	0	0	0	0	0	2	0.08333333
58148	2018	Garden	Nebraska	41.4499137	-102.53066	contemporary	13	Lisco	Male	4	0	2	4	4	1	0.625
1803-25409	2016	Sedgwick	Colorado	40.932974	-102.48678	contemporary	14	Sedgwick	Male	1	2	4	1	4	3	0.625
1803-25410	2016	Sedgwick	Colorado	40.932974	-102.48678	contemporary	14	Sedgwick	Female	1	0	NA	1	2	0	0.2
1833-36504	2016	Sedgwick	Colorado	40.932974	-102.48678	contemporary	14	Sedgwick	Female	1	1	NA	2	2	3	0.45
56722	2016	Deuel	Nebraska	41.0423944	-102.13668	contemporary	15	Big Springs	Male	0	0	0	0	0	0	0
57686	2017	Deuel	Nebraska	41.0423944	-102.13668	contemporary	15	Big Springs	Male	0	0	0	0	2	0	0.08333333
56728	2016	NA	Nebraska	41.2976611	-102.02668	contemporary	16	Lewellen	Male	0	0	1	0	0	0	0.04166667
56737	2016	NA	Nebraska	41.2976611	-102.02668	contemporary	16	Lewellen	Male	0	0	0	0	0	0	0
58091	2018	Keith	Nebraska	41.301746	-102.01262	contemporary	16	Lewellen	Male	0	0	0	0	0	2	0.08333333
58095	2018	Keith	Nebraska	41.301746	-102.01262	contemporary	16	Lewellen	Male	0	0	1	0	0	0	0.04166667
58096	2018	Keith	Nebraska	41.301746	-102.01262	contemporary	16	Lewellen	Female	0	0	NA	0	0	0	0
58146	2018	Keith	Nebraska	41.301746	-102.01262	contemporary	16	Lewellen	Female	1	0	NA	0	0	0	0.05
58147	2018	Keith	Nebraska	41.301746	-102.01262	contemporary	16	Lewellen	Male	0	0	0	0	0	0	0
1803-25403	2016	Keith	Nebraska	41.298255	-102.05192	contemporary	16	Lewellen	Male	0	0	1	1	0	1	0.125
1803-25404	2016	Keith	Nebraska	41.298255	-102.05192	contemporary	16	Lewellen	Male	2	0	1	0	0	0	0.125
1803-25405	2016	Keith	Nebraska	41.298255	-102.05192	contemporary	16	Lewellen	Male	0	0	0	1	0	0	0.04166667
1803-25401	2016	Keith	Nebraska	41.22806	-101.74345	contemporary	17	Ogallala	Male	0	0	0	0	0	0	0
1803-25402	2016	Keith	Nebraska	41.22806	-101.74345	contemporary	17	Ogallala	Male	0	0	0	0	0	0	0

(Table A1 continued)

1833-36501	2016	Keith	Nebraska	41.22806	-101.74345	contemporary	17	Ogallala	Male	0	0	0	0	0	0	0
56720	2016	Lincoln	Nebraska	41.1495917	-101.07404	contemporary	18	Sutherland	Male	0	0	0	0	0	0	0
56733	2016	Lincoln	Nebraska	41.1495917	-101.07404	contemporary	18	Sutherland	Female	0	0	NA	0	0	0	0
57708	2017	Lincoln	Nebraska	41.1495917	-101.07404	contemporary	18	Sutherland	Male	0	0	0	0	0	0	0
57709	2017	Lincoln	Nebraska	41.1495917	-101.07404	contemporary	18	Sutherland	Male	0	0	1	1	0	0	0.08333333
57764	2017	Lincoln	Nebraska	41.1495917	-101.07404	contemporary	18	Sutherland	Female	0	0	NA	0	0	0	0
1803-25406	2016	Lincoln	Nebraska	41.17314	-100.78951	contemporary	19	North Platte	Male	0	2	2	0	0	3	0.29166667
1803-25407	2016	Lincoln	Nebraska	41.17314	-100.78951	contemporary	19	North Platte	Male	0	0	0	0	0	0	0
56718	2016	Lincoln	Nebraska	40.9493611	-100.26863	contemporary	21	Gothenberg	Male	0	0	0	0	0	0	0
56719	2016	Lincoln	Nebraska	40.9493611	-100.26863	contemporary	21	Gothenberg	Female	0	0	NA	0	0	0	0
56732	2016	Lincoln	Nebraska	40.9493611	-100.26863	contemporary	21	Gothenberg	Female	0	0	NA	0	0	0	0
57728	2017	Dawson	Nebraska	40.9493611	-100.26863	contemporary	21	Gothenberg	Male	0	0	0	0	0	0	0
57729	2017	Dawson	Nebraska	40.9493611	-100.26863	contemporary	21	Gothenberg	Female	0	0	NA	0	0	0	0
56717	2016	Buffalo	Nebraska	40.6849528	-99.391019	contemporary	22	Elm Creek	Male	0	0	0	0	0	1	0.04166667
56731	2016	Buffalo	Nebraska	40.6849528	-99.391019	contemporary	22	Elm Creek	Male	0	0	1	0	0	0	0.04166667
56740	2016	Buffalo	Nebraska	40.6849528	-99.391019	contemporary	22	Elm Creek	Female	0	0	NA	0	0	0	0
57669	2017	Buffalo	Nebraska	40.6849528	-99.391019	contemporary	22	Elm Creek	Male	0	0	0	0	0	1	0.04166667
57985	2017	Buffalo	Nebraska	40.6849528	-99.391019	contemporary	22	Elm Creek	Male	0	0	0	0	0	0	0
57697	2017	Hall	Nebraska	40.8143194	-98.426661	contemporary	24	Grand Island	Male	0	0	0	0	0	0	0
56716	2016	Polk	Nebraska	41.3323694	-97.599622	contemporary	25	Silver Creek	Female	1	0	NA	0	0	0	0.05
56739	2016	Polk	Nebraska	41.3323694	-97.599622	contemporary	25	Silver Creek	Female	0	0	NA	0	0	0	0
56715	2016	Saunders	Nebraska	41.0333889	-96.820339	contemporary	26	Schuyler	Female	0	0	NA	0	0	0	0
56730	2016	Butler	Nebraska	41.4114944	-97.027417	contemporary	26	Schuyler	Female	0	0	NA	0	0	0	0
56738	2016	Butler	Nebraska	41.4114944	-97.027417	contemporary	26	Schuyler	Male	0	0	0	0	0	0	0
57888	2017	Colfax	Nebraska	41.4059111	-97.083072	contemporary	26	Schuyler	Male	0	0	0	0	0	0	0
56729	2016	Washington	Nebraska	41.491075	-96.065614	contemporary	27	Eastern	Male	0	0	0	0	0	0	0
1803-25411	2016	Douglas	Nebraska	41.218737	-96.351863	contemporary	27	Eastern	Female	0	0	NA	0	0	0	0
1803-25412	2016	Douglas	Nebraska	41.218737	-96.351863	contemporary	27	Eastern	Male	0	0	0	0	0	0	0
1803-25413	2016	Douglas	Nebraska	41.218737	-96.351863	contemporary	27	Eastern	Male	1	0	0	0	0	0	0.04166667
57593	2016	Tompkins	New York	42.44413	-76.43883	photos	28	Allopatric YSFL	Male	NA						
51231	2004	Tompkins	New York			photos	28	Allopatric YSFL	Male	NA						
55005	2012	Tompkins	New York	42.4381028	-76.509476	photos	28	Allopatric YSFL	Female	NA						
48696	1996	Onondaga	New York			photos	28	Allopatric YSFL	Female	NA						
58944	2015	King	Washington	47.60621	-122.33207	photos	0	Allopatric RSFL	Male	NA						
57207	2015	King	Washington	47.60621	-122.33207	photos	0	Allopatric RSFL	Female	NA						
6143	1930	Catron	New Mexico			photos	0	Allopatric RSFL	Male	NA						
6156	1938		Coahuila, Mexico			photos	0	Allopatric RSFL	Male	NA						
24648	1953	Comanche	Oklahoma	34.6806523	-98.510284	photos	0	Allopatric RSFL	Male	NA						
27344	1956	El Paso	Texas			photos	0	Allopatric RSFL	Female	NA						
6151	1918	Boulder	Colorado	39.98949	-105.23018	photos	0	Allopatric RSFL	Female	NA						
48643	1998	Alameda	California			photos	0	Allopatric RSFL	Male	NA						

**Table A2.** Details on the qualitative scoring of six phenotypic trait differences between red-shafted and yellow-shafted flickers. This method is slightly adapted from Short (1965).

Phenotype score	Description
<i>Crown color</i>	
0	Gray, as in yellow-shafted
1	Gray with brown traces in forehead and crown
2	Mixed gray and brown (crown half brown with more gray on hind neck)
3	Crown brown with hind neck gray toward back
4	Brown, as in red-shafted
<i>Ear covert color</i>	
0	Tan, as in yellow-shafted
1	Tan with gray traces
2	Mixed gray and tan
3	Gray with tan traces (especially below eye)
4	Gray, as in red-shafted
<i>Malar stripe color (males only)</i>	
0	Black, as in yellow-shafted
1	Black with <20% red
2	Mixed black and red
3	Red with <20% black
4	Red, as in red-shafted
<i>Nuchal patch presence</i>	
0	Present and broad, as in yellow-shafted
1	Present and restricted in width (less than one-half of normal width)
2	Present and broken in one or more places
3	Traces present, usually at sides of nape
4	Absent, as in red-shafted
<i>Shaft color</i>	
0	Bright yellow, as in yellow-shafted
1	Yellow-orange
2	Orange
3	Red-orange
4	Deep salmon red, as in red-shafted
<i>Throat color</i>	
0	Tan, as in yellow-shafted
1	Tan with gray traces (usually on lower throat)
2	Mixed gray and tan
3	Gray with tan traces (usually near chin)
4	Gray, as in red-shafted

**Table A3.** Sampling localities used in the geographic cline analyses and shown in the inset map in Figure 1.1.

Locality ID	Locality Name	Latitude	Longitude	Distance	Transect
0	Allopatric RSFL			-100	photos only
1	Western	40.8830559	-105.51687	0	contemporary
2	Greeley	40.346603	-104.82279	58.3646979	historic
3	Kersey	40.3693671	-104.44526	90.1103961	contemporary
4	Orchard	40.351842	-104.06838	121.800573	historic and contemporary
5	W Fort Morgan	40.267982	-103.94052	132.552561	historic
6	Morrill	41.9594945	-103.92463	133.888098	contemporary
7	E Fort Morgan	40.2825194	-103.70253	152.564017	contemporary
8	Brush	40.3272657	-103.57831	163.008856	contemporary
9	Minatare	41.8984992	-103.42772	175.670701	contemporary
10	Merino	40.4047694	-103.39182	178.689349	contemporary
11	Bridgeport	41.6895056	-103.16821	197.490627	contemporary
12	Crook	40.8444414	-102.77278	230.73844	historic and contemporary
13	Lisco	41.4499137	-102.53066	251.096087	contemporary
14	Sedgwick	40.932974	-102.48678	254.784719	contemporary
15	Big Springs	40.9935125	-102.17377	281.10142	historic and contemporary
16	Lewellen	41.2998817	-102.02722	293.422112	contemporary
17	Ogallala	41.22806	-101.74345	317.279115	contemporary
18	Sutherland	41.1451911	-101.11715	369.929707	historic and contemporary
19	North Platte	41.17314	-100.78951	397.471743	contemporary
20	Halsey	41.903358	-100.31039	437.743998	historic
21	Gothenberg	40.9061571	-100.16424	450.027689	historic and contemporary
22	Elm Creek	40.686218	-99.347335	518.683376	historic and contemporary
23	Burwell	41.756348	-99.282391	524.140991	historic
24	Grand Island	40.853711	-98.406833	597.712064	historic and contemporary
25	Silver Creek	41.2795413	-97.680686	658.717108	historic and contemporary
26	Schuyler	41.4080137	-97.031092	713.281209	historic and contemporary
27	Eastern	41.3335076	-96.238837	779.814775	historic and contemporary
28	Allopatric YSFL			880	photos only

**Table A4.** Model results for the geographic clines using qualitative scoring in the historic and contemporary transects.

model	trait	transect	center	center_low	center_high	width	width_low	width_high	pMin	pMin_low	pMin_high	pMax	pMax_low	pMax_high
2	hybrid index	historic	228.68320	161.56219	275.91522	129.19850	3.32159	333.83536	0.04019	0.01378	0.07553	0.85358	0.69120	0.99996
2	crown	historic	221.92670	176.42163	261.40843	122.43880	1.47662	239.31715	0.13284	0.09253	0.18792	0.97141	0.85270	0.99994
1	ear coverts	historic	192.39540	141.52467	241.83138	228.53800	151.91124	340.15064						
2	male malar	historic	212.46660	161.11708	274.36755	164.76820	1.16819	325.08454	0.03700	0.00660	0.08688	0.98426	0.76163	1.00000
2	nuchal	historic	236.29490	190.07687	277.63731	146.83380	4.92274	263.70432	0.01545	0.00199	0.04391	0.93487	0.78341	0.99986
2	shaft	historic	231.32890	188.49253	279.94341	3.40810	0.01501	249.58180	0.01446	0.00168	0.03548	0.83239	0.68336	0.99866
2	throat	historic	241.84830	138.76503	309.75439	222.01730	52.85077	445.49191	0.02422	0.00005	0.05770	0.77395	0.57338	1.00000
1	hybrid index	contemporary	138.69080	87.32768	174.55890	260.51620	168.07635	451.39875						
1	crown	contemporary	114.83320	49.38160	154.41112	294.91410	189.52713	523.12076						
1	ear coverts	contemporary	132.73050	96.05198	160.20280	170.34320	108.14908	288.27724						
1	male malar	contemporary	179.53520	132.66409	222.16418	261.35450	165.25173	463.67747						
1	nuchal	contemporary	130.27530	67.65079	170.41115	258.85970	160.52765	478.27984						
1	shaft	contemporary	124.34120	68.78629	161.34235	256.72800	164.31097	450.86122						
1	throat	contemporary	174.27820	131.92614	209.84245	261.96480	171.57909	440.31226						

**Table A5.** Model results for the geographic clines using quantitative scoring in the contemporary transect.

Columns #1-15

model	trait	parameter	center	center_low	center_high	width	width_low	width_high	muL	muL_low	muL_high	muR	muR_low	muR_high
5	crown	short wave (blue)	43.66617	1.14577099	89.6726296	2.243035	0.00085461	84.0112316	0.06711949	0.06218299	0.07290727	0.08425488	0.08197262	0.08642149
2	crown	UV wave	136.0485	7.41110913	291.965138	1.654745	0.01665523	55.7645917	0.05695795	0.04675828	0.06413285	0.07125147	0.06719137	0.07755064
1	ear coverts	long wave (red)	134.5512	82.0724156	162.088736	140.0108	86.8845322	274.044267						
1	malar	long wave (red)	189.6729	144.694272	230.292357	357.8445	293.236743	446.547328						
2	malar	med wave (green)	202.1533	188.293386	212.365052	2.492393	0.0752683	10.3136493	0.05177183	0.04463349	0.05667491	0.02828251	0.02450882	0.03301426
5	malar	short wave (blue)	204.7335	189.06869	211.679116	6.70439	0.09209876	17.6208442	0.04511785	0.04094112	0.04765061	0.03167555	0.02902582	0.03426476
2	nuchal	area	138.4743	4.66787484	159.770366	145.6179	34.281262	233.030542	104.0749	-467.7201	573.504412	11698.18	9102.82864	12861.6735
2	shaft	long wave (red)	56.19493	0.88654678	145.08392	1.626527	0.00124021	13.7731074	0.1429817	0.12464743	0.16322257	0.1789578	0.17420235	0.18426259
5	shaft	med wave (green)	111.3254	84.231407	131.882353	178.9396	88.706712	360.856384	0.07948163	0.0669843	0.08473363	0.1514433	0.14122858	0.16480561
1	throat	long wave (red)	151.9305	117.232674	179.875496	208.0041	126.301941	354.621335						
2	throat	luminance	108.4203	65.5581825	146.312909	67.79958	0.53566257	202.158944	0.1284577	0.12057454	0.13966551	0.1615339	0.15714361	0.16509761

Columns #16-30

varL	varL_low	varL_high	varR	varR_low	varR_high	varH	varH_low	varH_high	deltaR	deltaR_low	deltaR_high	tauR	tauR_low	tauR_high
8.51E-05	4.20E-05	0.00020312	0.00011583	8.82E-05	0.00015539	18.78479	4.18E-06	123.129322	641.5833	0.33010044	1039.88145	0.1351632	0.00047032	0.99999211
0.00022516	9.23E-05	0.00036787	0.00020001	0.0001661	0.0003766	0.00317002	2.47E-05	316.005784						
						0.00189348	0.00098985	0.0040156						
						0.00316846	0.00207356	0.00526826						
0.00029709	0.00020015	0.00050898	0.00010653	7.59E-05	0.00020926	2.507712	0.03153954	166578.428						
0.00010236	6.81E-05	0.00016745	5.30E-05	3.42E-05	8.94E-05	0.03400838	0.00167679	169.108913	604.3228	1.60842032	1039.24535	0.1595306	0.00034134	0.99981283
11982.06	9.99E+01	594787.885	10031523	6614032.81	28993089.2	42069164	1.60E+07	62290228.8						
0.00097838	0.0005003	0.00248264	0.00054604	0.00041613	0.0007422	64.16742	1.04454284	112122848						
0.00022187	9.79E-05	0.00039417	0.00018656	3.34E-06	0.00056347	0.00066151	0.00031306	0.00104341	32.55537	6.13913723	76.8934201	0.1912548	0.03171442	0.37629537
						0.00101014	0.00058443	0.0019355						
0.00016941	0.00012473	0.00050343	0.00034859	0.00023011	0.00052682	0.00026609	2.26E-06	0.0132605						

CHAPTER 2 APPENDIX

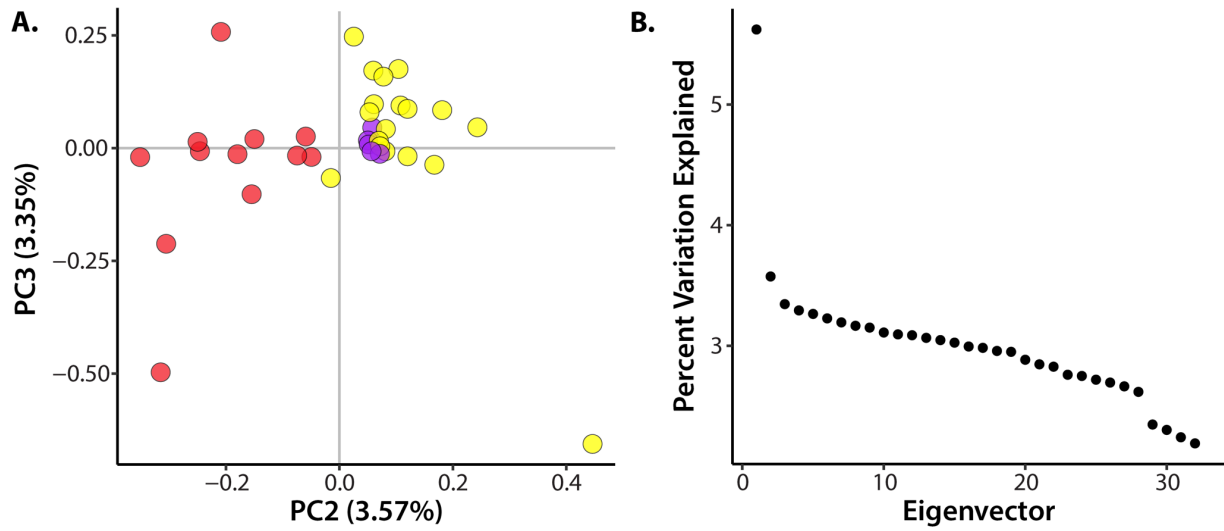


**Figure B1.** (A) Additional axes of the principal component analysis (PCA) and (B) percent of variation explained by each eigenvector for the PCA demonstrating that eigenvectors beyond PC2 do not provide additional useful information on clustering.

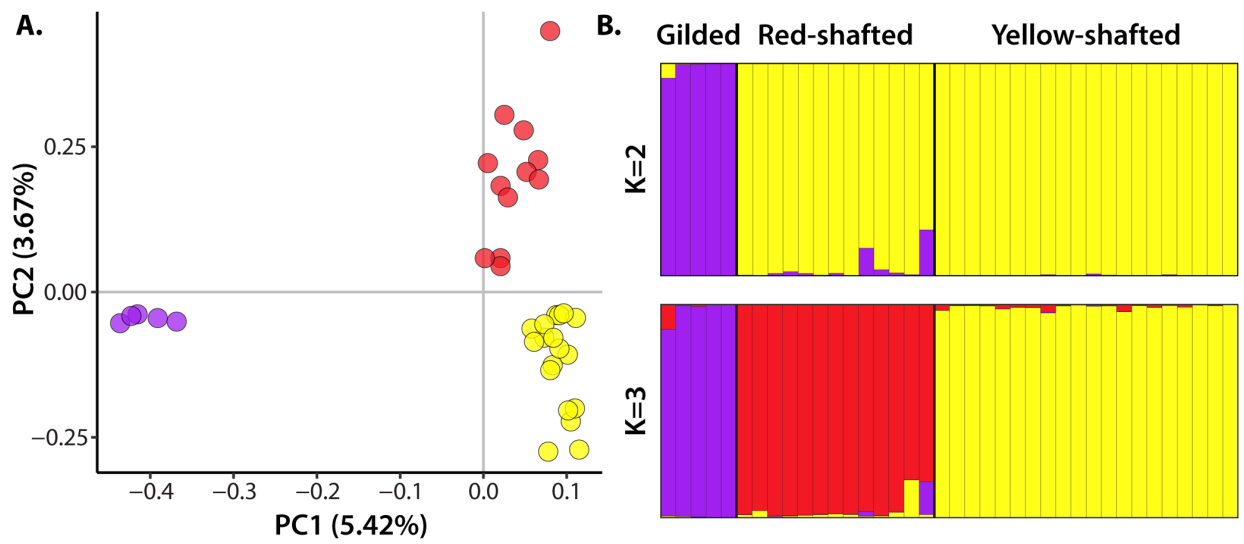


**Figure B2.** (A) PCA and (B) STRUCTURE results from the reference-based assembly demonstrating the similarity between the de novo and reference-based SNP datasets.

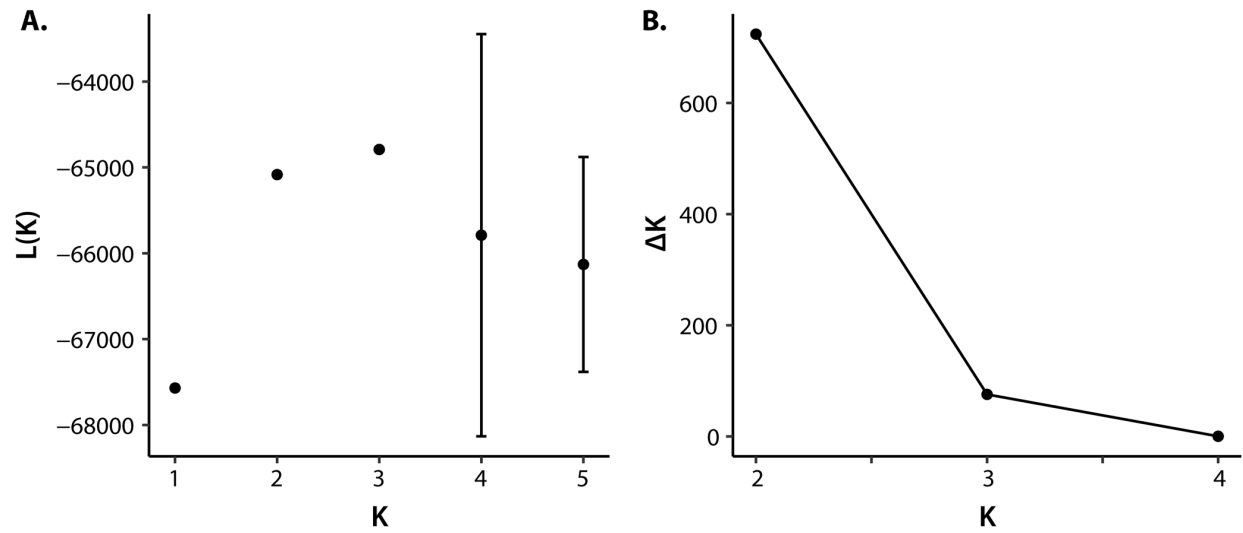


**Figure B3.** (A) Log likelihood and (B)  $\Delta K$  plots from the STRUCTURE analysis showing  $K = 2$  is preferred by the  $\Delta K$  method, but  $K = 3$  has the highest log likelihood value.

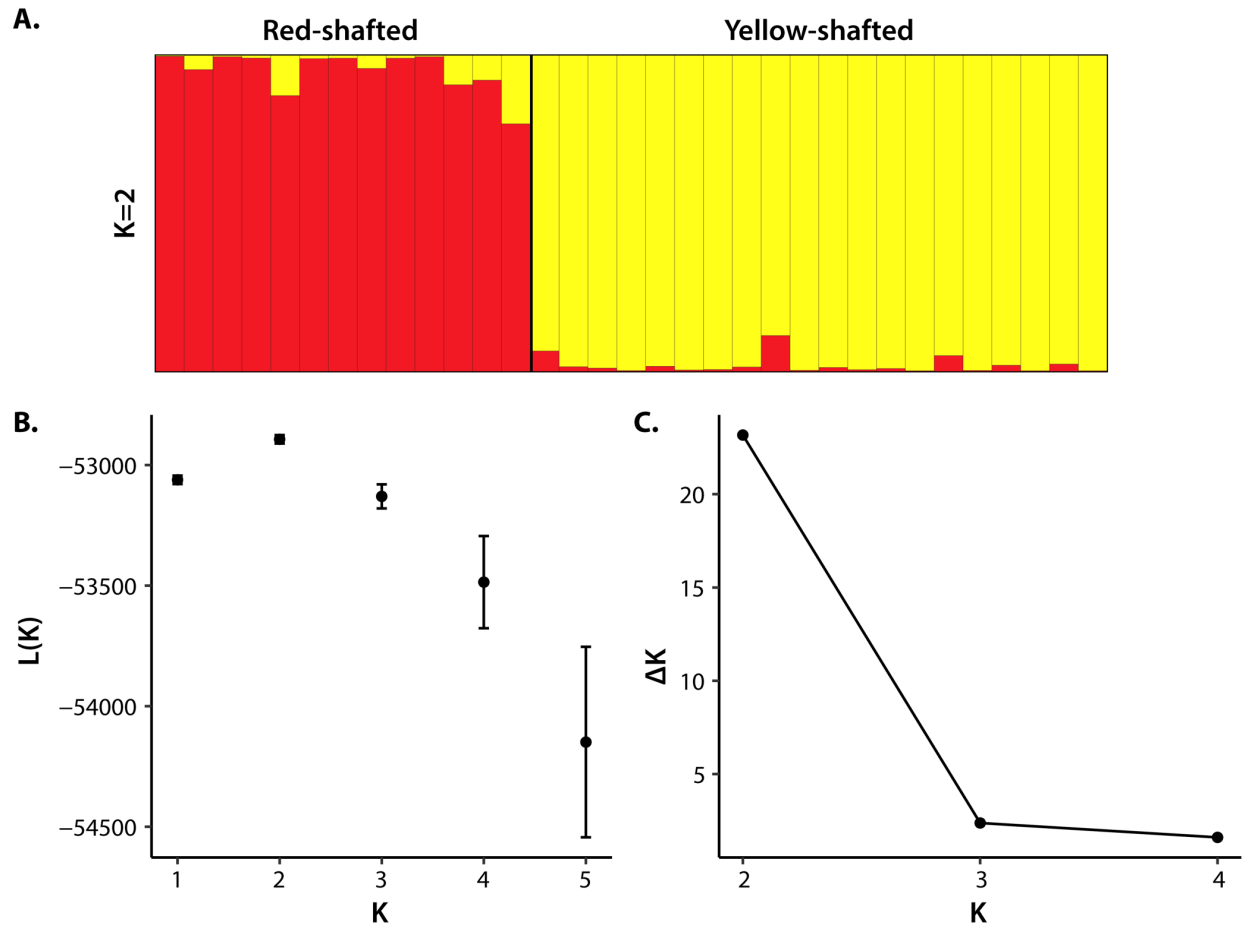


**Figure B4.** (A) STRUCTURE plot for the analysis in Red-shafted and Yellow-shafted flickers (i.e. excluding Gilded Flickers) based on 1,737 SNPs.  $K = 2$  is preferred with both the highest (B) log likelihood and (C)  $\Delta K$  value.

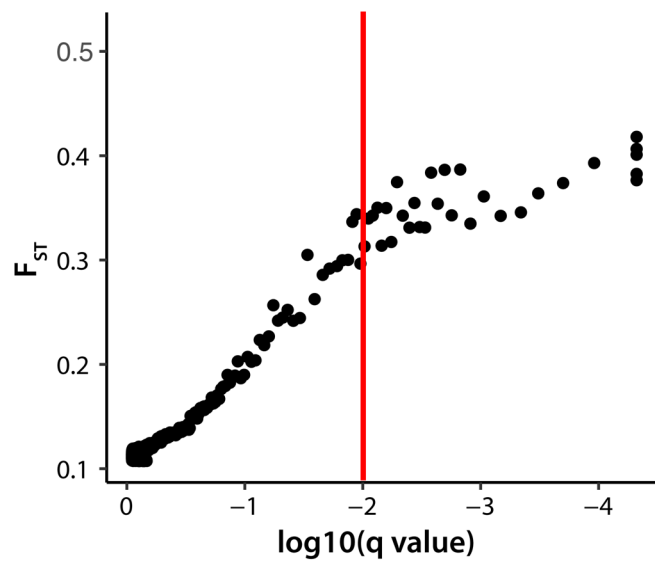


**Figure B5.** Results from the BayeScan analysis showing the  $F_{ST}$  estimated in BayeScan and the corresponding q value for each SNP. The red vertical line shows the false discovery rate of 0.05 used in the analysis. SNPs to the right of the line were identified as outlier SNPs under selection.

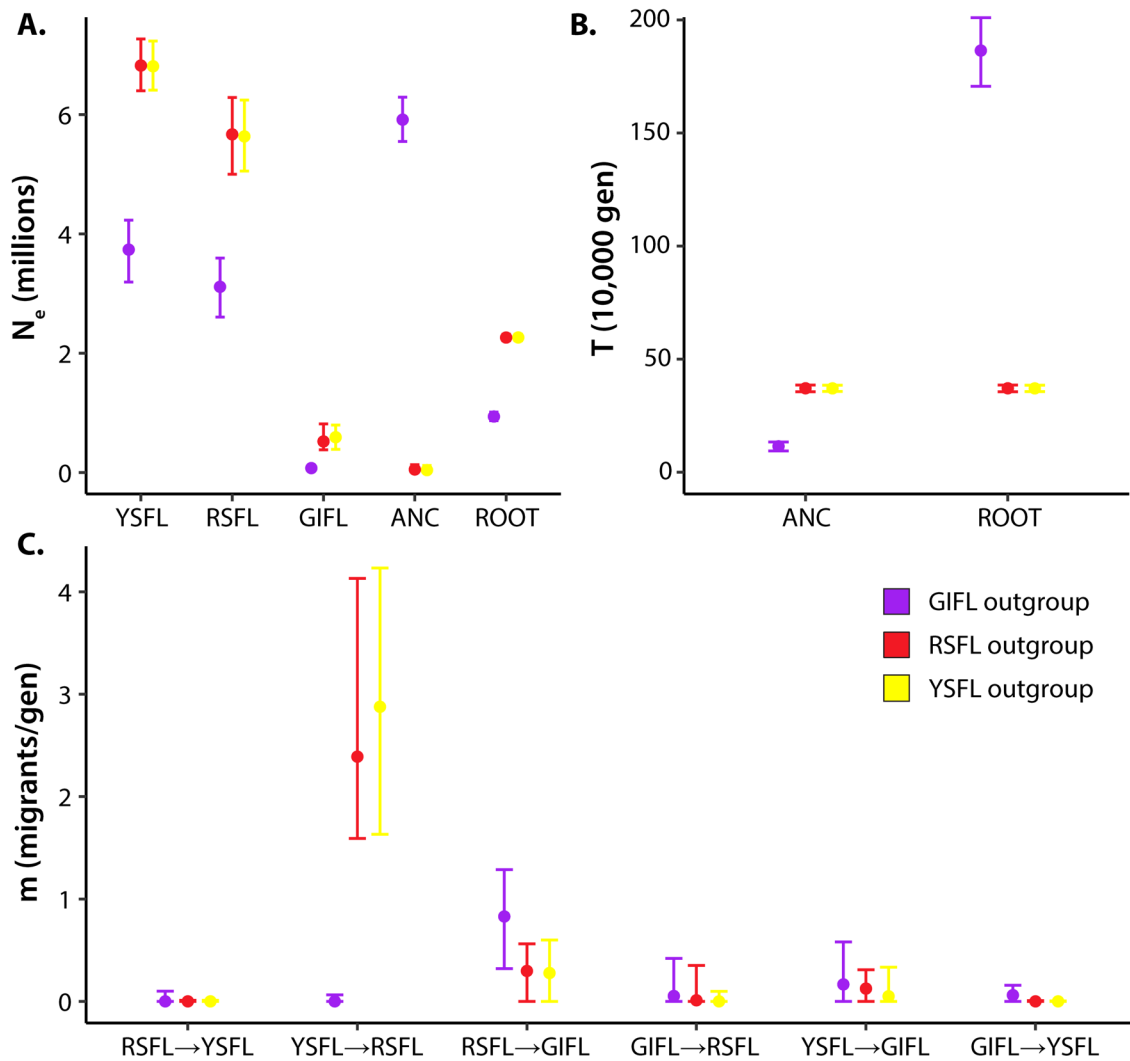


**Figure B6.** G-PhoCS estimates for (A) effective population sizes ( $N_e$ ), (B) divergence times (T), and (C) gene flow (m) from the three models shown as medians with 95% Bayesian CI. Values are colored based on the model's outgroup: Gilded Flicker (purple), Red-shafted Flicker (red), and Yellow-shafted Flicker (yellow). ANC and ROOT indicate the divergence between the model's two sister taxa and their outgroup, respectively. Actual values of parameter estimates should be interpreted with caution as they are based on an approximate mutation rate of  $10^{-9}$  mutations per bp per generation. Taxa abbreviations: GIFL = Gilded Flicker, RSFL = Red-shafted Flicker, YSFL = Yellow-shafted Flicker.

**Table B1.** Details on samples included in this study, including the museum voucher number, year collected, phenotypic group (GIFL = Gilded Flicker, RSFL = Red-shafted Flicker, YSFL = Yellow-shafted Flicker), and locality information. Estimated latitude/longitude are indicated with asterisks.

Voucher No.	Year	Group	State, Country	County	Latitude	Longitude
UWBM 84071	2007	GIFL	Sinaloa, MX	Municipio El Fuerte	26.310000	-108.810000
UWBM 90812	2011	GIFL	Sinaloa, MX	Municipio El Fuerte	26.421389*	-108.620000*
UWBM 108767	2006	GIFL	Nevada, USA	Clark	35.516667	-115.050000
UWBM 109555	2001	GIFL	Nevada, USA	Clark	35.330000	-115.500000
UWBM 115674	2006	GIFL	Nevada, USA	Clark	34.450000	-115.200000
AMNH 14039	2005	RSFL	Washington, USA	Whatcom	48.750278*	-122.475000*
AMNH 14040	2002	RSFL	Washington, USA	Whatcom	48.750278*	-122.475000*
AMNH 14041	1999	RSFL	Washington, USA	Whatcom	48.750278*	-122.475000*
AMNH 14042	2005	RSFL	Washington, USA	Whatcom	48.750278*	-122.475000*
AMNH 15767	2006	RSFL	Oregon, USA	Wallowa	45.220000	-117.056667
LSUMZ B-22912	1993	RSFL	California, USA	San Bernardino	34.125833*	-117.619167*
LSUMZ B-24450	2000	RSFL	California, USA	Riverside	33.895000*	-117.055278*
MVZ 181836	2002	RSFL	California, USA	Contra Costa	37.8635598	-122.0183027
MVZ 182088	2006	RSFL	California, USA	Marin	37.96176667	-122.6011333
MVZ 182198	2006	RSFL	California, USA	Lassen	40.66357	-120.79506
MVZ 182962	2007	RSFL	California, USA	Contra Costa	37.959599	-122.093861
MVZ 184137	2004	RSFL	California, USA	Contra Costa	37.98388	-122.046745
MVZ 184140	2004	RSFL	California, USA	Contra Costa	37.855279	-122.046754
CUMV 50481	2003	YSFL	New York, USA	Onondaga	42.946667*	-76.428333*
CUMV 51231	2004	YSFL	New York, USA	Tompkins	42.470833*	-76.461667*
CUMV 51593	2005	YSFL	New York, USA	Tompkins	42.395000*	-76.367222*
CUMV 52028	2006	YSFL	New York, USA	Oneida	43.334498	-75.748017
CUMV 52454	2006	YSFL	New York, USA	Tompkins	42.443333*	-76.500000*
CUMV 52455	2006	YSFL	New York, USA	Tompkins	42.409167*	-76.374167*
CUMV 52670	2008	YSFL	New York, USA	Tompkins	42.440786	-76.496727
CUMV 52999	2009	YSFL	New York, USA	Tompkins	42.442079	-76.449035
CUMV 54489	2010	YSFL	New York, USA	Tompkins	42.440786	-76.496727
CUMV 54562	2011	YSFL	New York, USA	Tompkins	42.479900	-76.451000
CUMV 54913	2012	YSFL	New York, USA	Seneca	42.826389*	-76.7375*
CUMV 55005	2012	YSFL	New York, USA	Tompkins	42.4381028	-76.5094764
CUMV 55258	2013	YSFL	New York, USA	Tompkins	42.4799000	-76.451000
LSUMZ B-48981	2002	YSFL	Florida, USA	Brevard	28.319167*	-80.665833*
LSUMZ B-50722	2003	YSFL	Florida, USA	Escambia	30.433333*	-87.200000*
LSUMZ B-58995	2004	YSFL	Florida, USA	Escambia	30.433333*	-87.200000*
LSUMZ B-59061	2004	YSFL	Florida, USA	Escambia	30.433333*	-87.200000*
LSUMZ B-83282	2009	YSFL	Florida, USA	Escambia	30.433333*	-87.200000*
FMNH 465427	2009	YSFL	Illinois, USA	Cook	41.886111*	-87.626389*
FMNH 481942	2012	YSFL	Illinois, USA	Cook	42.058333*	-87.673611*

**Table B2.** Details on average coverage and missing data from the de novo and reference-based assemblies for samples included in this study. \* indicates sample was removed from the PC analysis. \*\* indicates sample was used to infer a species tree in SNAPP.

Voucher No.	STACKS de novo output		STACKS reference-based output	
	Coverage	% Missing Data	Coverage	% Missing Data
UWBM 84071**	48.73	5.02	51.41	2.91
UWBM 90812**	46.42	5.07	49.42	1.77
UWBM 108767**	88.87	5.43	89.50	2.23
UWBM 109555**	49.65	4.09	52.64	2.18
UWBM 115674**	51.22	3.97	53.60	1.85
AMNH 14039	46.29	2.56	48.49	1.08
AMNH 14040**	33.94	4.31	35.28	3.77
AMNH 14041*	23.22	82.62	20.48	83.17
AMNH 14042	29.65	11.41	30.18	9.50
AMNH 15767	25.71	38.38	24.86	33.65
LSUMZ B-22912**	72.74	7.13	78.81	1.54
LSUMZ B-24450**	59.39	4.93	62.71	1.21
MVZ 181836	26.58	35.07	26.07	40.43
MVZ 182088	44.75	3.19	46.85	1.91
MVZ 182198**	68.42	6.74	74.93	1.27
MVZ 182962	29.08	18.61	29.57	20.33
MVZ 184137	44.58	4.26	47.34	2.25
MVZ 184140**	58.54	6.93	63.01	1.79
CUMV 50481	57.13	2.12	57.95	2.09
CUMV 51231	27.78	11.36	29.05	10.13
CUMV 51593**	38.30	2.76	39.49	2.04
CUMV 52028	43.76	3.50	46.50	1.58
CUMV 52454	28.96	8.36	29.95	7.72
CUMV 52455*	21.59	83.66	18.68	80.21
CUMV 52670*	22.84	86.59	18.75	84.75
CUMV 52999	33.29	7.88	34.29	7.95
CUMV 54489	37.26	2.83	38.57	2.66
CUMV 54562**	59.91	3.23	64.58	1.08
CUMV 54913	36.25	4.79	36.61	4.11
CUMV 55005**	64.67	4.18	67.89	1.85
CUMV 55258	40.98	3.35	42.97	3.42
LSUMZ B-48981	52.90	2.30	54.83	1.90
LSUMZ B-50722	60.09	4.00	63.58	1.93
LSUMZ B-58995	44.09	4.81	46.23	2.76
LSUMZ B-59061	41.70	3.12	42.36	1.80
LSUMZ B-83282	34.88	5.31	35.89	3.87
FMNH 465427**	61.64	2.54	64.57	1.31
FMNH 481942**	47.97	3.01	50.95	2.11

**Table B3.** Pairwise  $F_{ST}$  estimates (uncorrected for sample sizes) for 16,670 SNPs with mean  $F_{ST}$  shown below the diagonal and range shown above.

	<b>Gilded Flickers</b>	<b>Red-shafted Flickers</b>	<b>Yellow-shafted Flickers</b>
<b>Gilded Flickers</b>	—	[0-1.0]	[0-1.0]
<b>Red-shafted Flickers</b>	0.0616	—	[0-0.8037]
<b>Yellow-shafted Flickers</b>	0.0744	0.0092	—

**Table B4.** Pairwise mean  $F_{ST}$  estimates between populations within the three taxa for 16,670 SNPs. Range of per SNP  $F_{ST}$  is shown in brackets.

<b>Population comparison</b>	<b><math>F_{ST}</math> estimate</b>
<b>Gilded Flickers</b>	
Nevada ( $N = 3$ ) vs. Sinaloa, Mexico ( $N = 2$ )	0.0547 [0-1.0]
<b>Red-shafted Flickers</b>	
Washington/Oregon ( $N = 5$ ) vs. Northern California ( $N = 6$ )	0.0034 [0-1.0]
Washington/Oregon ( $N = 5$ ) vs. Southern California ( $N = 2$ )	0.0173 [0-1.0]
Northern California ( $N = 6$ ) vs. Southern California ( $N = 2$ )	0.0094 [0-1.0]
<b>Yellow-shafted Flickers</b>	
New York ( $N = 13$ ) vs. Illinois ( $N = 2$ )	0.0039 [0-1.0]
New York ( $N = 13$ ) vs. Florida ( $N = 5$ )	0.0060 [0-0.6512]
Illinois ( $N = 2$ ) vs. Florida ( $N = 5$ )	0.0108 [0-1.0]

**Table B5.** Details on BLAST hits for all outlier SNPs, including locus name, outlier identification method, locus  $F_{ST}$ , annotation of the region in the Zebra Finch genome, % query coverage, % match, and the associated E value.

Locus ID	Outlier Method	$F_{ST}$	BLAST Results	Query%	Match%	E value
590_21	BayeScan	0.736	No confident match			
996_76	BayeScan	0.4636	No confident match			
1072_49	Elevated FST	0.9713	No confident match			
1361_103	BayeScan	0.8185	No confident match			
2207_89	Both	0.8221	PREDICTED: Taeniopygia guttata l(3)mbt-like 2 (Drosophila) (L3MBTL2), mRNA	94%	73%	4.00E-14
3542_73	BayeScan	0.6986	No confident match			
4042_20	Elevated FST	0.8941	No confident match			
4044_127	BayeScan	0.6942	No confident match			
4213_118	Both	0.8976	No confident match			
4213_131	Both	0.8976	No confident match			
4426_22	Both	0.8541	No confident match			
4583_103	BayeScan	0.7209	No confident match			
4597_128	Elevated FST	0.8299	No confident match			
4757_60	Elevated FST	0.9151	No confident match			
4934_8	BayeScan	0.6088	PREDICTED: Taeniopygia guttata G patch domain containing 11 (GPATCH11), transcript variant X2, mRNA	65%	77%	6.00E-12
4934_60	Both	0.9494	PREDICTED: Taeniopygia guttata G patch domain containing 11 (GPATCH11), transcript variant X2, mRNA	65%	77%	6.00E-12
5078_51	BayeScan	0.8042	No confident match			
5078_57	BayeScan	0.8042	No confident match			
5078_138	BayeScan	0.8042	No confident match			
5332_23	Elevated FST	0.8328	No confident match			
5732_26	Elevated FST	0.8648	No confident match			
6521_123	BayeScan	0.7264	PREDICTED: Taeniopygia guttata glucosidase, beta (bile acid) 2 (GBA2), mRNA	98%	85%	1.00E-37
7982_98	BayeScan	0.7974	No confident match			
7982_133	BayeScan	0.7974	No confident match			
8325_87	Both	0.8528	No confident match			
8516_15	Elevated FST	0.8544	No confident match			
8612_89	BayeScan	0.4594	No confident match			
9134_52	BayeScan	0.6609	No confident match			
9832_20	BayeScan	0.7463	No confident match			
9832_48	BayeScan	0.7125	No confident match			
9832_56	BayeScan	0.7805	No confident match			
11150_30	BayeScan	0.532	No confident match			
11250_48	Elevated FST	0.8817	PREDICTED: Taeniopygia guttata RING finger protein 151-like (LOC100224067), mRNA	80%	75%	1.00E-13
11958_28	BayeScan	0.6831	No confident match			
12946_41	BayeScan	0.75	No confident match			
12946_77	Both	0.8584	No confident match			
12946_115	BayeScan	0.6359	No confident match			
13181_108	BayeScan	0.7817	No confident match			
13298_92	BayeScan	0.7406	No confident match			
13409_128	BayeScan	0.7266	No confident match			
13768_88	BayeScan	0.6182	No confident match			
14120_85	BayeScan	0.58	No confident match			
14120_109	BayeScan	0.7255	No confident match			
14142_14	Both	0.8433	No confident match			
14306_65	BayeScan	0.676	No confident match			
14306_85	BayeScan	0.6694	No confident match			
14306_96	BayeScan	0.6694	No confident match			
14306_132	BayeScan	0.6694	No confident match			
15393_126	BayeScan	0.5759	PREDICTED: Taeniopygia guttata coxsackie virus and adenovirus receptor (CXADR), mRNA	65%	84%	2.00E-19
15393_130	Both	0.9441	PREDICTED: Taeniopygia guttata coxsackie virus and adenovirus receptor (CXADR), mRNA	65%	84%	2.00E-19

CHAPTER 3 APPENDIX

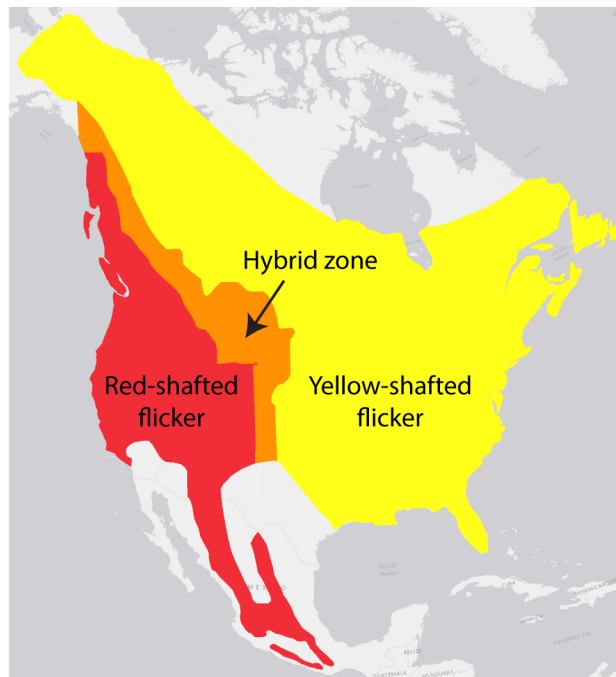


**Figure C1.** Geographic distribution of the red-shafted and yellow-shafted flickers in North America with the approximate location of the hybrid zone shown in orange.

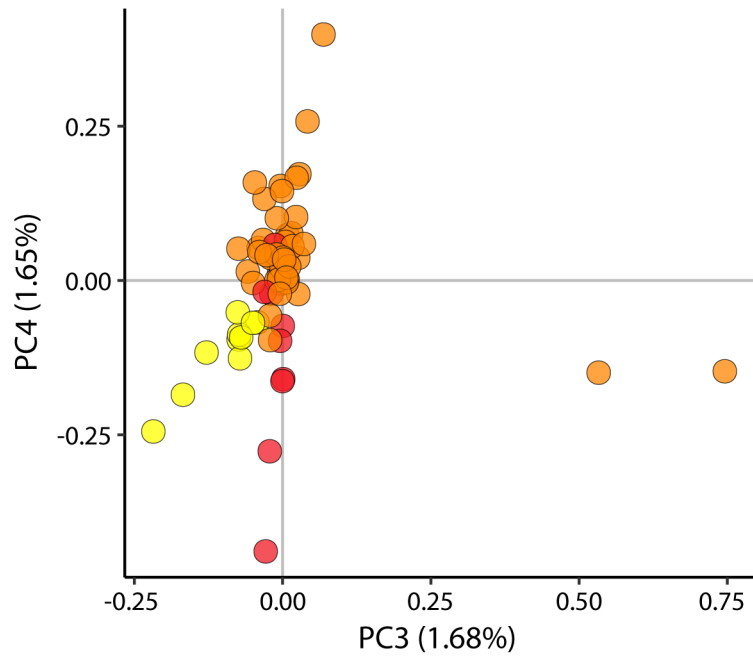


**Figure C2.** PC3 and PC4 of the principal component analysis (PCA) showing the hybrid flickers (orange points) separating from red-shafted (red points) and yellow-shafted (yellow points) flickers on these axes.

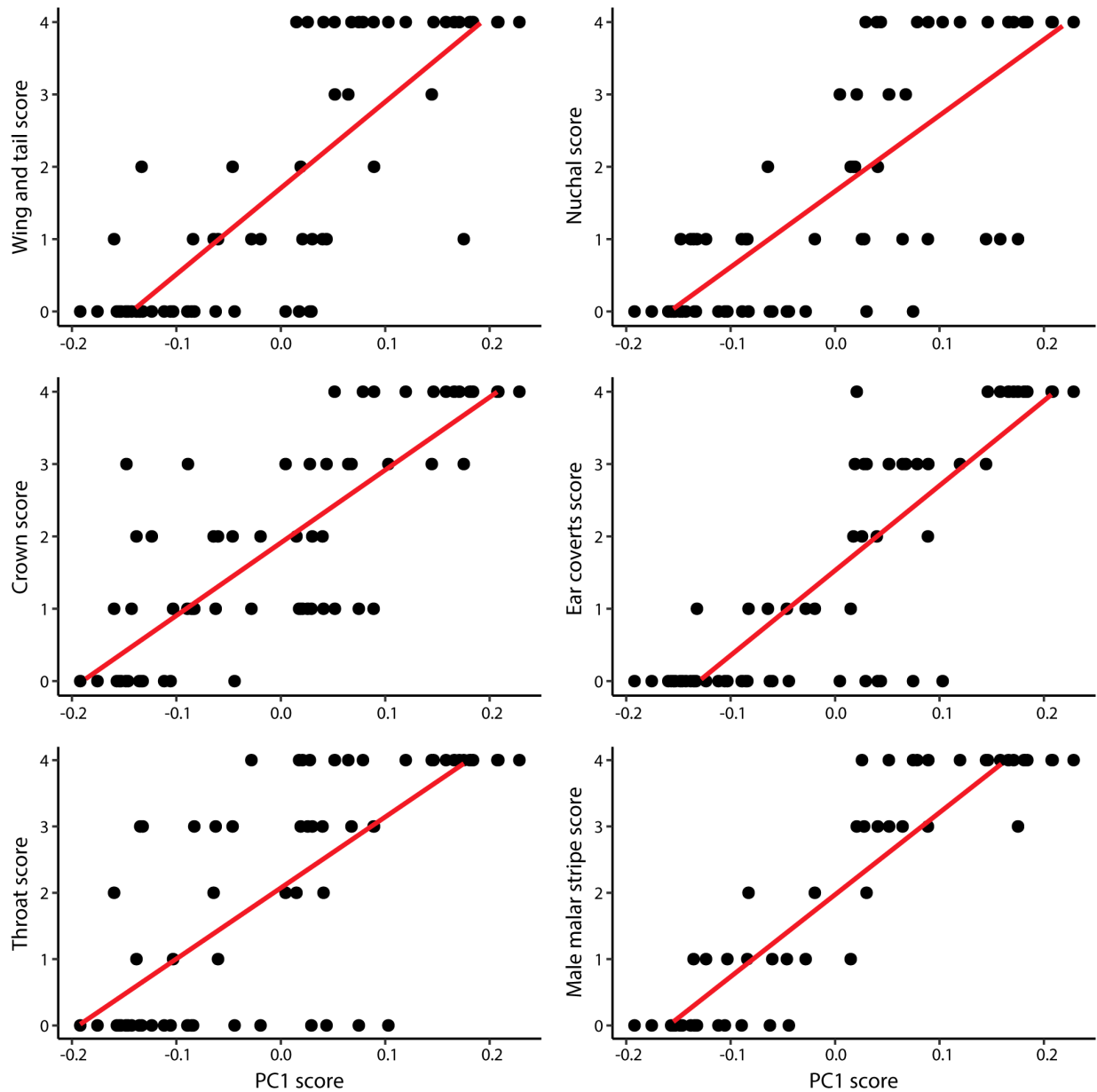


**Figure C3.** PC1 is significantly associated with each individual plumage trait: wing and tail ( $\rho = 0.83$ ,  $p < 2.2 \times 10^{-16}$ ), nuchal patch ( $\rho = 0.78$ ,  $p = 5.4 \times 10^{-15}$ ), crown ( $\rho = 0.82$ ,  $p < 2.2 \times 10^{-16}$ ), ear coverts ( $\rho = 0.86$ ,  $p < 2.2 \times 10^{-16}$ ), throat ( $\rho = 0.74$ ,  $p = 3.4 \times 10^{-13}$ ), and male malar stripe ( $\rho = 0.93$ ,  $p < 2.2 \times 10^{-16}$ ). Scores ranges from 0 for pure yellow-shafted flickers to 4 for pure red-shafted flickers. The analysis for malar stripe includes only males, as females do not possess a malar stripe.

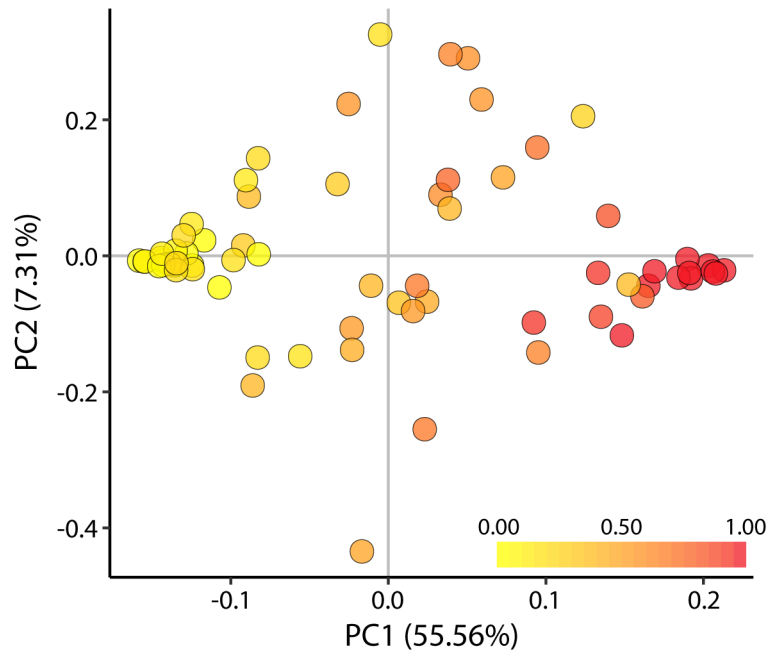


**Figure C4.** PCA using 780 fixed SNPs ( $F_{ST} = 1$ ) between allopatric red-shafted and allopatric yellow-shafted flickers with points coloured by phenotype score.

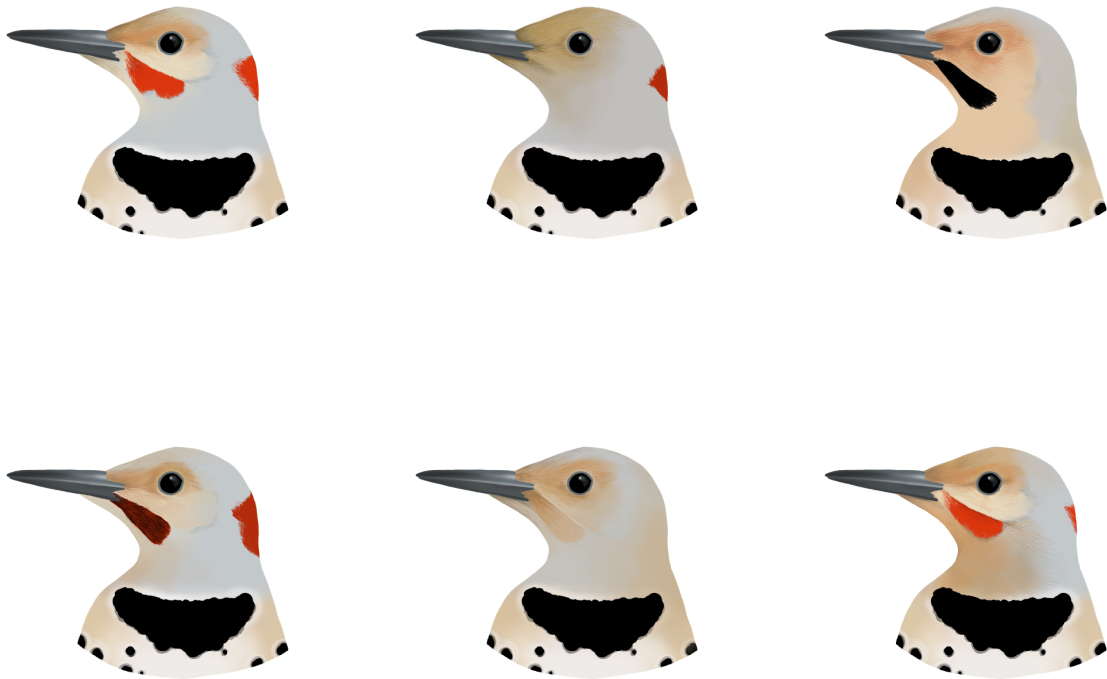


**Figure C5.** Example phenotypes of six hybrids between yellow-shafted and red-shafted flickers (note that these do not represent particular individuals included in this study).  
Illustrations by Megan Bishop.

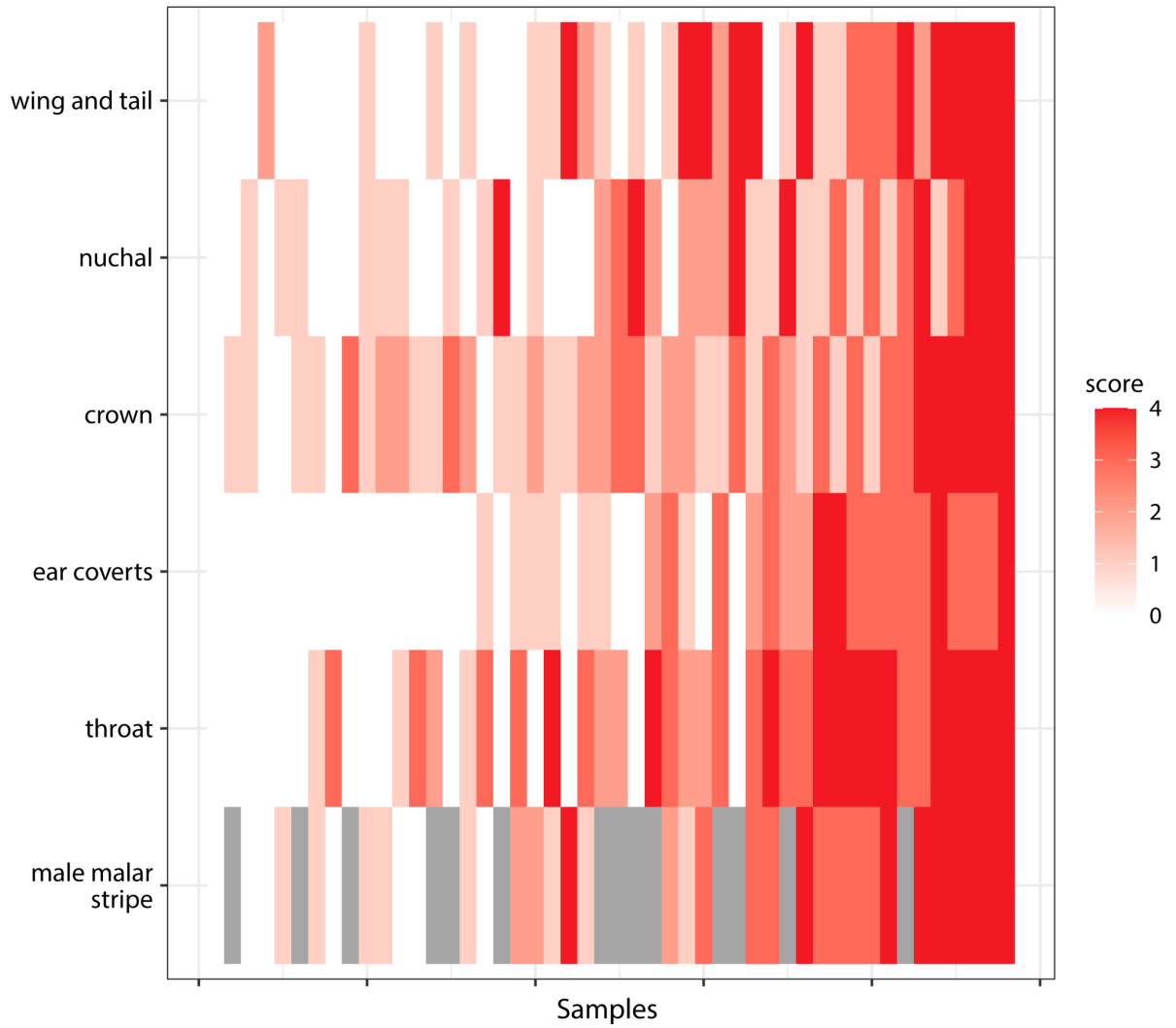


**Figure C6.** Variability in phenotype scores across the six focal plumage traits in hybrid flickers. Individuals are arranged along the x-axis by their overall phenotypic hybrid score. Individuals with grey coloration denote females that lack the malar stripe.

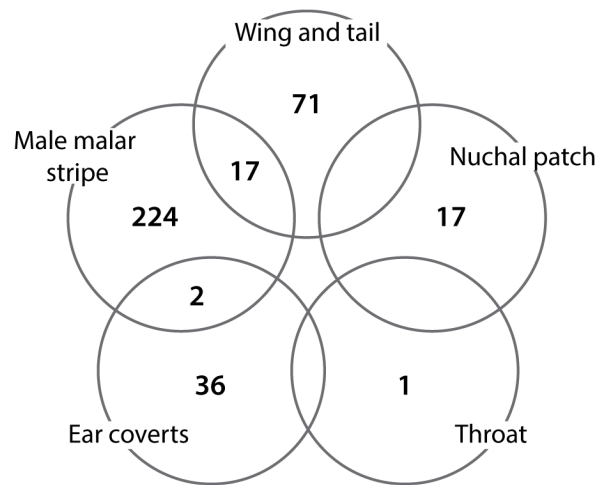


**Figure C7.** Venn diagram showing how individual SNPs identified as significantly associated with coloration traits in the independent GWAs are shared across analyses. See Table C3 for the full list of identified SNPs.

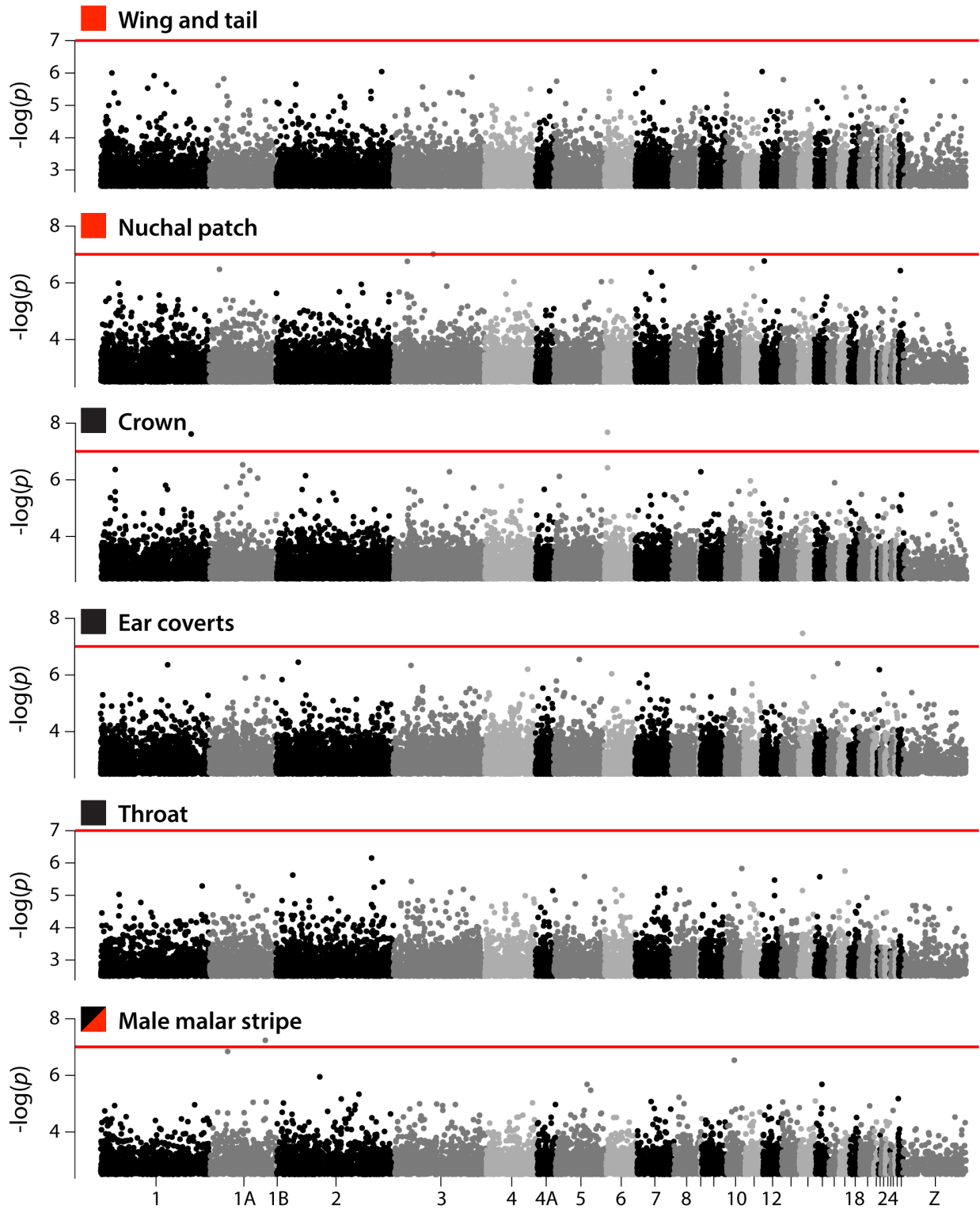


**Figure C8.** Results from the GWAs comparing individual SNPs with the six plumage patches after the phenotypes were randomized across individuals. For visualization purposes we show only points with  $-\log_{10}(p) > 2.5$ .

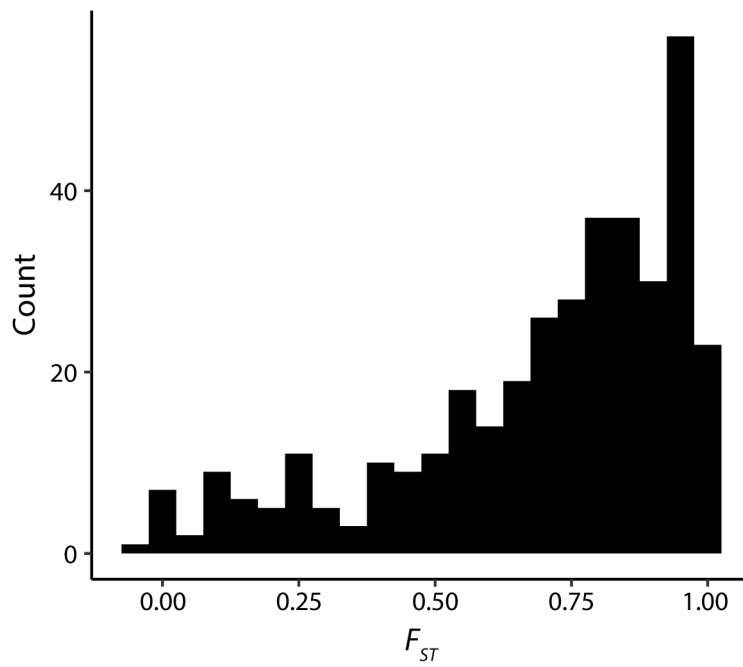


**Figure C9.** Distribution of per-SNP  $F_{ST}$  values of SNPs identified as significantly associated with coloration traits in the GWAs.

**Table C1.** Details on the six plumage patch coloration differences between red-shafted and yellow-shafted flickers. Individuals are scored from 0 (pure yellow-shafted) to 4 (pure red-shafted) for each trait. An overall phenotype score is calculated by summing across the six traits and transforming to range from 0-1 (to allow comparisons between the sexes). Phenotypic scoring is adapted from Short (1965).

Phenotype score	Description
<i>Wing and tail ("shaft") colour, Carotenoid</i>	
0	Bright yellow, as in yellow-shafted
1	Yellow-orange traces, faint in all feathers or heavy in one or several
2	Orange to red rachises with yellow-orange vanes
3	Orange-red
4	Deep salmon red, as in red-shafted
<i>Nuchal patch presence, Carotenoid</i>	
0	Present and broad, as in yellow-shafted
1	Present and restricted in width (less than one-half of normal width)
2	Present and broken in one or more places
3	Traces present, usually at sides of nape
4	Absent, as in red-shafted
<i>Crown colour, Melanin</i>	
0	Grey, as in yellow-shafted
1	Grey with brown traces in forehead and crown
2	Mixed grey and brown (crown half brown with more grey on hind neck)
3	Crown brown with hind neck grey toward back
4	Brown confluent with back colour, as in red-shafted
<i>Ear covert colour, Melanin</i>	
0	Tan, as in yellow-shafted
1	Tan with grey traces
2	Mixed grey and tan
3	Grey with tan traces (especially below eye)
4	Grey, as in red-shafted
<i>Throat colour, Melanin</i>	
0	Tan, as in yellow-shafted
1	Tan with grey traces (usually on lower throat)
2	Mixed grey and tan
3	Grey with tan traces (usually near chin)
4	Grey, as in red-shafted
<i>Malar stripe colour (males only), Melanin and Carotenoid</i>	
0	Black, as in yellow-shafted
1	Black with <20% red
2	Mixed black and red
3	Red with <20% black
4	Red, as in red-shafted

**Table C2.** Details on samples included in this study.

Individual ID	Taxa	Sex	Year	County, State	Phenotype score
LSU B48981	Yellow-shafted	Male	2002	Brevard, FL	0.000
LSU B48980	Yellow-shafted	Male	2002	Escambia, FL	0.000
LSU B50722	Yellow-shafted	Male	2003	Escambia, FL	0.000
LSU B59061	Yellow-shafted	Male	2004	Escambia, FL	0.000
LSU B59422	Yellow-shafted	Male	2005	Escambia, FL	0.000
CUMV 51231	Yellow-shafted	Male	2004	Tompkins, NY	0.000
CUMV 52455	Yellow-shafted	Male	2006	Tompkins, NY	0.000
CUMV 52999	Yellow-shafted	Male	2009	Tompkins, NY	0.000
CUMV 54562	Yellow-shafted	Male	2011	Tompkins, NY	0.000
CUMV 58977	Yellow-shafted	Male	2017	Tompkins, NY	0.000
1803-25407	Hybrid	Male	2016	Lincoln, NE	0.000
CUMV 56730	Hybrid	Female	2016	Butler, NE	0.050
CUMV 57686	Hybrid	Male	2017	Deuel, NE	0.083
1803-25405	Hybrid	Male	2016	Keith, NE	0.083
1803-25403	Hybrid	Male	2016	Keith, NE	0.083
1803-25410	Hybrid	Female	2016	Sedgwick, CO	0.100
CUMV 56731	Hybrid	Male	2016	Buffalo, NE	0.125
CUMV 58091	Hybrid	Male	2018	Keith, NE	0.125
CUMV 56715	Hybrid	Female	2016	Lancaster, NE	0.150
CUMV 56717	Hybrid	Male	2016	Buffalo, NE	0.167
CUMV 58065	Hybrid	Male	2018	Garden, NE	0.167
CUMV 56728	Hybrid	Male	2016	Keith, NE	0.167
1803-25404	Hybrid	Male	2016	Keith, NE	0.167
CUMV 57607	Hybrid	Female	2017	Logan, CO	0.200
CUMV 56716	Hybrid	Female	2016	Polk, NE	0.200
CUMV 58072	Hybrid	Male	2018	Logan, CO	0.208
CUMV 56725	Hybrid	Male	2016	Morrill, NE	0.208
CUMV 58060	Hybrid	Female	2018	Morgan, CO	0.250
1803-25406	Hybrid	Male	2016	Lincoln, NE	0.292
CUMV 56724	Hybrid	Male	2016	Morrill, NE	0.292
CUMV 58090	Hybrid	Male	2018	Morgan, CO	0.333
CUMV 58084	Hybrid	Male	2018	Logan, CO	0.375
CUMV 58067	Hybrid	Male	2018	Weld, CO	0.375
CUMV 57608	Hybrid	Female	2017	Logan, CO	0.400
CUMV 56734	Hybrid	Female	2016	Morrill, NE	0.400
1833-36504	Hybrid	Female	2016	Sedgwick, CO	0.400
CUMV 58076	Hybrid	Female	2018	Weld, CO	0.450
CUMV 57988	Hybrid	Male	2017	Morgan, CO	0.458
CUMV 58148	Hybrid	Male	2018	Garden, NE	0.500
CUMV 56726	Hybrid	Male	2016	Scotts Bluff, NE	0.500
CUMV 57610	Hybrid	Female	2017	Logan, CO	0.550
CUMV 58085	Hybrid	Female	2018	Logan, CO	0.550
1833-36502	Hybrid	Male	2016	Morgan, CO	0.583
CUMV 58079	Hybrid	Male	2018	Morgan, CO	0.583
1803-25408	Hybrid	Female	2016	Morgan, CO	0.600
1803-25409	Hybrid	Male	2016	Sedgwick, CO	0.625
CUMV 58068	Hybrid	Male	2018	Scotts Bluff, NE	0.667
CUMV 57967	Hybrid	Male	2017	Weld, CO	0.667
CUMV 58080	Hybrid	Male	2018	Morgan, CO	0.708
CUMV 58069	Hybrid	Male	2018	Weld, CO	0.708
CUMV 58070	Hybrid	Male	2018	Weld, CO	0.750
CUMV 56723	Hybrid	Female	2016	Kimball, NE	0.800
CUMV 56736	Hybrid	Male	2016	Scotts Bluff, NE	0.833
CUMV 58078	Hybrid	Male	2018	Larimer, CO	0.875
CUMV 56727	Hybrid	Male	2016	Scotts Bluff, NE	0.917
CUMV 58063	Hybrid	Male	2018	Larimer, CO	0.958
CUMV 58077	Hybrid	Male	2018	Larimer, CO	0.958
1833-36503	Hybrid	Male	2016	Larimer, CO	1.000
BURKE 109367	Red-shafted	Male	2002	Josephine, OR	1.000
BURKE 113386	Red-shafted	Male	2002	Josephine, OR	1.000
BURKE 112778	Red-shafted	Male	2002	Josephine, OR	1.000
BURKE 101882	Red-shafted	Male	2002	Josephine, OR	1.000
BURKE 101883	Red-shafted	Male	2002	Josephine, OR	1.000
BURKE 100969	Red-shafted	Male	2003	Inyo, CA	1.000
LSU B34359	Red-shafted	Male	1999	San Bernardino, CA	1.000
LSU B24273	Red-shafted	Male	2000	San Bernardino, CA	1.000
LSU B60069	Red-shafted	Male	2007	San Bernardino, CA	1.000
BURKE 66173	Red-shafted	Male	1996	Tulare, CA	1.000

**Table C3.** List of SNPs identified as significant in the six genome-wide association (GWA) analyses of hybrid flickers. Chromosomal and base pair positional information is based on alignment to the zebra finch genome.

Chromosome	Position	Trait(s)
1	39,415,098	nuchal
1	52,626,705	nuchal
1	52,626,737	nuchal
1	52,653,356	nuchal
1	52,653,706	nuchal
1	52,700,655	nuchal
1	52,756,992	nuchal
1	53,801,061	ear coverts
1	53,806,326	ear coverts
1	53,829,371	ear coverts
1	53,829,377	ear coverts
1	53,832,167	ear coverts
1	111,041,277	ear coverts
1	111,224,664	nuchal
1	111,456,749	ear coverts
1	111,603,710	malar
1	111,609,155	malar
1	111,613,466	wing and tail
1	111,629,266	malar
1	111,633,439	malar
1	111,636,647	malar
1	111,636,955	malar
1	111,639,298	malar
1	111,641,462	malar
1	111,647,668	malar, wing and tail
1	111,648,047	malar, wing and tail
1	111,662,337	malar
1	111,662,847	malar
1	111,662,886	malar
1	111,676,311	malar
1	111,769,605	malar
1	111,777,708	malar
1	111,777,787	malar
1	111,778,815	malar
1	111,778,865	malar, wing and tail
1	111,782,790	malar, wing and tail
1	111,783,610	malar, wing and tail
1	111,796,830	malar
1	111,797,835	malar, wing and tail
1	111,798,058	malar
1	111,798,422	malar
1	111,805,636	malar
1	111,853,738	malar
1	111,867,006	malar
1	111,867,015	malar
1	111,867,074	malar
1	111,876,834	malar
1	111,877,448	malar
1	111,877,454	malar
1	111,917,531	malar
1	111,918,025	malar
1	111,925,977	malar
1	111,928,144	ear coverts, malar
1	111,929,075	malar
1	111,932,397	malar
1	111,977,285	malar
1	111,978,572	malar
1	111,978,580	malar
1	111,982,609	malar
1	111,985,919	malar
1	111,986,496	malar
1	111,986,548	malar
1	111,986,827	malar
1	111,987,440	malar
1	111,987,468	malar
1	111,987,673	malar
1	111,990,874	malar
1	111,990,966	malar
1	111,990,987	malar

(Table C3 continued)

1	111,991,008	Malar
1	112,001,088	malar
1	112,002,842	malar
1	112,003,373	malar
1	112,005,105	malar
1	112,033,916	malar
1	112,035,669	malar
1	112,041,366	malar
1	112,057,492	malar
1	112,057,524	malar
1	112,058,369	malar
1	112,061,267	wing and tail
1	112,065,123	malar
1	112,065,143	ear coverts, malar
1	112,065,154	malar
1	112,068,325	malar
1	112,068,702	malar
1	112,068,888	malar
1	112,069,628	malar
1	112,069,670	malar
1	112,069,794	malar
1	112,069,819	malar
1	112,070,296	malar, wing and tail
1	112,070,608	malar, wing and tail
1	112,072,446	malar
1	112,084,931	malar
1	112,089,208	malar
1	112,089,238	malar
1	112,190,161	malar
1	112,190,360	ear coverts
1	112,226,857	ear coverts
1	112,296,408	nuchal
1	112,296,423	nuchal
1	112,297,985	nuchal
1	112,330,428	nuchal
1	112,376,343	nuchal
1	112,376,369	nuchal
1A	11,531,381	malar
1A	60,758,627	malar
1A	60,759,066	malar
1A	60,759,256	malar
1A	63,674,004	malar
2	68,050,522	throat
2	95,007,724	malar
2	95,010,031	malar
2	95,012,939	malar
2	140,675,410	malar
2	140,714,420	malar
3	8,951,128	wing and tail
3	10,312,247	malar, wing and tail
3	10,312,762	wing and tail
3	10,352,404	wing and tail
3	10,353,497	wing and tail
3	10,375,489	wing and tail
3	10,413,965	wing and tail
3	10,434,258	wing and tail
3	10,439,619	wing and tail
3	10,476,003	wing and tail
3	10,566,449	wing and tail
3	10,575,314	wing and tail
3	10,577,787	wing and tail
3	10,597,979	wing and tail
3	10,611,115	malar, wing and tail
3	10,612,379	malar
3	10,612,404	malar, wing and tail
3	10,615,068	malar, wing and tail
3	10,615,188	malar, wing and tail
3	10,734,204	wing and tail
3	10,904,459	malar
3	13,831,349	ear coverts
3	13,838,289	ear coverts
3	13,870,656	ear coverts
3	13,872,939	ear coverts
3	13,873,199	ear coverts

(Table C3 continued)

3	14,330,585	wing and tail
3	14,337,000	wing and tail
3	14,337,398	wing and tail
3	60,436,190	Malar
3	99,683,829	malar
4	25,315,868	ear coverts
4	38,859,047	malar
4	47,523,614	malar
4A	22,320,367	malar
4A	22,335,118	malar
4A	22,335,344	malar
5	7,102,593	nuchal
5	51,844,026	wing and tail
5	51,912,496	wing and tail
5	51,945,436	wing and tail
5	51,969,576	wing and tail
5	52,017,499	wing and tail
5	52,021,455	wing and tail
5	52,037,928	wing and tail
6	6,355,445	ear coverts
6	6,358,127	ear coverts
6	6,371,374	ear coverts
6	6,399,896	ear coverts
6	6,408,378	ear coverts
6	6,439,162	ear coverts
6	6,447,141	ear coverts
6	6,459,398	ear coverts
6	6,460,610	ear coverts
6	6,466,613	ear coverts
6	6,492,415	ear coverts
6	6,492,432	ear coverts
6	6,494,236	ear coverts
6	6,506,303	ear coverts
6	16,226,196	malar
6	16,226,199	malar
7	21,501,858	ear coverts
8	32,308,115	wing and tail
8	32,308,697	wing and tail
8	32,390,642	malar
8	32,422,287	wing and tail
8	32,428,368	wing and tail
8	32,464,211	wing and tail
8	32,885,769	wing and tail
8_random	1,165,267	wing and tail
9	9,570,463	wing and tail
11	6,870,506	ear coverts
12	4,269,475	wing and tail
12	4,450,671	wing and tail
12	4,493,867	wing and tail
12	4,494,447	wing and tail
12	4,501,149	wing and tail
12	4,538,964	wing and tail
12	4,543,047	wing and tail
12	4,547,356	wing and tail
12	4,547,433	wing and tail
12	4,551,440	wing and tail
12	4,557,142	wing and tail
12	4,625,995	nuchal
12	4,814,729	wing and tail
12	12,777,199	ear coverts
12	21,220,664	malar
13	11,349,592	malar
13	11,384,895	malar
13	11,403,495	ear coverts
28	361,396	wing and tail
28	361,416	wing and tail
28	361,944	wing and tail
28	362,880	ear coverts
28	363,157	ear coverts
28	366,803	ear coverts
28	1,136,931	wing and tail
28	2,900,628	nuchal
28	3,113,797	malar
28	3,170,382	wing and tail

(Table C3 continued)

28	3,217,874	wing and tail
28	3,222,090	wing and tail
28	3,235,155	wing and tail
28	3,250,388	wing and tail
28	3,252,636	malar
28	3,332,023	malar
28	3,333,691	malar, wing and tail
28	3,336,903	wing and tail
28	3,337,858	malar
28	3,337,956	malar
28	3,339,244	malar
28	3,363,067	wing and tail
28	3,364,820	wing and tail
28	3,364,865	wing and tail
28	3,365,001	wing and tail
28	3,401,371	wing and tail
28	3,401,827	wing and tail
28	3,463,580	malar
28	3,471,032	wing and tail
28	3,505,003	wing and tail
28	3,505,017	wing and tail
28	3,515,639	wing and tail
28	3,518,785	malar, wing and tail
28	3,570,206	wing and tail
28	3,592,412	wing and tail
28	3,665,221	wing and tail
28	3,684,589	malar
28	4,710,776	malar, wing and tail
28	4,711,391	malar
28	4,711,449	wing and tail
28	5,847,087	wing and tail
Z	1,675,485	malar
Z	1,689,369	malar
Z	1,874,629	malar
Z	1,937,058	malar
Z	2,204,018	malar
Z	2,412,780	malar
Z	2,524,238	malar
Z	2,608,546	malar
Z	2,735,902	malar
Z	2,736,084	malar
Z	2,736,158	malar
Z	2,836,782	malar
Z	2,849,883	malar
Z	2,851,245	malar
Z	2,895,513	malar
Z	2,905,125	malar
Z	3,011,096	malar
Z	3,081,467	malar
Z	3,303,871	malar
Z	3,324,810	malar
Z	3,340,821	malar
Z	23,752,174	malar
Z	24,690,090	malar
Z	24,691,332	malar
Z	24,718,875	malar
Z	24,807,103	malar
Z	24,825,966	malar
Z	25,099,799	malar
Z	25,221,113	malar
Z	25,442,799	malar
Z	25,487,407	malar
Z	25,526,775	malar
Z	25,527,463	malar
Z	25,552,962	malar
Z	26,742,443	malar
Z	26,743,841	malar
Z	26,748,088	malar
Z	26,749,563	malar
Z	26,750,225	malar
Z	26,751,908	malar
Z	26,839,283	malar
Z	26,846,689	malar
Z	26,846,781	malar

(Table C3 continued)

Z	26,846,866	malar
Z	26,846,889	malar
Z	26,846,906	malar
Z	26,847,344	malar
Z	26,847,350	malar
Z	26,848,823	malar
Z	26,848,974	malar
Z	26,861,247	malar
Z	26,868,101	malar
Z	26,875,438	malar
Z	26,915,982	malar
Z	26,916,070	malar
Z	26,919,261	malar
Z	26,919,290	malar
Z	26,924,800	malar
Z	26,936,299	malar
Z	26,936,531	malar
Z	26,936,820	malar
Z	26,938,249	malar
Z	26,941,800	malar
Z	26,941,846	malar
Z	26,941,907	malar
Z	26,962,012	malar
Z	27,013,819	malar
Z	27,013,895	malar
Z	27,014,288	malar
Z	27,083,567	malar
Z	27,090,452	malar
Z	27,215,683	malar
Z	27,215,689	malar
Z	27,215,728	malar
Z	27,219,187	malar
Z	27,219,403	malar
Z	27,220,453	malar
Z	27,220,515	malar
Z	27,221,098	malar
Z	27,329,433	malar
Z	29,848,816	malar
Z	29,882,788	malar
Z	29,912,192	malar, wing and tail
Z	29,921,834	malar
Z	35,476,033	malar
Z	35,482,169	malar
Z	35,490,637	malar
Z	35,498,903	malar
Z	35,499,475	malar
Z	35,514,777	malar
Z	35,515,952	malar
Z	35,515,958	malar
Z	38,083,371	malar
Z	38,083,562	malar
Z	48,224,055	malar
Z	48,224,213	malar
Z	48,225,978	malar
Z	48,226,965	malar
Z	48,227,051	malar
Z	48,227,101	malar
Z	48,227,216	malar
Z	48,227,220	malar
Z	48,227,221	malar
Z	48,227,225	malar
Z	48,227,497	malar
Z	48,227,501	malar
Z	48,304,252	malar
Z	48,307,509	malar
Z	48,319,420	malar
Z	48,332,084	malar
Z	69,174,342	malar
Z	69,308,275	malar
Z	70,636,027	malar
Z	70,970,163	malar
Z	73,541,236	malar
scaffold 3709	15,832	malar
scaffold 3761	1,283	malar
scaffold 5826	8,630	malar
scaffold 5826	8,635	malar
scaffold 9005	543	malar

**Table C4.** List of candidate genes located within 20kb of the SNPs identified in Table C3. Gene functions of potential relevance to melanin or carotenoid pigmentation are included (e.g., vesicles, WNT signalling pathway). The strongest candidate genes, those with known or suspected roles in pigmentation, are shaded in grey. Chromosomal and base pair positional information is based on alignment to the zebra finch genome.

Chrom.	Trait(s)	Gene ID from Flicker Genome	Gene Position	Ensembl Gene ID	Gene	Putative Function	Figure	Citations
1	nuchal	maker-Chromosome_1-snap-gene-175.1	52,671,908 -> 52,708,829	ENSTGUG00000012986	HIKESHI		3.3A	
1	<b>nuchal</b>	<b>maker-Chromosome_1-snap-gene-175.2</b>	<b>52,709,708 -&gt; 52,691,390</b>	<b>ENSTGUG00000012982</b>	<b>EED</b>	<b>known melanin gene</b>	<b>3.3A</b>	<b>Poelstra et al. 2015</b>
1	nuchal	maker-Chromosome_1-snap-gene-176.2	52,764,742 -> 52,850,165	ENSTGUG00000012969	PICALM	vesicle	3.3A	
1	ear coverts	maker-Chromosome_1-snap-gene-179.3	53,860,621 -> 53,713,396	ENSTGUG00000010346	GABRB3			
1A	malar	maker-Chromosome_1A-snap-gene-202.1	60,768,998 -> 60,761,565	ENSTGUG00000000892	FAM174A			
3	wing and tail	maker-Chromosome_3-snap-gene-30.2	9,019,049 -> 8,906,066	ENSTGUG00000002443	MACROD2	candidate pigmentation gene		Rodríguez et al. 2020
3	wing and tail	snap_masked-Chromosome_3-processed-gene-30.5	8,895,771 -> 9,018,107	ENSTGUG00000002440	FLRT3			
3	malar, wing and tail	maker-Chromosome_3-snap-gene-34.20	10,378,574 -> 10,317,976	ENSTGUG00000006163	ANKEF1		3.3B	
3	wing and tail	maker-Chromosome_3-snap-gene-34.21	10,403,056 -> 10,389,227	ENSTGUG00000006175	unk		3.3B	
3	wing and tail	maker-Chromosome_3-snap-gene-35.2	10,469,740 -> 10,564,745	ENSTGUG00000006182	PAK5		3.3B	
3	wing and tail	maker-Chromosome_3-snap-gene-35.3	10,583,266 -> 10,574,406	ENSTGUG00000006211	LAMP5		3.3B	
3	<b>malar, wing and tail</b>	<b>maker-Chromosome_3-snap-gene-37.8</b>	<b>10,793,362 -&gt; 10,620,855</b>	<b>ENSTGUG00000006214</b>	<b>PLCB4</b>	<b>known melanin gene, lipid</b>	<b>3.3B</b>	<b>Poelstra et al. 2015</b>
3	<b>malar</b>	<b>maker-Chromosome_3-snap-gene-37.13</b>	<b>11,099,970 -&gt; 10,898,437</b>	<b>ENSTGUG00000006294</b>	<b>PLCB1</b>	<b>known melanin gene, WNT signal, JNK cascade, lipid</b>	<b>3.3B</b>	<b>Poelstra et al. 2015</b>
3	wing and tail	maker-Chromosome_3-snap-gene-47.0	14,345,946 -> 13,946,705	ENSTGUG00000006863	CCDC85A	WNT/beta-catenin signal		
4	malar	maker-Chromosome_4-snap-gene-129.2	38,835,916 -> 38,911,484	ENSTGUG00000006243	GALNT7	known melanin gene family		
4	malar	maker-Chromosome_4-snap-gene-129.3	38,911,724 -> 38,835,906	ENSTGUG00000006267	HMG2	WNT signal		
4	malar	maker-Chromosome_4-snap-gene-158.4	47,573,951 -> 47,572,407	ENSTGUG00000008581	SHISA3	WNT signal, FGF signal		
4	malar	snap_masked-Chromosome_4-processed-gene-158.1	47,572,116 -> 47,352,661	ENSTGUG00000008477	GRXCR1			
5	nuchal	maker-Chromosome_5-snap-gene-23.2	7,033,310 -> 7,088,236	ENSTGUG00000026634	PARVA			
5	wing and tail	maker-Chromosome_5-snap-gene-172.3	51,835,816 -> 51,843,671	ENSTGUG00000011618	GPR176			
5	wing and tail	maker-Chromosome_5-snap-gene-173.25	51,935,021 -> 51,922,959	ENSTGUG00000011624	THBS1	MAPK signal, TGFB binding		
5	wing and tail	maker-Chromosome_5-snap-gene-173.24	51,913,700 -> 51,928,707	ENSTGUG00000011622	FSIP1			
6	<b>ear coverts</b>	<b>maker-Chromosome_6-snap-gene-21.9</b>	<b>6,485,210 -&gt; 6,492,457</b>	<b>ENSTGUG00000005207</b>	<b>JMJD1C</b>	<b>known melanin gene family</b>		<b>Poelstra et al. 2015</b>
6	malar	snap_masked-Chromosome_6-processed-gene-54.6	16,309,555 -> 16,236,385	ENSTGUG00000006706	VCL			
6	<b>malar</b>	<b>maker-Chromosome_6-snap-gene-54.13</b>	<b>16,242,935 -&gt; 16,268,213</b>	<b>ENSTGUG00000006678</b>	<b>AP3M1</b>	<b>known melanin gene family, vesicle</b>		<b>Poelstra et al. 2015; Rodríguez et al. 2020</b>
7	ear coverts	maker-Chromosome_7-snap-gene-71.15	21,475,276 -> 21,503,308	ENSTGUG00000008201	DCAF17			
7	ear coverts	maker-Chromosome_7-snap-gene-71.16	21,503,439 -> 21,514,050	ENSTGUG00000008221	CYBRD1			
8	malar, wing and tail	maker-Chromosome_8-snap-gene-108.14	32,391,574 -> 32,424,405	ENSTGUG00000009700	HOOK1	vesicle	3.3C	
8	<b>wing and tail</b>	<b>maker-Chromosome_8-snap-gene-108.17</b>	<b>32,465,680 -&gt; 32,429,366</b>	<b>ENSTGUG00000009722</b>	<b>CYP2J19</b>	<b>known carotenoid gene</b>	<b>3.3C</b>	<b>Lopes et al. 2016; Mundy et al. 2016</b>
8_rand	wing and tail	maker-Chromosome_8-random-snap-gene-4.44	1,176,692 -> 1,192,840	ENSTGUG00000017294	FMO4			
9	wing and tail	maker-Chromosome_9-snap-gene-31.21	9,559,286 -> 9,519,807	ENSTGUG00000007788	FARSB			
9	wing and tail	maker-Chromosome_9-snap-gene-32.0	9,564,202 -> 9,591,606	ENSTGUG00000007842	MOGAT1	lipid		
11	ear coverts	maker-Chromosome_11-snap-gene-22.9	6,810,780 -> 6,851,662	ENSTGUG00000006986	ESRP2	FGF signal		
11	ear coverts	maker-Chromosome_11-snap-gene-23.12	6,932,171 -> 6,857,241	ENSTGUG00000007006	NFATC3			
12	wing and tail	maker-Chromosome_12-snap-gene-14.28	4,250,558 -> 4,241,380	ENSTGUG00000005100	APEH		3.3D	
12	wing and tail	maker-Chromosome_12-snap-gene-14.29	4,268,946 -> 4,257,610	ENSTGUG00000005096	BSN	candidate pigmentation gene, vesicle	3.3D	Rodríguez et al. 2020
12	wing and tail	maker-Chromosome_12-snap-gene-14.34	4,434,700 -> 4,432,029	ENSTGUG00000005027	MONIA		3.3D	
12	wing and tail	maker-Chromosome_12-snap-gene-15.21	4,437,364 -> 4,498,200	ENSTGUG00000004964	RBM6		3.3D	
12	<b>wing and tail</b>	<b>maker-Chromosome_12-snap-gene-15.22</b>	<b>4,525,217 -&gt; 4,530,903</b>	<b>ENSTGUG00000006529</b>	<b>SEMA3B</b>	<b>known melanin gene family</b>	<b>3.3D</b>	<b>Poelstra et al. 2015</b>

(Table C4 continued)

12	wing and tail	maker-Chromosome_12-snap-gene-15.28	4,560,800 -> 4,536,803	ENSTGUG00000004888	RAD54L2			3.3D	
12	nuchal	maker-Chromosome_12-snap-gene-15.27	4,631,946 -> 4,670,685	ENSTGUG00000004855	DCAF1			3.3D	
12	wing and tail	maker-Chromosome_12-snap-gene-16.0	4,900,226 -> 4,707,979	ENSTGUG00000004762	DOCK3			3.3D	
28	ear coverts, wing and tail	maker-Chromosome_28-snap-gene-1.1	340,511 -> 348,174	ENSTGUG00000000181	FZR1			3.3E	
28	ear coverts, wing and tail	<b>maker-Chromosome_28-snap-gene-1.9</b>	<b>370,481 -&gt; 362,387</b>	<b>ENSTGUG00000000177</b>	<b>MFSD12</b>	<b>candidate melanin gene</b>		3.3E	<b>Abolins-Abols et al. 2018; Rodríguez et al. 2020</b>
28	ear coverts, wing and tail	maker-Chromosome_28-snap-gene-1.2	374,985 -> 377,309	ENSTGUG00000000169	HMG20B	candidate pigmentation gene		3.3E	Rodríguez et al. 2020
28	ear coverts, wing and tail	maker-Chromosome_28-snap-gene-1.3	378,835 -> 381,355	ENSTGUG00000000168	GIPC3			3.3E	
28	ear coverts, wing and tail	maker-Chromosome_28-snap-gene-1.10	383,383 -> 381,880	ENSTGUG00000000167	TBXA2R			3.3E	
28	wing and tail	snap_masked-Chromosome_28-processed-gene-3.30	1,145,704 -> 1,144,538	ENSTGUG00000000201	MEX3D				
28	nuchal	maker-Chromosome_28-snap-gene-9.30	2,923,071 -> 2,916,346	ENSTGUG000000013909	MAU2				
28	<b>malar</b>	<b>maker-Chromosome_28-snap-gene-10.10</b>	<b>3,096,137 -&gt; 3,091,560</b>	<b>ENSTGUG00000001090</b>	<b>ARMC6</b>	<b>known melanin gene family</b>		<b>Fig. 3f</b>	<b>Poelstra et al. 2015; Rodríguez et al. 2020</b>
28	malar	maker-Chromosome_28-snap-gene-10.3	3,097,965 -> 3,105,617	ENSTGUG00000001088	SUGP2			3.3F	
28	wing and tail	maker-Chromosome_28-snap-gene-10.7	3,155,623 -> 3,156,267	ENSTGUG000000014035	CERS1	lipid metabolism		3.3F	
28	wing and tail	snap_masked-Chromosome_28-processed-gene-10.19	3,162,454 -> 3,163,191	ENSTGUG000000014084	GDF1	MAPK signal, TGFB signal		3.3F	
28	wing and tail	snap_masked-Chromosome_28-processed-gene-10.28	3,180,618 -> 3,173,691	ENSTGUG00000001057	UPF1			3.3F	
28	wing and tail	maker-Chromosome_28-snap-gene-10.8	3,209,003 -> 3,216,285	ENSTGUG000000014102	COMP			3.3F	
28	malar, wing and tail	maker-Chromosome_28-snap-gene-10.14	3,242,942 -> 3,224,926	ENSTGUG00000001067	CRTC1			3.3F	
28	malar, wing and tail	snap_masked-Chromosome_28-processed-gene-10.31	3,267,485 -> 3,265,908	ENSTGUG00000001064	KLHL26			3.3F	
28	malar, wing and tail	maker-Chromosome_28-snap-gene-11.6	3,314,609 -> 3,314,098	ENSTGUG00000001051	KXD1	vesicle		3.3F	
28	<b>malar, wing and tail</b>	<b>maker-Chromosome_28-snap-gene-11.1</b>	<b>3,315,620 -&gt; 3,319,941</b>	<b>ENSTGUG00000001043</b>	<b>FKBP8</b>	<b>known melanin gene</b>		<b>3.3F</b>	<b>Poelstra et al. 2015</b>
28	malar, wing and tail	maker-Chromosome_28-snap-gene-11.2	3,347,564 -> 3,363,970	ENSTGUG00000001031	ELL			3.3F	
28	wing and tail	maker-Chromosome_28-snap-gene-11.7	3,408,947 -> 3,408,060	ENSTGUG000000008630	PGPEP1L			3.3F	
28	wing and tail	maker-Chromosome_28-snap-gene-11.3	3,418,013 -> 3,421,135	ENSTGUG00000001027	LSM4			3.3F	
28	malar, wing and tail	maker-Chromosome_28-snap-gene-11.4	3,438,740 -> 3,445,058	ENSTGUG00000001025	PDE4C			3.3F	
28	malar, wing and tail	<b>maker-Chromosome_28-snap-gene-11.5</b>	<b>3,448,481 -&gt; 3,449,841</b>	<b>ENSTGUG00000000716</b>	<b>RAB8A</b>	<b>known melanin gene family, vesicle trafficking</b>		<b>3.3F</b>	<b>Poelstra et al. 2015</b>
28	malar, wing and tail	maker-Chromosome_28-snap-gene-11.8	3,454,392 -> 3,452,329	ENSTGUG00000001023	MPV17L2	candidate pigmentation gene		3.3F	Rodríguez et al. 2020
28	malar, wing and tail	maker-Chromosome_28-snap-gene-11.9	3,456,215 -> 3,455,098	ENSTGUG00000000388	IFI30			3.3F	
28	malar, wing and tail	maker-Chromosome_28-snap-gene-11.10	3,470,396 -> 3,463,027	ENSTGUG00000000392	PIK3R2	MAPK signal		3.3F	
28	malar, wing and tail	snap_masked-Chromosome_28-processed-gene-11.38	3,491,736 -> 3,479,309	ENSTGUG00000000403	MAST3			3.3F	
28	malar, wing and tail	maker-Chromosome_28-snap-gene-11.13	3,523,469 -> 3,519,953	ENSTGUG00000000411	ARRDC2			3.3F	
28	malar, wing and tail	snap_masked-Chromosome_28-processed-gene-11.27	3,532,938 -> 3,534,707	ENSTGUG00000000415	ENC1-like			3.3F	
28	wing and tail	maker-Chromosome_28-snap-gene-11.14	3,558,614 -> 3,543,477	ENSTGUG00000000416	ARHGEF18	TGFB signal		3.3F	
28	wing and tail	maker-Chromosome_28-snap-gene-12.8	3,609,350 -> 3,590,247	ENSTGUG00000000426	INSR	MAPK signal		3.3F	
28	<b>malar, wing and tail</b>	<b>maker-Chromosome_28-snap-gene-12.10</b>	<b>3,669,011 -&gt; 3,639,812</b>	<b>ENSTGUG00000000453</b>	<b>MYO9B</b>	<b>known melanin gene family, CaM signal</b>		<b>3.3F</b>	<b>Poelstra et al. 2015</b>
28	malar, wing and tail	maker-Chromosome_28-snap-gene-12.0	3,678,113 -> 3,683,712	ENSTGUG00000000469	HAUS8			3.3F	
28	malar, wing and tail	maker-Chromosome_28-snap-gene-12.1	3,690,823 -> 3,723,601	ENSTGUG00000000470	CPAMD8				
28	malar, wing and tail	maker-Chromosome_28-snap-gene-15.30	4,684,401 -> 4,711,811	ENSTGUG00000000641	PTBP1	FGF signal			
28	malar, wing and tail	maker-Chromosome_28-snap-gene-15.37	4,725,567 -> 4,721,961	ENSTGUG00000000652	PLPPR3	lipid			
28	malar, wing and tail	maker-Chromosome_28-snap-gene-15.31	4,729,208 -> 4,730,933	ENSTGUG00000000658	CFD-like				
28	wing and tail	maker-Chromosome_28-snap-gene-19.23	5,837,622 -> 5,842,500	ENSTGUG00000000893	MIDN				
Z	malar	snap_masked-Chromosome_Z-processed-gene-5.10	1,637,460 -> 1,696,079	ENSTGUG00000000096	RNF38				

(Table C4 continued)

Z	malar	maker-Chromosome_Z-snap-gene-5.3	1,699,756 -> 1,712,155	ENSTGUG00000000103	TRIM14			
Z	malar	maker-Chromosome_Z-snap-gene-5.5	1,723,579 -> 1,701,377	ENSTGUG00000000113	NANS			
Z	malar	maker-Chromosome_Z-snap-gene-7.5	2,202,423 -> 2,133,925	ENSTGUG00000000132	PCGF3			
Z	malar	maker-Chromosome_Z-snap-gene-8.3	2,318,377 -> 2,408,627	ENSTGUG00000000135	CHRNA7-like	MAPK signal		
Z	malar	maker-Chromosome_Z-snap-gene-9.1	2,731,109 -> 2,637,419	ENSTGUG00000000146	PIGG			
Z	malar	maker-Chromosome_Z-snap-gene-9.5	2,881,763 -> 2,851,106	ENSTGUG00000000167	MAT1A			
Z	malar	maker-Chromosome_Z-snap-gene-9.0	2,891,453 -> 2,901,465	ENSTGUG00000000170	TMEM175			
Z	malar	maker-Chromosome_Z-snap-gene-10.10	2,940,395 -> 2,915,807	ENSTGUG00000000179	PDE6B	WNT signal		
Z	malar	maker-Chromosome_Z-snap-gene-10.7	3,005,642 -> 3,009,139	ENSTGUG00000000214	SLC26A1			
Z	malar	maker-Chromosome_Z-snap-gene-10.8	3,023,699 -> 3,079,852	ENSTGUG00000000237	THAP1			
Z	malar	maker-Chromosome_Z-snap-gene-10.12	3,083,308 -> 3,023,352	ENSTGUG00000000227	CHRN3			
Z	malar	maker-Chromosome_Z-snap-gene-11.15	3,313,091 -> 3,260,927	ENSTGUG00000000265	KCMF1			
Z	malar	maker-Chromosome_Z-snap-gene-11.16	3,339,984 -> 3,314,791	ENSTGUG00000000273	FNTA	TGFB signal		
Z	malar	maker-Chromosome_Z-snap-gene-11.12	3,347,725 -> 3,432,475	ENSTGUG00000000279	FUT10			
Z	<b>malar</b>	<b>maker-Chromosome_Z-snap-gene-82.1</b>	<b>24,652,494 -&gt; 24,773,591</b>	<b>ENSTGUG00000000903</b>	<b>PAM</b>	<b>known melanin gene</b>	<b>3.3G</b>	<b>Poelstra et al. 2015</b>
Z	malar	maker-Chromosome_Z-snap-gene-82.5	24,797,311 -> 24,652,580	ENSTGUG00000000926	GIN1		3.3G	
Z	malar	maker-Chromosome_Z-snap-gene-82.3	24,817,864 -> 24,864,805	ENSTGUG00000000931	PP1P5K2		3.3G	
Z	<b>malar</b>	<b>maker-Chromosome_Z-snap-gene-89.0</b>	<b>26,868,639 -&gt; 26,946,338</b>	<b>ENSTGUG00000001015</b>	<b>APC</b>	<b>known melanin gene, candidate carotenoid gene, WNT signal</b>	<b>3.3H</b>	<b>Poelstra et al. 2015; Gao et al. 2018</b>
Z	malar	maker-Chromosome_Z-snap-gene-90.8	26,963,344 -> 27,013,932	ENSTGUG00000001019	SRP19		3.3H	
Z	malar	maker-Chromosome_Z-snap-gene-90.10	27,006,224 -> 27,002,598	ENSTGUG00000001029	REEP5		3.3H	
Z	malar	maker-Chromosome_Z-snap-gene-90.12	27,106,155 -> 27,055,165	ENSTGUG00000001036	MCC	WNT/beta-catenin signal	3.3H	
Z	malar	maker-Chromosome_Z-snap-gene-91.0	27,284,135 -> 27,356,788	ENSTGUG00000003755	YTHDC2		3.3H	
Z	malar	maker-Chromosome_Z-snap-gene-118.0	35,498,523 -> 35,541,658	ENSTGUG00000001185	CHD1			
Z	malar	maker-Chromosome_Z-snap-gene-118.2	35,562,052 -> 35,534,707	ENSTGUG00000001184	RGMB	BMP signal		
Z	malar	maker-Chromosome_Z-snap-gene-127.0	38,007,636 -> 38,120,307	ENSTGUG00000001335	FEM1C			
Z	malar	maker-Chromosome_Z-snap-gene-160.16	48,224,144 -> 48,211,432	ENSTGUG00000001845	GBA2	lipid	3.3I	
Z	<b>malar</b>	<b>maker-Chromosome_Z-snap-gene-160.6</b>	<b>48,229,062 -&gt; 48,240,140</b>	<b>ENSTGUG00000001841</b>	<b>RGP1</b>	<b>candidate melanin gene, vesicle</b>	<b>3.3I</b>	<b>Brelsford, Toews, and Irwin 2017</b>
Z	malar	snap_masked-Chromosome_Z-processed-gene-160.49	48,243,929 -> 48,241,867	ENSTGUG00000001838	MSMP		3.3I	
Z	malar	maker-Chromosome_Z-snap-gene-161.24	48,288,734 -> 48,296,125	ENSTGUG00000001820	TMEM8B		3.3I	
Z	malar	maker-Chromosome_Z-snap-gene-161.26	48,318,493 -> 48,324,728	ENSTGUG00000001818	unk		3.3I	
Z	malar	snap_masked-Chromosome_Z-processed-gene-161.19	48,337,940 -> 48,336,573	ENSTGUG00000001815	TESK1		3.3I	
Z	malar	maker-Chromosome_Z-snap-gene-160.9	48,254,027 -> 48,262,735	ENSTGUG00000001828	NPR2-like		3.3I	

CHAPTER 4 APPENDIX

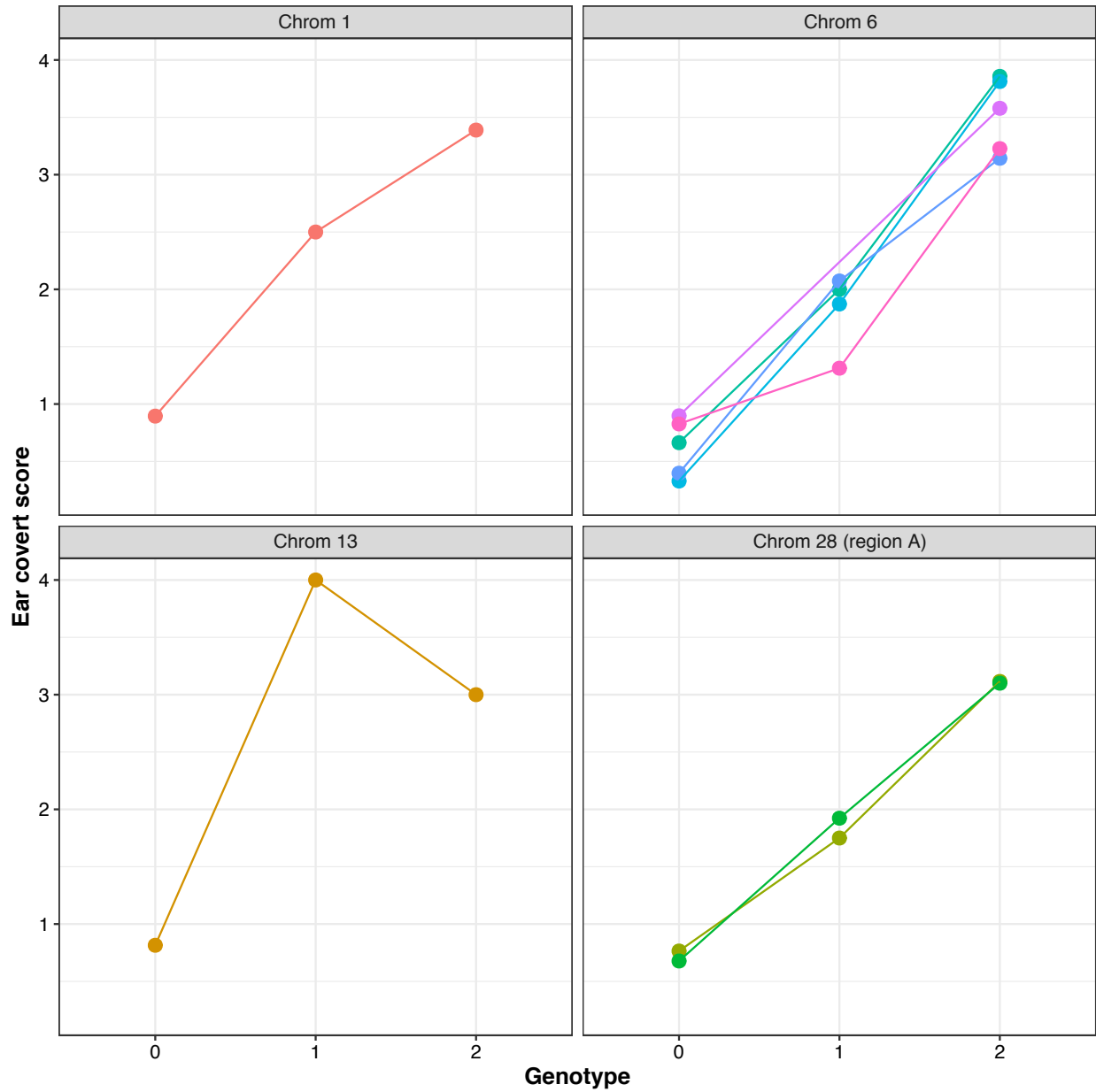


**Figure D1.** The relationship between ear cover score and the genotype of targeted SNPs separated by chromosome. The non-zero slopes in these relationships demonstrate the genotype-phenotype associations found in Aguilon et al. (2021) are still present when additional samples are included in the analysis.

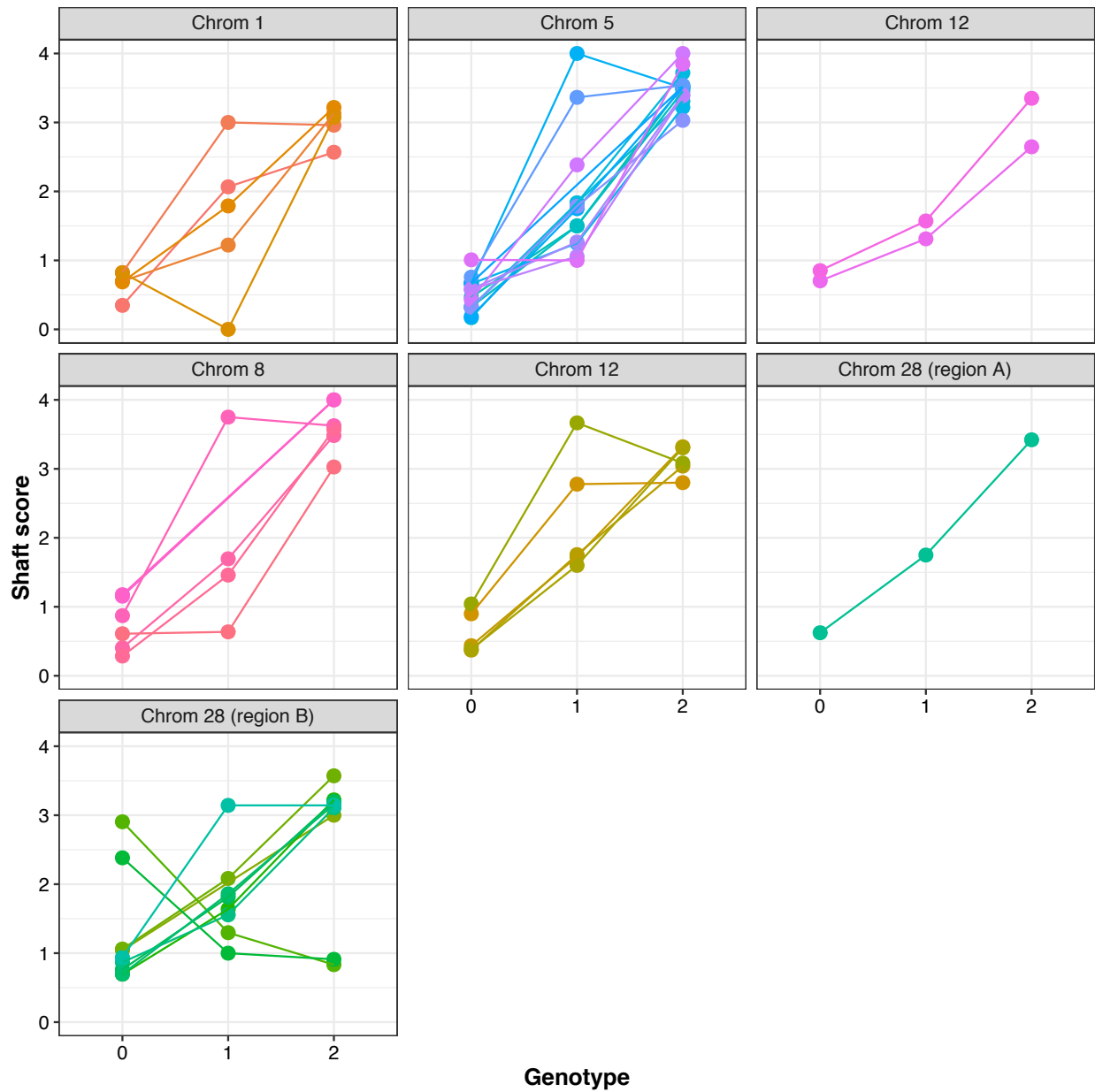


**Figure D2.** The relationship between shaft score and the genotype of targeted SNPs separated by chromosome (and additionally, region, for chromosome 28). The non-zero slopes in these relationships demonstrate the genotype-phenotype associations found in Aguillon et al. (2021) are still present when additional samples are included in the analysis.

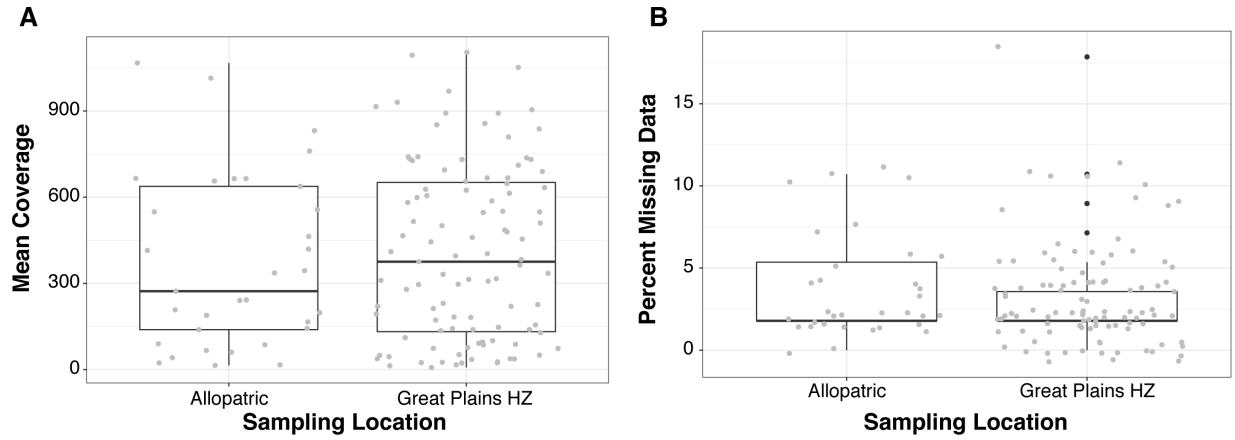


**Figure D3.** (A) Mean coverage and (B) percent missing data of individual samples across all targeted SNPs. Individuals are separated by their location—allopatric or hybrid zone—as indicated in Table D1.

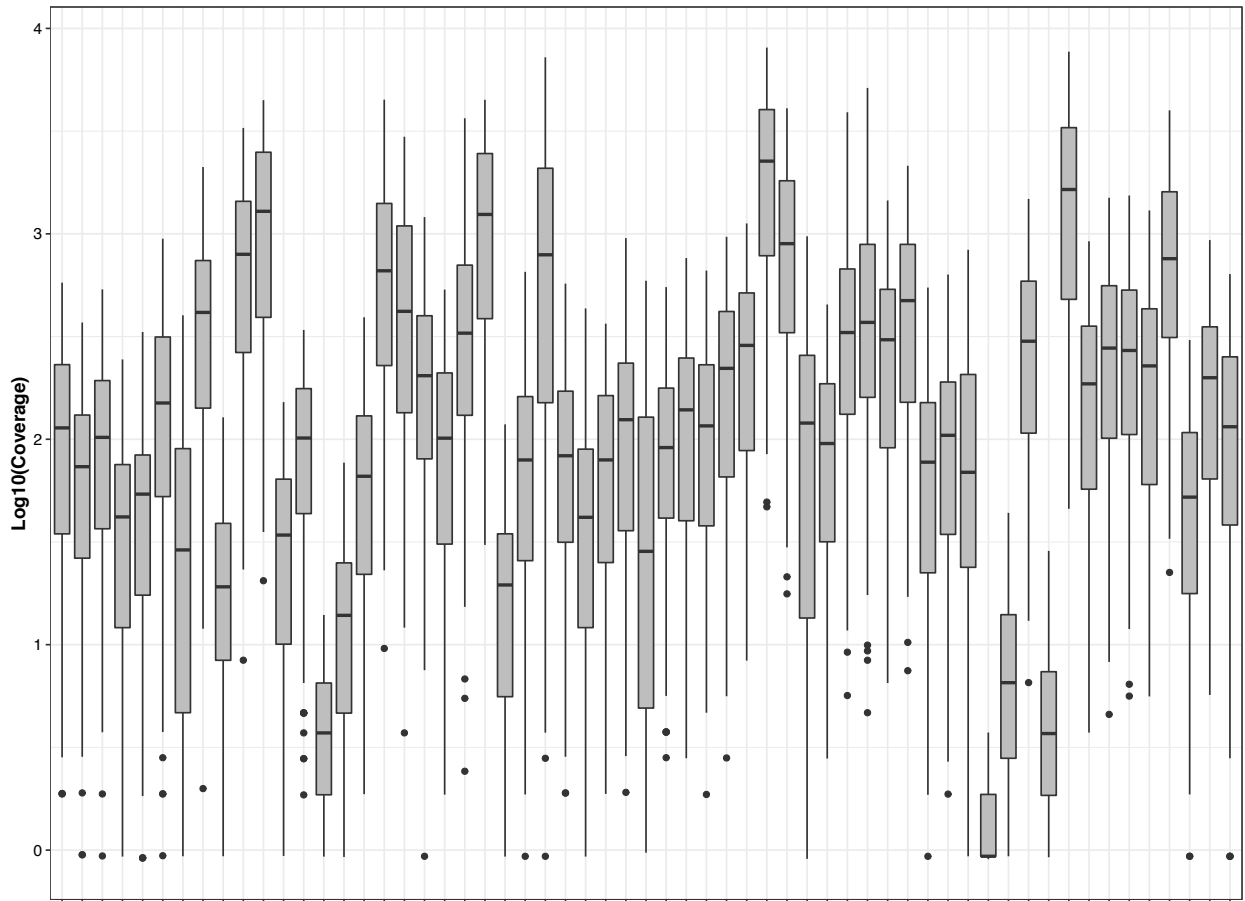
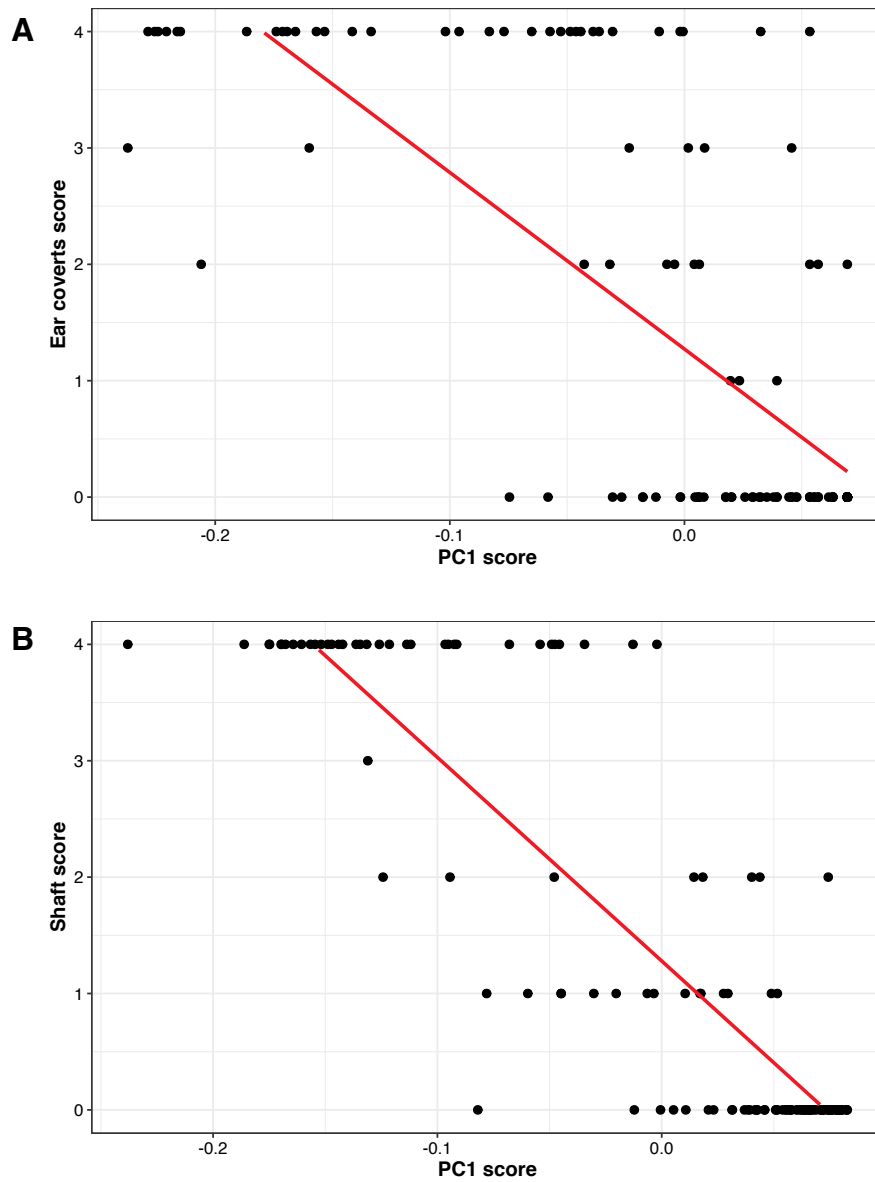
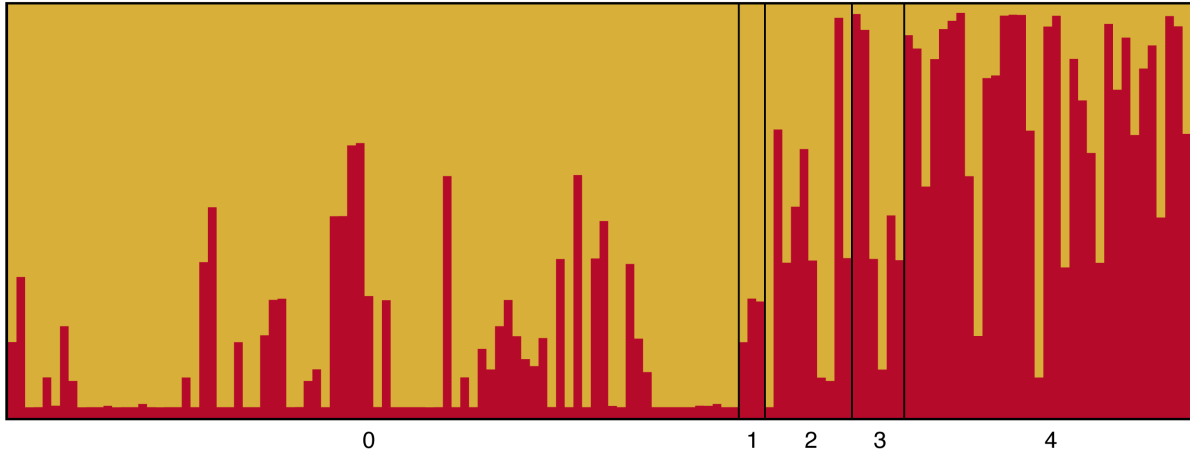


**Figure D4.** The sequencing coverage of each targeted SNP across all individuals. Coverage is shown on a log scale.



**Ear covers**



**Shaft**

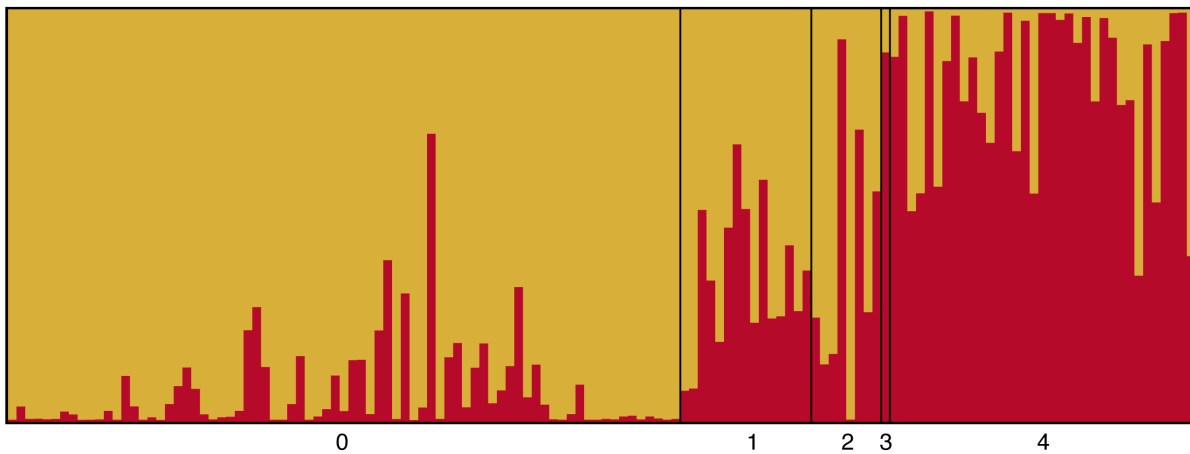


**Figure D6.** STRUCTURE plots for ear cover and shaft color showing the ancestry proportions for individual samples with  $K=2$  (the optimal value of  $K$  in both analyses). Individuals are grouped and ordered by their phenotype score (0 = yellow-shafted, 4 = red-shafted). Corresponding averages for each phenotype score are shown in Figure 4.1B and 4.1D.

**Table D1.** Detailed information on samples included in this study. Phenotype scores range from 0 (yellow-shafted) to 4 (red-shafted) for the ear coverts and shaft. Scores for the overall phenotype have been transformed to range from 0 (yellow-shafted) to 1 (red-shafted) to allow comparisons between the sexes.

Sample ID	Museum	Sex	State	Population	Ear Covert Score	Shaft Score	Overall Score
51231	CUMV	male	New York	allopatric	0	0	0
52454	CUMV	male	New York	allopatric	0	0	0
54562	CUMV	male	New York	allopatric	0	0	0
466387	FMNH	female	Illinois	allopatric	0	0	0
481942	FMNH	male	Illinois	allopatric	0	0	0
488431	FMNH	female	Illinois	allopatric	0	0	0
488432	FMNH	female	Illinois	allopatric	0	0	0
490404	FMNH	male	Illinois	allopatric	0	0	0
B48980	LSUMNS	male	Florida	allopatric	0	0	0
B50721	LSUMNS	female	Florida	allopatric	0	0	0
B50722	LSUMNS	male	Florida	allopatric	0	0	0
B58995	LSUMNS	female	Florida	allopatric	0	0	0
B59061	LSUMNS	male	Florida	allopatric	0	0	0
B83282	LSUMNS	female	Florida	allopatric	0	0	0
1803-25401	NA	male	Nebraska	hybrid zone	0	0	0
1803-25402	NA	male	Nebraska	hybrid zone	0	0	0
1803-25407	NA	male	Nebraska	hybrid zone	0	0	0
1803-25411	NA	female	Nebraska	hybrid zone	0	0	0
1803-25412	NA	male	Nebraska	hybrid zone	0	0	0
56715	CUMV	female	Nebraska	hybrid zone	0	0	0
56718	CUMV	male	Nebraska	hybrid zone	0	0	0
56719	CUMV	female	Nebraska	hybrid zone	0	0	0
56720	CUMV	male	Nebraska	hybrid zone	0	0	0
56721	CUMV	female	Nebraska	hybrid zone	0	0	0
56722	CUMV	male	Nebraska	hybrid zone	0	0	0
56729	CUMV	male	Nebraska	hybrid zone	0	0	0
56730	CUMV	female	Nebraska	hybrid zone	0	0	0
56732	CUMV	female	Nebraska	hybrid zone	0	0	0
56733	CUMV	female	Nebraska	hybrid zone	0	0	0
56735	CUMV	female	Nebraska	hybrid zone	0	0	0
56737	CUMV	male	Nebraska	hybrid zone	0	0	0
56738	CUMV	male	Nebraska	hybrid zone	0	0	0
56739	CUMV	female	Nebraska	hybrid zone	0	0	0
56740	CUMV	female	Nebraska	hybrid zone	0	0	0
57697	CUMV	male	Nebraska	hybrid zone	0	0	0
57708	CUMV	male	Nebraska	hybrid zone	0	0	0
57728	CUMV	male	Nebraska	hybrid zone	0	0	0
57729	CUMV	female	Nebraska	hybrid zone	0	0	0
57764	CUMV	female	Nebraska	hybrid zone	0	0	0
57985	CUMV	male	Nebraska	hybrid zone	0	0	0
57987	CUMV	male	Colorado	hybrid zone	0	0	0
58061	CUMV	male	Colorado	hybrid zone	0	0	0
58073	CUMV	female	Colorado	hybrid zone	0	0	0
58081	CUMV	female	Colorado	hybrid zone	0	0	0
58086	CUMV	female	Colorado	hybrid zone	0	0	0
58096	CUMV	female	Nebraska	hybrid zone	0	0	0
58147	CUMV	male	Nebraska	hybrid zone	0	0	0

(Table D1 continued)

1803-25405	NA	male	Nebraska	hybrid zone	0	0	0.041666667
1803-25413	NA	male	Nebraska	hybrid zone	0	0	0.041666667
56717	CUMV	male	Nebraska	hybrid zone	0	0	0.041666667
56728	CUMV	male	Nebraska	hybrid zone	0	0	0.041666667
56731	CUMV	male	Nebraska	hybrid zone	0	0	0.041666667
57669	CUMV	male	Nebraska	hybrid zone	0	0	0.041666667
58087	CUMV	male	Colorado	hybrid zone	0	0	0.041666667
58095	CUMV	male	Nebraska	hybrid zone	0	0	0.041666667
56716	CUMV	female	Nebraska	hybrid zone	0	0	0.05
57607	CUMV	female	Colorado	hybrid zone	0	0	0.05
58093	CUMV	female	Colorado	hybrid zone	0	0	0.05
58146	CUMV	female	Nebraska	hybrid zone	0	0	0.05
56725	CUMV	male	Nebraska	hybrid zone	0	1	0.083333333
57609	CUMV	male	Colorado	hybrid zone	0	1	0.083333333
57686	CUMV	male	Nebraska	hybrid zone	0	2	0.083333333
57709	CUMV	male	Nebraska	hybrid zone	0	0	0.083333333
58065	CUMV	male	Nebraska	hybrid zone	0	0	0.083333333
58072	CUMV	male	Colorado	hybrid zone	0	0	0.083333333
58091	CUMV	male	Nebraska	hybrid zone	0	0	0.083333333
58092	CUMV	male	Colorado	hybrid zone	0	0	0.083333333
1803-25403	NA	male	Nebraska	hybrid zone	0	0	0.125
1803-25404	NA	male	Nebraska	hybrid zone	0	0	0.125
56724	CUMV	male	Nebraska	hybrid zone	0	1	0.125
58097	CUMV	male	Colorado	hybrid zone	0	1	0.125
57986	CUMV	female	Colorado	hybrid zone	0	1	0.15
58094	CUMV	female	Colorado	hybrid zone	0	1	0.15
58067	CUMV	male	Nebraska	hybrid zone	0	0	0.166666667
58084	CUMV	male	Colorado	hybrid zone	0	1	0.166666667
1803-25410	NA	female	Colorado	hybrid zone	0	2	0.2
58151	CUMV	female	Colorado	hybrid zone	0	1	0.2
56726	CUMV	male	Nebraska	hybrid zone	0	4	0.208333333
58088	CUMV	male	Colorado	hybrid zone	2	0	0.208333333
57642	CUMV	female	Colorado	hybrid zone	0	1	0.25
58060	CUMV	female	Colorado	hybrid zone	0	0	0.25
1803-25406	NA	male	Nebraska	hybrid zone	2	0	0.291666667
58083	CUMV	male	Colorado	hybrid zone	1	0	0.291666667
58090	CUMV	male	Colorado	hybrid zone	2	0	0.291666667
57608	CUMV	female	Colorado	hybrid zone	0	1	0.35
58076	CUMV	female	Colorado	hybrid zone	3	0	0.4
58079	CUMV	male	Colorado	hybrid zone	3	0	0.416666667
1833-36504	NA	female	Colorado	hybrid zone	1	2	0.45
58085	CUMV	female	Colorado	hybrid zone	1	2	0.45
57988	CUMV	male	Colorado	hybrid zone	3	1	0.458333333
56734	CUMV	female	Nebraska	hybrid zone	0	0	0.5
58069	CUMV	male	Nebraska	hybrid zone	4	1	0.5
57967	CUMV	male	Colorado	hybrid zone	4	1	0.541666667
57610	CUMV	female	Colorado	hybrid zone	0	4	0.55
1833-36502	NA	male	Colorado	hybrid zone	2	4	0.583333333
58068	CUMV	male	Nebraska	hybrid zone	4	0	0.583333333
58064	CUMV	female	Nebraska	hybrid zone	2	0	0.6
1803-25409	NA	male	Colorado	hybrid zone	2	4	0.625
58148	CUMV	male	Nebraska	hybrid zone	0	4	0.625
1803-25408	NA	female	Colorado	hybrid zone	2	2	0.65

(Table D1 continued)

58150	CUMV	male	Colorado	hybrid zone	2	4	0.666666667
58070	CUMV	male	Colorado	hybrid zone	4	1	0.708333333
58089	CUMV	male	Colorado	hybrid zone	3	4	0.708333333
58154	CUMV	male	Colorado	hybrid zone	2	2	0.75
56723	CUMV	female	Nebraska	hybrid zone	3	4	0.8
56727	CUMV	male	Nebraska	hybrid zone	2	4	0.833333333
58071	CUMV	male	Colorado	hybrid zone	4	2	0.833333333
56736	CUMV	male	Nebraska	hybrid zone	4	2	0.875
58078	CUMV	male	Colorado	hybrid zone	4	4	0.875
58153	CUMV	male	Colorado	hybrid zone	4	1	0.875
1833-36503	NA	male	Colorado	hybrid zone	3	4	0.958333333
58063	CUMV	male	Colorado	hybrid zone	4	3	0.958333333
58066	CUMV	male	Colorado	hybrid zone	4	4	0.958333333
58062	CUMV	male	Colorado	hybrid zone	4	4	1
58075	CUMV	female	Colorado	hybrid zone	4	4	1
58077	CUMV	male	Colorado	hybrid zone	4	4	1
58152	CUMV	male	Colorado	hybrid zone	4	4	1
14042	AMNH	female	Washington	allopatric	4	4	1
17496	AMNH	male	Washington	allopatric	4	4	1
66173	BMUW	male	California	allopatric	4	4	1
100969	BMUW	male	California	allopatric	4	4	1
101883	BMUW	male	Oregon	allopatric	4	4	1
109367	BMUW	male	Oregon	allopatric	4	4	1
112778	BMUW	male	Oregon	allopatric	4	4	1
116098	BMUW	male	Oregon	allopatric	4	4	1
182046	MVZ	female	California	allopatric	4	4	1
182088	MVZ	male	California	allopatric	4	4	1
182380	MVZ	male	California	allopatric	4	4	1
182962	MVZ	female	California	allopatric	4	4	1
B22912	LSUMNS	unknown	California	allopatric	4	4	1
B24273	LSUMNS	male	California	allopatric	4	4	1
B24450	LSUMNS	female	California	allopatric	4	4	1
B34359	LSUMNS	male	California	allopatric	4	4	1
B34447	LSUMNS	female	California	allopatric	4	4	1
B41840	LSUMNS	female	California	allopatric	4	4	1
B42138	LSUMNS	female	California	allopatric	4	4	1

**Table D2.** Detailed information on the SNPs we targeted in this study. SNPs were identified as significantly associated with color differences in either the ear coverts or shaft in Aguillon et al. (2021). The strength of the association in the genome-wide association (GWA) and the  $F_{ST}$  between allopatric populations of red-shafted and yellow-shafted flickers from Aguillon et al. (2021) are included.

Chromosome	Position	Trait	GWA log(P)	$F_{ST}$
1	111456749	ear coverts	7.364264094	0.571429
1	111613466	shaft	7.947607746	0.802637
1	111647668	shaft	7.19338622	0.85675
1	111778865	shaft	7.947463802	0.619185
1	111782790	shaft	7.362767221	0.774397
1	112061267	shaft	8.649358968	0.941478
3	10312247	shaft	8.35105014	0.86762
3	10312762	shaft	10.10363993	0.866925
3	10352404	shaft	8.815952825	0.941176
3	10353497	shaft	10.29274127	0.944581
3	10375489	shaft	7.090095552	1
3	10413965	shaft	7.742057809	1
3	10439619	shaft	8.858493788	0.888889
3	10566449	shaft	7.428951145	0.944581
3	10577787	shaft	7.988428711	1
3	10612404	shaft	8.058980433	0.865672
3	10615068	shaft	8.551425843	1
3	10615188	shaft	8.00683638	1
3	10734204	shaft	7.052811533	0.63074
3	14337000	shaft	7.109014151	0.865135
5	51844026	shaft	7.667061077	0.659646
5	51912496	shaft	7.684634941	0.470199
5	51945436	shaft	7.825798844	0.542418
6	6355445	ear coverts	7.876230001	0.705847
6	6358127	ear coverts	8.56309555	0.619185
6	6447141	ear coverts	7.792428641	0.76352
6	6494236	ear coverts	7.519868826	0.774806
6	6506303	ear coverts	8.870432552	0.503367
8	32308115	shaft	8.164013385	0.0833333
8	32308697	shaft	7.699864921	0.112742
8	32422287	shaft	7.835043716	0.806589
8	32464211	shaft	8.343237347	0.889811
8	32885769	shaft	7.802039167	0.573276
8_random	1165267	shaft	7.288242444	0.566864
12	4269475	shaft	7.448065351	0.865672
12	4450671	shaft	8.030236558	0.74882
12	4493867	shaft	7.629254189	0.674587
12	4543047	shaft	7.972613693	0.816667
12	4547433	shaft	7.252227388	0.419704
12	4557142	shaft	8.27683012	0.767141
12	4814729	shaft	8.136582855	0.461455
13	11384895	ear coverts	7.052559661	0.721854
28 (region A)	361944	shaft	7.231039738	0.674603
28 (region A)	363157	ear coverts	7.127296977	0.825709
28 (region A)	366803	ear coverts	7.079998575	0.595115
28 (region B)	3170382	shaft	9.223335202	0.375
28 (region B)	3235155	shaft	7.594353341	0.285714
28 (region B)	3250388	shaft	7.149910435	-0.0061838
28 (region B)	3336903	shaft	11.23864042	0.123917
28 (region B)	3365001	shaft	7.439080485	0.390625
28 (region B)	3401827	shaft	9.257351525	0.216507
28 (region B)	3471032	shaft	8.707403495	0.240741
28 (region B)	3570206	shaft	8.204204001	0.286145
28 (region B)	3665221	shaft	7.614060359	0.292795

**Table S3.** The representative SNPs chosen to assess the additive and interactive effects between different genomic regions in producing the ear covert and shaft phenotypes.

The full list of targeted SNPs is shown in Table D2.

<b>Trait</b>	<b>Chromosome</b>	<b>Position</b>
Ear covert	1	111456749
Ear covert	6	6506303
Ear covert	13	11384895
Ear covert	28 (region A)	363157
Shaft	1	112061267
Shaft	3	10353497
Shaft	5	51912496
Shaft	8	32464211
Shaft	12	4450671
Shaft	28 (region A)	361944
Shaft	28 (region B)	3336903